# A QUANTITATIVE ANALYSIS AND MODELING OF HUMAN THERMAL SENSATION AND COMFORT IN OUTDOOR SPACES

**XIE YONGXIN**

**PhD**

**The Hong Kong Polytechnic University**

**2020**

**The Hong Kong Polytechnic University**

**Department of Building Services Engineering**

# A Quantitative Analysis and Modeling of Human Thermal Sensation and Comfort in Outdoor Spaces

**XIE YONGXIN**

**A thesis submitted in partial fulfillment of the requirements for the degree of Doctor of Philosophy**

**February, 2020**

# Certificate of originality

I hereby declare that this thesis is my own work and that, to the best of my knowledge and belief, it reproduces no material previously published or written, nor material that has been accepted for the award of any other degree or diploma, except where due acknowledgements has been made in the text.

______________________(Signed)

__Xie Yongxin_____(Name of Student)

# Abstract


Abstract of thesis entitled : A Quantitative Analysis and Modeling of Human Thermal Sensation and Comfort in Outdoor Spaces

Submitted by : Xie Yongxin

For the degree of : Doctor of Philosophy

To be involved in the outdoor environment is human nature, especially for the residents living in the cities. However, their desire of outdoor activities are hindered by the uncomfortable thermal conditions in the outdoors. For the residents living in the cities located in the subtropical and tropical areas, the humid and warm to hot outdoor conditions are those causing uncomfortable feelings. In recent years, cities located in the subtropical and tropical areas are experiencing an extended warm-biased period. The high-rise buildings built in the high-density cities weaken the wind environment and thus intensify the heat island effect. The building's structure, the arrangement of building clusters and vegetation such as trees and grass, and the infrastructures in human-height in the outdoor environment can have a significant influence on the micro-thermal environment. Different arrangements can create a various micro-thermal environment. Previous studies lack a clear understanding of the complex outdoor thermal environment and its influence on the residents.

Therefore, this thesis aims at providing knowledge in a better understanding of the outdoor thermal environment and its influence on the thermal perception of actual users. The research goal will be achieved through numerical modeling based on the physiological parameters and statistical modeling using a large amount of field survey data. Three sub-works are included in this thesis to achieve the research goal. Namely, (1) investigating the application of the CBE model in the outdoor environment from the aspects of wind and solar sensitivity; (2) the development of a model for accurate prediction of thermal sensation in the outdoor environment based on measured skin temperature; (3) locating the thermal neutral and thermal comfort ranges of meteorological parameters in Hong Kong through statistical modeling.

The thesis is based on a large amount of field measurement data of different micro-thermal environments using a microclimate station and survey response from actual users. The collected data covered four seasons. The parameters including air temperature ($T_a$, °C), globe temperature ($T_g$, °C), relative humidity (RH, %), wind speed ( $V$ , m/s), wind direction, black globe temperature ($T_b$, °C), long-wave irradiance ($Q_l$, W/m2), and short-wave irradiance ($Q_s$, W/m2) were collected simultaneously. At the same time, the human subjects were invited to experience the specific outdoor conditions. The physiological parameters, such as core and skin temperature, were collected simultaneously for certain experiment settings.

A multi-nodal thermal regulation model developed by the University of California-Berkeley targeted at the prediction of thermal sensation and thermal comfort in the transient and asymmetry thermal environment was selected for the prediction of thermal perception in the outdoor environment and the prediction accuracy was first investigated through the comparison of the field surveyed thermal response of human subjects. The preliminary study points out that human subjects were highly sensitive to the outdoor wind and solar environment. The human subjects were highly sensitive to the changing wind speed in the low-radiation conditions. The CBE model failed to predict such a high sensitivity. Besides, the human subjects had a higher tolerance to high air temperatures in outdoor environments than indoors when the solar radiation was acceptable, but the UCB model over-predicted the thermal sensation in such conditions. Both the field survey results and the predictions by the CBE model showed that subjects were more sensitive to wind speed in hotter environments while they were the least sensitive to solar radiation in neutral thermal conditions.

Physiological parameters such as local and overall skin temperatures were used in the CBE model as bridges to link the measured meteorological parameters and the prediction of thermal perception. Therefore, to identify the causes of prediction error, the field measured local and overall skin temperatures were compared with the simulated skin temperatures from the CBE model using the meteorological parameters as input. The measured and simulated skin temperatures were similar to each other merely in the range of 32.5 to 34.0 ℃. The prediction gap existed when the human body was experiencing cold and hot conditions. In the comparison between the relation of field-measured mean and local skin temperatures and overall and local thermal sensations, it is discovered that there was a wide range of mean and local skin temperatures corresponded to the thermal neutral range. Such a phenomenon was not observed in the prediction results from the CBE model due to the setting of ‘set-point’. A discussion about the usage of 'set-point' was introduced. Due to the characteristics of fluctuating wind environment in the outdoors and human subjects’ adaptation, we propose replacing ‘set-point’ with ‘null-zone’. The range of ‘null-zone’ was determined for different genders and applied to the calculation of local thermal sensation in the CBE model. Including the forehead as one of the dominant parts other than chest, abdomen, back, and pelvis in the logic of determining overall thermal sensation was another development. The prediction accuracy improved to 93.7% for the revised model.

The collected 1600 human subject responses from the field survey with the concurrent measurement results of meteorological parameters were used for the statistic modeling of locating thermal neutral and comfort ranges. Probit analysis was used for searching for the thermal neutral range of Hong Kong residents in a year span. Logistic regression was used for locating the meteorological parameter ranges for thermal neutral and comfort conditions. The results from Probit analysis showed residents had difficulties in determining their actual thermal feelings near the thermal neutral status when using the nine-point thermal sensation scale to describe their thermal feelings. The logistics regression models for thermal neutrality and thermal comfort were built using the combination of meteorological parameters. The results of the regression models showed that wind and solar radiation had an interaction effect with air temperature in determining thermal sensation and thermal comfort. Wind can effectively offset the negative effect of solar radiation in summer when the air temperature was lower than 31 ℃. The thermal comfort condition allowed a higher limit of solar radiation than the thermal neutral condition when the air temperature was lower than 31℃.

The present thesis investigates the human thermal perception in the outdoor environment. The findings in the present thesis contribute to a better understanding of creating a comfortable outdoor thermal environment. The revised CBE model can help to give an accurate prediction of thermal sensation in the outdoor thermal environment. The results from logistic regression modeling provide the reference of thermal neutral and comfort ranges for the planners and designers in the subtropical cities.

# Publications arising from this thesis

## Journal publications

[1] Xie, Y., Huang, T., Li, J., Liu, J., Niu, J., Mak, C. M., & Lin, Z. (2018). Evaluation of a multi-nodal thermal regulation model for assessment of outdoor thermal comfort: Sensitivity to wind speed and solar radiation. Building and Environment, 132, 45-56.

[2] Xie, Y., Liu, J., Huang, T., Li, J., Niu, J., Mak, C. M., & Lee, T. C. (2019). Outdoor thermal sensation and logistic regression analysis of comfort range of meteorological parameters in Hong Kong. Building and Environment, 155, 175-186.

[3] Xie, Y., Niu, J., Zhang, H., Liu, S., Liu, J., Huang, T., ... & Mak, C. M. (2020). Development of a multi-nodal thermal regulation and comfort model for the outdoor environment assessment. Building and Environment, 106809.

## Conference publications

[1] Xie, Y., Huang, T., Li, J., Niu, J., & Mak, C. M. (2018) The Sensitivity of Wind Speed and Solar Radiation in Determining Outdoor Thermal Sensation and Comparison with UC-Berkeley Model in the 4th International Conference on Building Energy and Environment (COBEE), Melbourne, Australia.

[2] Xie, Y., Niu, J., Mak, C. M., Li, J., Huang, T. (2018). Describing neutral thermal status in the urban area using physiological parameters in the 10th International Conference on Urban Climate/ 14th Symposium on the Urban Environment, New York, USA.

[3] Xie, Y., Niu, J., Mak, C. M. (2019). Further evaluation of a multi-nodal thermal regulation model: behavior of physiological parameters and sensitivity to convective heat transfer parameters in the 11th International Symposium on Heating, Ventilation and Air Conditioning (ISHVAC), Harbin, China.

# Acknowledgements

I want to dedicate this thesis to my husband and my parents. Special thanks to my husband, Yufeng Liu, for his support and patience during my Ph.D study. Without his support, it would have been impossible for me to finish my project. I would like to also acknowledge the CRF project of the Research Grant Council (Hong Kong) for its financial support to my experiment.

My sincere appreciation is given to my supervisor, Prof. Niu Jianlei, for his invaluable guidance, continued inspiration, and tireless support. Prof. Niu is the expert in the field of heat and mass transfer. He guided me into the research world, showed me how awesome it is when making improvements and new achievements. He always shows me the right direction to head for during my PhD study.

I sincerely thank Prof. Mak Cheuk-Ming of being one of my supervisors. Without his guidance and support, it would be impossible for me to finish my experiment. He is genuinely a kind gentleman and a scholar.

I thank all my colleagues and friends in Hong Kong, especially Prof. Jianlin Liu, Mr. Taiyang Huang, Ms. Jianong Li, Ms. Yuhang Fang, Mr. Ping Shue Shum, for their valuable help and suggestions. Special thanks to Prof. Richard de Dear and my lab mates in the IEQ lab, Dr. Sijie Liu, Ms. Yichen Yu, Mr. James Love, Dr. Jing Xiong, Dr. Lijuan Wang, Dr. Yan Xiong, Dr. Wenjie Ji and Dr. Yuchen Ji for their

kind support during my exchange at The University of Sydney. I would also like to thank all the participants in my experiment.

# Table of contents

Certificate of originality ........ I

Abstract ........ II

Publications arising from this thesis ........ VII

Acknowledgements ........ VIII

Table of contents ........ X

List of Figures ........ XVII

List of Tables ........ XXII

Nomenclature ........ XXIV

Chapter 1 Introduction ........ 1

1.1 Background ........ 1

1.2 Statement of the problem and research objectives ........ 7

1.3 Thesis outline ........ 11

Chapter 2 Literature review ........ 14

2.1 Outdoor thermal comfort studies in recent years .................................. 14

2.1.1 Brief introduction of the research area .......................................... 14

2.1.2 Methods for the outdoor thermal environment evaluation ............. 16

2.1.3 Strategies for improving the outdoor thermal conditions .............. 19

2.2 The mainstream thermal comfort indexes and models applied in the outdoors ........................................................................................................ 27

2.3 The Principles and development of the thermal indexes and models ... 32

2.3.1 PET (physiological equivalent temperature) .................................. 32

2.3.2 SET* (Standard effective temperature) .......................................... 37

2.3.3 UTCI ............................................................................................... 40

2.3.4 The CBE model .............................................................................. 48

2.3.5 The validation of the listed models in the outdoor environment ... 55

2.4 The basic theory related to the physiological models ........................... 59

2.4.1 Basic thermoregulation process and triggering conditions ............ 59

2.4.2 Thermal receptors ........................................................................... 60

2.4.3 Control theory and set-point ........................................................ 64

2.5 The studies related to the pedestrian wind environment....................... 70

2.5.1 Simulation techniques for the outdoor wind environment (CFD and wind tunnel) ............................................................................................. 70

2.5.2 Wind comfort criterion and scales ................................................ 72

2.6 Thermal comfort studies in Hong Kong............................................... 76

2.7 Summary and research gap .................................................................. 80

Chapter 3 Methodology......................................................................... 84

3.1 Introduction ........................................................................................... 84

3.2 The brief introduction of field survey ...................................................... 84

3.2.1 Survey location........................................................................ 85

3.2.2 Human subject......................................................................... 87

3.2.3 Survey sample ......................................................................... 89

3.2.4 Equipment .............................................................................. 91

3.2.5 Experiment procedure .............................................................. 97

3.3 The calculation method of main parameters .......................................... 100

3.3.1 The operative temperature ($Top$) .................................................... 100

3.3.2 The mean radiant temperature ($Tmrt$)............................................ 101

3.3.3 The calculation of direct and diffuse solar radiation........................ 102

3.4 The statistic method ................................................................... 105

3.4.1 Unclear voting near thermal neutral range...................................... 105

3.4.2 Probit analysis ...................................................................... 105

3.4.3 Logistic regression ................................................................ 109

3.5 Setting of the CBE model ........................................................... 112

Chapter 4 Evaluation of a multi-nodal thermal regulation model for assessment of outdoor thermal comfort: sensitivity to wind speed and solar radiation............. 114

4.1 Introduction.............................................................................. 114

4.2 Meteorological data analysis...................................................... 115

4.3 Comparison of the surveyed TSV and the simulated TSV (by the CBE model) over the whole range of operative temperature ...................................... 121

4.4 Comparison of the surveyed TSV and the simulated TSV (by CBE model) over the change in wind speed ............................................................. 125

4.5 Comparison of the surveyed TSV and simulated TSV (by the CBE model) over the change of solar radiation levels ............................................................. 129

4.6 Thermal sensation sensitivity to wind speed and mean radiation temperature ............................................................. 133

Chapter 5 Further evaluation and development of a multi-nodal thermal regulation model for the usage in the micro urban environment ............................. 138

5.1 Introduction ............................................................. 138

5.2 General description of the microclimate conditions ............................. 139

5.3 Primary comparison of the field data and the simulated data ................. 140

5.4 Comparison of the thermal sensation based on local and mean skin temperatures ............................................................. 146

5.5 The concept of “null zone” versus “set-point” ....................................... 155

5.6 Further development of the multi-nodal model ..................................... 165

Chapter 6 Outdoor thermal sensation and logistic regression analysis of comfort range of meteorological parameters in Hong Kong ................................................ 170

6.1 Introduction ........ 170

6.2 Hong Kong air temperature data analysis ........ 171

6.3 Data analysis related to the thermal neutral condition ........ 173

6.3.1 Unclear voting around the thermal neutral range ........ 174

6.3.2 Defining outdoor thermal neutral range in Hong Kong ........ 175

6.4 Thermal neutral and comfort ranges of meteorological parameters in Hong Kong summer ........ 183

6.5 Design recommendations for outdoor thermal comfort improvement ........ 201

6.5.1 Improving pedestrian wind environment ........ 202

6.5.2 Providing shading ........ 206

Chapter 7 Conclusions and recommendations for future study ........ 208

7.1 Summary of main works ........ 208

7.2 Evaluation of a multi-nodal thermal regulation model for assessment of outdoor thermal comfort- Sensitivity to wind speed and solar radiation ........ 210

7.3 Development of a multi-nodal thermal regulation and comfort model for the outdoor environment ........ 212

7.4 Outdoor thermal sensation and logistic regression analysis of comfort range of meteorological parameters in Hong Kong ............................................ 214

7.5 Recommendations for the future study .................................................. 216

Reference......................................................................................... 218

# List of Figures

Figure 2.1 cooling strategies during summer (Osmond & Sharifi, 2017)................. 26

Figure 2.2 The passive system of Fiala model (Fiala et al., 2010) ............................ 41

Figure 2.3 Schematic diagram of the logic flow in whole-body thermal sensation model (reproduced based on the reference (H. Zhang et al., 2010b) ......................... 54

Figure 2.4 Respective correlations between mean thermal sensation vote (MTSV) and three models in UEB and Open areas: (1) Correlation between MTSV and UTCI; (2) Correlation between MTSV and PET; (3) Correlation between MTSV and UCBTSV. ............................................................................................................. 57

Figure 2.5 Relationship between SET* and thermal sensation vote (TSV) (Xi et al., 2012) ................................................................................................................. 58

Figure 2.6 The relationship between MRT and thermal sensation vote (TSV) (Xi et al., 2012)................................................................................................................. 59

Figure 2.7 Discharge frequencies at different skin temperatures of thermoreceptors, along with potential transient receptor potential (TRP) channels associated with receptor function (Tansey & Johnson, 2015) ............................................................ 63

Figure 2.8 General properties of thermoreceptors. Static and dynamic responses of warm and cold receptors as they response to the static and transient temperature change (E. A. Arens & Zhang, 2006) ........................................................... 64

Figure 3.1 Survey locations for the first set of experiment....................................... 87

Figure 3.2 Survey locations for the second set of experiment (left) Sydney; (right) Hong Kong ............................................................................................................ 87

Figure 3.3 Microclimate station (Yongxin Xie et al., 2018) ..................................... 94

Figure 3.4 Equipment for core temperature measurement (a) CorTemp (HQInc, 2019) (b) inner structure of CoreTemp (HQInc, 2019) (c) HT150002 data logger (HQInc, 2019) ................................................................................................................. 95

Figure 3.5 Equipment for skin temperature measurement (a) T type thermal couple; (b) data logger; (c) thermal resistance; (d) i-button .................................................. 96

Figure 3.6 Measurement sites of local skin temperature......................................... 100

Figure 4.2 The wind rose distribution (a)Wind rose distribution at Site 1 (b) Wind rose distribution at Site 2 (c) Wind rose distribution at Site 3 ................................ 121

Figure 4.3 Thermal sensation data over the experiment period (a)Top vs TSV; (b)Top vs TSV-CBE.......................................................................................................... 122

Figure 4.4 Comparison of on-site TSV and CBE-simulated TSV over a range of wind speeds (a) on-site data, (b) CBE data ........ 125

Figure 4.5 Comparison of on-site TSV and CBE-simulated TSV at different solar radiation levels (a) on-site data, (b) CBE data ........ 129

Figure 4.6 Percentage distribution of people's feelings on sun radiation ........ 130

Figure 4.7 Thermal sensation sensitivity to wind speed (a: on-site data, b: CBE-simulated data) and mean radiation temperature (c: on-site data, d: CBE-simulated data) ........ 135

Figure 5.1 The relation between the field surveyed and simulated: (a) thermal sensation vote (TSV); (b) thermal comfort votes (TCV). (*The simulated TSV and TCV data were obtained by using the measured environmental parameters, and the surveyed subject physiology data as inputs.) ........ 141

Figure 5.2 Comparison between the measured and simulated mean skin temperatures ($T_{skin,m}$) ........ 145

Figure 5.3 Correlation between thermal sensation vote (TSV) and skin temperature: (a) between the Overall TSV and Mean skin temperature; and between the local TSV and local skin temperature: (b) Forehead; (c) Abdomen; (d) Left lower arm; (e) Left hand; (f) Left upper leg; (g) Left lower leg; (h) Left foot. ........ 151

Figure 5.4 Forehead skin temperature change with the change of wind speed (a) continuous sensible wind environment; (b) sudden strong wind environment........ 156

Figure 5.5 Local body temperature null zone in thermal neutral status (a) Male; (b) Female (c) thermal adaptation range derived from Zhang's study (H. Zhang, 2003) ........................................................................................................................ 162

Figure 5.6 The relation between field-surveyed forehead TSV and overall TSV.... 167

Figure 5.7 Prediction results compared with the field survey data (the revised model vs. the original model)............................................................................................ 168

Figure 6.1 Monthly average air temperature for the past 10 years in King's Park Observation point ....................................................................................................... 172

Figure 6.2 The record of extreme hot days in Hong Kong in the past 10 years (a) daytime record; (b) nighttime record ....................................................................... 173

Figure 6.3 P-P plot of on-site survey thermal sensation vote data ........................... 176

Figure 6.4 Normal distribution residual plot of on-site survey thermal sensation vote data ............................................................................................................................ 177

Figure 6.5 The seven probit regression lines ........................................................... 178

Figure 6.6 Sigmoid curves of the "neutral and warmer" and "warmer than neutral" groups ........................................................................................................................ 178

Figure 6.7 Transitional curves of thermal neutral for different seasons in Hong Kong ............................................................................................................................ 181

Figure 6.8 Determining the classification cutoff points (a) ROC curve of thermal neutral from the saturated logistic model; (b) ROC curve of thermal comfort from the saturated logistic model; (c) the difference between the sensitivity and 1-specificity in the ROC curve of thermal neutral logistic regression result; (d) the difference between the sensitivity and 1-specificity in the ROC curve of thermal comfort logistic regression result............................................................................................ 186

Fig.6.9 The meteorological parameters combinations for thermal neutrality and thermal comfort in the Hong Kong summer (a) Wind speed range: 0~0.5 m/s; (b) Wind speed range: 0.6~1.0 m/s; (c) Wind speed range: 1.1~1.5 m/s; (d) Wind speed range: 1.6~2.0 m/s; (e) Wind speed range: 2.1~2.5 m/s; (f) Wind speed range: 2.5~3.0 m/s.............................................................................................................. 195

Fig.6.10 The meteorological parameters combinations for thermal neutrality and thermal comfort in the September of Hong Kong (a) Wind speed range: 1.1~1.5 m/s; (b) Wind speed range: 2.1~2.5 m/s. ............................................................ 199

Fig. 6.11 Example of the area under the elevated building...................................... 203

Fig. 6.13 Hong Kong government building ............................................................ 205

# List of Tables


Table 1.1 The most citied articles in the field of outdoor thermal comfort................ 15

Table 2.1 UTCI equivalent temperatures categorized in terms of thermal stress (Bröde et al., 2012)......................................................................................... 46

Table 2.2 Neutral UTCI range and regression models of UTCI in different seasons for different climates ......................................................................................... 46

Table 2.3 Extended Land Beaufort Scale showing wind effect on people (B. Blocken & J. Carmeliet, 2004)......................................................................................... 73

Table 3.1 General information of the human subjects .............................................. 89

Table 3.2 Technical information of experimental equipment .................................... 96

Table 3.3 Technical information of physiological data collection ............................. 97

Table. 3.4 Example of thermal sensation *v*ote combination.................................... 108

Table. 5.1 The microclimate condition distribution of experiment.......................... 139

Table 5.2. Spearman correlation coefficient (rs) for the correlation between selected local body parts and the overall thermal sensation vote .......................................... 168

Table. 6.1 Significant level of comparison between original data and random data 175

Table. 6.2 Independent variables and the evaluation index in the logistics regression of thermal neutrality ........................................................................................ 187

Table. 6.3 Independent variables and the evaluation index in the logistics regression of thermal comfort.......................................................................................... 188

# Nomenclature

| | |
|---|---|
| $\lambda$ | The intensity of the thermal stimulus |
| $\lambda_0$ | A certain thermal stimulus intensity |
| $\gamma$ | The surface is rotated by $\gamma$ degrees (with north facing being 90° and upper facing being zero) |
| $\mu$ | The mean value of a normal distribution |
| $\sigma$ | The standard deviation of a normal distribution |
| $\varepsilon_p$ | Emissivity of the clothed human body in long-wave radiation; suggested value 0.97 |
| σ | Stefan-Boltzmann constant, 5.67*10-8 $\mathrm{W}/m^2K^4$ |
| $\rho$ | The average albedo |
| $\rho_b$ | Blood density, kg/l |
| ΔT | The difference between mean radiant temperature and air temperature |
| $az$ | The azimuthal angle |
| $a_k$ | Absorption coefficients of the clothed human body in short-wave radiation; suggested value 0.7 |
| AVA | Air Ventilation Assessment scheme |
| Berkeley Comfort model | The UC-Berkeley Thermal Comfort Model |
| $\frac{A_r}{A_D}$ | Ratio of effective radiation area and Dubois surface area; the value is 0.73 for a standing person |
| $c_b$ | Specific heat, $W \cdot s/K \cdot kg$ |
| clo | Cloting value |
| C+R | Sensible heat loss from skin, $W/m^2$ |
| *Centered-z* | Centered independent *v*ariables |
| $dP$ | Increment of probability |
| $d\lambda$ | The increment of thermal stimulus |
| DHI | Direct normal irradiance |
| DNI | Diffuse horizontal irradiance |
| $elv$ | Elevation angle, measured from the horizon to the solar position |
| $E_D$ | Total rate of evaporative heat loss from skin, $W/m^2$ |
| $E_{Re}$ | Rate of evaporative heat loss from respiration, $W/m^2$ |
| $E_{Sw}$ | Rate of evaporative heat loss from sweating, $W/m^2$ |
| $ET^*$ | Effective temperature |
| $f(\lambda)$ | Distribution function |
| $F_{CS}$ | Heat flows from body core to skin surface, W/m2 |
| $F_{SC}$ | Heat flows from skin surface to the clothing, W/m2 |
| GHI | Global horizontal irradiance |
| GTI | Global titled irradiance |
| $GHI_{lower}$ | The global horizontal irradiance received by the pyranometers facing ground |
| $GHI_{upper}$ | The global horizontal irradiance received by the pyranometers facing sky |

| | |
|---|---|
| $h_e$ | Evaporative heat transfer coefficient, describe outer surface resistances, W/(m2·kpa) |
| $h_r$ | Radiative heat transfer coefficient, $4.71 \mathrm{W/M^2K}$ |
| $h_c$ | Convective heat transfer coefficient, $\mathrm{W/M^2K}$ |
| $i_m$ | Total vapor permeation efficiency: ratio of actual evaporative heat flow capability between skin and environment o sensible heat flow capability as compared to Lewis ratio |
| $I_{cl}$ | The heat resistance of the clothing, $Km^2/kg$ |
| $I$ | Turbulence intensity, % |
| *ln (odds)* | Logit transformation |
| $k$ | The peak factor (or gust factor) |
| LIF | Laser-induced fluorescence |
| LR | Total vapor permeation efficiency: ratio of actual evaporative heat flow capability between skin and environment o sensible heat flow capability as compared to Lewis ratio |
| M | Rate of metabolic heat production, W/m$^2$ |
| MEMI | The Munich Energy-balance Model for Individuals |
| Met | The unit of metabolic rate |
| MTSV | Mean thermal sensation vote |
| $p_{ET*,S}$ | The saturated vapor pressure at ET*, kpa |
| $p_a$ | The vapor pressure at a point of air temperature , kpa |
| $P$ | The proportion of response in the overall population |
| $PET$ | The Physiologically Equivalent Temperature |
| PMV | predicted mean vote |
| PIV | particle image velocimetry |
| P-P plot | Probability–probability plot |
| $Q_l$ | Long-wave irradiance, W/m$^2$ |
| $Q_s$ | Short-wave irradiance, W/m$^2$ |
| $r_s$ | The spearman correlation coefficient |
| RH | Relative humidity, % |
| ROC curve | Receiver operating characteristic curve |
| $sza$ | Solar zenith angle, measured from the vertical to the solar position; |
| $sza_r$ | The angle of incidence of the DNI with respect to the tilted surface |
| $S$ | Rate of heat storage, W/m$^2$ |
| t | the time elapsed since the occurrence of $\frac{dT^+_{skin,m}}{dt_{max}}$ |
| $T$ | The surface is titled by T degrees (with north facing being 90° and upper facing being zero) |
| $T_{hy}$ | head core temperature, ℃ |
| $T_{skin}$ | The mean skin temperature |
| $T_{core}$ | Core temperature, ℃ |
| $T_{skin}$ | Skin temperature, ℃ |

| | |
|---|---|
| $T_{skin,m}$ | Mean skin temperature, ℃ |
| $T_{forehead}$ | The skin temperature of forehead, ℃ |
| $T_{abdomen}$ | The skin temperature of abdomen, ℃ |
| $T_{left\ lower\ arm}$ | The skin temperature of left lower arm, ℃ |
| $T_{left\ hand}$ | The skin temperature of left hand, ℃ |
| $T_{left\ upper\ leg}$ | The skin temperature of left upper leg, ℃ |
| $T_{left\ lower\ leg}$ | The skin temperature of left lower leg, ℃ |
| $T_{left\ foot}$ | The skin temperature of left foot, ℃ |
| $T_{cl}$ | Clothing temperature, ℃ |
| $T_a$ | Air temperature, ℃ |
| $Ta'$ | Centered air temperature (°C) |
| $T_g$ | Globe temperature, ℃ |
| $T_b$ | Black globe temperature, ℃ |
| $T_{mrt}$ | Mean radiant temperature, ℃ |
| $T_{mrt}{}'$ | Centered mean radiant temperature (°C) |
| $T_{mrt-i}$ | Six directional mean radiant temperatures of the imaginary room, ℃ |
| $T_{op}$ | Operative temperature, ℃ |
| $T_{si-i}$ | Equivalent surface temperature of the wall in the imaginary room, i=1-6 |
| TS*V* | Thermal sensation *v*ote |
| TC*V* | Thermal comfort *v*ote |
| The CBE model | A multi-node human body thermal regulation model developed by the University of California-Berkeley |
| *UTCI* | The Universal Thermal Climate Index |
| $U_e$ | The equivalent wind speed, m/s |
| $\bar{u}$ | The wind speed measured at the height of 1.75m |
| $u_{max,2s}$ | The peak 2-s gust within a 10-min period |
| *v* | Wind speed (m/s) |
| $v'$ | Centered wind speed (m/s) |
| $v_b$ | The blood flow from body core to skin, $l/s \cdot m^2$ |
| VP | Vapor pressure, hpa |
| *w* | Skin wittedness, dimensionless |
| W | Rate of mechanical work accomplished, W/m$^2$ |
| WBGT | wet bulb globe temperature |
| *SET** | Standard effective temperature |
| SPMV | Spatial predicted mean vote |
| *Y* | The probit value of *P* |
| $Z_0$ | Centered variables |

# Chapter 1 Introduction

## 1.1 Background

The need of building a comfortable and energy-efficient living environment has always been pursued by the society. Comfortable indoor environment needs huge amount of energy support, while comfortable outdoor environment can be realized by better planning in the developing stage of a neighborhood or even a city. Improved thermal conditions in the outdoor environment help accommodating daily traffic related to pedestrians and cyclists, and encouraging citizens to conduct various activities outdoors, such as dinning outdoors, spending leisure time and doing sports. Human nature determines people’s desirability for going outside especially after spending longtime in the indoor built environment. It is well known that spending more time in the outdoor environment is beneficial to both physical and mental health. In a word, outdoor environment is important for building sustainable cities and will be benefit to urban livability. Therefore, the government and city planners show growing concern of building a better outdoor environment and making outdoor spaces attractive to citizens in the designing and planning stage of the sustainable cities (Maruani, & Amit-Cohen, 2007). Thermal and wind effects are the two most influential factors that could affect comfort in outdoor spaces. (Thorsson et al., 2007).

Especially when the function of the outdoor spaces is for leisure and entertainment (e.g. parks), the usage of such kind of spaces is influenced more by thermal conditions than the spaces such as outdoor squares (practical function) (Thorsson et al., 2007). A study from Lai et al. (2014) showed thermal comfort accounted for 35% of the relative importance in selecting an outdoor space for activities among the other factors including air quality and acoustic environment, functionality and convenience. As a result of which, the concern about the thermal issues in the built environment has recorded growing number of studies all around the world during the past decades (Ahmed, 2003; Chen, & Ng, 2012; Vicky Cheng et al., 2012; Givoni et al., 2003; Höppe, 2002; Soligo et al., 1998; Spagnolo, & de Dear, 2003; Tseliou et al., 2010).

The majority of urban climate phenomena can be divided by scale: the microscale, local scale and mesoscale domains (Oke et al., 2017). According to Urban Climates by Oke et al., (2017) subtle changes of sky condition with airflow distribution, micro- and local phenomena and the effects of surface properties like albedo, emissivity and thermal properties establishes different urban microclimates. The thermal comfort in the outdoor spaces is greatly influenced by the local microclimate. Different climate regions form specific thermal conditions for different districts. In the urban area, neighborhoods surrounded by high buildings of various building density with different kinds of façade materials and different building structures, and the infrastructures in human-height providing or blocking direct solar radiation and wind passages form its own microclimate. Moreover, the water body and the arrangement of greenery (different types of trees and grasslands) also have great impact on the microclimate. Therefore, thermal comfort in the outdoor environment in different areas should be considered case by case and there is no one solution for all. This explains why different regions and cities having their own thermal comfort studies related to their own outdoor conditions. Besides, the difference in thermal environment, physiological and psychological factors from actual users also play an important role in determining thermal comfort status. The dressing patterns and behaviors, adaptation effects to certain climate conditions and recent thermal history as well as psychological feelings of people from different regions and areas could be the influencing factors. A study performed by Nikolopoulou and Lykoudis (2006) showed the neutral temperature difference across Europe could be over 10 °C. The vast amount of outdoor thermal comfort studies in recent two decades have two main focuses: evaluating the performance of the methods for the improvement of outdoor thermal environment and building proper thermal comfort indexes to describe outdoor thermal comfort.

In the past two decades, a vast number of studies related to evaluating the ways for the improvement of urban thermal comfort conditions appear around the whole world. Researchers devoted themselves in searching for a proper way to improve the thermal conditions of the outdoor spaces for local climate conditions. Among the studies searching for the strategies of improving outdoor thermal conditions, some consider the effect of H/W ratio (height-to-width ratio) of the street canyons and street axis orientations; some focus on the building arrangement and building structures while some focus on the landscapes. The H/W ratio and the street orientations as well as the building structures and clusters affect the amount of solar and wind access (Ali-Toudert, & Mayer, 2006; Johansson, 2006). A study in Fez, Morocco (hot and dry climate) compared the effect of H/W ratio (height-to-width ratio) of street canyons and found deep canyon is comfortable in summer and the shading created by deep canyon provide a 10 ℃ temperature drop compared to the shallow canyon but is not comfortable in the winter for blocking solar access (Johansson, 2006). Rodríguez-Algeciras et al. (2018) studied the street axis orientations and founded that the E-W streets had the highest thermal stress to pedestrian with extreme PET values of 36 ℃ in the summer of Cuba. Gulyas et al. (2018) used the thermal index PET to perform the human-biometeorological assessment using RayMan for the microclimate of the urban area surrounded by buildings of different surface materials and plants and found that the difference in PET index can reach 15-20 ℃. Huang et al. (2017) found the open space under an elevated building can provide a PET drop of 6.2 ℃ compared to the open space surrounded by buildings. The landscape design parameters included grass, trees of different heights and water body were assessed to have different performances in ameliorating thermal environment (S. Sun et al., 2017). Regarding the greenery, the improvement of thermal environment by the greenery depends on the choice and arrangement of plants. The configuration parameters: leaf area index, tree height and trunk height were found to be three of the most influential parameters to the improvement of thermal environment (Morakinyo et al., 2017).

The neutral temperatures of different regions and areas in the worldwide are the representative of district difference and adaptation in thermal sensation and comfort. There have been many outdoor thermal comfort studies related to searching for the neutral temperature using various thermal indexes. Spagnolo and de Dear (2003) investigated the outdoor and semi-outdoor locations in subtropical Sydney and found the thermal neutrality in the index of OUT_SET* was 26.2 ℃. The neutral temperature described by SET* in Taiwan (a representative of hot and humid climate regions) was 27.1 ℃ for the outdoor environments and 25.8 ℃ for semi-outdoor environments (Hwang, & Lin, 2007). The neutral PET (physiological equivalent temperature) in the summer of Hong Kong, China was around 28.0 ℃ from the observations by Ng and Cheng (2012). The PET neutral temperature in Changsha, China and Singapore was 27.9 ℃ and 28.1 ℃, respectively (Yang et al., 2013). The field study in the summer of Cambridge showed that neutral temperature was about 27.0 ℃ of $T_a$ (air temperature) (Nikolopoulou et al., 2001). From the studies worldwide, the thermal neutrality and thermal comfort range was defined according to the local microclimate characteristics using different thermal comfort indexes. Through listing the studies from different regions and the results of assessment from different strategies, we can find that it is difficult to do the comparison due to the disunity of thermal indexes.

From the research listed above, it is noticeable that there is a clear need for a thermal comfort index or model that can be used to accurately evaluate the outdoor thermal environment in the designing and planning stage. At present, the thermal indexes can normally be divided into two groups: empirical models and rational models. The models built through regression are empirical models; those energy budget model and physiological models are rational models. The regression models are to build up a correlation between thermal sensation vote and a combination of meteorological parameters (solar radiation, wind speed, air temperature, and humidity) (Lai et al., 2017b; Yongxin Xie et al., 2018). The application for such kind of model is limited to certain climate conditions, because of the sample size and the characteristics of local human subjects. The existing energy balance models, such as the PMV (Predicted Mean Vote) index, focus on stable thermal environment where human subjects are required to reach a thermally equivalent status (Höppe, 2002; Yongxin Xie et al., 2018). The requirements of such kind of models render them not suitable for the transient changing thermal environment like the outdoors. The models based on thermo-physiological parameters, however, involves the stimulation of the dynamic thermal regulation mechanism of a human body (Yongxin Xie et al., 2018). Divided by the compartment nodes of the models related to thermo-physiological parameters, the mainstream models are the two-node model (SET*, OUT_SET* and PET) and the multi-nodal model (UTCI and the CBE model). Our study did a general comparison of the performance of such kind of models in the evaluation of thermal sensation in the outdoor environment (Huang et al., 2017). We have found that the multi-nodal models (UTCI and the CBE model) have higher prediction accuracy than the two-node model (PET) (Huang et al., 2017). Still, the multi-nodal models have their own short-comings and cannot provide thermal sensation prediction in the outdoor environment in high accuracy (Yongxin Xie et al., 2018). The main reason is that such kind of models were built based on the experimental data obtained in the indoor chambers or indoor experiments, which were different from the actual outdoor environment considering the transient wind environment and asymmetric solar radiation conditions. In summary, there is still a lack of a thermal comfort model to give accurate thermal sensation and comfort predictions in outdoor settings.

### 1.2 Statement of the problem and research objectives

This study focuses on the searching for a proper way to evaluate the thermal comfort in the scale of sub-microclimate. The main objective is to acquire a better knowledge of how to evaluate and improve the thermal environment in the urban setting, to understand people's thermal perception and its importance in the outdoor environment, in order to provide a reference for the planning and designing stage of an outdoor neighborhood. It is expected that the increased usability of the outdoor environment will be beneficial to the physical and mental health of the public. It can also make contribution to energy saving in private residences by reducing the time people stay indoors.

The research questions of this study are listed as below:

1) The outdoor thermal environment is a highly transient and asymmetric thermal environment, the main fluctuating factors are wind environment and solar radiation. The outdoor wind environment is highly transient with much higher turbulence intensity and frequently occurring gust wind. However, the current ASHRAE standard recommends limited air movement for the indoor mechanical system. The current thermal comfort models are developed in the indoor chamber, where complex outdoor wind condition cannot be simulated. The outdoor asymmetric radiation environment is caused by the direct solar radiation from the sun and the reflected long-wave radiation from different surface materials of the surroundings. The indoor thermal environments usually have limited radiation difference. And thus, the popular two-node models (PET and SET* etc.) might

not be able to give accurate predictions in the outdoors. With these main differences from the indoor environment, is it appropriate to continue using the thermal indexes or models developed in the indoor chamber to evaluate the outdoor context? What is the gap of applying such kind of models in the outdoor environment?

2) The model developed by applying the physiological parameters seems to be capable of coping with the transient thermal environment in comparison with other models developed by simple regressions, but the existing perception model linked with physiological thermal regulation model output was based on the data obtained in the indoor experiment. Do the logic structures for the relationship of physiological parameters and thermal perceptions developed based on the indoor environment applicable to the outdoor thermal environment? Will the continuous thermal stimulus in the outdoor environment have different impact on the physiological parameters than that of the indoors? How does the physiological parameters adapt to the outdoor environment?

3) The wind environment in the outdoors is highly transient. The turbulence intensity level in the outdoor environment is much higher than that in the indoors; however, the existing research about the cooling effect of turbulence intensity such as the heat transfer coefficients were developed at the conditions of low turbulence intensity (<20%) (R. J. de Dear et al., 1997). The existing studies

related to the wind environment are mainly about wind safety and wind comfort, there is a gap of the study focusing on the wind characteristics and thermal comfort in the outdoor environment. How does the wind environment in the outdoors affect the local skin temperatures? How does people in the urban settings react to and adapt to different wind characteristics? How to quantify the cooling effect of different wind characteristics?

4) The thermal environment affects thermal perception as a whole system. The air temperature, solar radiation, relative humidity, and wind environment should be considered as a whole system. However, the existing studies tend to discuss these parameters separately. Therefore, we are wondering what the proper way is to search for the comfort range combining all the environmental parameters together. What is the comfort ranges for wind and solar conditions under different air temperatures? Is there any difference for the climate conditions when achieving thermal neutral status and thermal comfort status?

Three sub-works were done to solve the listed research questions. A multi-nodal thermal regulation model was evaluated in different outdoor settings, including the fully open area, and the semi-open area under an elevated building. People's sensitivity to solar radiation and wind environment in the outdoor environment was examined. Skin temperature was used as a bridge to link the environmental parameters and the thermal feelings together. The behavior of skin temperature of 17 local body parts were observed in a large scale of human subject surveys over a whole year period in the outdoor setting to explore the relation between these three aspects. A statistic method was used to locate the thermal comfort range of different combinations of the environmental parameters.

### 1.3 Thesis outline

This chapter (Chapter 1) presents a brief description of the background and the statement of the problems, points out the research questions and also draws the outline of this thesis (Figure 1.1).

Chapter 2 provides the literature review about the whole study. It mainly covers three aspects: outdoor thermal comfort studies in recent years; mainstream thermal comfort indexes and models; basic theory and findings related to the physiological models; studies related to outdoor wind environment.

Chapter 3 gives the description about the methodology used in this thesis, including the methods and equipment of microclimate monitoring and field data collection; the methods related to the original data processing and input to the multi-nodal thermal regulation model; and the description of a statistic model (probit analysis and logistic regression).

Chapter 4 provides the results of field monitoring and field thermal perception survey response along with the initial comparison of the prediction results from the multi-nodal thermal regulation model (the CBE model).

Chapter 5 provides the results of field measured local skin temperatures from a year span along with the comparison of the simulation results from the CBE model. A discussion between “null zone” and “set-point” will be presented and a further development of the CBE model for the outdoor environment will be provided.

Chapter 6 presents the analysis of searching for the thermal neutral and thermal comfort ranges of the combination of meteorological parameters using the statistical methods.

Chapter 7 is the conclusion of the whole thesis and the recommendations for future studies.

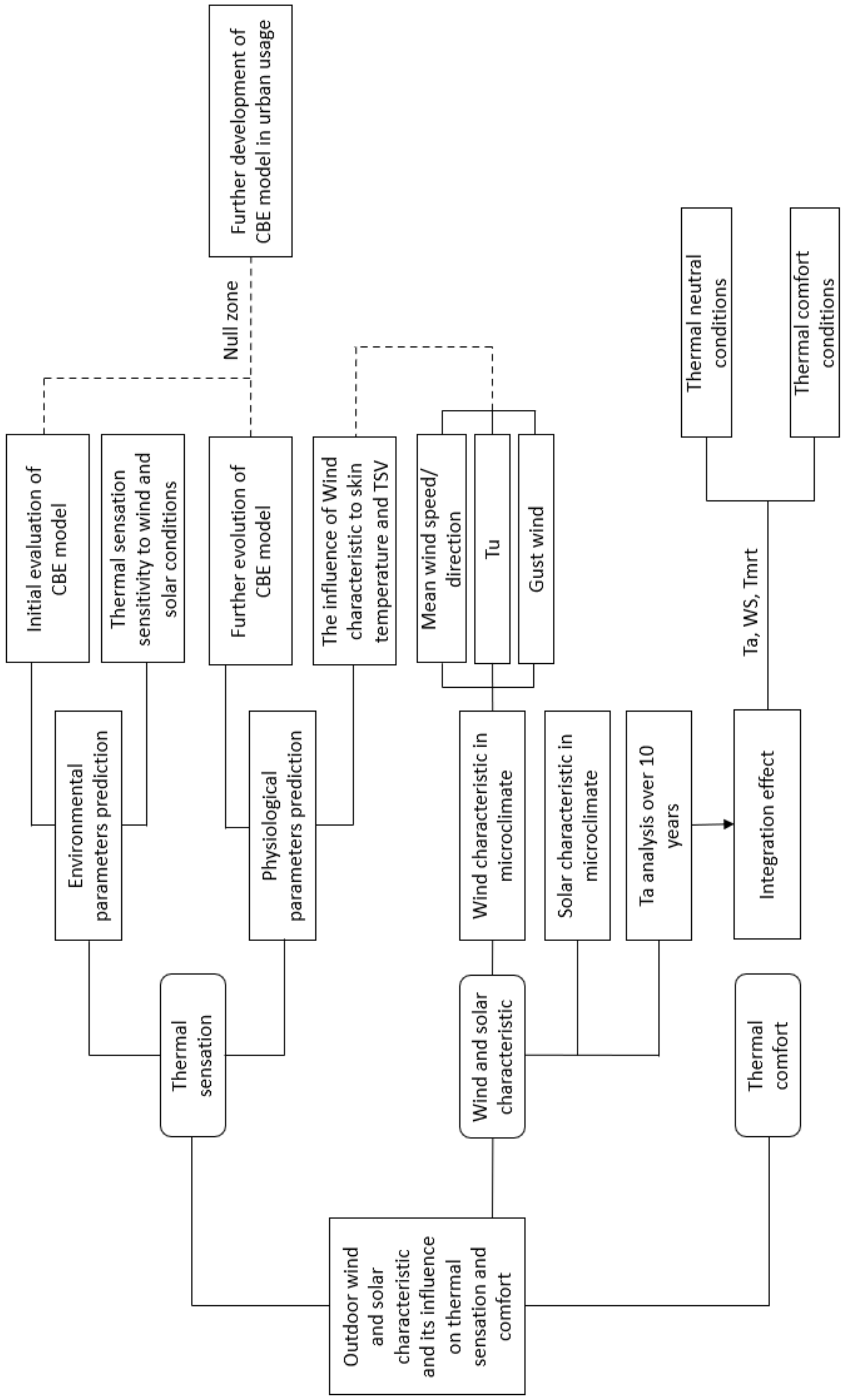


Figure 1.1 The outline of this study

# Chapter 2 Literature review

## 2.1 Outdoor thermal comfort studies in recent years

### 2.1.1 Brief introduction of the research area

In order to give a brief idea of the studies related to “outdoor thermal comfort”, the author did a search in the Web of Science using the key word of “outdoor thermal comfort”. The listed results show the increasing interest of this field, with the number of published articles from the record of two publications in the year of 2000 to 327 publications in the year of 2018. Table 1 shows the most citied articles in the field of outdoor thermal comfort, within which, one of them is the evaluation of thermal index (Jendritzky et al., 2012); nine of them focus on the strategies of the improvement of urban thermal environment, such as greenery (Lee et al., 2016; T.-P. Lin et al., 2010; Ng et al., 2012; Norton et al., 2015; Skelhorn et al., 2014) and rearranging urban geometry (Ali-Toudert, & Mayer, 2006; E. L. Krüger et al., 2011; Taleghani et al., 2015; Y. Wang et al., 2016); four of them focus on on-site measurement (Harlan et al., 2006; D. Lai, D. Guo, et al., 2014; T.-P. Lin, 2009; Spagnolo, & de Dear, 2003) and one of them uses CFD to simulate wind environment in the urban setting (Ramponi, & Blocken, 2012). Almost half of them mentioned the urban heat island effect (UHI) (Harlan et al., 2006; Lee et al., 2016; Ng et al., 2012; Norton et al., 2015; Skelhorn et al., 2014; Taleghani et al., 2015; Y.

Wang et al., 2016) and offered solutions trying to solve such problem.

Table 1.1 The most citied articles in the field of outdoor thermal comfort

| Authors | Title | No. of citations | Year of publication | Area |
|---|---|---|---|---|
| Sharon L. Harlan, Anthony J. Brazel, Lela Prashad, William L. Stefanov, Larissa Larsen | Neighborhood microclimates and vulnerability to heat stress | 402 | 2006 | Onsite measurement |
| Fazia Ali-Toudert, Helmut Mayer | Numerical study on the effects of aspect ratio and orientation of an urban street canyon on outdoor thermal comfort in hot and dry climate | 324 | 2006 | Urban geometry |
| Jennifer Spagnolo, Richard de Dear | A field study of thermal comfort in outdoor and semi-outdoor environments in subtropical Sydney Australia | 301 | 2003 | Onsite measurement |
| Edward Ng, Liang Chen, Yingna Wang, Chao Yuan | A study on the cooling effects of greening in a high-density city: An experience from Hong Kong | 253 | 2012 | Greenery |
| Tzu-Ping Lin | Thermal perception, adaptation and attendance in a public square in hot and humid regions | 249 | 2009 | Onsite measurement |
| Gerd Jendritzky, Richard de Dear, George Havenith | UTCI-Why another thermal index? | 241 | 2012 | Evaluation of model |
| Tzu-Ping Lin, Andreas Matzarakis, Ruey-Lung Hwang | Shading effect on long-term outdoor thermal comfort | 226 | 2010 | Onsite measurement |
| R. Ramponi, B. Blocken | CFD simulation of cross-ventilation for a generic isolated building: Impact of computational parameters | 213 | 2012 | CFD |
| Briony A. Norton, Andrew M. Coutts, Stephen J. Livesley, Richard | Planning for cooler cities: A framework to prioritise green infrastructure to mitigate high temperatures in urban landscapes | 196 | 2015 | Greenery |

| | | | | |
|---|---|---|---|---|
| J. Harris, Annie M. Hunter, Nicholas S.G. Williams | | | | |
| E.L. Krüger, F.O. Minella, F. Rasia | Impact of urban geometry on outdoor thermal comfort and air quality from field measurements in Curitiba, Brazil | 149 | 2011 | Urban geometry |
| Mohammad Taleghani, Laura Kleerekoper, Martin Tenpierik, Andy van den Dobbelsteen | Outdoor thermal comfort within five different urban forms in the Netherlands | 139 | 2015 | Onsite measurement |
| Dayi Lai, Deheng Guo, Yuefei Hou, Chenyi Lin, Qingyan Chen | Studies of outdoor thermal comfort in northern China | 102 | 2014 | Onsite measurement |
| Hyunjung, Helmut Mayer, Liang Chen | Contribution of trees and grasslands to the mitigation of human heat stress in a residential district of Freiburg, Southwest Germany | 99 | 2016 | Greenery |
| Yupeng Wang, Umberto Berardi, Hashem Akbari | Comparing the effects of urban heat island mitigation strategies for Toronto, Canada | 89 | 2016 | Greenery |
| Cynthia Skelhorn, Sarah Lindley, Geoff Levermore | The impact of vegetation types on air and surface temperatures in a temperate city: A fine scale assessment in Manchester, UK | 84 | 2014 | Greenery |

### 2.1.2 Methods for the outdoor thermal environment evaluation

For the evaluation of outdoor thermal environment, the precise knowledge about the microclimate conditions is preferred. Unlike the indoor environment, the outdoor thermal environment is well known as highly transient and asymmetric. The earlier studies for the onsite measurement only provided rough values such as the hourly value, which is not able to catch the instant characteristics of the climate data (C. S. C. Cheung, & M. A. Hart, 2014; Dimoudi et al., 2013; Tseliou et al., 2010). These kinds of measurement data could be used to discover the long-term effect on thermal perception but could not distinguish the transient characteristics of the outdoor thermal environment. Later in recent years, more studies concerned about the instant properties of the thermal environment (Lai et al., 2017a; Niu et al., 2015). The wind characteristics were clearer in the data collected in a higher frequency.

The shortcoming of onsite measurement of outdoor thermal environment is that it can merely provide point measurement results, a detailed cognition of the thermal environment can only be obtained with the help of simulation tools. CFD simulation and wind tunnel can help to provide a more comprehensive idea of the wind environment (Du et al., 2018; Liu, & Niu, 2016; Liu et al., 2017; Toparlar et al., 2015) while ENVI-Met is able to provide the simulation results including the thermal effect of solar radiation (Ali-Toudert, & Mayer, 2006). These simulation tools are widely used combining with the existing thermal comfort indexes or models to predict or evaluate a given outdoor thermal environment (Du, Mak, Huang, et al., 2017; Liu et al., 2016).

With the help of computers and the well-developed turbulence models, the characteristic of outdoor thermal environment can be described using simulation;

however, the field survey from local residents and actual users in the given outdoor space is still the most reliable way to know how human interact with the thermal environment. It is usually very time-consuming to have a comprehensive idea of the thermal perception of users to a specific outdoor space covering different time of a year. Usually, to ensure the accuracy of the study, a continuous on-site measurement covering a year span or targeted at specific seasons with the survey response of a large number of people is needed. Spangnolo and de Dear (2003) validated the thermal environment for outdoor and semi-outdoor in subtropical Sydney through 1018 subjects and found the thermal neutrality described using the OUT_SET* index was 26.2 ℃. Lin (2009) conducted an on-site measurement in the square of Taiwan, where he counted the number of people visiting the square and collected 505 survey response in total to observe people's adaptation pattern throughout a whole year and found that people's preferred temperature in different seasons varied, which were 23 ℃ for the cool season and 24.5 for the warm season. Lam and Lau (2018) studied the long-term acclimatization effect by comparing the local citizens' thermal perception in two cities: Melbourne and Hong Kong by collecting a large amount of samples (over 2000 samples in Melbourne and over 400 in Hong Kong) and found Hong Kong residents show stronger thermal resistance to hot weather. The field measurement and survey can also cope with the dynamic problem and help to figure out the change of thermal sensation when moving between different microclimate environments and its causes, such as thermal adaptation, thermal imbalance, transient change of physiological parameters and even psychological issues. Lau et al. (2019) considered the dynamic thermal comfort for the pedestrians walking in different urban geometries and found that thermal sensation was associated with the participants' short-term thermal memory. To conclude, onsite measurement and survey response from the actual users are important for understanding how human interact with the outdoor thermal environment and provide guidance for further improvement. The relation between human and the outdoor environment is so complex that the existing thermal comfort prediction models can hardly provide accurate description covering most of the possible causes for the thermal comfort feelings.

### 2.1.3 Strategies for improving the outdoor thermal conditions

The aim of outdoor thermal comfort studies is to make the outdoor thermal environment more comfortable and encourage the usage of outdoor environment. Therefore, studies related to the strategies of improving the outdoor thermal environment has emerged in the last decades. The common strategies discussed in the studies are rearranging the building clusters, changing building structures, providing greening and shading and creating water bodies. The effect of the listed strategies on thermal environment will be discussed separately.

#### 2.1.3.1 Rearranging building clusters

The placement of the building clusters has influence on the wind environment and solar access. The placement of building clusters, the site coverage and the building stories effect the street orientation along with the H/W ratio (aspect ratio) of street canyon determines the urban morphology (Wei et al., 2016). Its influence on thermal comfort should be discussed with the local microclimate characteristics such as the climatic region, the geographical position, the prevailing wind direction, the dominating wind speed, humidity conditions, and the irradiance intensity. The thermal preference of local residents should also be listed in the consideration factors. The regions and cities having the problems related to heat stress are the main research target.

The target of the studies in the hot-humid area is to improve pedestrian wind environment and provide shading to alleviate hot discomfort. The tropical coastal cities in hot-humid regions can take advantage of the wind environment to improve thermal comfort conditions, such as cities located in southern China (Y. Zhang et al., 2017), Dares Sallam in Tanzania (Ndetto, & Matzarakis, 2013) and Netherlands (Taleghani et al., 2015). The streets oriented north-south (N-S) in such cities were found to be able to provide higher wind speed in the pedestrian level.

The studies in the hot-arid climate concern more about the solar orientation. Ali-

Toudert and Mayer (2006) compared the urban canyons with various H/W ratios and different solar orientations when hot stress occur and found solar radiation was the most decisive parameter. Heat stress in wide streets was the most difficult to mitigate and a N-S orientation combined with a H/W ratio greater than or equal to 2 provided a much better thermal environment compared with the other conditions (Ali-Toudert, & Mayer, 2006). However, wide streets were more comfortable as solar access was possible (Johansson, 2006). The effect of shading devices through overhanging faces was also investigated by their team and its contribution to mitigating hot discomfort was significant (Ali-Toudert, & Mayer, 2007). Pearlmutter et al. (2006) studied the energy exchange in the urban environment by an example of arid Negev Highlands of southern Israel and found that the coherent urban design in hot-arid regions had the ability to reduce the daytime heat burden and can provide microclimate benefits. Narrow streets seem to be preferred in the hot regions.

Building built in high density and narrow streets are also preferred in cold region like Gothenburg, Sweden because the densely built structure is capable for mitigating extreme values in $T_{mrt}$ (mean radiant temperature) through the whole year (Thorsson et al., 2011).

Studies related to temperate climate were limited, mainly due to the reason that it is originally thermal comfort. Still, some researchers concerned about the increasing air temperature in the future and studied the thermal conditions of different urban forms including singular, linear and courtyard. Courtyard showed best comfort situation for providing a more protected microclimate with less solar radiation in summer (Taleghani et al., 2015).

#### 2.1.3.2 Changing building structures

Building structure also play an important role in influencing the thermal environment in the pedestrian level.

The buildings with hanging balcony which are broadly used in the southern China, can provide shading to the pedestrian walkway and have impact on the openness of sky. Lau et al. (2019) simulated the daily walking activity in Hong Kong, human subjects were asked to follow two different routes which covered different building types. Their results show that openness of sky was the dominant factor influencing pedestrians' thermal comfort: moving from sunlit to the shaded spots were found to be more comfortable (Lau et al., 2019).

Our research team focused on the relation between the building structures and wind environment, we successfully proved that the buildings with elevated structures ('lift-up' design) can help improving weak wind condition in pedestrian-level for the coastal cities like Hong Kong (Liu, Zhang, et al., 2019). Such kind of design allows wind to penetrate through buildings and provide shading in the open area underneath the building (Liu, Zhang, et al., 2019). The amplification effect on wind environment by the elevated design was first discussed focusing on a single building. It was first quantified by the wind velocity simulation results of CFD combined with the measured thermal parameters (Liu et al., 2016). Both wind comfort and thermal comfort conditions underneath the elevated building and in the limited surrounding area were proved to be improved by the elevated design (Liu et al., 2016). This design was further examined in a more complex context by discussing different H/W ratios (aspect ratios) (X. Zhang, K. T. Tse, et al., 2017) and other key design parameters of a single building (X. Zhang et al., 2018a). The H/W ratio from 4:1 to 0.5:1 was examined in the boundary level wind tunnel (X. Zhang, K. T. Tse, et al., 2017). A building with H/W ratio between 0.33 and 1.25 were proved to have better performance in improving pedestrian wind comfort (X. Zhang, K. T. Tse, et al., 2017). Building height showed a significant influence on the maximum wind speed in the lift-up area while the width of the central core limits the low wind speed area (X. Zhang et al., 2018a). The effects of the elevated design in four building structures (“-”, “L”, “U” and “□”) was investigated by Du et al. (2017) using CFD and they found that the elevated design can improve the wind comfort condition in pedestrian level in the building surroundings. Later, they combined the wind tunnel tests and the on-site monitoring results to calculate PET (physiologically equivalent temperature) values and proved that the elevated design can provide a comfortable microclimate in summer and at the mean time not causing much cold stress in winter (X. Zhang, K. T. Tse, et al., 2017). The influence of surrounding buildings on the pedestrian level wind around an elevated building was studied using the LES (large eddy simulation) approach in CFD by Liu et al.(2019). The amplification effect was found in the open area underneath the elevated building and also its surrounding area (Liu, Zhang, et al., 2019).

The wind environment underneath the elevated building was clearer from these studies. Solid evidence was provided for the amplification effect on wind environment and the improvement of wind comfort related to the elevated design. However, the general idea of outdoor thermal comfort benefitting from such kind of design was roughly discussed by generating a PET map (Du, Mak, Huang, et al., 2017), specific field survey or response from the actual users were not being provided.

**2.1.3.3 Greening and shading**

Urban vegetation is a mainstream technology to mitigate the urban heat island effect through evapotranspiration, shading and providing cooler surfaces to reduce mean radiant temperature (Osmond, & Sharifi, 2017).

Among the types of vegetation patterns, trees are proved to have the best effect on improving thermal comfort but its negative effect on decreasing wind velocity should also be considered (B. Lin et al., 2008). Sun et al. (2017) used ENVI-Met to simulate the thermal condition of the urban green spaces located in the city and found tall trees are the most significant influential factor on improving thermal comfort condition. Statistically, air temperature in the tree canopy is about 1 ℃ lower than the sunlit area (Klemm et al., 2015; Yoshida et al., 2015) while radiant temperature in the urban parks is about 2-4 ℃ lower than the adjacent unvegetated areas (Osmond, & Sharifi, 2017). The morphological properties of trees effect the solar attenuation capacity and might block the wind passage to a certain extent. Studies by Kong et al. (2017a) found the most efficient tree types in reducing mean radiant temperature was with a large crown, short trunk and dense canopy. Morakinyo et al. (2017) studied eight common types of trees planted in the city to study the main parameters affecting thermal comfort. Leaf area index, tree height and trunk height are the most influential ones among the other parameters. They suggested tall trees of low canopy density with high trunk should be planted in deeper canyons and vice-versa. Except from the tree types, the location of planting also have influence on thermal comfort level. Research shows that trees planted in the high density setting are more effective than those planted in the open spaces in improving pedestrians' thermal comfort (Kong et al., 2017a).

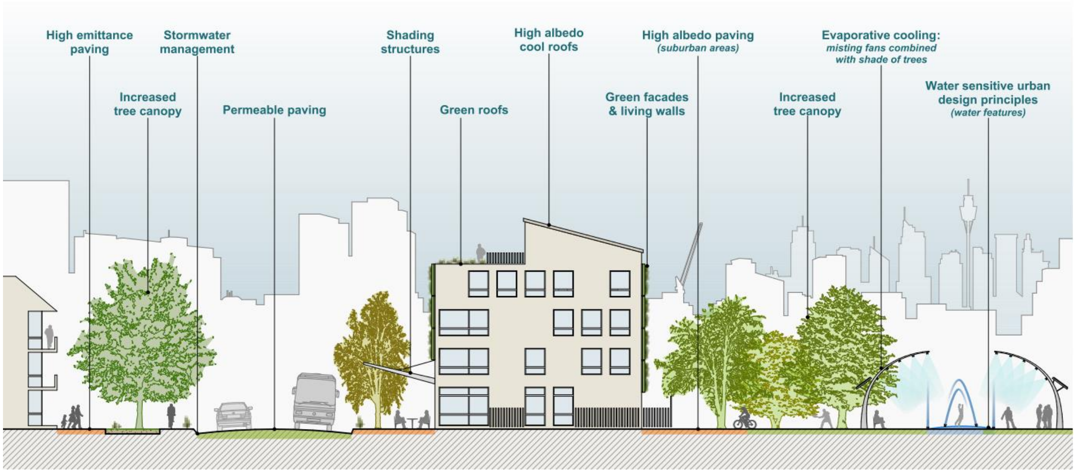


Figure 2.1 cooling strategies during summer (Osmond, & Sharifi, 2017)

#### 2.1.3.4 Water surfaces

Water bodies or water surfaces in the urban area are usually described as a permanent or temporary collection of water in the form of small stationary water or pond (Syafii et al., 2016). Water surfaces are friendly to urban microclimate design because air temperature and humidity could remain at a comfortable level through evaporation of ponds. Water surfaces also have low solar reflectance which is able to absorb solar radiation. Based on the listed characteristics, water surfaces or water body have a positive impact on the cities in hot summer times. The existing research has provided solid proof of the benefits of water surfaces or water bodies to the hot summer. Syafii et al. (2016) simulated the urban condition using an outdoor-scaled model consists of an array of 1.5m concrete cubes, trying to isolate the pond to study its cooling effect and found up to 2.6 ℃ of air temperature decrease during the hottest time of the day and 0.7 ℃ drop during the coolest time of the day. More studies were conducted in the real urban settings. Saaroni and Ziv (2003) found lakes have the capacity of decreasing air temperature by 1.6 ℃ and increasing relative humidity by 6% during the days with moderate heat stress, they defined it as "lake effect". Sun et al. (2012) tried to quantify the cooling island intensity of water bodies, they found four landscape descriptors have significant impact to microclimate surrounding the water bodies, including water body's area, geometry, location and the surrounding built-up proportions. Interestingly, they found the flowing water bodies such as rivers can further reduce the air temperature than stagnant water surface such as lakes (air temperature difference of 3.15 ℃ and 1.5 ℃) (R. Sun et al., 2012). The benefits of water bodies were not merely limited to its cooling effect. It also brings in ornamental pleasure. Chan et al. (2017) found water ponds in the park which was visible for the park visitors can improve their thermal acceptability in summer but not in winter.

## 2.2 The mainstream thermal comfort indexes and models applied in the outdoors

This chapter will focus on introducing the mainstream thermal comfort indexes and models which researchers applied to the outdoor environment. The examples and cases of their applications will be first introduced, followed by the principles of the models and considerations when dealing with thermal sensation and comfort prediction in the outdoor environment.

It is widely known that six variables affect outdoor thermal sensation, including four meteorological variables (solar radiation, wind, ambient air temperature, and humidity) and two personal variables (activity level and clothing value) (E. Arens, & Bosselmann, 1989). Many thermal indices addressing these six variables have been developed to evaluate and predict thermal sensation and thermal comfort, such as PET (physiologically equivalent temperature) (Höppe, 1999), SET* (standard effective temperature) (ASHRAE Standard Committee, 2013), SPMV (standard predicted mean vote) (Höppe, 2002), UTCI (the Universal Thermal Climate Index) (Fiala et al., 2012) and the CBE model (a multi-node human body thermal regulation model developed by the University of California-Berkeley) (H. Zhang et al., 2010c) etc. Several companies and research institutes have used these thermal comfort indices when designing and assessing urban environments. Swire Properties (Yau et al., 2017) used the SPMV method to predict pedestrian thermal comfort levels for the Brickell City Centre project located in Miami. Distribution maps of SPMV were produced to evaluate the improvement of thermal sensation level after an innovative outdoor corridor design. Murakami et al. (1999) combined the CFD simulation results with a radiation simulation of a Tokyo city block to produce a spatial distribution map of SET* values. Middel et al. (2017) increased the prediction accuracy of solar radiation spatial distribution by generating synthetic hemispherical fisheye views from Google Earth. A distribution map of PET based on the solar radiation prediction results was generated, hoping to increase the prediction accuracy of outdoor thermal comfort level (Middel et al., 2017). Liu et al. (2016) reported a simplified method combining with the measured thermal parameters and the simulated wind velocity by CFD to predict thermal comfort in pedestrian level around an underneath-elevated building. Wind tunnel test results were also adopted in developing a thermal comfort map based on the PET index (Du, Mak, Huang, et al., 2017). In general, there is a strong expectation of having a tool to accurately predict spatial outdoor thermal sensation and comfort when designing a sustainable community. But whether the existing thermal indices can accurately predict thermal sensation and comfort in an outdoor urban environment remains unknown and further assessment is needed.

These thermal indices were mainly developed by three approaches. The most direct and simple way is to build up a linear correlation between thermal sensation vote and a combination of meteorological parameters (solar radiation, wind speed, air temperature, and humidity) (Lai et al., 2017b). This method is the most straightforward one to determine the relationship between thermal sensation and meteorological parameters. However, it is region-specific. The linear correlation result can only be applied to a limited region and a group of subjects. Applying these results to build up models for the regions with climate condition differ from that of the experimental location should be revised with correlation factors (T. P. Lin, & Matzarakis, 2008). In the outdoors, the asymmetric distribution of solar radiation and transient wind environment form different microclimates, which make the linear regression results more difficult to be applied. Moreover, the accuracy of a linear relation largely depends on the number of subjects and the variety of test conditions.

The second approach is based on energy budget models, such as the PMV (predicted mean vote) index (Höppe, 2002). The heat flux exchange between a human body and the ambient environment is the main concern of this approach. Existing thermal indices of this kind were all developed under steady thermal conditions, where subjects were assumed to reach thermally equivalent status (Höppe, 2002). The thermal indices developed based on this assumption might not be suitable for the outdoors. Human bodies might be exposed to very different thermal conditions, such as simply walking from an air-conditioned indoor space (comfortably neutral condition) to an extreme outdoor environment (cold winter or hot summer). A thermally stable condition is practically impossible to be reached for this instance (Höppe, 2002), which makes the existing thermal indices developed from the energy balance models inappropriate for outdoor environments.

The third approach relates to thermo-physiological aspects (Höppe, 2002; Lai et al., 2017b) such as SET* (ASHRAE Standard Committee, 2013), OUT-SET* (Pickup, & de Dear, 2000), PET (Höppe, 1999), the UTCI (Fiala et al., 2012), and the CBE model (H. Zhang et al., 2010c). This approach focus on the stimulation of the thermal receptors located in the skin and the core, which perceive different levels of cold and warmth, then send signals to the brain (Craig, 2003; Hall, 2011). The main development of this approach in these years maintains at improving its details. The primitive ones were all based on the two-node model (the core node and the skin node), for instance, SET* (ASHRAE Standard Committee, 2013; A. Gagge, 1973; Xi et al., 2012), OUT-SET* (Pickup, & de Dear, 2000) and PET (Höppe, 1999). Simply treating the human body as a two-node model often creates prediction errors when the thermal conditions are asymmetric and unstable. Xi et al. (2012) discovered that the neutral SET* varied when tested near different building blocks in the outdoors. Huang et al. (2017) found different linear regression relations between PET and surveyed MTSV (mean thermal sensation vote) existed in different microclimates within one campus area. Human bodies are divided into more specific compartments in the UTCI compared to the early-stage thermal indices. In total, 12 compartments and 187 nodes are consisted in the UTCI model. It was expected to be available to solve the asymmetry problem by considering the heat transfer function separately for different body tissues and segments. Though this model has considered the rate of change of $T_{skin}$ and $T_{core}$ to cover transient conditions, its experimental validations was obtained at thermal uniform conditions (Fiala et al., 2001). Recently, some researchers attempted to verify its application in the outdoors: some focused on the operating parameters (Weihs et al., 2012) and some on the result comparisons (D. Lai, D. Guo, et al., 2014). From the results of Weihs et al. (2012), asymmetric solar radiation condition could lead to misprediction in the UTCI model. When solar elevation was low, an error up to 2K appeared (Weihs et al., 2012). Acclimatization effects could also cause prediction difference in the outdoor usage of the UTCI model (Eduardo L Krüger et al., 2017). Longer exposure (minimum 30 minutes) could reduce prediction errors (Eduardo L Krüger et al., 2017), which suggested that the UCTI model might perform better when thermal balance was established. Lai et al. (2014) found substantial differences in the UTCI prediction results when comparing the climates in northern China and the Mediterranean (Salata et al., 2016). UTCI is able to give better prediction results than its older counterparts, but its application in the outdoors still needs further validation and amendment (Blazejczyk et al., 2012). Whether it is the best choice for outdoor thermal condition prediction remains controversy.

## 2.3 The Principles and development of the thermal indexes and models

### 2.3.1 PET (physiological equivalent temperature)

#### 2.3.1.1 Principles of PET

The physiological equivalent temperature was based on the Munich Energy-balance Model for Individuals (MEMI) (Höppe, 1999). PET was defined as the air temperature (no extra air movement and radiation) at which the heat budget of a human body was balanced with the same core and skin temperature as under the concerned complex thermal conditions (Höppe, 1999). PET was orientated to be an easily understandable method to assess the thermal environment.

The MEMI was based on the heat balance equation for human body (Equation 2.1) (ASHRAE Standard Committee, 2017a) and some of the parameters of the Gagge two-node model:

$$M + W + R + C + E_D + E_{Re} + E_{Sw} + S = 0 \qquad \text{Equation (2.1)}$$

where:

M: rate of metabolic heat production, $W/m^2$;

W: rate of mechanical work accomplished, $W/m^2$;

C+R: sensible heat loss from skin, $W/m^2$;

$E_D$: total rate of evaporative heat loss from skin, $W/m^2$;

$E_{Re}$: rate of evaporative heat loss from respiration, $W/m^2$;

$E_{Sw}$: rate of evaporative heat loss from sweating, $W/m^2$;

$S$: rate of heat storage, W/m$^2$.

To solve Equation 2.1, three unknown parameters have to be calculated: the mean temperature of the clothing ($T_{cl}$), the mean skin temperature ($T_{sk}$), and the core temperature ($T_c$). These three parameters were solved based on the listed two equations (Equation 2.2 and 2.3).

$$F_{CS} = \nu_b \times \rho_b \times c_b \times (T_c - T_{sk})) \qquad \text{Equation (2.2)}$$

$F_{CS}$: heat flows from body core to skin surface, W/m$^2$;

$\nu_b$: the blood flow from body core to skin, $l/s \cdot m^2$;

$\rho_b$: blood density, kg/l;

$c_b$: specific heat, $W \cdot s/K \cdot kg$;

$T_c$: core temperature, ℃;

$T_{sk}$: skin temperature, ℃.

$$F_{SC} = (1/I_{cl}) \times (T_{sk} - T_{cl}) \qquad \text{Equation (2.3)}$$

$F_{SC}$: heat flows from skin surface to the clothing, W/m$^2$;

$I_{cl}$: the heat resistance of the clothing, $Km^2/kg$;

$T_{sk}$: skin temperature, ℃;

$T_{cl}$: clothing temperature, ℃.

Equation 2.1 to 2.3 show heat flow between the environment and human body for each individual, and it is directly affected by the following meteorological parameters: air temperature ($T_a$), humidity (RH), velocity($\nu$) and mean radiant temperature ($T_{mrt}$). The main difference between PET and MEMI was that the PET limited the equivalent thermal environment to a specific level to assume an indoor reference condition. Within the reference thermal environment, three parameters were limited: $\nu$ =0.1 m/s, VP=12 hPa and $T_{mrt} = T_a$ (Mayer, & Hoppe, 1987). By limiting these parameters, the calculated $T_a$ represented the same thermal state as in the complex outdoor conditions and it is referred to the PET value.

The limitation of such model is that it simply considers human as a two-node model: core and skin, and assuming that the skin temperature distributes evenly for different body parts, which is far different from the real condition. Moreover, it assumed human body reaching its steady status in the given thermal condition and the physiological parameters in human body remain unchanged. Such limitations make it more suitable for the stable thermal environment instead of the transient changing thermal environment.

#### 2.3.1.2 The application of the PET in the outdoor conditions

PET was preferable to the other thermal indexes because of its unit (℃) which maked it more understandable. The PET results could also be presented in the bioclimatic map with the help of computing software. Therefore, PET was widely applied to the outdoor conditions, mostly when assessing the overall thermal environment and evaluating the strategies for the improvement of thermal environment. Matzarakis et al. (1999) showed the examples of applying PET to evaluate the thermal environment of different climate conditions. Gulyás et al. (2006) conducted the human-biometeorological assessment using PET for different urban conditions in the city of Szeged, a South-Hungarian city. PET index was used to discuss the contribution of different street designs on thermal comfort in several studies (Ali-Toudert, & Mayer, 2006; Johansson, 2006). Some studies visualized the PET value in a microclimate region to evaluate the thermal conditions of different designs. Bouyer et al. generated a map of bioclimate based on the PET index for stadium of different shapes and compared the influence of structure to thermal comfort conditions. Du et al. (2017) assessed the improvement of thermal comfort conditions by the ‘lift-up’ design using the map showing PET levels. Niu et al. (2015) developed a new index called the thermally-perceivable environment parameter difference based on PET (physiological equivalent temperature) to evaluate the simultaneous differences of microclimate parameters. The listed studies have one common point of the attempt of using the PET index to show the relative difference in thermal conditions of different building structures or arrangement designs. It is undoubtable that PET is able to reflect the relative change of thermal conditions generated by the difference of $T_a$, $T_{mrt}$ and $v$ if leaving aside the accuracy, but all the studies are based on the assumption that the considered thermal parameters remain unchanged during the experiment period or only a certain point of time is considered.

In recent years, some studies focus on comparing PET with other indexes and investigate its accuracy for the application in the outdoor context. Tseliou et al. (2010) compared different thermal indexes (including PET, the temperature-humidity index and the wind chill index) to the surveyed five-scale thermal sensation in seven European cities and found each thermal index showed a strong correlation with the climatic mean temperature and therefore misclassification of the thermal sensation. Fang et al. (2018) obtained the neutral PET and UTCI temperatures from the filed survey conducted in Guangzhou were 21.9 and 23.2 ℃ respectively for the metabolic rate under 2.0 met. Huang et al. (2017) compared the PET index with the UTCI index and the CBE model through large amount of field survey from different outdoor settings and found that all three thermal indexes showed different levels of inaccuracies when changed to different outdoor settings.

### 2.3.2 SET* (Standard effective temperature)

#### 2.3.2.1 Principles of SET*

SET* was developed based on ET* (effective temperature), which combined temperature and humidity into a single index. Two environments having the same ET* and same air velocities were assumed to evoke the same thermal sensation though they might have different air temperatures and humidities (ASHRAE Standard Committee, 2017a). The definition now widely accepted was developed by Gagge et al. (1971; 1941), which was the temperature of an environment at 50% RH that resulted in the same total heat loss from the skin as in the actual environment. The definition of ET* was based on the two-node model. ET* has $t_0$ and vapor pressor in its equation, and thus combining $T_{mrt}$, $T_a$, $v$ and vapor pressor. Vapor pressor depended on skin wettedness and clothing moisture permeability and thus ET* at $T_a$ and RH depends on a person's actual activity and clothing (ASHRAE Standard Committee, 2017a). A standard set of conditions which were representative of a typical indoor environment at 50% RH was used to define a standard effective temperature (SET*) to generate a universal ET* chart (ASHRAE Standard Committee, 2017a). SET* was an equivalent air temperature of an isothermal environment when $T_{mrt} = T_a$, RH=50% and $v = 0.15\ m/s$, in which a person wearing standardized clothing and activity level experienced the same heat stress and thus having the same skin wittedness (ASHRAE Standard Committee, 2017a).

$$ET^{*} = T_{op} + wi_m LR(p_a - 0.5p_{ET*,S}) \qquad \text{Equation (2.4)}$$

$p_a$: the vapor pressure at a point of air temperature, kPa;

$p_{ET*,S}$: the saturated vapor pressure at ET*, kPa;

$T_{op}$: the operative temperature;

$w$: skin wettedness, dimensionless;

$i_m$: total vapor permeation efficiency; the ratio of actual evaporative heat flow capability between skin and environment sensible heat flow capability as compared to Lewis ratio;

LR: the Lewis ratio at typical indoor conditions, equals approximately 16,5 K/kPa;

$LR = h_e/h_c$ Equation (2.5)

LR: the Lewis ratio at typical indoor conditions, equals approximately 16,5 K/kPa;

$h_e, h_c$: the evaporative heat transfer coefficient and convective heat transfer coefficient, W/(m2·kPa).

#### 2.3.2.2 The application of the SET* in the outdoor conditions

Lin et al. (2011) used the SET* to represent the comprehensive effect of the outdoor thermal environment and studied the adaptive behavior in central Taiwan. Their results demonstrate that people’s thermal perceptions were strongly related to solar radiation and air temperature but was not significantly related to air speed and humidity. Lin et al. (2008) used SET* to compare the difference of pedestrian thermal comfort by different vegetation patterns on the pedestrian level, they found that trees were better than the other vegetation types if considered the average SET* around the pedestrian space. Later, they exanimated a more complex condition by considering the arrangement of trees and building layout by SET* (Hong, & Lin, 2015). They found the configurations that contained a square central space surrounded by buildings which oriented toward the prevailing wind direction could offer better thermal environment (Hong, & Lin, 2015). Xi (2012) used SET* to investigate the improvement brought by the building design with pilotis. One concern about applying SET* to the outdoor condition was that the original SET* index assumed $T_{mrt} = T_a$ which made it could merely be applicable to the indoor thermal environment where the radiation level could be ignored. To solve this problem, Pickup and de Dear (2000) developed an OUT_SET* to include the mean radiant temperature into consideration.

### 2.3.3 UTCI

#### 2.3.3.1 Principles

In the past forty years, the simple two-node thermal regulation model (only consider the core and skin) have evolved into more complex multi-nodal models, such as the Stolwijk model (J. A. Stolwijk, 1971), the Wissler model (Wissler, 1985) and the Tanabe 65-node model (Tanabe et al., 2002) and the Huizenga model (Huizenga et al., 2001). These kinds of multi-segment models took into account of the actual human body structure, physiological properties of human body segments and also the response from central nervous system. The results from the models included the physiological response and also the thermal response as a side product. The development of multi-nodal thermal regulation model provided the technical support and knowledge for the development of the UTCI model. The UTCI model was a numerical model which linked the thermo physiological properties and thermal sensation response together (Fiala et al., 2010). It was developed to be applied in a wide range of thermal conditions, such as steady and transient conditions (Fiala et al., 2010).

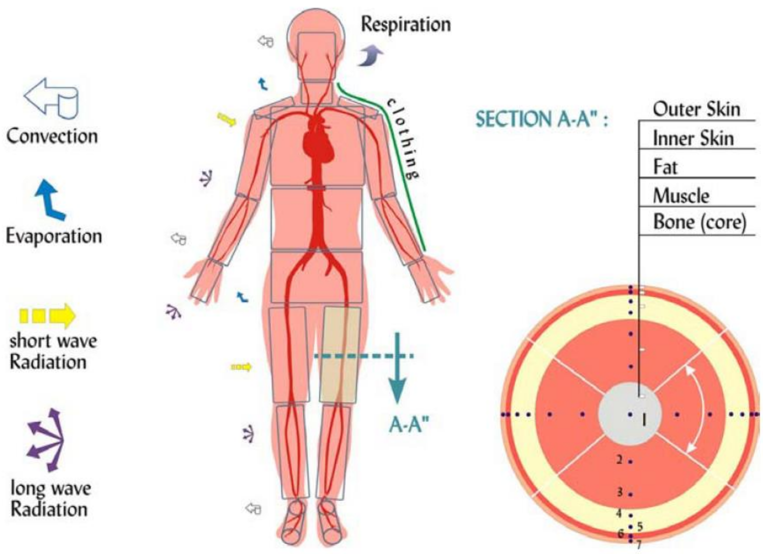


Figure 2.2 The passive system of Fiala model (Fiala et al., 2010)

The UTCI model included two systems: the passive system and the active system. Figure 2.2 shows the layers of human body. The human body was divided into 20 spherical and cylindrical elements. Each element was built of annular concentric tissue layers which consist of bone, muscle, fat, inner skin and outer skin (Fiala et al., 2010). The inner skin was the blood perfused region where generated metabolic heat while the outer skin was where the sweat glands locate and it was responsible for skin evaporation (Weinbaum et al., 1984). The metabolic heat was distributed to all the body parts through blood circulation. The Pennes's Bio-Heat Transfer Equation (shown as Equation 2.6 here) for polar and spherical coordinates are used for the heat transfer within each node in the UTCI model and also the heat exchange between adjacent nodes were realized through hybrid matrix solution techniques (Fiala, 1998). As the heat transfer process for each local body part was considered separately, it was assumed that the cases of human body in the asymmetric thermal environment or the thermal difference created by the clothed and unclothed part could now be considered.

$$\rho c \frac{dT}{dt} = k\left(\frac{d^2T}{dr^2} + \frac{g}{r}\frac{dT}{dr}\right) + q_m + \rho_{bl}\omega_{bl}c_{bl}(T_{bla} - T)$$ Equation (2.6)

$\rho$: the tissue density, $kg/m^3$;

$c$: heat capacitance, $J/kg \cdot K$;

$k$: heat conductivity, $W/m \cdot K$;

$T$: tissue temperature, ℃;

t: time, s;

r: radius, m;

g: a geometry factor (equals to 1 and 2 for polar and spherical co-ordinates respectively);

$\rho_{bl}$: blood density, $kg/m^3$;

$\omega_{bl}$: blood perfusion rate, $m^3/s \cdot m^3$;

$c_{bl}$: heat capacitance of blood, $J/kg \cdot K$;

$T_{bla}$: arterial blood temperature, ℃.

The passive system focused on the heat transfer issues by passive blood flow, while the active system considered of the thermoregulatory responses of central nervous system due to the outside thermal effect, which were shivering, sweating vessel dilatation and vessel constriction (Fiala et al., 2010). The model was developed based on the word-wide research results covering a wide range of environmental temperature from 5-50 ℃ and metabolic rate from 0.8-10 met (Fiala et al., 2010). Regression analysis was employed to investigate the contribution level or significant level of the parameters. Skin temperature $T_{skin,m}$, head core temperature

$T_{hy}$ and rate of change of skin temperature $\Delta T_{skin,m}$ were included in the governing equation for thermoregulatory response (Fiala et al., 2010). DTS (dynamic thermal sensation) is developed in the UTCI model to relate physiological parameters with thermal sensation (Equation 2.7 and 2.8). Both the static $T_{skin,m}$ and the rate of change of $\Delta T_{skin,m}$ were considered in the DTS so it was assumed to be applicable to the transient thermal environment.

$$DTS = 3 \times \tanh\left(\frac{0.11\frac{dT^{-}_{skin,m}}{dt} + 1.91\frac{dT^{+}_{skin,m}}{dt_{max}}e^{-0.681t}}{1+G} + m\left(T_{skin,m} - 34.4\right) + G\right)$$

Equation (2.7)

m: 0.30/K for $T_{skin,m} < 34.4$ and 1.08/K for $T_{skin,m} > 34.4$;

$\frac{dT^{+}_{skin,m}}{dt_{max}}$: the maximum positive rate of change of skin temperature;

t: the time elapsed since the occurrence of $\frac{dT^{+}_{skin,m}}{dt_{max}}$;

$T_{skin,m}$: mean skin temperature, °C;

$$G = 7.94 \times \exp\left(\frac{-0.902}{T_{hy} - 36.6} + \frac{7.612}{T_{skin,m} - 38.4}\right) \quad \text{Equation (2.8)}$$

$T_{hy}$: head core temperature, °C.

The limitation of this model relied on the database it used, only the data from indoor chamber was included in the model development, making the application to the outdoor environment a question to ask.

#### 2.3.3.2 The application of the UTCI index in the outdoor conditions

Similar to PET and SET*, the UTCI model provided an equivalent temperature for fast lookup. Many researchers applied the equivalent temperature from the UTCI model to different climate regions. Thus, there are available datasets in different climate regions for comparison. The equivalent temperature of the UTCI model was quite similar to which in the SET* index, it defined a reference thermal environment within which $T_{mrt} = T_a$, RH=50% and air movement was limited (calm air) (Bröde et al., 2012). With the usage of equivalent temperature, it was clearer to discover the trend of change. Cheung and Hart (2014) did a prediction of the outdoor thermal condition in Hong Kong using the UTCI and found that there was a shift from ‘No thermal stress’ toward ‘Moderate heat stress’ and ‘Strong heat stress’ during the period of 2046-2065. However, when an index was used to compare the thermal conditions for different regions, the basic requirement was to give accurate descriptions.

Table 2.1 UTCI equivalent temperatures categorized in terms of thermal stress

(Bröde et al., 2012)

| UTCI range (°C) | Stress category |
|---|---|
| Above +46 | Extreme heat stress |
| +38 to +46 | Very strong heat stress |
| +32 to +38 | Strong heat stress |
| +26 to +32 | Moderate heat stress |
| +9 to +26 | No thermal stress[a] |
| +9 to 0 | Slight cold stress |
| 0 to −13 | Moderate cold stress |
| −13 to −27 | Strong cold stress |
| −27 to −40 | Very strong cold stress |
| Below −40 | Extreme cold stress |

Table 2.2 Neutral UTCI range and regression models of UTCI in different seasons

for different climates

| Year | Authors | Location | Climate | Neutral UTCI ranges, ℃ |
|---|---|---|---|---|
| 2012 | Bröde (2012) | Southern Brazil | Tropical | 18-23 |
| 2013, 2018 | Pantavou et al. (2018; 2013) | Athens | Mediterranean climate | 17.4- 24.5 |

| | | | | |
|---|---|---|---|---|
| 2014 | Lai et al. (2014) | TianJin | Sub-humid warm tempe rate monsoon climate | 12-25 |
| 2018 | Cheung and Jim (2018) | Hong Kong | Humid subtropical climate | 19.9-33.1 |
| 2018 | Xu et al. (2018) | Xi An | semi-humid continental monsoon climate | 14.9 – 23.2 |
| 2018, 2019 | Hadianpour et al. (2019; 2018) | Tehran | Cold semi-arid climate | 16.7-25 (Spring)<br>23.5-28.1(Summer)<br>17.7-25.4(Autumn)<br>14.2-20.1 (Winter) |

The UTCI equivalent temperatures are shown in Table 2.1. To compare the UTCI equivalent temperatures in a more specific way, the neutral equivalent temperature from studies in the recent years are listed in Table 2.2. It seems the neutral temperature varies a lot in different climate regions. Two passible reasons might lead to such phenomenon: one was the adaptation to local climates and the other one was that even the model built based on the world-wide database was not suitable to be simply applied in different regions. To answer this question, studies focus on the comparison of the UTCI equivalent temperatures and the actual field survey response should be applied. Some of the mentioned studies in Table 2.2 have done the liner regression between the UTCI equivalent temperature with the TSV values. The comparisons which were done targeting in different microclimates in similar experiment time were able to figure out whether the UTCI was able to give accurate descriptions. One of the studies listed in Table 2.2 have investigated the effect of wind direction on thermal sensation (Hadianpour et al., 2019). In their analysis focusing on windward and leeward directions, linear regression was done between the UTCI and the mean TSV. Significant sensitivity difference was found when describing TSV using UTCI in different wind directions, the slopes were 0.1089 and 0.1326 for windward and leeward respectively (Hadianpour et al., 2019). Although this study focused on the cooling effect from different wind directions, the finding can also reflect a fact that UTCI was not able to describe the cooling effect from different wind directions. Our previous study compared the UTCI values with surveyed TSV response in different microclimate conditions, including the open areas, the areas beneath an elevated building where covered weak wind condition and strong wind condition (Huang et al., 2017), still different sensitivities between the UTCI and mean TSV were found. Therefore, the outdoor thermal conditions were much different than the indoors and using the models developed based on the indoor climate data. Even though the models developed based on the datasets collected world-wide like the UTCI, were not able to cover the outdoor thermal condition accurately.

### 2.3.4 The CBE model

#### 2.3.4.1 Principles

Much like the UTCI index, the CBE model was developed in the early 2000s which was based on the development of the multi-nodal models. The CBE model was based on the Tanabe 65-node model (Tanabe et al., 2002), which meant the Stolwijk model (J. A. Stolwijk, 1971) also contributed to its basic structure. The CBE model made improvement in the blood flow model, added a clothing node for better simulation of heat and moisture transfer via clothing, and built up the correlations between the physiological parameters with thermal sensation and comfort vote based on the experimental data (Huizenga et al., 2001). Compared to the UTCI model, which was based on the universal database, the specific logic underline the rational models and the listed coefficients in the publications related to the CBE model provide the possibility for further development (H. Zhang et al., 2010b).

The CBE model was developed in the indoor climate chamber, based on the measured thermo-physiological measurements (skin and core temperatures) and was then validated with real passengers sitting in automobiles within a climate chamber (H. Zhang et al., 2010c). It was hypothesized in this model that the thermal sensation feeling was based on a self-thermoregulation system, which was triggered by the sensory organs (thermal receptors) located in the skin, spin and some abdominal organs (E. A. Arens, & Zhang, 2006). The number and depth of warm and cold receptors varied from part to part in human body (E. A. Arens, & Zhang, 2006), which was the reason a multi-nodal model should be adopted when the asymmetric thermal environment was concerned. During the experiment, human subjects were asked to wear air sleeves of conditioned air that enclosed specific body segment to force the individual body parts through a range of temperatures. The subjects' local skin temperatures and core temperatures were measured and they were repeatedly surveyed for local and whole-body sensation and comfort level (H. Zhang, 2003). An extended ASHRAE seven-point scale, adding "+4 very hot" and "-4 very cold", was used to evaluate thermal sensation (H. Zhang et al., 2010c). The thermal comfort level scale was a symmetric six-point scale : "+4 very comfortable", "+2 comfortable", "0 just comfortable", "-0 just uncomfortable", "-2 uncomfortable", "-4 very uncomfortable" (H. Zhang et al., 2010a). To obtain thermal responses in individual body segments under transient and asymmetric conditions, most of the tests involved cooling local body parts under warm conditions followed by warm recovery, and a limited number of tests warmed local body parts under cool conditions (H. Zhang et al., 2010c).

In the CBE model, the local thermal sensation was divided into two parts: static and dynamic parts (Equation 2.9) (H. Zhang et al., 2010c). The entire local sensation equation followed the form as Equation 2.10 (H. Zhang et al., 2010c). The static local sensation was a logistic function of the difference between local skin temperature and its set-point, while the dynamic local sensation was determined by the derivatives of skin and core temperature (Equation 2.11) (H. Zhang et al., 2010c). Both the local skin temperature and the mean skin temperature had the impact to the local thermal sensation. The mean skin temperature represented the modifying effect of whole-body thermal status on local sensation (H. Zhang et al., 2010c). The coefficients for the cold and warm sides were different and thus the model was asymmetric. The dynamic local sensation mainly dealt with the conditions when human body was experiencing skin temperature change which is caused by the changing thermal environment such as step change of air temperature. The dynamic part is described using the form as Equation 2.12 (H. Zhang et al., 2010c).

$$\text{Local Sensation} = Local\ sensation_{static} + Local\ sensation_{dynamic} \quad \text{Equation (2.9)}$$

$$\text{Local Sensation} = \int (T_{skin,i}, \frac{dT_{skin,i}}{dt}, \bar{T}_{skin}, \frac{dT_{core}}{dt}) \quad \text{Equation (2.10)}$$

$$\text{Local sensation}_{static} = 4\left(\frac{2}{1+e^{[-(C1+K1)(T_{skin,i}-T_{skin,i,set-point})+K1(T_{skin,m}-T_{skin,m,set-point})]}} - 1\right) \quad \text{Equation (2.11)}$$

$$\text{Local sensation}_{dynamic} = \text{C2}\ dT_{skin,i}/dt + \text{C3}\ dT_{core}/dt \quad \text{Equation (2.12)}$$

The logic flow of determining the overall TSV is shown in Fig. 2.3. The body parts were categorized into two groups: the dominant group and the others. The dominant group was the trunk area of human body, which was consist of chest, back and pelvis. The dominant group had larger contribution to the overall thermal sensation (H. Zhang et al., 2010b). The overall thermal sensation was considered by two different conditions separately: “no opposite sensation” and “opposite sensation” conditions (H. Zhang et al., 2010b). To categorize the two conditions, each local body sensation was divided into two groups: the group of positive thermal sensation and the group of negative thermal sensation. The local body parts which was voted as “TSV = 0” was classified into the bigger group.

The “no opposite sensation” was defined as two conditions:

(a). the sensation of all the local body parts located in the same side;

(b). the body parts in the smaller group had thermal sensation no stronger than “slightly cool” or “slightly warm”, and the dominant body parts were warmer than “slightly cool” when local cooling applied.

The “no opposite sensation” part could be defined as no body parts feeling significantly opposite to the other body parts; otherwise, “opposite sensation” condition was termed (H. Zhang et al., 2010b).

The “opposite sensation” was defined as two conditions in order:

(a). the dominant body parts had higher priority: the “opposite sensation” is satisfied if they have strong cooling sensation: “TSV < -1”;

(b). if condition (a) was not applicable and at least one of the local thermal sensations of the smaller group was cooler than “slightly cool”.

Each body part accounted for a certain weight in determining overall thermal sensation if “no opposite sensation” condition was considered (H. Zhang et al., 2010b). If “opposite sensation” condition was considered, the whole body sensation led the overall thermal sensation while the “opposite parts” modify it (H. Zhang et al., 2010b). The coefficients of each local body part in determining overall thermal sensation are obtained from experimental data and vary considering of the “no opposite condition” and the “opposite condition”.

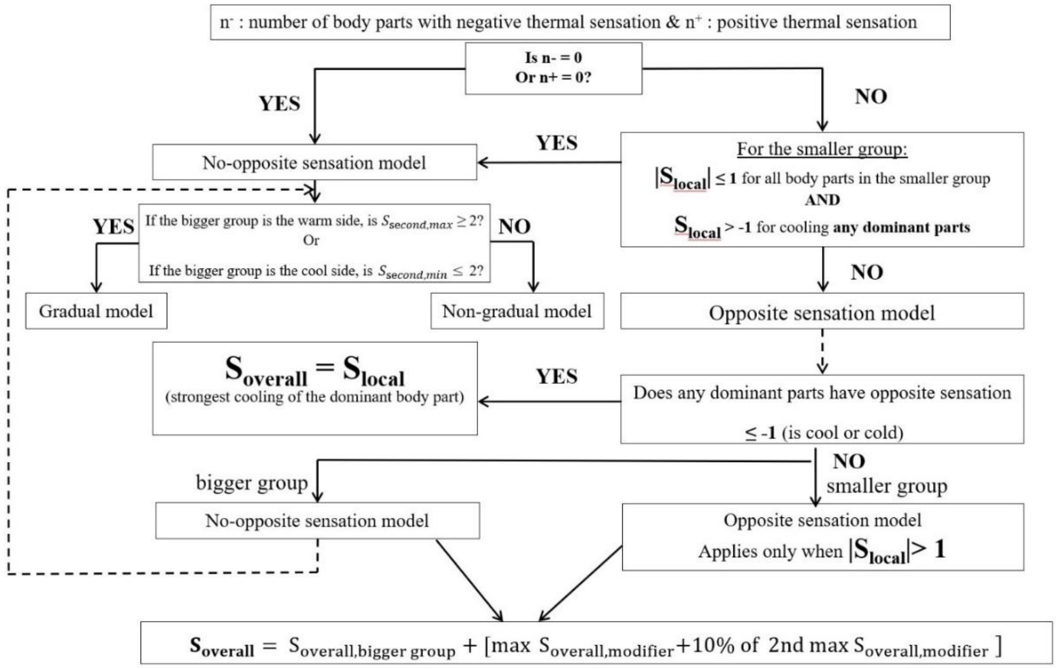


Figure 2.3 Schematic diagram of the logic flow in whole-body thermal sensation model (reproduced based on the reference (H. Zhang et al., 2010b))

### 2.3.4.2 The application of the CBE model in the outdoor conditions

The application of the CBE model in the outdoor conditions was rare, most of the application of the CBE model were applied in the indoor environment (Makhoul et al., 2013; Schellen et al., 2013; Zhou et al., 2014; Zolfaghari, & Maerefat, 2010). Our team did a preliminary study of applying the CBE model in the outdoor environment by comparing with the PET index and the UTCI index in different microclimates in the campus of the Hong Kong Polytechnic University (Huang et al., 2017). Three different microclimate conditions were considered in the study, including the fully open area where human subjects can be exposed to direct sunlight;

two open areas under the elevated building covering the weak wind condition and the strong wind condition (Huang et al., 2017). The CBE model gave better prediction than the other two indexes in the listed three environments (Huang et al., 2017).

I am quite surprised about the limited application of the CBE model in the outdoor environment before our team's effort for the reason that the CBE model targeted at the transient and asymmetric thermal environment which was the main characteristics of the outdoor thermal environment. Though it behaved better than the other indexes, still more validation studies should be done before its application in the outdoor environment to ensure the model's accuracy.

### 2.3.5 The validation of the listed models in the outdoor environment

Though the previous reviews listed the application of the listed models for the evaluation of the outdoor thermal environment, the accuracy of such application still needs verification as the listed models were all developed in indoor chamber or based on the experiment data from indoor chamber. Our research team have conducted a preliminary study trying to answer this question (Huang et al., 2017). We compared the prediction results of three listed models, PET, UTCI and the CBE model to the field-surveyed data of actual users in different outdoor contexts regarding their prediction accuracies (Huang et al., 2017). Two different outdoor environments were selected, a semi-outdoor space created by the elevated building (UEB area) and a fully open outdoor space (Open area). In the UEB area, the actual users cannot receive direct sunlight and the wind environment was relatively stronger than the open area. In the Open area, the actual users were exposed to direct sunlight with weak wind condition. Figure 2.4 shows the correlations between mean thermal sensation vote and three models in the UEB and open areas. The corresponded data in each sub-figure in Figure 2.4 was organized by the prediction values from each model. It is obvious that the data from UEB and Open area are separated into two different correlation lines for the listed three models. Take PET as an example, when PET equals 30 ℃, it corresponds to MTSV = 0 in the UEB dataset and MTSV = 1 in the Open dataset. This phenomenon indicates that one prediction value corresponds to different actual thermal sensation feelings in different outdoor thermal conditions. In other words, the prediction values from the PET model was not able to reflect the actual thermal sensation. The larger the gap between two correlation lines, the bigger the difference it is. Both the PET and UTCI had large prediction gaps throughout the whole range; however, the data from the CBE model had similar prediction from two different sites around the thermal neutral status. Therefore, we see the chance of further applying this model in the outdoor conditions.

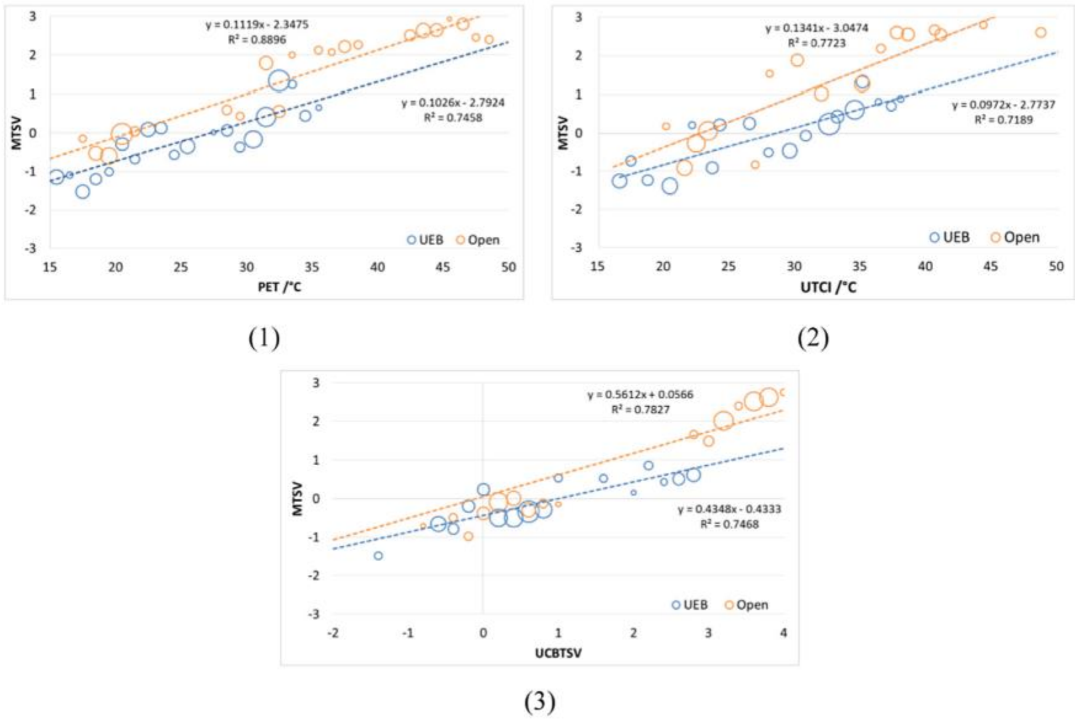


Figure 2.4 Respective correlations between mean thermal sensation vote (MTSV) and three models in UEB and Open areas: (1) Correlation between MTSV and UTCI; (2) Correlation between MTSV and PET; (3) Correlation between MTSV and UCBTSV.

We did not include the SET* model in the previous comparison considering its own model structure, which assumes mean radiant temperature equals air temperature. Such assumption hinders the SET* model from reflecting the thermal stress of solar radiation. An early research conducted in Guangzhou, China has proved the insensitivity of SET* to the change of solar radiation by correlating the prediction results from SET* to the actual thermal sensation vote (Xi et al., 2012). Their results show cumulative SET* values in the range between 30 ℃ to 34 ℃

correspond to wide range of TSV from “TSV = 0” to “TSV = 2.5”. Combining the correlation results between mean radiant temperature and TSV, where shows TSV is sensitive to the mean radiant temperature, it is reasonable to infer that the cumulative SET* values to a wide range of TSV is because of such model not being able to reflect the thermal stress from solar radiation.

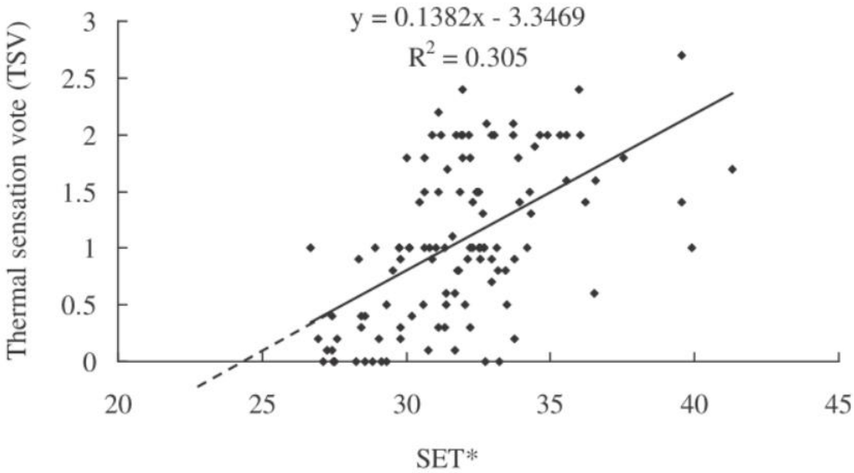


Figure 2.5 Relationship between SET* and thermal sensation vote (TSV) (Xi et al., 2012)

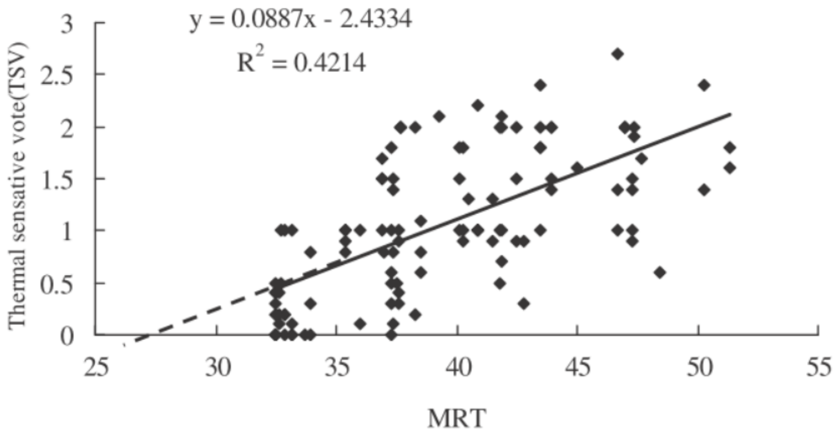


Figure 2.6 The relationship between MRT and thermal sensation vote (TSV) (Xi et al., 2012)

## 2.4 The basic theory related to the physiological models

### 2.4.1 Basic thermoregulation process and triggering conditions

The thermoregulation functions in human body generally refer to four mechanisms: sweating, shivering, vasodilation and vasoconstriction. The objective of thermoregulation is to regulate deep body temperature. Normal core temperature is around 37.0 ℃ and is controlled within a limited range of 34.4-37.8 ℃ when measured in rectal (Sund‐Levander et al., 2002). The range of body temperature might have slight difference when measured using different ways and it is summarized from the studies with strong evidence that the range measured in oral was 33.2-38.2 ℃, when measured in tympanic was 35.4-37.8 ℃ and when measured in axillary was 35.5-37.0 ℃ (Sund‐Levander et al., 2002).

Sweating is the function of increasing heat loss from human body to the environment through water evaporation from skin surface, it is triggered to prevent deep body temperature from further increasing. Shivering is an automatic heat production by muscle to prevent the deep body temperature from further decreasing. When human body is exposed to mild cold environment, it will conserve heat by vasoconstriction. But if it is exposed to the serve cold environment, vasoconstriction is insufficient to maintain core temperature, shivering happens. It is believed that when shivering emerged, the maximum vasoconstriction has already been achieved (DeGroot, & Kenney, 2007). There exists a thermoregulatory "null zone" in core temperature between the threshold for shivering and sweating and its magnitude was measured to be $0.57 \pm 0.20$ for rectal temperature (Mekjavic et al., 1991).

Vasodilation and vasoconstriction are the states of blood vessel, such states response to the increased and decreased internal temperatures. When vasodilation happens, the vessel diameter enlarges and more blood pass through, and thus enhanced transfer of metabolic heat. Adversely, when vasoconstriction happens, transfer of metabolic heat is restrained. Both vasodilation and vasoconstriction have direct result on skin temperature.

### 2.4.2 Thermal receptors

Both the core and skin temperatures serve as the feedback thermal signal in thermoregulation system (Romanovsky et al. 2009, Werner 2010). The feedback signal was represented by heavy weighted core temperature and light weighted skin temperature, and thus the core temperatures was the main feedback signal and skin temperature was the secondary (auxiliary) feedback signal (Romanovsky et al. 2009, Werner 2010). Different effectors within the thermoregulation system were driven by different combinations of core and skin temperatures (Romanovsky et al. 2009, Werner 2010). Skin temperatures were considered relatively more important for triggering most thermoregulatory behaviors compared to the deep core temperature, while the deep core temperature was more important for driving autonomic responses (Jessen, 1981; Sakurada et al., 1993). Werner pointed out that the auxiliary characteristics of skin temperature in thermoregulation was similar to that in the engineering field, which was a quick response to disturbances compared to the main control variable (core temperature) (Jürgen Werner, 2010) and it responded to not only the temperature but also the rate of change of temperature (H Hensel, & Schafer, 1984).

The listed physiological findings provide the theoretical foundation of this study. The nervous structures (thermoreceptors) detect the organism’s temperature fluctuations and send signals to the hypothalamus (H Hensel, & Schafer, 1984). Thermoreceptors were located mainly in the peripheral area and in the hypothalamus and some were found in the spinal cord, abdominal viscera and in or around the large veins of the upper abdomen and thorax (E. A. Arens, & Zhang, 2006). The hypothalamus was the recognized as the integration center to deal with the signals for thermoregulation (Tansey, & Johnson, 2015), while the preoptic anterior hypothalamus was the most important region for autonomic temperature control (Romanovsky, 2007).

The discovery of TRP (Transient receptor potential) family of ion channels in the last decade made advance in understanding the transduction processes in peripheral thermal sensation (Wu et al., 2010). The TRP family channels were a superfamily of proteins that could be expressed in cell membranes and in membranes of internal structures (Tansey, & Johnson, 2015). Individual TRP channel (sensation receptor) response to a specific narrow temperature range and overlapped for certain range of temperature (shown in Figure 2.7). The warm receptors (TRPV4 and TRPV3) were activated in the temperature range of 25 and 31 ℃ while the cold receptors (TRPM8) were activated below 27 ℃ (Tansey, & Johnson, 2015). The warm receptors located deeper (0.3-0.6 mm) than the cold receptors (0.15 to 0.17 mm) in the dermis (E. A. Arens, & Zhang, 2006). The number of cold receptors was ten times of the warm receptors located in the peripheral area. These characteristics made human body more sensitive to cold stimulus than warm stimulus (E. A. Arens, & Zhang, 2006).

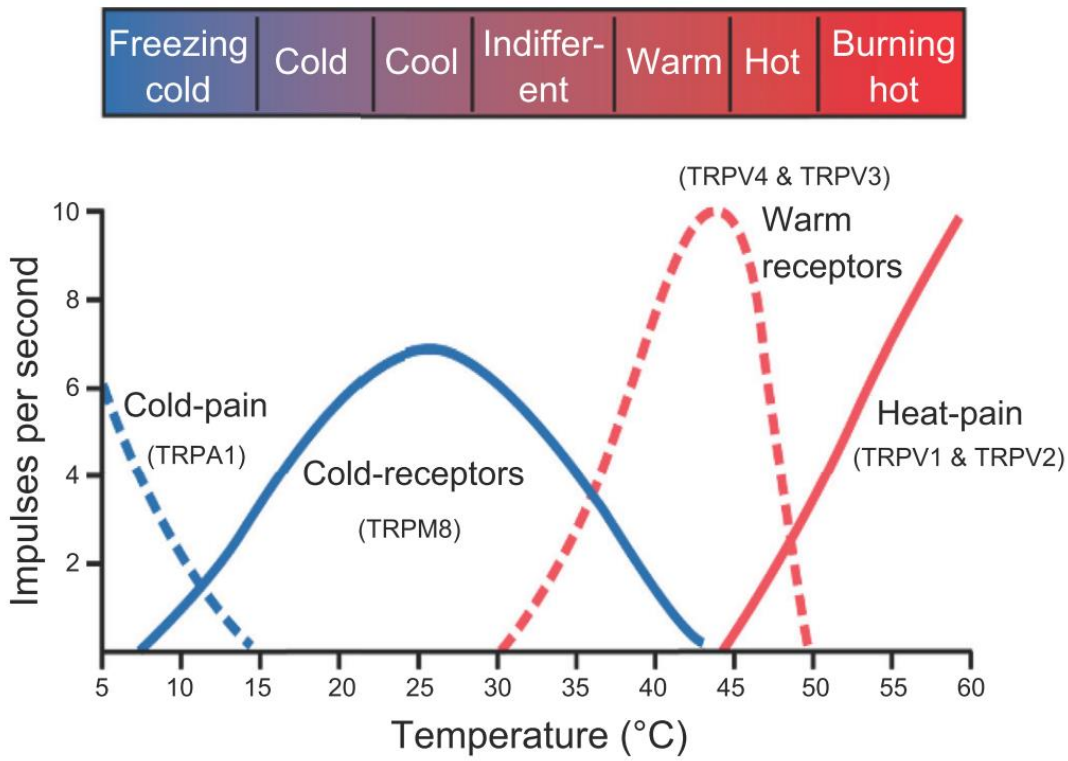


Figure 2.7 Discharge frequencies at different skin temperatures of thermoreceptors, along with potential transient receptor potential (TRP) channels associated with receptor function (Tansey, & Johnson, 2015)

A thermoreceptor was able to response to static and transient thermal stimulus. Fig. 2.8 shows the general properties of thermoreceptor when responding to static and dynamic thermal stimulus. When static thermal stimulus was applied, both warm and cold receptors at low rate. But when transient thermal stimulus was applied, both of the receptors had an abrupt high frequency at first and then it faded away quickly, and the receptor stabled at a higher impulse frequency than the thermal stimulus starts. Thus, this explains the much stronger thermal sensation felt when a person was experiencing a sudden change of temperature. This phenomenon is termed "overshoot". In contrast to the "overshoot" is adaptation. When chronic deviations from neutral status happens, adaptive modification of short-term thermoregulatory processes take place. The degree of adaptation not only depended on the strength of stimulus and the duration, but also on its time structures (such as constant, slowly changing, continuous and intermittent) (H Hensel, & Schafer, 1984).

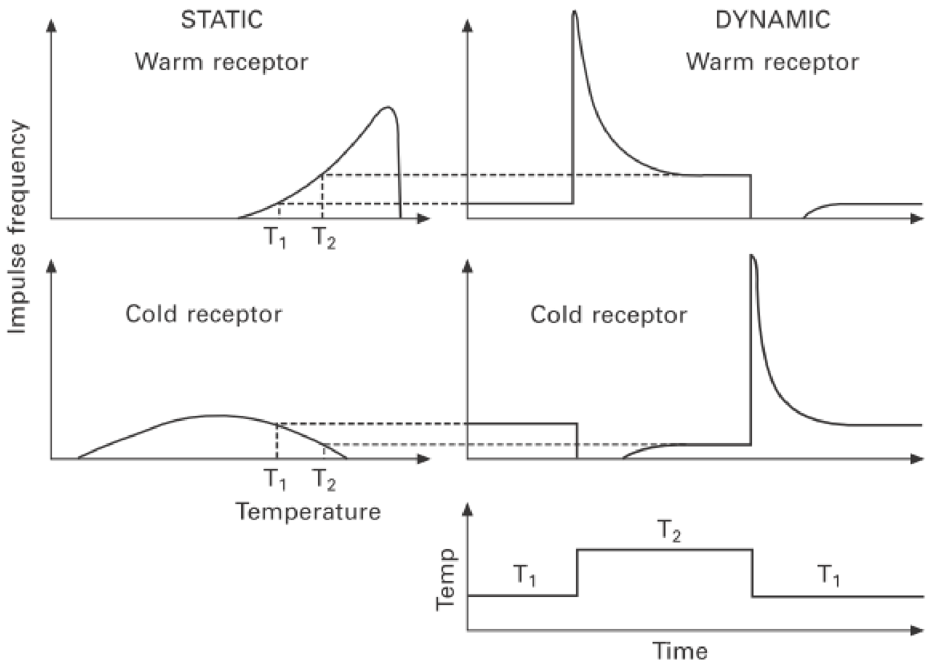


Figure 2.8 General properties of thermoreceptors. Static and dynamic responses of warm and cold receptors as they response to the static and transient temperature change (E. A. Arens, & Zhang, 2006)

### 2.4.3 Control theory and set-point

Thermoregulation aims at stabilizing the body temperature ($T_b$) with thermal sensation being its side product (Romanovsky, 2007). The Stolwijk's 25-node model deeply rooted the control theory in thermoregulation models, including the CBE model (Parkinson, & De Dear, 2015). "Load error" which triggers the regulatory processes is the soul of the control theory. "Set-point" is used as the reference temperature to calculate the load error, which serves as a feedback signal (J Werner, 1980), to regulate the human body and to evaluate the thermal state (J. A. Stolwijk, 1971). The "load error" is defined as the deviation from the set-point of the regulated variable (Jürgen Werner, 1988). Set-point temperature is defined as the weighted average of $T_{core}$ (core temperature) and $T_{skin}$ (skin temperature) (C. Cheng et al., 1995; Cotter, & Taylor, 2005; Frank et al., 1999). $T_{skin}$ contributes about 5-20% to the thermoregulatory response while $T_{core}$ contributes to the more substantial proportion, the proportion varies depending on cold or warm conditions (E. A. Arens, & Zhang, 2006; C. Cheng et al., 1995; J. Stolwijk et al., 1971; Tikuisis, & Giesbrecht, 1999). $T_{skin}$ seems to be the auxiliary variable in the thermoregulation process. Nevertheless, given the warmth and cold thermoreceptors located in different depths of the skin, which sense thermal stimulation, the role of skin in the perception of thermal sensation is non-negligible (E. A. Arens, & Zhang, 2006). The activation of thermoreceptors also depends on "load error" (C. Cheng et al., 1995; R. De Dear, 2011; Herbert Hensel, 1982), and thus quantifying the deviation from the set-point has a direct effect on the intensity of thermal sensation perception. Therefore, the

CBE model defines “load error” for the perception of thermal sensation in a given local body part as the deviation of the actual local skin temperature and its local “set-point” (H. Zhang et al., 2010c). The set-point for thermal sensation and comfort prediction of a given local body part is obtained in its thermal neutral status (H. Zhang et al., 2010c; Zhao et al., 2014). Therefore, the particular concern should be given to the thermal neutral status.

Terms like “set-point" have been disputed for decades in thermal physiology. The original meaning of “set-point” comes from the engineering field and refers to an externally assigned physical reference signal in a unified control system. The term “set-point” has evoked much confusion for its usage in various situations: “set-point” is regarded as “the regulated body temperature of steady-state”; “the central reference signal” and “the thermal effector threshold” in the field of thermal physiology (Jürgen Werner, 2010). In the thermal comfort studies such as the Pierce model (Foda, & Sirén, 2011), the UTCI model (Fiala et al., 2012), and the CBE model (H. Zhang et al., 2010c; Zhao et al., 2014), it is referred to the physiological parameters in its “thermal neutral status”. The controversy regarding such usage mainly comes from three aspects: the reference signal hypothesis, the unified entire system, the disturbance and acclimation. The first two controversies come from the field of thermal physiology, while the last one comes from the field of thermal sensation and comfort studies. We will briefly describe these three aspects below.

In recent years, the biologists and physiologists have come to an agreement that the reference signal hypothesis was untenable. Firstly, the clear evidence of the neurons in the hypothalamic region of the brain that are supportive of the reference signal hypothesis has remained elusive (Bligh, 2006; Romanovsky, 2007; J Werner, 1980). Secondly, Romanovsky (Romanovsky, 2007) concluded that $T_b$ is regulated by independent thermoeffector loops, each having its afferent and efferent branches and independent thresholds, respectively. The regulation activity of each thermoeffector is triggered by a unique combination of skin and core temperatures. The response of thermoeffector is the result of the temperature-dependent phase transitions of the thermosensory neurons in sequential order (Romanovsky, 2007). Therefore, no comparison of integrated body temperature or a hidden set-point is necessary.

The early research comparing the core temperature with its set-point was a simplified explanation of the thermoregulation process in the human body. However, such cognition would have to treat the human body as a unified entire system with a single controller or a single reference threshold, which has been proved as inappropriate and bringing in misunderstanding. Complex as the thermoregulation system in the human body, abundant thermoreffector loops exist (Romanovsky, 2007), and their thresholds often change independently (Romanovsky, 2007). Furthermore, the integration of the responses to a particular external stimulation depends on abundant sensor-to-effector pathway connections (Romanovsky, 2007). Such complex interconnections through the central nervous system make it unlikely that any particular response is merely the outcome of one particular stimulus and thus requires some degree of variability or flexibility in temperature regulation (Bligh, 2006).

The above arguments are all in the field of thermoregulation. As for the set-point related to the thermal neutral state, it is the value when the thermal balance is obtained, and the rate of heat storage is equal to zero (Belding, & Hatch, 1955). "Set-point" here mainly refers to the "reference point" used in the thermal sensation and comfort models. If one strict value was considered without any variability, a slight change of the thermal environment could break the thermal neutral state corresponded to the given "set-point", and thus changing thermal sensation correspondingly. It is barely impossible for the "steady state" or "thermal neutral state" to be established if the term "set-point" is considered (Jürgen Werner, 2010), especially in the transient changing thermal environment. Moreover, the human body can adapt to a new steady level when persistent thermal disturbances happen. The balance of body temperature is further achieved in a new level due to the inherent property of dynamical stability of the thermoregulatory feedback loop (Jürgen Werner, 2010), thus shifting of thermal sensation response after adaption. Thermal adaptation is a higher level of control, on which either the heat transfer process or the thermoeffector properties (e.g., thresholds) are adjusted (Bittel, 1987; Brück et al., 1976), and hence a fixed "set-point" is not able to describe thermal adaption.

Based on the listed reasons, the biologists consider the term "set-point" in thermoregulation invalid almost unanimously and suggest eliminating the usage of this term (Romanovsky, 2007). However, how to handle the term "set-point" in the thermal sensation and comfort model is a different matter, especially in the case of an urban open environment where unstable and asymmetric thermal stimulus becomes dominating. The existing CBE model has built a base structure that supports the change of "set-point" and has attempted to locate the adaptation thresholds (H. Zhang, 2003). However, the related datasets were too limited to establish the adaptation thresholds, and the datasets were obtained in the indoor setting where the transient thermal environment was created by step change of air temperature. Moreover, the complex wind environment in the outdoors could not be reproduced in the indoor chamber. The major difference between indoor and outdoor wind characteristics are turbulent intensity and gust wind. The existing studies based on the research results from indoor chamber are not able to describe the convective heat transfer effect of the outdoor wind environment due to limited experiment results in high turbulent intensity, needless to mention the transient effect by gust wind (R. J. de Dear et al., 1997). The wind tunnel experiment from Yu et al. (2019) have confirmed that stronger heat transfer process existed under high turbulence intensity level. Due to these factors, there is a room for improvement if the CBE thermal sensation and thermal comfort model are to be applied for the outdoor environment.

## 2.5 The studies related to the pedestrian wind environment

### 2.5.1 Simulation techniques for the outdoor wind environment (CFD and wind tunnel)

The pedestrian wind environment is mainly analyzed through three methods: on-site measurements, wind tunnel tests and CFD simulations. On-site measurement provides the most accurate data for actual pedestrian-level wind environment, but it only limit to point measurement. Wind tunnel tests and CFD simulations are the frequently used techniques for wind environment simulation at present. A global understanding of whole-flow field data can be achieved through the reduced-scale test of the wind environment in the wind tunnel tests aiding by particle image velocimetry (PIV) and laser-induced fluorescence (LIF). CFD simulations are a powerful alternative but its accuracy is an important matter of concern. Careful handling in grid generation and selection in proper solution strategies and parameters are needed (Blocken et al., 2011).

The CFD analyses of outdoor wind environment concerns about the listed aspects below:

- The wind environment around a building or the building blocks;

- The microclimate analysis in the pedestrian level;
- The overall urban climate.

The studies about the outdoor wind environment concern about the wind flow around buildings at first. The isolated building with a cubical shape laid the foundation (Blocken et al., 2011), the wind-flow pattern for different sides of the building was identified (Hosker, 1984). The earlier studies focus on simple building structures was aimed at obtaining the detail of flow behavior and CFD validation (Blocken, & Carmeliet, 2007; Franke, 2005; Yoshie et al., 2007). Later, more applied studies which provide the detail knowledge of the wind environment in the complex urban settings appeared, covering from the building scale to microscale and even the mesoscale. (Antoniou et al., 2019; Bert Blocken, & Jan Carmeliet, 2004; Blocken, & Persoon, 2009; Richards et al., 2002; Toparlar et al., 2017).

With the work done in recent years, we have a clearer understanding of the wind flow pattern in the pedestrian level for different building types and wind comfort (B. Blocken, & J. Carmeliet, 2004; Mochida, & Lun, 2008). Xia et al. (2017) measured the mean wind flow pattern for a square building with elevated structural pillars using a wind tunnel. The pedestrian wind environment and wind comfort in the similar design for a group of buildings with 'lift-up' design were further simulated by Zhang et al. using a wind tunnel (X. Zhang, K.-T. Tse, et al., 2017; X. Zhang et al., 2018b). Du et al. examined the wind comfort conditions around the building of four common building configurations with lift-up design (Du, Mak, Liu, et al., 2017). Druenen et al. (2019) evaluated different modifications of building geometry in reducing the pedestrian wind speed around an isolated high-rise building and found that a canopy or a podium can significantly reduce the area-averaged wind speed in pedestrian level up to 29%. Liu et al. did the assessments of pedestrian wind environment using LES for a single building and buildings arrays with the 'lift-up' design (Liu, & Niu, 2019; Liu, Niu, et al., 2019).

### 2.5.2 Wind comfort criterion and scales

The construction of a building brings inevitably changes to the microclimate. Whether the changes are favorable should be considered case by case given the original need of the construction sites considered. The building structures which are able to lead wind are not welcomed in the sites where extreme wind speed happens in high probability (Blocken, & Persoon, 2009); however, the wind leading ability is favorable in the weak wind environment for removing air pollution and improving thermal conditions (Liu et al., 2016). The wind fluctuation pattern at pedestrian level results from the complex wind flow pattern around the building blocks (Blocken, & Persoon, 2009) and the obstacles in pedestrian height such as trees.

There are many criteria assessing wind comfort (or wind discomfort). Such as the Beaufort scale of winds (Engineers, 2003), the wind comfort criteria and the effect of wind gustiness for wind comfort (Hunt et al., 1976a). The wind speed in Beaufort scale refers to the value that measured in pedestrian height and are the average value over the period of 10 minutes or 1 hour. Gust wind has important influence on the average value.

Table 2.2 Extended Land Beaufort Scale showing wind effect on people (B. Blocken, & J. Carmeliet, 2004)

| Beaufort Number | Description | Wind Speed at 1.75 m height (m/s) | Effect |
|---|---|---|---|
| 0 | Calm | 0.0–0.1 | |
| 1 | Light air | 0.2–1.0 | No noticeable wind |
| 2 | Light breeze | 1.1–2.3 | Wind felt on face |
| 3 | Gentle breeze | 2.4–3.8 | Hair disturbed, clothing flaps, newspaper difficult to read |
| 4 | Moderate breeze | 3.9–5.5 | Raises dust and loose paper, hair disarranged |
| 5 | Fresh breeze | 5.6–7.5 | Force of wind felt on body, danger of stumbling when entering a windy zone |
| 6 | Strong breeze | 7.6–9.7 | Umbrellas used with difficulty, hair blown straight, difficult to walk steadily, sideways wind force about equal to forwards walking force, wind noise on ears unpleasant |
| 7 | Near gale | 9.8–12.0 | Inconvenience felt when walking |
| 8 | Gale | 12.1–14.5 | Generally impedes progress, great difficulty with balance in gusts |
| 9 | Strong gale | 14.6–17.1 | People blown over |

Murakami reported that a steady wind of 5 m/s cause minor disturbances on hair and clothes and wind is felt on the face, while a steady wind of 10 m/s cause blowy hair and fluttering clothes (S Murakami et al., 1980). The data reported by Murakami causing the same effect was much higher than that listed in the Beaufort scale. In other words, when mechanical wind effects are considered, people are more affected by non-uniform winds and by wind gusts than by uniform winds (Hunt et al., 1976b).

The wind comfort criteria are defined as a combination of the discomfort threshold and a exceedance probability of the threshold (B. Blocken, & J. Carmeliet, 2004). A representative of wind comfort criteria shown below is concluded and corrected by Bottema (Bottema, 2000). He compared about 30 criteria and selected the criterion for evaluating wind comfort shown in the following mathematical structure (Equation 2.13 and 2.14) (known as the shop owners criterion from Lawson and Penwarden (1975)) and the discomfort threshold from the field data obtained by the long-term survey from Murakami (Shuzo Murakami et al., 1986).

$$U_e = U + \sigma_u > 6\ m/s \qquad \text{Equation (2.13)}$$

$$P_{max} = 15\ \% \qquad \text{Equation (2.14)}$$

The wind gustiness intends to describe the fluctuating quantity of wind. In several publications, the equivalent wind speed $U_e$ was used to define the wind gusts, which include both the mean wind speed and the turbulence intensity (Soligo et al., 1998).

$$U_e = \bar{u} + k\sigma = \bar{u}(1 + kI) \qquad \text{Equation (2.15)}$$

$$k = \frac{u_{max,2s}}{\bar{u}}$$ Equation (2.16)

$U_e$: the equivalent wind speed, m/s;

$\bar{u}$: the wind speed measured at the height of 1.75m;

$k$: the peak factor (or gust factor);

$I$: turbulence intensity, %;

$\sigma$: the standard deviation;

$u_{max,2s}$: the peak 2-s gust within a 10-min period.

The $\sigma$ is not always defined in same way, sometime it refers to the u-component only and sometimes refers to the total horizontal turbulence (Bottema, 2000). The gust factor was indicated by many studies and the main problem of converting gust speeds into equivalent wind speeds was the determination of gust factor $k$. For the highly turbulent winds, the large gust value makes the turbulent characteristic more important and for the less turbulent winds, small gust value instead (Soligo et al., 1998). The gust factor is calculated using Equation 2.16. A moving average is used to locate the peak 2-s average gust wind with a time period of 10 min.

The existing criteria are related to wind comfort and wind danger, which are the mechanical wind effect. The Hong Kong SAR Government has the Air Ventilation

Assessment (AVA) scheme serving as a technical guideline to guide urban planning and building design, the concept of 'wind for thermal comfort' was first suggested for Hong Kong (Ng, 2009). However, only a suggested comfort chart showing the comfort range of meteorological parameters, further analysis related to the correlation of outdoor wind pattern and the thermal effect was neglected. The thermal effect of wind was less discussed. Because several parameters need to be considered when the thermal effect is discussed: air temperature, relative humidity, radiation and the personal parameters including clothing and metabolic rate. The experimental data of outdoor thermal comfort related to wind is now remain limited (Bottema, 2000). The cooling effect caused by outdoor wind and high turbulent level also remains uncertain. From the limited experimental data indoors, the investigated highest turbulent intensity was below 10% (R. J. de Dear et al., 1997).

Yet the current studies related to the outdoor wind environment lacks the understanding of the mechanism of how the outdoor wind environment affects human body and the corresponding thermal perception.

## 2.6 Thermal comfort studies in Hong Kong

Hong Kong is a representative of the typical high-density city located at the sub-tropical area. It has the typical climate characteristics of the cities located in the sub-tropical and tropical area: long and hot summer along with warm and short winter.

Normally, Hong Kong has high humidity from spring to summer, ranging from 60% to 80%. Ginn et al. (2010) conducted a historical analysis of the meteorological observations in Tsim Sha Tsui since the year of 1885. Their results show that cold episodes are becoming rarer while hot days are happening in higher frequency (Wing-lui et al., 2010). They also found that the raise of temperature in Hong Kong was slightly higher than the global mean in the 21st century (Wing-lui et al., 2010). Therefore, the thermal comfort studies related to Hong Kong should focus more on warm and hot days.

Being a seaside city, Hong Kong has its historical problem of constructing high-rise buildings at the coastal area. These buildings are like the “screen buildings” and block the coastal wind from approaching further inland. The high-rise buildings in downtown area are built in high density, which further lower the permeability of wind flow and cause stagnant air in the pedestrian level. Such weak wind condition and stagnant air are adverse to the dispersion of hot and sticky feeling in hot days and the dispersion of air pollution. The downtown observation points from the Hong Kong Observatory recorded continue decreasing annual wind speed data from the year of 1968 to 2013 (Niu et al., 2015).The Urban Climatic Map and Standards for Wind Environment report stated the recommended desirable wind condition is of a median probability of 50% over a whole year achieving 1.5 m/s mean wind speed (Ng, & Ren, 2015). The report also recommended a need of 0.4 m/s increase of mean wind speed to offset every 1 ° C of air temperature (Vicky Cheng et al., 2009).

Many studies focus on thermal comfort of the subtropical area in recent years. Some studies focus on searching for the most suitable thermal comfort model to evaluate the local thermal environment (P. K. Cheung, & C. Jim, 2018; Fang et al., 2017; Fang et al., 2019; Golasi et al., 2018; Huang et al., 2017). The differences of the predicted performance by some frequently used thermal indices, including PMV (predicted mean vote), WBGT (wet bulb globe temperature), PET (physiologically equivalent temperature), $SET^*$ (standard effective temperature), the Berkeley Comfort model (CBE model) and the UTCI (the universal thermal climate index), have been indicated for the subtropical climate (P. K. Cheung, & C. Jim, 2018; Fang et al., 2017; Fang et al., 2019; Golasi et al., 2018; Huang et al., 2017). On the other hand, some studies focus on evaluating the practical measures for improving thermal comfort. Liu et al. (Liu et al., 2016) proposed that the elevated building design can help to provide better thermal comfort in the summer conditions in the open space underneath the building. Kong et al. (Kong et al., 2017b) compared various types of trees on improving thermal comfort condition and found that trees grown in the high-density settings performed better than the open settings by reducing the similar amount of solar radiation incident on urban surfaces (maximum value 3.9 and 5.1 °C respectively) and at the same time maintaining the wind speed level. Chen and Ng (Chen, & Ng, 2013) simulated the cooling effect of downtown greenery on the urban microclimate using ENVI-met and found both the greenery design scenarios with tree and grass can help reducing the average PET of the domain by 0.4 K. The other studies focus on the local characteristic of Hong Kong residents. Li et al. (Li et al., 2018) investigated the UTCI ranges where wind or solar radiation would take the dominant places based on the desirability of Hong Kong residents and found the UTCI of 26 °C was the breaking point. Lam and Lau (Lam, & Lau, 2018) examined the thermal perception differences in the summer of Hong Kong and Melbourne, and found that Hong Kong residents had higher UTCI (23.5 °C) for thermal neutrality than Melbourne residents (19.3 °C).

Many efforts aimed at providing a reference to the city planners by building up thermal comfort prediction models and improving the evaluation methods or simulation tools. The suitable ranges of meteorological parameters combination to achieve thermal neutrality and thermal comfort conditions targeted at Hong Kong residents can serve as an effective reference. For instance, Ng and Cheng (V Cheng, & Ng, 2006) proposed a comfortable outdoor temperature chart of Hong Kong to guide the local urban design, which was based on the studies conducted in regions that had similar climate conditions like Hong Kong. Still, given the thermal adaptation effect of local residents to their own city pattern, there is a need to provide such kind of reference based on the local characteristics of Hong Kong residents.

## 2.7 Summary and research gap

The topic of outdoor thermal comfort is gaining increasing importance in these years, especially for those cities suffering from severe hot or cold conditions. Hong Kong is a typical high-density city located in the sub-tropical area with air temperature of almost half a year time over 30 ℃ with high humidity, outdoor thermal comfort study conducted in Hong Kong can be a proper representative for the cities in sub-tropical and tropical areas. Better design of the outdoor environment needs to address the issues related to thermal comfort, and thus the planners and architectures have desires to know about the influence of the building structures and the arrangement of building blocks on the ambient micro thermal environment. Guidance of meteorological parameter ranges which provide thermal comfort are also meaningful for regional construction design. The current simulation tool for the prediction of thermal comfort conditions are all developed based on the data obtained indoors, such as the PET, the UTCI and the SET*. The application of such models directly in the outdoor environment would lead to errors given the listed reasons：

1) The thermal environment in the outdoor is much more complicated than that in the indoors. Air temperature is the main consideration for the indoor environment. The air velocity in the indoors is normally kept in a narrow range (under 0.80 m/s if no occupant control and $T_{op} > 25.5$ ℃)

(ASHRAE Standard Committee, 2017b). Turbulence is unwanted and draft is avoided. The radiative environment is relatively symmetrical considered the indoor environment is surrounded by walls, the limited source that can create asymmetry radiative environment are windows or some appliances that have temperature higher than the surroundings. The outdoor environment in pedestrian height, however, have complex wind environment and solar radiation environment. The building blocks and the trees increase the roughness near the ground and thus increase the turbulence level. Wind gusts increase the complexity of the wind environment. The experiment conducted in the indoor chamber was not able to reproduce the characteristics of the outdoor wind environment. Therefore, the thermal effect of the outdoor wind environment might not be included in the existing model and the thermal effect of the cases with high turbulent intensity is not being discussed in-depth. When people are exposed to the open area in the outdoors, they receive the short-wave radiation from the direct sunlight and also the long-wave radiation reflected from the surrounding building surfaces. Thus, the solar radiation is highly asymmetric.

2) Besides the objective difference exists between the indoor and the outdoor thermal environment. The subjective need of people when using

these two environments is different. People work and study in the indoors, stable thermal environment and less air movement is needed to avoid distraction. However, the entertainment and relax functions are valued more when choosing to stay in the outdoors, such as doing physical exercise, dinning and other social activities. The change of subjective need might welcome more dynamic thermal environment.

3) The two-node models (e.g. the PET, the SET*) might not be the suitable model to deal with the dynamic and asymmetric thermal environment. The multi-nodal models have proved to give more accurate results in the asymmetric and transient indoor thermal environment, but its performance in the outdoor environment still needs to be validated.

The final objective of evaluating the thermal environment is to provide the outdoor areas which people are willing to stay. Therefore, it is needed to know the range of meteorological conditions where the actual users feel thermally comfortable. The thermal history and thermal adaption effect of local residents are critical factors which might have influence on their thermal preference. However, the previous studies which focusing on the meteorological ranges for thermal comfort conditions in Hong Kong were not based on the survey results of a large number of local residents. Moreover, the previous studies listed in the literature review only focus on one or two meteorological parameters; however, the thermal effect of the meteorological parameters is needed to be discussed as a whole. The combination of meteorological parameters which actual users consider as thermally comfortable should be located to provide the reference for the building industries.

# Chapter 3 Methodology

## 3.1 Introduction

This chapter presents the main methodology used in this study, including the brief introduction of field experiment procedure and field data collection, the data processing method, the data needed for the input in the CBE model software and the statistic models used in the data analysis. The field measurement was conducted on a university campus to collect real-time meteorological data and thermal response of actual users along with the collection of their physiological data. The data processing method for preparing the radiation data for the data input of the CBE model is introduced. Three statistic methods including how to estimate the boundary of thermal neutral status using t-test, probit analysis and logistic analysis are presented in this part.

## 3.2 The brief introduction of field survey

We conducted filed measurement and survey in several outdoor scenarios to quantify the thermal perceptions. In total, three sets of experiments were conducted focusing on three different purposes. These two sets of experiment were named according to different kinds of outdoor environment for exposure.

- Elevated area (shaded) - open area (sunny) - elevated area (shaded);
- Choose one outdoor condition to stay for a certain period of time.

The first set of experiment focus on the dynamic process of changing thermal environment, while the second set of the experiment focus on the stable process of staying at a given thermal outdoor environment.

For each set of experiment, the human subjects were invited to experience the outdoor setting for a certain time period and finish the questionnaires distributed to their cellphone. Meanwhile, the microclimate station was used to monitor and collect the meteorological parameters of the given outdoor environment. Local skin temperatures were collected in the second and third sets of experiment settings. More details about the filed measurement will be described in the following sections.

### 3.2.1 Survey location

All of the field measurement and survey in the transitional seasons and summer and limited winter data were conducted on the campus of the Hong Kong Polytechnic University located in Hong Kong. Hong Kong is a crowded city with typical characteristics of the subtropical climate. It normally has long hot and humid summers and warm winters accompanied with the short and unobvious transitional seasons. The winter data of the second set of experiment was collected on the campus of the University of Sydney. Both the selected campuses are located in the central area of the city. Therefore, they are able to represent the typical microclimate conditions within the city. Both experimental sites were surrounded by academic buildings with external wall material of red brick (approximate albedo is 0.3) (Bradley et al., 2002) or glass curtain wall (the external reflectance ($ER_{Glass}$) in Hong Kong should be no more than 0.2 according to the Design and Construction Requirements for Energy Efficiency of Residential Buildings in Hong Kong (APP-156) (Buildings Department, 2014)). The pavement material for the sites were grass (approximate albedo is 0.2) (Bradley et al., 2002) and concrete (approximate albedo is 0.225) (Bradley et al., 2002) for Sydney and Hong Kong respectively. The meteorological parameters for the given set of experiment will be analyzed in the results shown in each part.

Fig. 3.1 shows the locations for the first set of experiment. Three sites were selected to cover different microthermal environments, as shown in Fig. 3.1. Sites 1 and 3, which were located in a passage of the underneath-elevated buildings, represented semi-outdoor environments. The wind environment on Site 3 was more complex than Site 1 in the aspect of fast-changing wind speed. Site 2 was an open square that receive direct sunlight.

Fig. 3.2 shows the outdoor environment for the second set of experiment. The outdoor scenarios were divided into four kinds of conditions: sunny and windy;

sunny and less wind; shaded and windy; shaded and less wind.

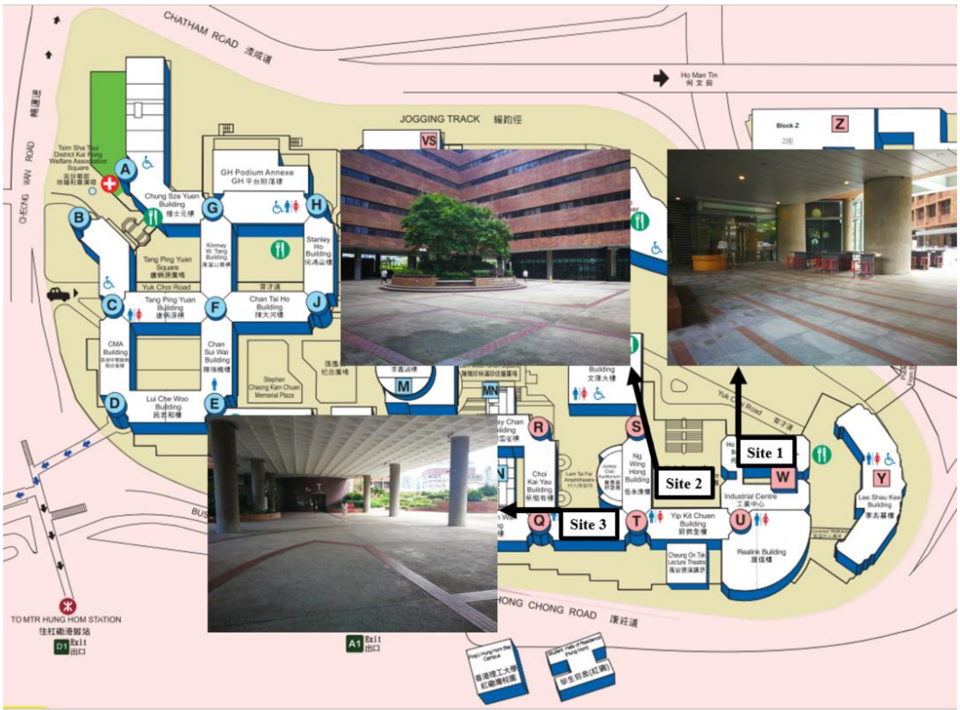


Figure 3.1 Survey locations for the first set of experiment

Figure 3.2 Survey locations for the second set of experiment (left) Sydney; (right) Hong Kong

### 3.2.2 Human subject

Given different experiment purposes, the activity and exposure time varied for different experiments. Some requirements for the human subjects remain the same for all three sets of experiment. In order to investigate the actual thermal perceptions of actual users. For all three sets of experiment, the human subjects were required to wear normal clothing to join the experiment and do daily activities during the experiment. Most of the recruited human subjects were young adults, with the mean age of 24 years old. Table 3.1 shows the basic information about the human subjects.

For the first set of experiment, totally 1107 available questionnaire samples were collected. On each survey day, human subjects were invited to experience different microclimates following the sequence from Site 1 to Site 3. Subjects were asked to spend 15 minutes on each site, sitting, standing, or slowly walking around within a specific area, with their metabolic rates being recorded in the range between 0.79 and 2.34 Met. The mean value for the metabolic rate was 1.17 Met, with a standard deviation of 0.22 Met. The survey results that had a metabolic rate higher than 2.0 Met were abandoned in the data analysis. After a 15-minute adaptation to the given microthermal environment, each subject completed a thermal comfort questionnaire which was delivered to their mobile phone.

For the second set of experiment, totally 531 survey responses were collected. Human subjects were required to sit or stand or walk slightly during the whole experiment. 428 survey responses were available along with the measured skin temperature dataset after removing the missing data and limiting the activity level to sit or stand only. Within the available datasets, altogether 42 males (35 in Hong Kong and 7 in Sydney) and 32 females (28 in Hong Kong and 4 in Sydney) joined the experiment. Only the students and young colleges from China were invited to join the experiment to avoid difference in thermal feelings caused by culture difference.

Table 3.1 General information of the human subjects

| | **Age** | **Weight (kg)** | **Height (cm)** | **Metabolic Rate (Met)** | **Clothing Value (clo) Winter / Summer** |
|---|---|---|---|---|---|
| Mean | 24.5 | 59.3 | 166.8 | 1.17 | 0.68 / 0.35 |
| Standard deviation | 7.6 | 11.9 | 8.1 | 0.22 | 0.24 / 0.14 |
| Minimum | 15.0 | 40.0 | 148.0 | 0.79 | 0.18 / 0.16 |
| Maximum | 63.0 | 96.0 | 194.0 | 2.34 | 1.20 / 0.83 |

### 3.2.3 Survey sample

The survey was distributed to the mobile phone of each human subject through scanning the QR code. The researchers will distribute the QR code at certain point of time.

The questionnaires varied based on different purpose of the experiment. All three sets of the experiment collected basic personal details: name, gender, age, height, weight, clothing information, country and province. The questionnaire related to personal details was distributed before the start of experiment. The human subjects were required to answer the questions before joining the experiment.

The main questions relate to thermal perception. In the first set of experiment, the main questions were about the subject's activity level, the standing direction relative to the sun, thermal sensation, thermal comfort, and wind and radiation preference. The ASHRAE seven-point thermal sensation scale (ASHRAE Standard Committee, 2010) was adopted to evaluate the subjects' actual thermal sensation in the first part of the experiment. The thermal comfort scale followed a five-point scale as very uncomfortable, uncomfortable, neutral, comfortable, and very comfortable.

In the second set of experiment, activity level and standing direction relative to the sun were asked. The survey focused on the perception of overall and local thermal sensation and thermal comfort. An extended nine-point scale was adopted to evaluate the subject's thermal sensation and thermal comfort. The extended thermal sensation scale followed the ASHRAE seven-point scale (ASHRAE Standard Committee, 2017b) with "very hot" and "very cold" added at the terminals. The thermal comfort scale was stated as very uncomfortable (-4), uncomfortable (-3), slightly uncomfortable (-2), just uncomfortable (-1), neutral (0), just comfortable (1), slightly comfortable (2), comfortable (3) and very comfortable (4). The overall thermal sensation vote and overall thermal comfort vote were asked at the beginning of the questionnaire. Then the human subjects were asked to choose at least three local body parts where thermal sensation were different from the overall thermal sensation and choose the actual local thermal sensation for each mentioned local body part. The question related to local thermal comfort would appear right after the local thermal sensation parts were answered.

For the second set of experiment, the survey was distributed at the end of each experiment period (every 5 minutes). For the third set of experiment, the survey was distributed twice for each site: one was when the human subjects first arrived at the given site and one was 10 minutes later right after they finished experiencing the given site.

### 3.2.4 Equipment

A microclimate station was constructed to collect the meteorological parameters at the survey location. As shown in Fig. 3.3, the devices were supported by a tripod at 1.5 m height. Real-time collection of eight parameters was performed in the microclimate station, including air temperature ($T_a$, °C), globe temperature ($T_g$, °C), relative humidity (RH, %), wind speed ( $v$ , m/s), wind direction, black globe temperature ($T_b$, °C), long-wave irradiance ($Q_l$, W/m$^2$), and short-wave irradiance ($Q_s$, W/m$^2$). The specific information of the microclimate station is listed in Table 3.2.

A Ta/RH sensor (model 41382, R.M. YOUNG, USA) was used to collect air temperature and relative humidity data. An ultrasonic anemometer (model 81000, R.M. YOUNG, USA) recommended by ASHRAE handbook for the meteorological parameters measurement (ASHRAE Standard Committee, 2017a), was able to measure both wind speed and direction. They were calculated from the difference in the times of flight of an ultrasonic pulse travel along two reverse directions on each axis. It should be noted that the monitored wind direction range is 0 to 360°, while the elevation range is limited to ±60°. A black globe thermometer (model HQZY-1, TJHY, China) was used to measure the black globe temperature. In addition, a set of net radiometers (model CNR4, KIPP&ZONEN, the Netherlands) consisting of three pyranometer and pyrgeometer arms were used to collect long-wave and short-wave irradiation from six directions (the upper, ground and lateral directions). The sampling interval for all parameters was set as 10 seconds for the first set of experiment. The sampling interval of the anemometer was changed to 1 second per data in the second and third set of experiment, which was the fastest sampling period of the anemometer.

Table 3.3 lists the general information about the temperature sensors and data loggers for the data collection of core and skin temperature. Fig. 3.4 shows the equipment used in the core temperature measurement. A non-digestible CorTemp thermometer was used to collect core temperature. The human subjects were required to swallow the CorTemp thermometer at least three hours before joining the experiment to allow the CorTemp thermometer reaching the stomach. The data logger was wore at the waist height in order to allow the receiver closer to the signal generator and avoid missing data. The sampling rate of core temperature was 10s per data, which was the fastest sampling rate of its data logger. Fig. 3.5 shows the equipment for skin temperature measurement. T-type thermal couple and ibutton were used in the measurement of skin temperature. The local body parts which were not covered by clothing was measured by T-type thermal couples. Those covered with clothing and not sensitive to the change of environment were measured using ibuttons, such as foot and pelvis. One side of the upper arms and legs were also measured with ibutton as reference. The sampling rate of ibutton was 4s per data. The sampling rate of ibutton was limited by the length of experiment time and the limited storage size. The sampling rate of thermal couple was set as 1s per data, in order to capture the sudden change of skin temperature.

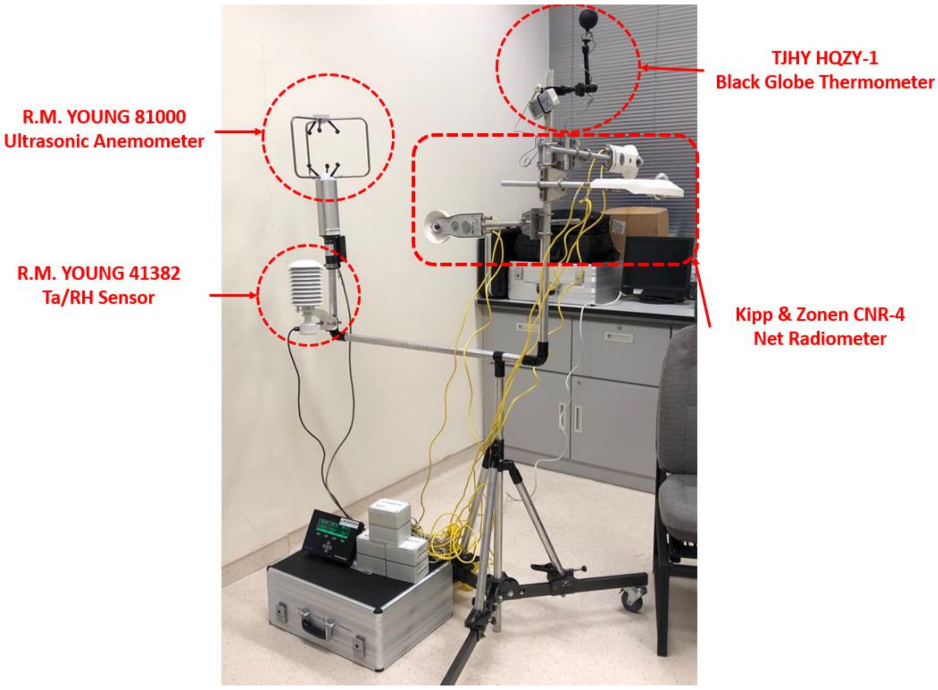


Figure 3.3 Microclimate station (Yongxin Xie et al., 2018)

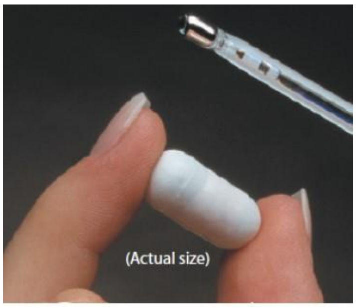


(a)

(c)

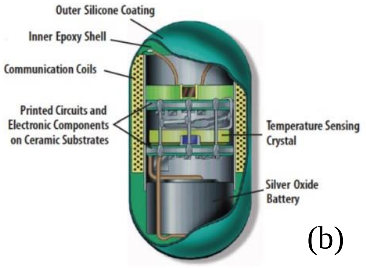


(b)

Figure 3.4 Equipment for core temperature measurement (a) CorTemp (HQInc, 2019) (b) inner structure of CoreTemp (HQInc, 2019) (c) HT150002 data logger (HQInc, 2019)

(a)

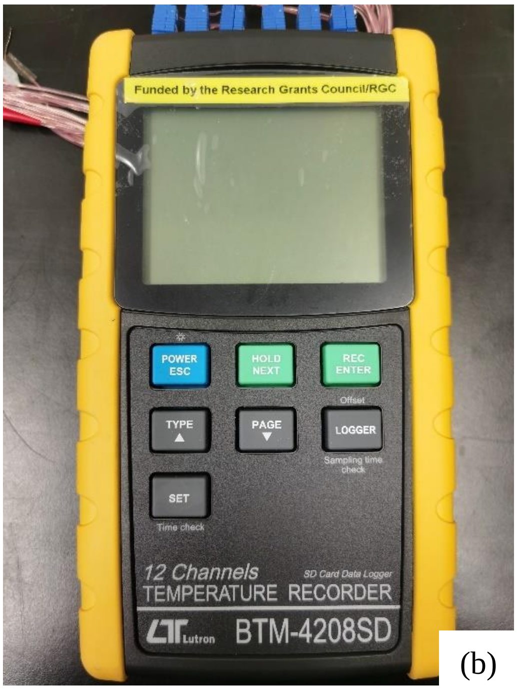


(b)



Figure 3.5 Equipment for skin temperature measurement (a) T type thermal couple; (b) data logger; (c) thermal resistance; (d) i-button

Table 3.2 Technical information of experimental equipment

| **Measured parameters** | **Sensor/Equipment** | **Range of measurement** | **Accuracy** |
|---|---|---|---|

| | | | |
|---|---|---|---|
| Air temperature ($T_a$) | RM 41382 | -50~50 °C | ±0.3 °C |
| Relative humidity ($RH$) | | 0~100 % | ±1 % |
| Wind speed ($v$) | R.M. YOUNG 81000 | 0~40 m/s | ±0.05 m/s |
| Long-wave radiation ($Q_l$) | Kipp & Zonen CNR-4 | -250~250 W | <10% |
| Short-wave radiation ($Q_s$) | | 0~2000 W | <5 % |

Table 3.3 Technical information of physiological data collection

| **Measured parameters** | **Sensor/Equipment** | **Range of measurement** | **Accuracy** |
|---|---|---|---|
| Core temperature ($\boldsymbol{T_c}$) | CorTemp ingestible thermometers (sensor) | +30~+45 ℃ | ±0.1 ℃ |
| | HT150002 (data logger) | 0~+50 ℃ | ±0.1 ℃ |
| Skin temperature ($\boldsymbol{T_{sk}}$) | i-button (DS1922L) | -40~+85 ℃ | ±0.5 ℃ |
| | TT-T-30-SLE (sensor) | -200~ 150 ℃ | ± (0.4 % or 0.5 ℃) |
| | BTM 4208 SD (data logger) | -50~ 400 ℃ | ± (0.4 % or 0.5 ℃) |
| | DataTaker DT 80 (data logger) | -270~+400 ℃ | ±0.1% |
| | TianJianHuaYi WZY-1 | -20~80 ℃ | ±0.3 ℃ |

### 3.2.5 Experiment procedure

#### 3.2.5.1 Elevated area (shaded) - open area (sunny) - elevated area (shaded)

The field survey of the first set of experiment was conducted from March 30th, 2016, to December 12th, 2016. A total of 25 survey dates were involved, covering the typical climate features of cool winter, hot summer, and the transitional seasons in southern China. On each survey day, human subjects were invited to experience different microclimates following the sequence from Site 1 to Site 3. Subjects were asked to spend 15 minutes on each site, sitting, standing, or slowly walking around within a specific area. The survey results that had a metabolic rate higher than 2.0 Met were abandoned in the data analysis. After a 15-minute adaptation to the given microthermal environment, each subject completed a thermal comfort questionnaire which was delivered to their mobile phone.

#### 3.2.5.2 Choose one outdoor condition to stay for a certain period of time

This set of field measurement was conducted from November 2017 to September 2018. The real-time meteorological data was collected by a micro-climate station. Parameters such as air temperature, globe temperature, relative humidity, wind speed, wind direction, long-wave irradiance, and short-wave irradiance were collected. The skin temperature of 17 local body parts were continuously collected. The temperature of pelvis, back, left foot and right foot which were not sensitive to slight thermal stimulations and covered by clothing were collected using the i-buttons. The other local body parts were measured using thermocouple or thermal resistance with a portable data logger. The skin temperature measurement sites are shown in Fig. 3.6. The data-logging interval for the skin temperature was 1 second. Detailed information of the skin temperature measurement sensors is listed in Table 3.3.

The data was collected from two cities, Hong Kong and Sydney. The experiment conducted in the campus of Hong Kong Polytechnic University belonged to the transitional seasons and hot summer, while the winter experiments were conducted in the campus of the University of Sydney. Both the selected campuses are located in the central area of the city. The human subjects were required to wear normal clothing suitable to the weather to join the experiment. About 30 minutes were allowed before the start of experiment for attaching the sensor and to allow the transient metabolic rate to reduce to a stable level. During the experiment, the human subjects were required to sit or stand, experience the specific outdoor thermal environment and fill in the survey. Fig. 3.2 shows two examples of experiment setup including the microclimate station, one in Sydney and one in Hong Kong. The microclimate stations used in two campuses were of the same type.

The survey focused on the perception of local and overall thermal sensation and thermal comfort, along with the collection of individual information (gender, age, height, weight, and clothing information). Ethical approval was obtained in both universities and the collected data was for research usage only. Each human subject experienced the specific outdoor environment for about 40 minutes and filled in the survey every 5 minute. An extended nine-point scale was adopted to evaluate the subject's thermal sensation and thermal comfort (Yongxin Xie et al., 2019). The onsite survey response and the collected local skin temperature data were then compared with the simulation data from the CBE model, detailed description of the model can be found in their previous studies (H. Zhang et al., 2010a, 2010b, 2010c;

Zhao et al., 2014).

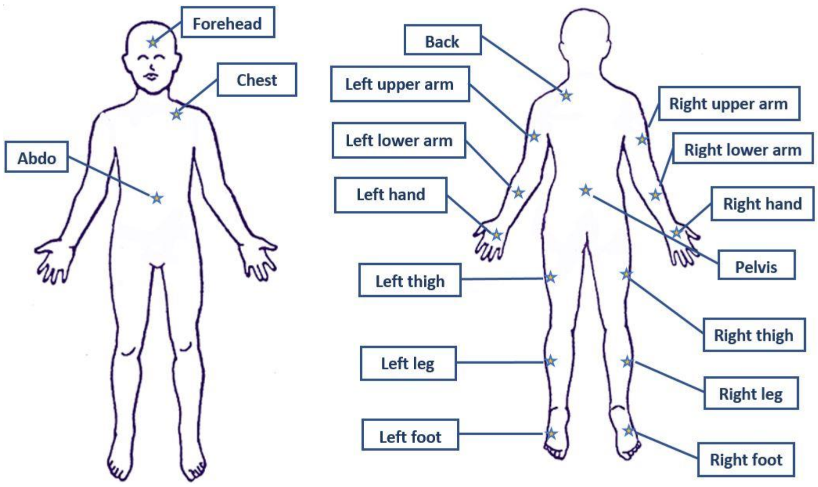


Figure 3.6 Measurement sites of local skin temperature

## 3.3 The calculation method of main parameters

### 3.3.1 The operative temperature ($T_{op}$)

The operative temperature $T_{op}$ describes the total sensible heat exchange by convection and radiation between human and ambient environment (ASHRAE Standard Committee, 2017a). As described in Equation (3.1), the operative temperature can be defined as the weighted average of the mean radiant and ambient air temperature. In this equation, the radiative heat transfer coefficient can be calculated by Equation (3.2), but it is not always possible to solve Equation (3.2) due to a lack of information for $T_{cl}$. Fortunately, $h_r$ is nearly constant for most conditions, and a value of $4.71\mathrm{W/m^2K}$ is sufficient for most calculations (ASHRAE Standard

Committee, 2010). However, the equations for estimation of $h_c$ are determined by relative wind speed. The highest wind speed for a standing person listed in the ASHRAE standard 55 table (ASHRAE Standard Committee, 2010) was 1.5 m/s, which was not applicable for some of our experimental conditions. Thus, de Dear's equation (R. J. de Dear et al., 1997) was referred in this study, in which the experimental wind speed for $h_c$ regression was up to 5 m/s. The estimation of $h_c$ is shown in Equation (3.3).

$$T_{op} = \frac{h_r T_{mrt} + h_c T_a}{h_r + h_c} \qquad \text{Equation (3.1)}$$

$$h_r = 4\varepsilon_p \sigma \frac{A_r}{A_D}(459.7 + \frac{T_{cl} + T_{mrt}}{2})^3 \qquad \text{Equation (3.2)}$$

$$h_c = 10.3v^{0.6} \qquad \text{Equation (3.3)}$$

### 3.3.2 The mean radiant temperature ($T_{mrt}$)

In the CBE model, it was assumed that a person was standing in an imaginary enclosed room (5 m × 5 m × 5 m) with different radiant temperatures of six wall surfaces. To simulate the asymmetric radiation condition in an outdoor environment, the long-wave data collected in six directions by the radiometers was used in the calculation of six directional radiant temperatures, $T_{mrt-i}$(i =1, 2, ⋯, 6). Then the equivalent temperatures of the six surfaces of the imaginary room were calculated. The radiometer was assumed to be at the center of the imaginary room, receiving equivalent radiation from the surface of the imaginary room. The surface of the radiometer facing in any one direction was assumed as a differential area, which formed an enclosure with those parts within the view in the imaginary room. Six surfaces formed six different enclosures. Within each enclosure, according to the method of calculating angle factor between a finite surface and a differential surface (Howell et al., 2010), six equations for calculating angle factors can be developed. The angle factor for the upper surface was 0.554126 in the imaginary enclosure and 0.111468 for the four lateral surfaces. Repeating this method in six directions, the equivalent surface temperature of the imaginary room can be obtained by solving the simultaneous linear equation of $T_{mrt-i}^4$ (i =1, 2, ⋯, 6) as shown in Equation (3.4).

$$T_{mrt-i}^4 = T_{s1}^4 F_{i-s1} + T_{s2}^4 F_{i-s2} + T_{s3}^4 F_{i-s3} + T_{s4}^4 F_{i-s4} + T_{s5}^4 F_{i-s5} + T_{s6}^4 F_{i-s6}$$

Equation (3.4)

### 3.3.3 The calculation of direct and diffuse solar radiation

One of the main differences of the thermal environment between the indoors and the outdoors comes from radiation. The main source of radiation in the indoor environment comes from long-wave irradiation (wavelength range equal to or longer than 3 μm); whereas, short-wave irradiation (wavelength range from 0.3 to 3 μm) is the main radiation source in the urban open space (Vignola et al., 2016). Meanwhile, long-wave irradiation cannot be neglected given the heat absorbed by the surroundings in the urban setting. Short-wave irradiation includes both the direct and diffuse solar irradiation (Vignola et al., 2016). The input of long-wave irradiation in the CBE model will follow the method described in Section 3.2.2, while the short-wave irradiation will be separated as direct and diffuse irradiation by the method described below. The pyranometer from CNR-4 gives the data of short-wave irradiation while the pyrgeometer gives the information related to long-wave irradiation. The global horizontal irradiance (GHI) was measured by the horizontal pyranometer facing sky, while the global titled irradiance (GTI) was measured by the north-facing pyranometer. When the surface is tilted with respect to the horizontal, the total irradiance comes from three aspects, which are the incident diffuse radiation on the titled surface, the direct normal irradiance projected onto the tilted surface and the ground-reflected irradiance that is incident on the tilted surface (Vignola et al., 2016).

By combining the measurement results facing the North and the sky together, DHI (diffuse horizontal irradiance) and DNI (direct normal irradiance) can be solved using the listed Equations (3.5-3.9) below and then as the inputs in the CBE model.

$$sza = 90° - elv \qquad \text{Equation (3.5)}$$

$$GHI_{upper} = DNI \cdot cos(sza) + DHI \qquad \text{Equation (3.6)}$$

$$cos(sza_r) = cos(T) \cdot cos(sza) + sin(T) \cdot sin(sza) \cdot cos(az - \gamma) \qquad \text{Equation (3.7)}$$

$$GTI = DNI \cdot cos(sza_r) + DHI \cdot (1 + cos(T))/2 + GHI \cdot \rho \cdot (1 - cos(T))/2$$

Equation (3.8)

$$\rho = GHI_{lower}/GHI_{upper}$$ Equation (3.9)

where:

$sza$: solar zenith angle, measured from the vertical to the solar position;

$elv$: elevation angle, measured from the horizon to the solar position;

$GHI_{upper}$: global irradiance received from the upper pyranometer;

DHI: diffuse horizontal irradiance;

DNI: direct normal irradiance;

$az$: the azimuthal angle;

$T$: the surface is titled by T degrees (with the north facing being 90° and the upper facing being zero);

$\gamma$: the surface is rotated by $\gamma$ degrees (with the north facing being 90° and the upper facing being zero);

GTI: the global tilted irradiance on a surface with a given tilt and azimuth orientation;

GHI: the global horizontal irradiance.

$sza_r$: the angle of incidence of the DNI with respect to the tilted surface;

$\rho$: the average albedo;

$GHI_{lower}$: the global horizontal irradiance received by the pyranometers facing ground;

$GHI_{upper}$: the global horizontal irradiance received by the pyranometers facing sky.

## 3.4 The statistic method

### 3.4.1 Unclear voting near thermal neutral range

An independent t-test was used to prove people had unclear voting near neutral status. A null hypothesis that people make no distinction among the categories of "slightly cool", "neutral" and "slightly warm" was made. The voting of these three categories was selected out of all the on-site results. Then, the original places of these categories were replaced by a set of random integers in the target ranges. The set of data which comprised of the original voting and random integers within target ranges was compared to the original set of data using an independent t-test. The null hypothesis would be satisfied when two sets of data were regarded as selecting from the same population from a statistical point of view ($p$-value > 0.05).

### 3.4.2 Probit analysis

The probit analysis was originally developed for the agricultural purpose, quantifying the toxicity of the pesticides. The response was binary: the insect was either dead or alive. This method was then extended with applications in analyzing thermal comfort field data starting from Charles Webb (Webb, 1959). The requisite binary response was obtained by separating the thermal response data into two groups (Nicol et al., 2012). In this case, the nine-point thermal sensation votes could be arranged in eight ways of response following the patterns listed in Table 3.4. Take the fourth row in Table 3.4 as an example, the Group 1 of the fourth row is the total percentage of people voting "cooler than neutral" while the Group 2 represents the total percentage of people voting "neutral and warmer". Grouping the data in the form of either Group 1 and Group 2 can be analysed in the same way, it is preferred to group the data in the manner of Group 2 in the following analysis.

The meaning of "Probit" is the probability unit. It describes the response probability to the certain stimulus which follows the normal distribution (Finney, & Tattersfield, 1952). In the field of thermal sensation, for any human subject, there will be a certain level of thermal stimulus intensity that below which the response does not occur and above which the response occurs. Such a value is designated as the threshold in this study. Though this threshold value varies from person to person for a certain level of thermal stimulus, when a group reaches a certain population, the distribution of threshold over the stimulus should have its own quantitative characteristics. The surveyed thermal sensation voting follows a normal distribution which fits the basic assumption of probit analysis, hence the probit analysis is used to reveal the characteristic of neutral thermal sensation for the Hong Kong residents.

If the intensity of the thermal stimulus is measured by λ, the distribution of thresholds may be expressed by Equation (3.10). $dP$ is a proportion of the whole population that consists of individuals whose thresholds lie between $\lambda$ and $\lambda + d\lambda$. If a thermal stimulus intensity $\lambda_0$ is given to the entire population, the proportion of response in the overall population is $P$, as stated in Equation (3.11). If $\lambda \in [0, +\infty]$, Equation (3.12) can be achieved. However, the physical explanation of one equation in the application of reality is what matters. For this consideration, the analysis shown in the result part will merely cover the real outdoor situation. When the response to the overall range of stimulus $f(\lambda)$ satisfies the assumption that it follows a normal distribution, Equation (3.10) can be written as Equation (3.13) and the sigmoid curve from probit regression can be generated (Finney, & Tattersfield, 1952).

$$dP = f(\lambda)\, d\lambda \qquad \text{Equation (3.10)}$$

$$P = \int_0^{\lambda_0} f(\lambda)\, d\lambda \qquad \text{Equation (3.11)}$$

$$\int_0^{\lambda_0} f(\lambda)\, d\lambda = 1 \qquad \text{Equation (3.12)}$$

$$P = \int \frac{1}{\sqrt{2\pi}\sigma} exp\, [-\frac{(\lambda-\mu)^2}{2\sigma^2}]\, d\lambda \qquad \text{Equation (3.13)}$$

$$P = \int_{-\infty}^{Y-5} \frac{1}{\sqrt{2\pi}} exp\,[-\frac{(\lambda)^2}{2}]\, d\lambda \qquad \text{Equation (3.14)}$$

$$Y = 5 + \frac{1}{\sigma}(\lambda - \mu) \qquad \text{Equation (3.15)}$$

Table. 3.4 Example of thermal sensation *v*ote combination

| **Group 1** | **Group 2** | **Abbreviation for Group 2** |
|---|---|---|
| P(-4) | P(3)+P(2)+P(1)+P(0)+P(+1)+P(+2)+P(+3)+P(+4) | P (TSV⩾-3) |
| P(-4)+P(-3) | P(-2)+ P(-1)+P(0)+P(+1)+P(+2)+P(+3)+P(+4) | P (TSV⩾-2) |
| P(-4)+P(-3)+P(-2) | P(-1)+P(0)+P(+1)+P(+2)+P(+3)+P(+4) | P (TSV⩾-1) |
| P(-4)+P(-3)+P(-2)+P(-1) | P(0)+P(+1)+P(+2)+P(+3)+P(+4) | P (TSV⩾0) |
| P(-4)+P(-3)+P(-2)+P(-1)+P(0) | P(+1)+P(+2)+P(+3)+P(+4) | P (TSV⩾+1) |
| P(-4)+P(-3)+P(-2)+P(-1)+P(0)+P(+1) | P(+2)+P(+3)+P(+4) | P (TSV⩾+2) |
| P(-4)+P(-3)+P(-2)+P(-1)+P(0)+P(+1)+P(+2) | P(+3)+P(+4) | P (TSV⩾+3) |
| P(-4)+P(-3)+P(-2)+P(-1)+P(0)+P(+1)+P(+2)+P(+3) | P(+4) | P (TSV = +4) |

The proportion $P$ under a certain thermal stimulus intensity $\lambda_0$ (Equation (3.13)) can be transferred to Equation (3.15) by a probit function Equation (3.14), $Y$ is the probit value of $P$ (Finney, & Tattersfield, 1952). $Y$ follows a normal distribution and has a mean value of 5 and a standard deviation of 1 (Finney, & Tattersfield, 1952). Further mathematic description about the probit transformation can be referred from the book by DJ Finney (Finney, & Tattersfield, 1952).

The eight ways of responses listed in Table 3.4 will produce eight probit regression lines which follow the pattern shown as Equation (3.15). $\frac{1}{\sigma}$ means the corresponding value change of the probability density function when the independent variable $\lambda$ change by one unit. The set of probit regression lines derived from different batches of thermal sensation voting data should be parallel, because the data follow the same normal distribution and have the same residual standard deviation of thermal sensation voting across the thermal stimulus range.

### 3.4.3 Logistic regression

Logistic regression was used in locating the meteorological parameters combinations for thermal neutral and thermal comfort status in the Hong Kong summer. Logistic regression was developed based on the logit transformation which was first introduced by Cox (Cox, 2018). The logit transformation dealt with the odds ratio as shown in Equation (3.16). Logit transformation was *ln (odds)* as shown in Equation (3.17) (Cox, 2018). The linear relationship between the independent variables and the dependent variables as shown in Equation (3.18) was able to be achieved through the logit transformation (Cox, 2018). Therefore, there is no need to make the linear relation assumption between the independent variables and the dependent variables. Equation (3.19) and Equation (3.20) were the transformations of Equation (3.18).

$$odds = P/(1 - P) \quad \text{Equation (3.16)}$$

$$Logit\ P = ln\ [\frac{P}{1-P}] \quad \text{Equation (3.17)}$$

$$Logit\ P = \beta_0 + \beta_1 x_1 + \beta_2 x_2 + \cdots + \beta_p x_p \qquad \text{Equation (3.18)}$$

$$P = \frac{\exp(\beta_0+\beta_1 x_1+\beta_2 x_2+\cdots+\beta_p x_p)}{1+\exp(\beta_0+\beta_1 x_1+\beta_2 x_2+\cdots+\beta_p x_p)} \qquad \text{Equation (3.19)}$$

$$1 - P = \frac{1}{1+\exp(\beta_0+\beta_1 x_1+\beta_2 x_2+\cdots+\beta_p x_p)} \qquad \text{Equation (3.20)}$$

$$Centered - z = z_0 - mean(z_0) \qquad \text{Equation (3.21)}$$

As the logistic regression aimed at dealing with the problems with a binary response, the thermal response from the survey was divided into two groups. The dependent variable $P$ was termed as the occurrence probability of the positive response in the logistic regression part. For the purpose of predicting thermal neutrality, the positive response was defined as when TSV was "-1 slightly cool", "0 neutral" and "+1 slightly warm"; other than the listed three TSVs were termed as zero response. For the purpose of predicting thermal comfort, the positive response was defined as TCV (thermal comfort vote) voted in the comfortable side; the zero response was defined as TCV voted in the uncomfortable side.

Only the meteorological parameters such as $T_a$ (air temperature), $T_{mrt}$ -$T_a$, $v$ (wind speed) and the product of these parameters were included as the independent variables. RH (relative humidity) was not included as RH remained almost constant throughout the whole summer in Hong Kong, except for the rainy days. The RH in Hong Kong summer was around 60% to 75%. The difference between $T_{mrt}$ (mean radiant temperature) and $T_a$, $(T_{mrt}-T_a)$ was used here to present the intensity of solar radiation. The higher the difference, the stronger the solar radiation is (T. P. Lin et al., 2012). The training data was selected from the survey response obtained on-site for two summers in Hong Kong. The highest clothing value in the selected data was limited to 0.48 clo, which represented the normal dressing pattern of Hong Kong residents during summer-time. The selected data covered the activity level up to 1.2 Met, mainly the sitting and standing conditions were considered.

As both the first-order parameters and their product terms were considered in the regression, multicollinearity problem should be considered. High level of multicollinearity was introduced by considering the product terms in the regression, which could produce large standard errors for the regression coefficients of the lower order variables (Aiken et al., 1991). To eliminate this effect, centered variables as the method in Equation (3.21) were used both in forming the product terms of the interaction effect and in the first-order variables for the logistic regression analysis (Aiken et al., 1991).

The concept of classification cutoff was used to distinguish the positive response from the logistic regression result. When $P$ was larger than the classification cutoff, the predictive response was termed as a positive response. The classification cutoff point was defined as the point where there had the highest sensitivity and specificity.

The ROC curve, which showed the relation between false positive rate and true positive rate, was utilized to find the classification cutoff (Allison, 2012). The result of the ROC curve is shown and discussed in the result part.

### 3.5 Setting of the CBE model

In the CBE model software, the collected personal details can be input in the body builder, such as height, weight, age, and gender. A clothing modeler was embedded in the CBE model, normal summer and winter clothing can be found in the clothing library. For each specific human subject, clothing as recorded in the survey was selected in the CBE simulation.

The air temperature and air speed can be set inside the imaginary room. The air temperature was set as uniform during the simulation, and the air speed had a maximum of 2 m/s. The asymmetric solar radiation condition was set using the "panel condition setting" in the software. To better simulate solar conditions, each panel in the imaginary room was set as a large window of 4.99 m width and height, with a 0.01 m wide wall frame. Each panel was set to the calculated surface radiant temperature according to its direction. The imaginary subject was located at the center of the room, in the actual standing direction as they were during the on-site experiment.

The short-wave irradiation was separated into direct normal irradiance (DNI) and diffuse horizontal irradiance (DHI) before being inputted in the solar setting of the CBE model. The absorption coefficient and emissivity were both set as 1.0 for the open window in the imaginary room to ensure the real radiant temperature as on-site. The albedo ($\rho$) was inputted in the solar setting.

# Chapter 4 Evaluation of a multi-nodal thermal regulation model for assessment of outdoor thermal comfort: sensitivity to wind speed and solar radiation

## 4.1 Introduction

This chapter evaluates a multi-nodal thermal regulation model for its application in the outdoor thermal environment. In this chapter, subjects' thermal sensation outdoors was surveyed and compared with the UCB model predictions. Meteorological parameters were monitored using a mobile weather station, and over a thousand human subjects' thermal sensation level were surveyed. Results point out that subjects were highly sensitive to the changes in wind speed, especially under low-radiation conditions. However, the UCB model failed to predict such a high sensitivity. Besides, subjects had a higher tolerance to high air temperatures in outdoor environments when the solar radiation was acceptable, but the UCB model over-predicted the TSV (thermal sensation vote) in such conditions. Both the on-site results and the predictions by UCB model showed that subjects were more sensitive to wind speed in hotter environments while they were the least sensitive to solar radiation in neutral thermal conditions. This chapter helps to reveal the potential of a multi-nodal thermal regulation model to address the asymmetric and transient features of outdoor environments and indicates the need of further refining the model for better quantitative prediction of outdoor thermal sensation.

## 4.2 Meteorological data analysis

Fig. 4.1 shows the meteorological data collected by the microclimate station in one typical survey day. The distribution of the solar radiation values from three survey sites are shown in Fig. 4.1 (a) to (c). The abbreviations in Fig. 4.4 (a-c): N, S, E, W, U, and D represent the direction of detected solar radiation, which are North, South, East, West, Up and Down respectively. A large variation of solar radiation was visible from six directions. These data were collected from 3:00 pm to 4:00 pm, for 15 minutes at each survey site. Although Sites 1 and 3 were sheltered by the underneath-elevated building block, the difference between these two sites was noteworthy. The solar radiation condition was greatly affected by the surrounding building clusters and sampling sites. There was a large directional difference in the radiation temperatures. The radiation temperature from the south was higher than that from the other directions at Site 1. It was followed by the radiation coming from the west. At Site 3, radiation from the south was slightly higher than the other directions, and radiation from the west was the lowest. Low radiation temperatures from the ground was detected at Sites 1 and 3; while, at Site 2, which received direct solar radiation, the radiation temperature from the ground was similar to that from the other directions. In the Site 2 dataset, the radiation temperatures from the upper side and the west were much higher than from other directions. Shadings can effectively reduce radiation coming from all directions, especially from the above.

Fig. 4.2 (d to f) shows the instantaneous distribution of wind speed, wind direction, and air temperature respectively. The air temperature at the three sites was fairly stable during the sampling time; the change remained within 0.5 ° C. The unstable parameters came from windy environments, especially for those in the urban area and surrounded by tall buildings. The highest wind speed was detected at Site 3. The transient wind speed could reach 7 m/s and generally stayed at around 2 to 3 m/s. The lowest wind speed was recorded at Site 2, which was around 0.4 m/s. Wind environment can differ greatly from location to location, even within one campus, affected by building arrangement and structure. The wind direction changed frequently during the survey period, but most of the time it stayed at the main direction as shown in the wind rose figure (Fig. 4.2). In the recording day, the wind mainly came from the NNE for Site 1, from the NW for Site 2, and from the WSW for Site 3. For Sites 1 and 3, the wind could pass through the underneath of the elevated building block without much obstruction. Thus, the wind followed the seasonal wind direction and fluctuated at a relatively stable range. Three buildings surrounded the measurement point at Site 2, so the wind flowed through Site 2 at pedestrian height was blocked.

The wind direction at Site 2, therefore, was more dispersed. Wind environments from the outdoor settings were much more complex than that indoors, introducing further uncertainty when defining thermal sensation and thermal comfort. For indoor thermal comfort studies, it is recommended that omnidirectional anemometers should be used for air velocity measurement to ensure the accuracy (ASHRAE Standard Committee, 2017a; Melikov et al., 2007). Limited by the measurement range of elevation angle in the ultrasonic anemometer of the microclimate station, measurement of omnidirectional air velocity might not be accurate where downdraft velocity was significant. An omnidirectional ultrasonic anemometer should be considered for further outdoor thermal comfort experiment.

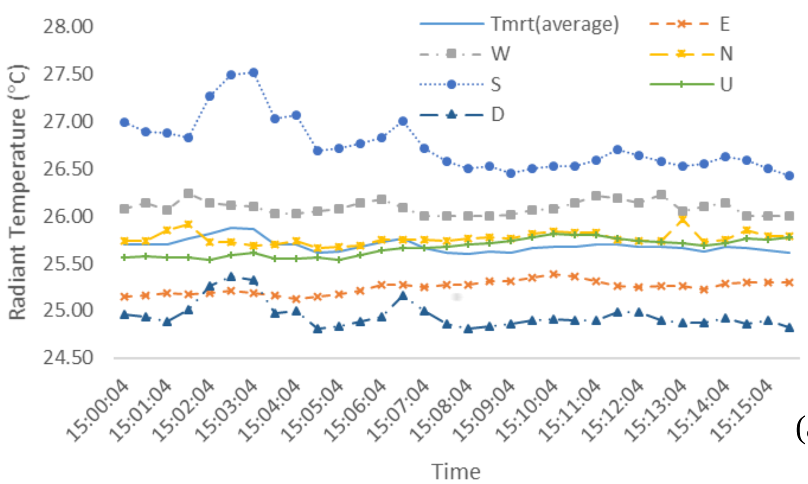

(a)

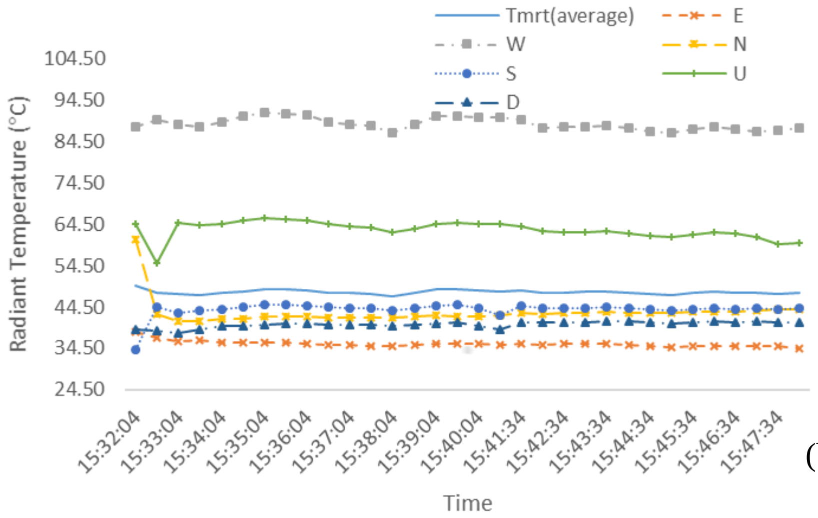

Tmrt(average)
E
W
N
S
U
D
Radiant Temperature (°C)
104.50
94.50
84.50
74.50
64.50
54.50
44.50
34.50
24.50
15:32:04
15:33:04
15:34:04
15:35:04
15:36:04
15:37:04
15:38:04
15:39:04
15:40:04
15:41:34
15:42:34
15:43:34
15:44:34
15:45:34
15:46:34
15:47:34
Time

(b)

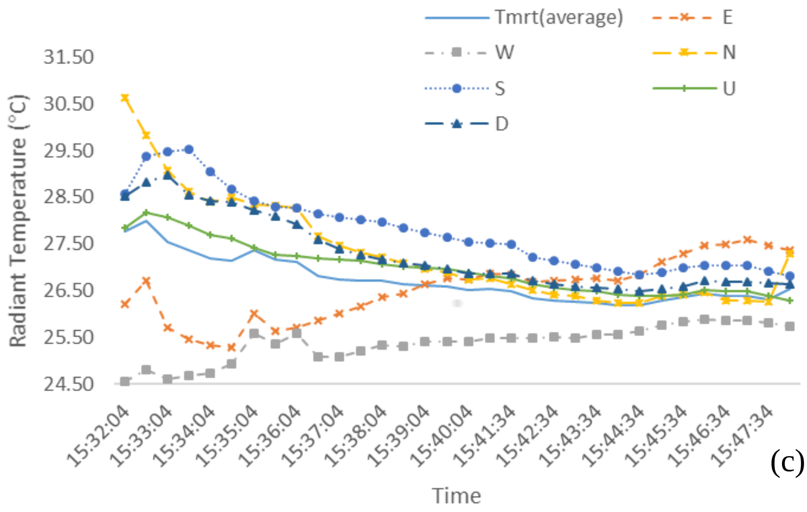

Tmrt(average)
E
W
N
S
U
D
Radiant Temperature (°C)
31.50
30.50
29.50
28.50
27.50
26.50
25.50
24.50
15:32:04
15:33:04
15:34:04
15:35:04
15:36:04
15:37:04
15:38:04
15:39:04
15:40:04
15:41:34
15:42:34
15:43:34
15:44:34
15:45:34
15:46:34
15:47:34
Time

(c)

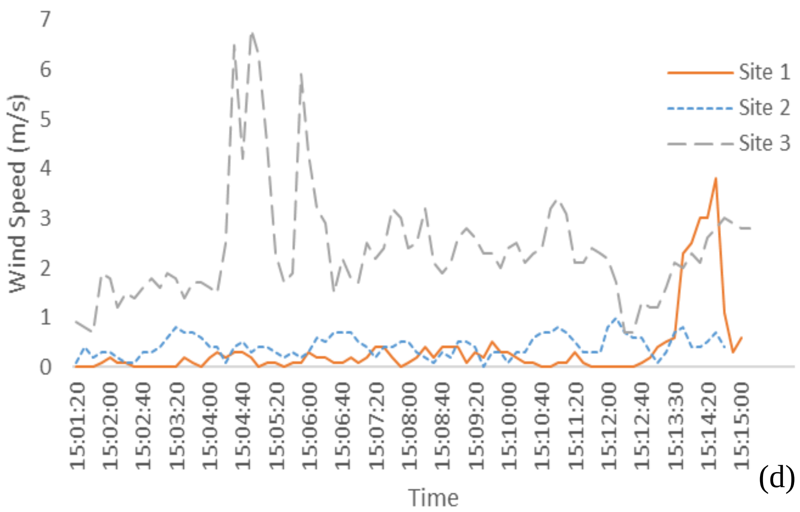

Wind Speed (m/s)
7
6
5
4
3
2
1
0
Site 1
Site 2
Site 3
15:01:20
15:02:00
15:02:40
15:03:20
15:04:00
15:04:40
15:05:20
15:06:00
15:06:40
15:07:20
15:08:00
15:08:40
15:09:20
15:10:00
15:10:40
15:11:20
15:12:00
15:12:40
15:13:30
15:14:20
15:15:00
Time

(d)

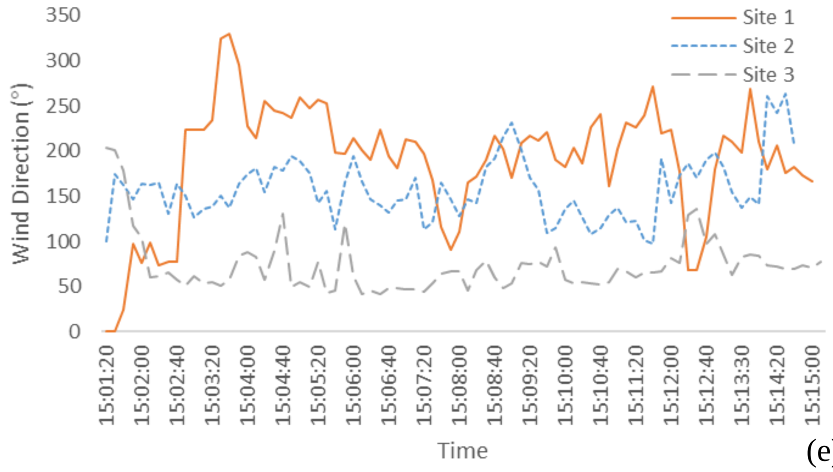


(e)

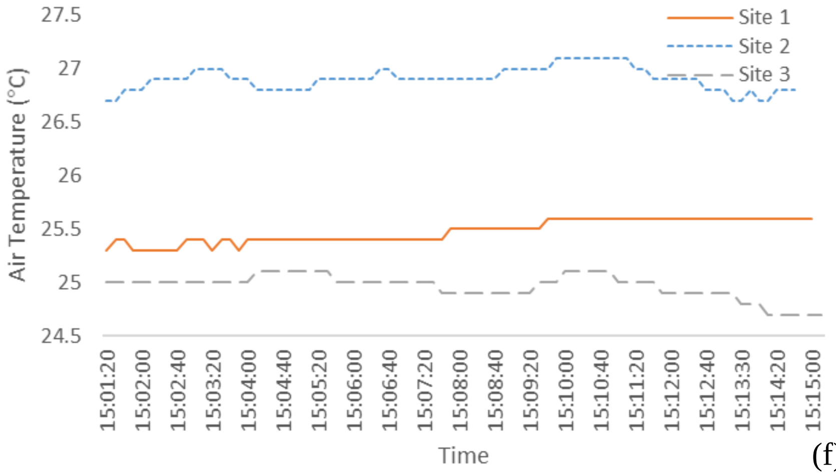


(f)

Figure 4.1 The meteorological data measurement results obtained by the microclimate station: (a) radiant temperature measured at Site 1; (b) radiant temperature measured at Site 2; (c) radiant temperature measured at Site 3; (d) wind speed measurement results for the three sites; (e) wind direction measurement results for the three sites; (f) air temperature measurement results for the three sites

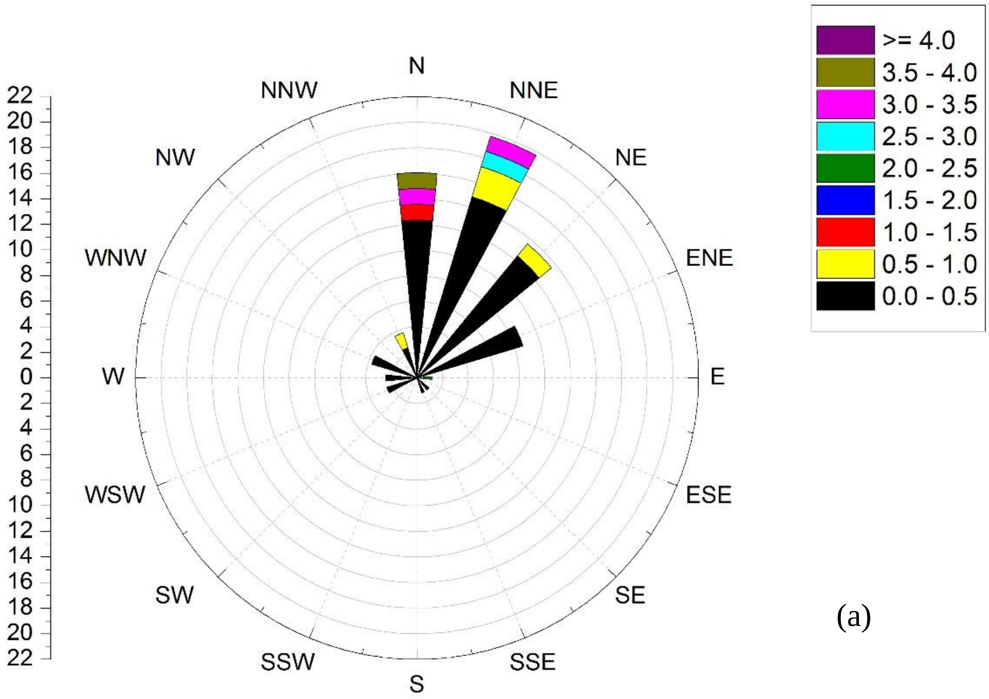
N
NNE
NE
ENE
E
ESE
SE
SSE
S
SSW
SW
WSW
W
WNW
NW
NNW
22
20
18
16
14
12
10
8
6
4
2
0
>= 4.0
3.5 - 4.0
3.0 - 3.5
2.5 - 3.0
2.0 - 2.5
1.5 - 2.0
1.0 - 1.5
0.5 - 1.0
0.0 - 0.5

(a)

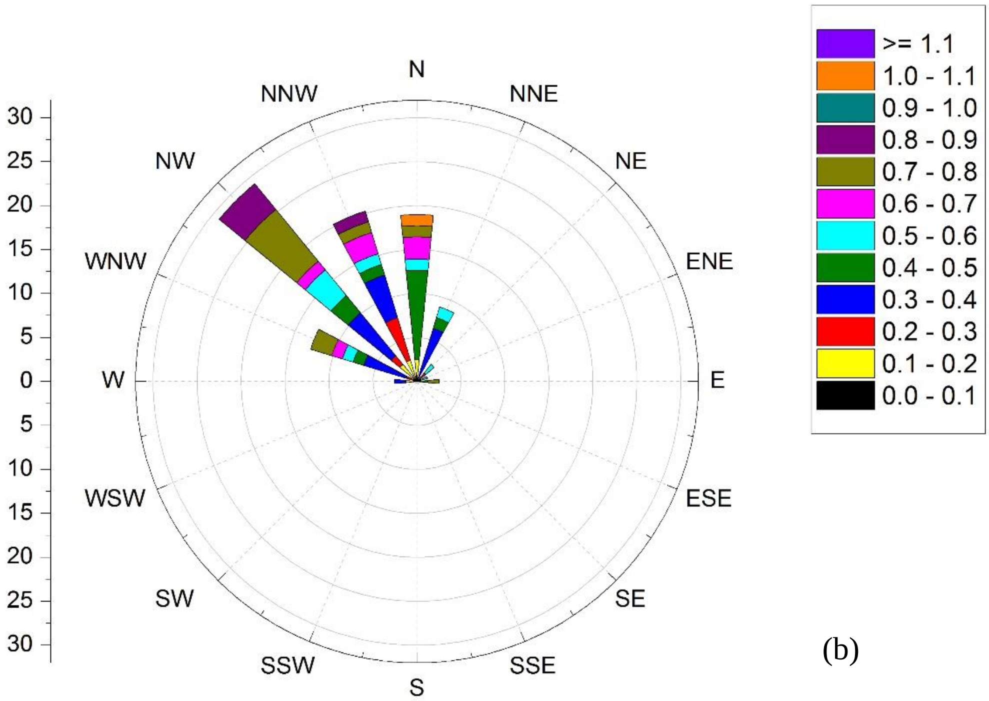
N
NNE
NE
ENE
E
ESE
SE
SSE
S
SSW
SW
WSW
W
WNW
NW
NNW
30
25
20
15
10
5
0
>= 1.1
1.0 - 1.1
0.9 - 1.0
0.8 - 0.9
0.7 - 0.8
0.6 - 0.7
0.5 - 0.6
0.4 - 0.5
0.3 - 0.4
0.2 - 0.3
0.1 - 0.2
0.0 - 0.1

(b)

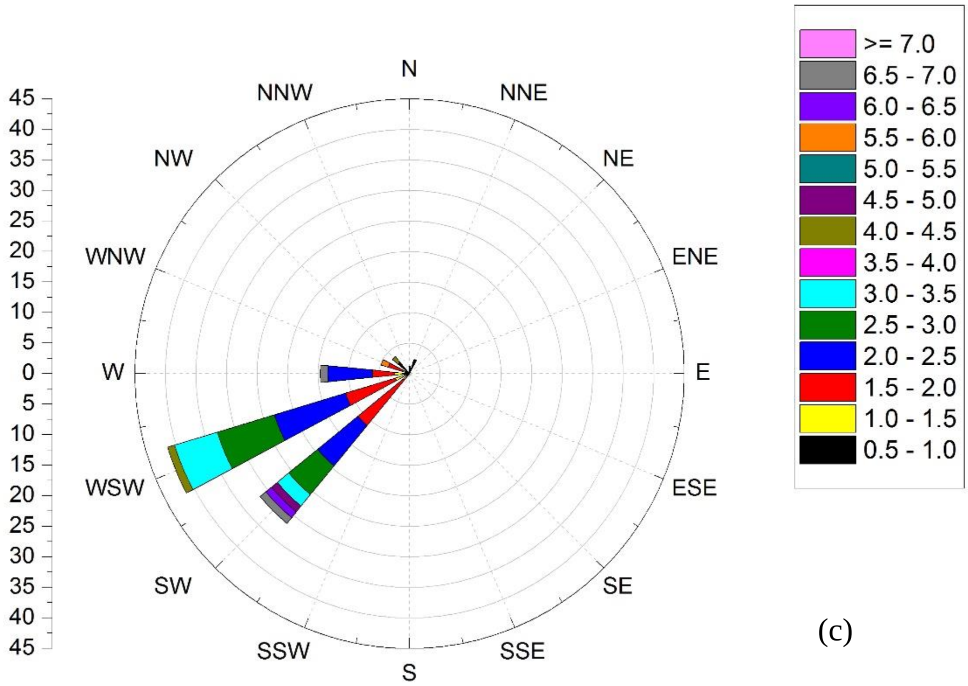


(c)

Figure 4.2 The wind rose distribution (a)Wind rose distribution at Site 1 (b) Wind rose distribution at Site 2 (c) Wind rose distribution at Site 3

### 4.3 Comparison of the surveyed TSV and the simulated TSV (by the CBE model) over the whole range of operative temperature

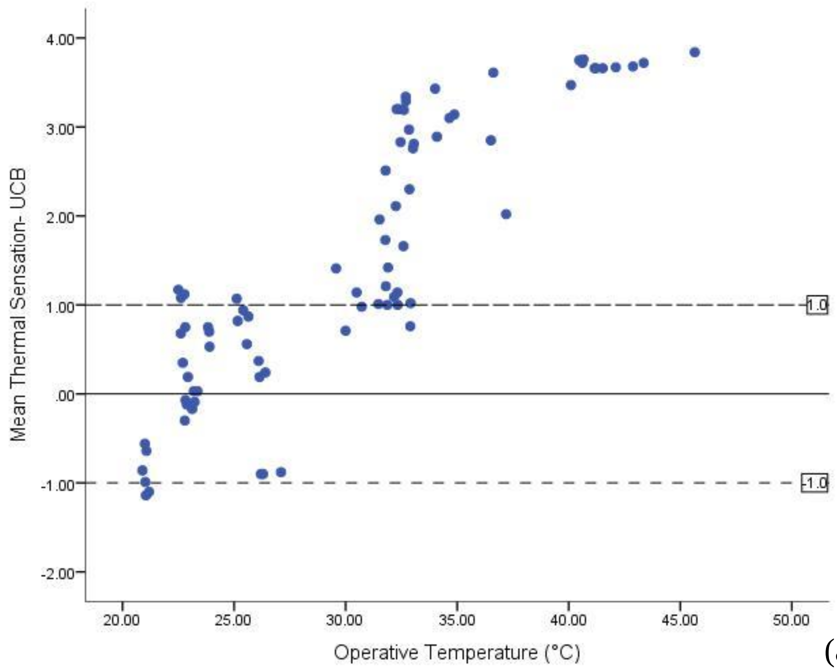


(a)

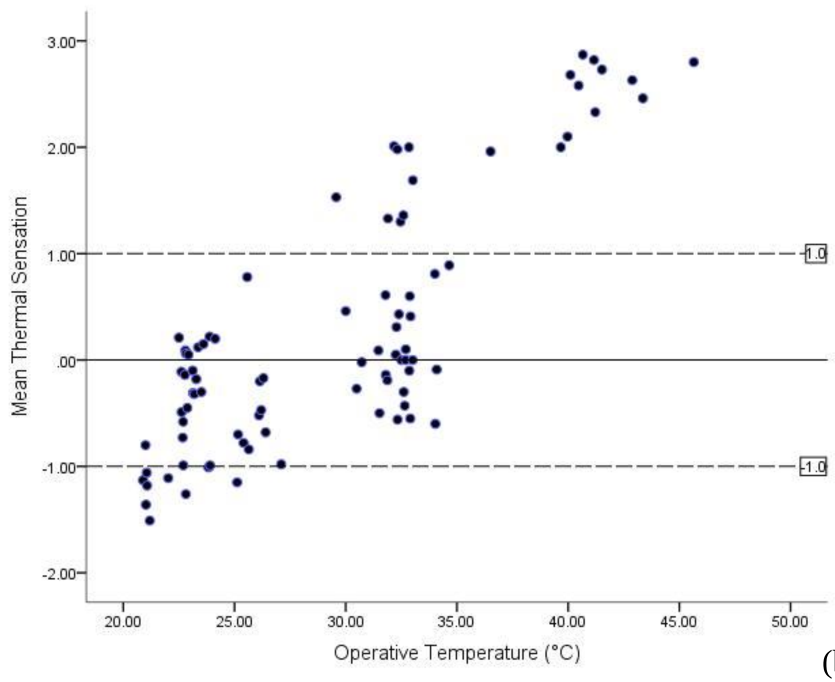


(b)

Figure 4.3 Thermal sensation data over the experiment period (a)Top vs TSV; (b)Top vs TSV-CBE

Fig. 4.3 presents the distribution of mean thermal sensation which covers all the experiment dates. Fig. 4.3 (a) covers subjects' actual thermal sensations from cool winter to hot spring in Hong Kong, which is a typical representation of hot and humid Asian climate. The collected air temperatures ranged from 21° C to 36 ° C. In 2016, Hong Kong had a warm winter, so thermal sensation in cold winter conditions was not able to be collected. However, the transitional seasons and the summer period during the experiment represent the city's typical climate. Fig. 4.3 (b) shows the CBE simulated TSV results.

When people expressed their thermal sensation in the range of acceptable conditions (between "-1 TSV" and "+1 TSV"), the mean operative temperature was 27 ° C. The corresponding operative temperature was 26° C when the simulated TSV remained at an acceptable range, which was close to the on-site survey result. Observed from Fig. 4.3 (a), the operative temperature which remained at acceptable condition was in the range of 20 ° C to 35 ° C. By contrast, most of the accepted TSV concentrated at around 25 ° C in the simulated TSV result. The range of acceptable operative temperature in the outdoors was much higher than that recorded indoors (in the literature, the range of acceptable temperature in an indoor environment was between 18 ° C and 26.8 ° C (Van Hoof, 2008)). The simulated TSV clustered at "+1 TSV" to "+3.2 TSV" when the operative temperature was in the range of 30 to 35 ° C (Fig. 4.3 (b)), which was much higher than the voted TSV. This phenomenon indicates that people have a higher tolerance for high temperatures when exposed to the outdoor environment.

It is interesting that there is a large variance shown in the range of voted thermal sensation around the operative temperature between 30 °C and 35 °C, from “-0.7 TSV” to “+2 TSV”. The long TSV span denotes that some factors in the outdoor environments could contribute more in decreasing subjects’ thermal sensation in the recorded cases. The authors’ previous study based on the climate characteristics of Hong Kong has pointed out solar radiation and wind speed were the two main factors that create thermal sensation difference of short-term exposure by comparing three microclimate conditions where air temperature and humidity remained similar (Huang et al., 2017). Thus, wind and solar radiation will be the focus of the following analysis.

In the range of 40 °C to 45 °C, where high solar radiation contributed to a further increase of operative temperature, the voted thermal sensation did not present an obvious increasing trend. The seven-point scale in ASHRAE standard 55 (ASHRAE Standard Committee, 2010) might not be appropriate for people to express their thermal sensation in hot summer outside, especially when high radiation circumstances are encountered. Instead, the nine-point scale used in the CBE model (H. Zhang et al., 2010c), adding “+4 TSV” and “-4 TSV” to express “too hot” and “too cold” respectively, is recommended for the application in the outdoor thermal comfort experiment and our further experiment.

## 4.4 Comparison of the surveyed TSV and the simulated TSV (by CBE model) over the change in wind speed

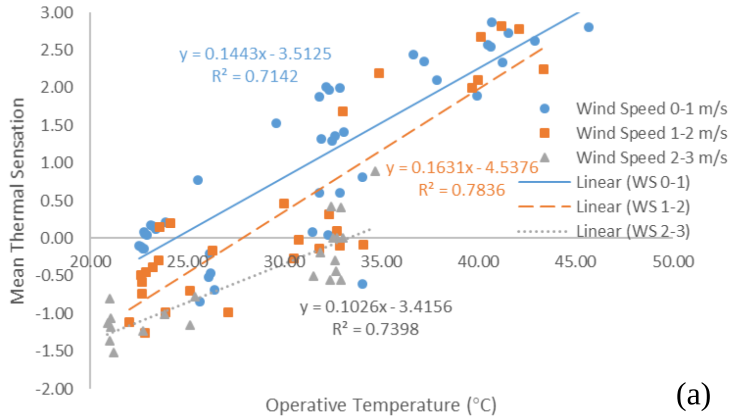


(a)

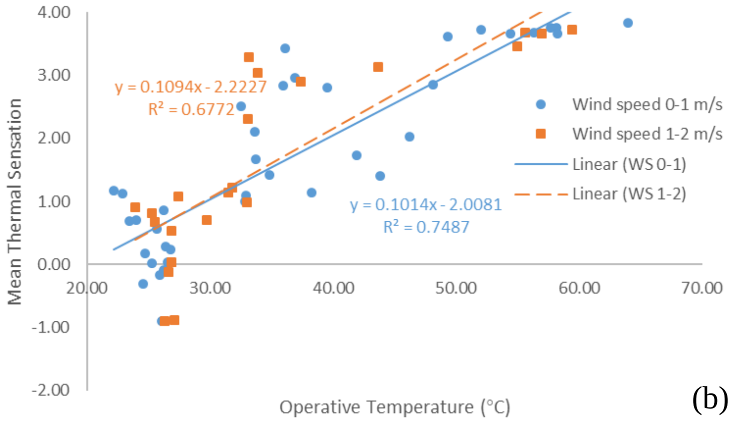


(b)

Figure 4.4 Comparison of the on-site TSV and the CBE-simulated TSV over a range of wind speeds (a) on-site data, (b) CBE data

To analyze the effects of wind speed in decreasing thermal sensation in outdoor environments, the collected data was split into three groups according to the level of wind speed in one experimental period. The group with the wind speed level lower than 1 m/s was termed the breeze group; between 1 m/s and 2 m/s was termed the mild wind group; and between 2 m/s and 3 m/s was termed the strong wind group. Generally, the strong wind group was only detected at Sites 1 and 3, where wind could blow through the elevated level. But the operative temperatures of Sites 1 and 3 were not as high as Site 2 due to the shading created by the elevated level. Thus, no data could be collected for the strong wind group when the operative temperature was high.

Linear regression was performed to describe the trend of thermal sensation with the increase of operative temperature. The R square for each linear regression was higher than 0.7. From Fig. 4.4 (a), it is obvious that when compared to the breeze group, the mild wind group made people feel cooler when the operative temperature remained the same. The cooling effect was stronger when the operative temperature was lower than 34 ° C. When the operative temperature was higher than 34 ° C, the cooling effect brought on by the increased wind speed was weakened. This was the interval where the radiant temperature was high. A t-test was conducted to verify the cooling effect of the increased wind speed within this interval. The p-value for the breeze group and the mild wind group was 0.098 (larger than 0.05), demonstrating that increasing the wind speed to mild wind group did not create a thermal sensation difference when the operative temperature was higher than 34 ° C. ANOVA analysis (An analysis of variance) was conducted to test the differentiation of the voted thermal sensation between the three wind speed groups. Only the data lower than 34 ° C was used in the analysis. They all satisfied the homogeneity test of variance, and thus the ANOVA result analyzed with the least significant difference (LSD) method was confidential. The p-value for the breeze and mild wind groups was 0.005 (lower than 0.05), indicating that increasing wind speed from 0-1 m/s to 1-2 m/s can create a significant thermal sensation difference. Similar results were found when the breeze and strong wind groups were compared. However, the p-value for the mild wind and strong wind groups was 0.092 (larger than 0.05), meaning that further increasing the wind speed from 1-2 m/s to 2-3 m/s did not make people feel cooler.

Considered the simulated thermal sensation results, only the breeze group and the mild wind group were simulated. Because the CBE model was developed in an indoor environment, where wind speed above 2 m/s rarely occurs, simulations of wind speed higher than 2 m/s were not able to be performed in the development stage of the CBE model software. The simulated thermal sensation result (Fig. 4.4 (b)) did not show any difference between two different wind speed groups. The dataset from the breeze group highly coincided with that of the mild wind group in full range of the operative temperatures. The t-test results supported this finding, with a p-value of 0.319 (much larger than 0.05). Increasing the wind speed from 0-1 m/s to 1-2 m/s did not create a difference in the predicted thermal sensation. It seems the cooling effect of increasing wind speed in an outdoor environment were more obvious than in the experimental results indoors. People were more sensitive to the changes in wind speed in the outdoors.

The most crucial part of the CBE model was building the prediction function of subjects' thermal sensation. The thermal sensation prediction model was developed from the dataset obtained from the local skin temperature control experiment, which was performed by controlling the air temperature within air sleeves (H. Zhang et al., 2010c). The heat was transferred to the air sleeves mostly through conduction. The cooling effect of air movement was weakened in the CBE model. Moreover, the highest tolerable wind speed was 0.8 m/s in an indoor environment, as recommended by ASHRAE 55 (ASHRAE Standard Committee, 2010). Wind speeds higher than this range lead to draft discomfort indoors. There is no doubt that the cooling effect of higher wind speeds was not the focus of the CBE model, as it was intended to predict thermal conditions indoors and in vehicles. Further experiments that combine the CBE model structure with the meteorological parameters and the physiological features of subjects in outdoor environments should focus more on the amendment of heat conduction and convection terms. The reasons that further increasing wind speed from 1-2 m/s to 2-3 m/s did not create thermal sensation difference should also be explained using physiological and psychological data.

## 4.5 Comparison of the surveyed TSV and simulated TSV (by the CBE model) over the change of solar radiation levels

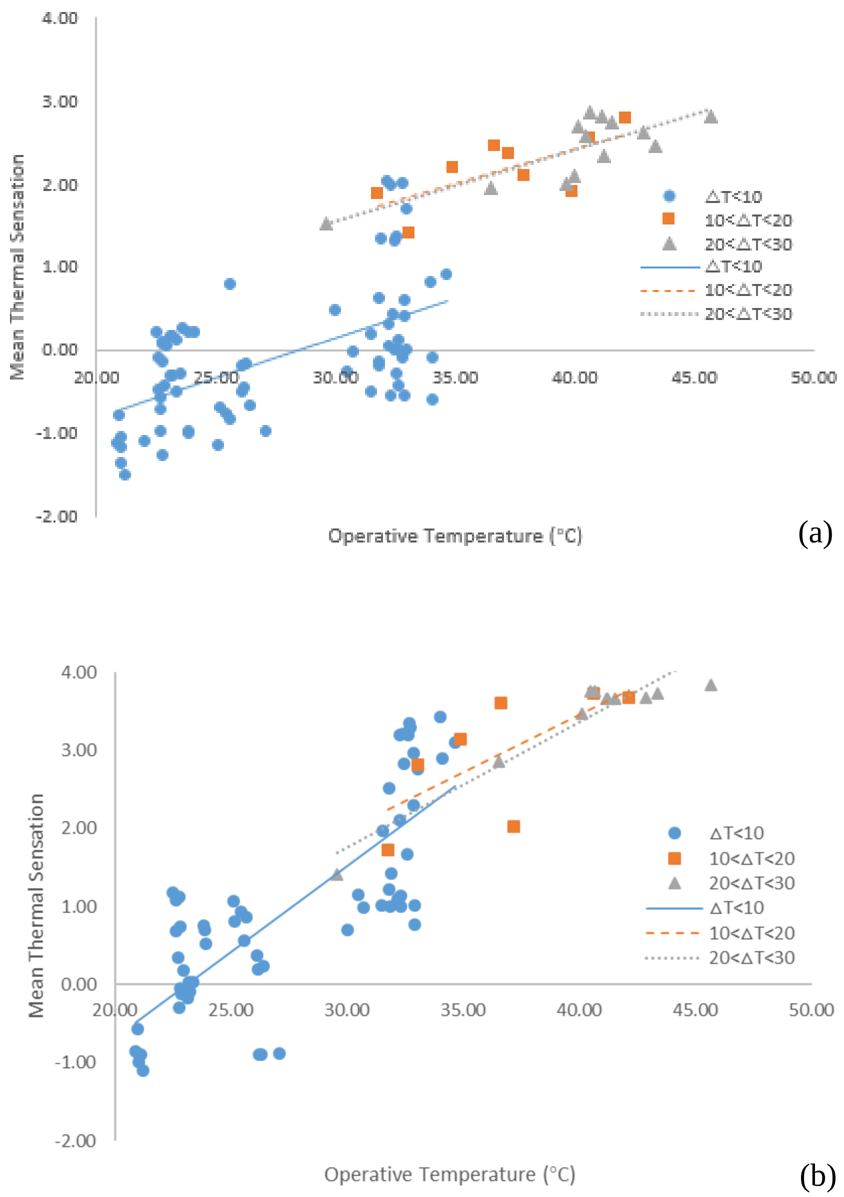


Figure 4.5 Comparison of on-site TSV and CBE-simulated TSV at different solar radiation levels (a) on-site data, (b) CBE data

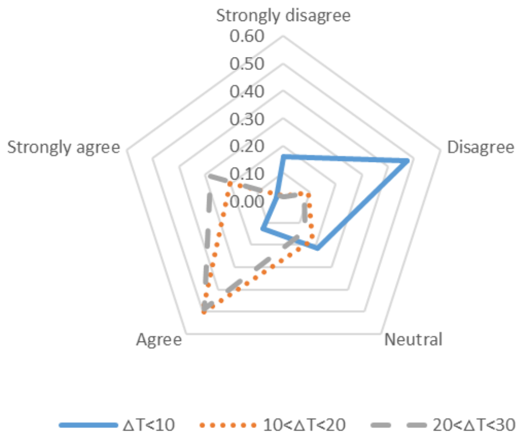


Figure 4.6 Percentage distribution of people's feelings on sun radiation

Fig. 4.5 shows the comparison of thermal sensation result difference (on-site surveyed data and CBE-simulated data) for different solar radiation levels. Solar radiation was divided into three groups according to the difference between mean radiant temperature and air temperature (ΔT). When ΔT was lower than 10 ° C, it was termed the low radiation group; when ΔT was between 10 ° C and 20 ° C, it was termed the mid radiation group; and when ΔT was between 20 ° C and 30 ° C, it was termed the high radiation group. The low radiation group only appeared in the operative temperature range of 20 ° C to 35 ° C, whereas the mid and high radiation groups appeared in the operative temperature range of 29 ° C to 45 ° C. The limitation of the distribution of different solar radiation levels was mostly attributed to the climate characteristics of Hong Kong.

From the on-site data (Fig. 4.5 (a)), it is obvious that the surveyed thermal sensation in the low radiation group is much lower than that in the mid and high radiation groups. It is interesting to note that although the operative temperature was as high as 30 °C to 35 °C, subjects still noted their thermal feelings to be acceptable (slightly warm) as long as the radiation level was low. However, this range of operative temperature was noted as unacceptable in indoor environments when the relative humidity was higher than 60% (ASHRAE Standard Committee, 2010) (in a typical summer of Hong Kong, the relative humidity is normally higher than 60%). This phenomenon indicates that people could better tolerate high air temperatures outdoors in the case of the radiation level was acceptable. In Fig. 4.5 (a), the trend line of the low radiation group is not in the same line as the mid and high radiation groups, but the slopes are similar. The sudden change of TSV demonstrates that even medium radiation could lead to intolerable hot feelings outdoors. Upgrading solar radiation from low- to mid-level could significantly increase people's thermal sensation levels. To understand subjects' feelings in radiation, the question "Do you agree that the sun is annoying?" was asked in the questionnaire. Five answers were provided: "strongly agree", "agree," "neutral", "disagree", and "strongly disagree". Fig. 4.6 shows the percentage of answers for each category. Nearly 50% of the subjects voted that the sun was not annoying when radiation was low. However, unpleasant feelings regarding sun radiation were strongly expressed when the radiation was medium or high.

Both the sudden increase of thermal sensation votes shown in Fig. 4.5 (a) and the change of subjects' opinions shown in Fig. 4.6 with increasing radiation levels illustrate that subjects were highly sensitive to the changes in the solar radiation level. People preferred a low radiation level and disliked even medium-level radiation. However, the trend lines of the low and mid radiation groups in the CBE-simulated thermal sensation results almost coincided. The leap in thermal sensation level when solar radiation changed from low to medium did not happen in the simulated result. The CBE model tended to give higher TSV results than the field-surveyed data in the low radiation group. Although the CBE model used an extended nine-point thermal sensation scale to ensure accurate expression of thermal sensation in extreme hot and cold environments, thermal sensation in a mild thermal environment should not be affected. However, the TSV from the CBE model was concentrated at the warm side, whereas the field-surveyed data was clustered at the cool side, in the operative temperature range of 20 °C to 25 °C. In the range of 30 °C to 35 °C of the low-radiation group, the CBE-simulated TSV was concentrated at "+1 slightly warm" and "+3 hot", whereas the field-surveyed TSV corresponding to those temperatures ranged from "-1 slightly cool" to "+1 slightly warm". The phenomenon observed in the survey was not reflected in the simulation data. According to the CBE model validation and the indoor survey results from Zhou et al. (Zhou et al., 2014), the discrepancy was only about 0.5 TSV scale unit. The CBE model seems to have larger discrepancy when predicting outdoor thermal sensation than indoor thermal sensation, especially under low-radiation conditions.

It is difficult to compare the CBE-simulated result and the on-site surveyed result when the operative temperature is high, owing to the application of different thermal sensation scales. However, both the surveyed points and the simulated points show that the TSV data for medium and high radiation coincide. There is no leap between the mid and high radiation groups.

### 4.6 Thermal sensation sensitivity to wind speed and mean radiation temperature

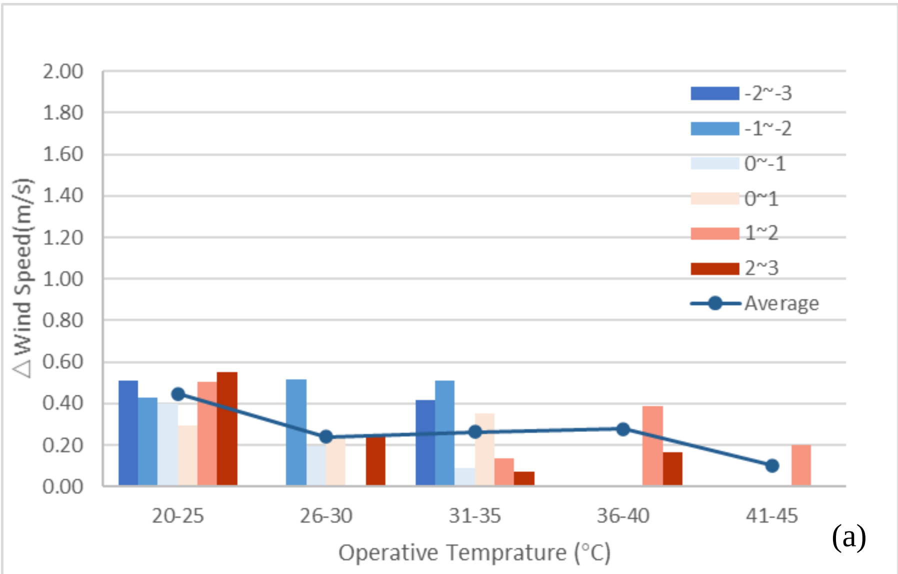

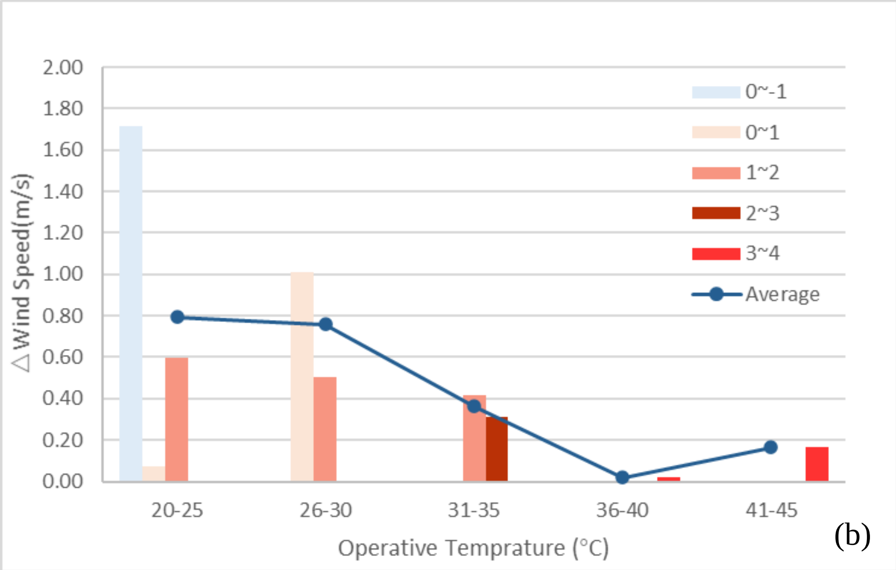

△Wind Speed(m/s)
2.00
1.80
1.60
1.40
1.20
1.00
0.80
0.60
0.40
0.20
0.00
0~-1
0~1
1~2
2~3
3~4
Average
20-25
26-30
31-35
36-40
41-45
Operative Temprature (°C)
(b)


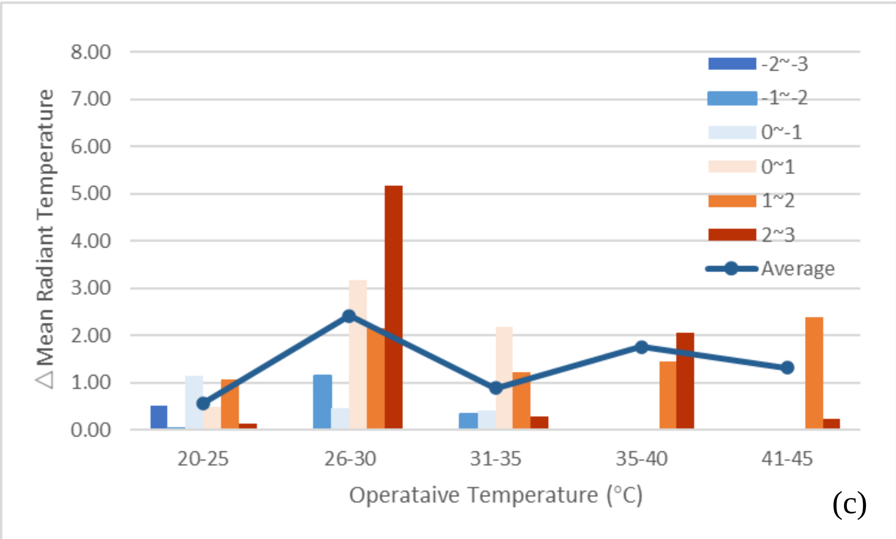

△Mean Radiant Temperature
8.00
7.00
6.00
5.00
4.00
3.00
2.00
1.00
0.00
-2~-3
-1~-2
0~-1
0~1
1~2
2~3
Average
20-25
26-30
31-35
35-40
41-45
Operataive Temperature (°C)
(c)

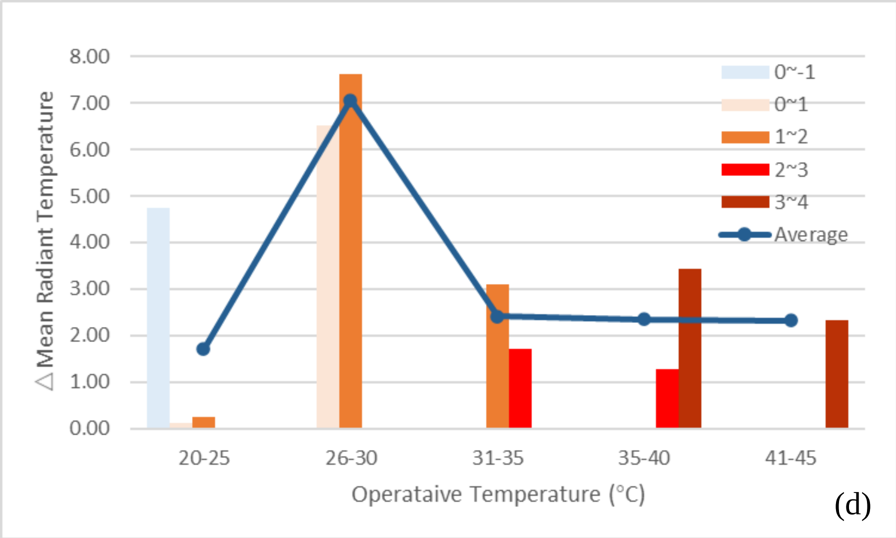


Figure 4.7 Thermal sensation sensitivity to wind speed (a: on-site data, b: CBE-simulated data) and mean radiation temperature (c: on-site data, d: CBE-simulated data)

This part of the study aims to discover thermal sensation sensitivity to wind and mean radiant temperature in different ranges of operative temperature. The whole dataset was separated into five groups of operative temperature, which spanned 5 °C each. Within each operative temperature group, the data were organized according to the level of thermal sensation. By changing each thermal sensation level, the change in mean radiant temperature or wind speed can be obtained. If the change in the observed parameter was large when the thermal sensation level changed one degree, the subjects were not sensitive to the observed parameter in the given range. On the contrary, if a slight change in the observed parameter can lead to a one-degree change in thermal sensation, the subjects were highly sensitive to the observed parameter.

When Fig. 4.7 (a) and (b) are compared, it is noticeable that the average change of wind speed causing a one-degree change of thermal sensation was much smaller than that of the CBE simulated result in each operative temperature range. As the CBE model was developed based on the experimental data obtained in the indoor chamber, the comparison result illustrates that subjects in the outdoor environment were more sensitive to the change of wind speed in the outdoors compared to the indoors. However, both two figures (Fig. 4.7 (a, b)) show much smaller scale in the change of wind speed when the operative temperature was higher than 40 °C. Thus, subjects became more sensitive to wind environment when the extreme hot condition happened in an outdoor environment. This finding is an explicit illustration that the city planners in the tropical and subtropical area should pay more attention to the wind environment in the neighborhood during the design stage. The building structures that improve air movement around building blocks, e.g. the elevated building block design in the campus of Hong Kong Polytechnic University, should be advocated.

Both the on-site data (Fig. 4.7 (c)) and the simulated data (Fig. 4.7 (d)) show that when the operative temperature was in the range of 26 °C to 30 °C, which was around the neutral state operative temperature (27 °C) in the outdoor environment, the subjects were less sensitive to solar radiation. The allowable change in mean radiant temperature in this range was much higher than that in any other operative temperature ranges. As shown in the on-site data (Fig. 4.7 (c)), a mean radiation temperature change of less than 2 °C can lead to a one-degree change in thermal sensation, except in the range 26 ° C to 30 ° C. This value was smaller than that of the simulated result. Hence, people in outdoor environments might be more sensitive to the changes in solar radiation than predicted in the CBE model.

The sensitivity comparison of the CBE-simulated result and the on-site surveyed result further illustrates that people were more sensitive to the changes in wind speed and solar radiation in outdoor environments than in indoor environments. The sensitivity to meteorological parameters varied under different operative temperature ranges. It cannot be generalized to one specific number. A reasonable inference is that the sensitivity of different body parts to these parameters might be changed with the range of operative temperature. The dominating body parts when defining overall thermal sensation might be varied as well. Therefore, based on the outline of the CBE model, for higher accuracy in predicting outdoor thermal comfort, further experiments in detecting skin and core temperatures and relating these physiological parameters to outdoor thermal sensations should be performed.

# Chapter 5 Further evaluation and development of a multi-nodal thermal regulation model for the usage in the micro urban environment

## 5.1 Introduction

This chapter presents a further evaluation of the multi-nodal thermal regulation model from the physiology point of view and discuss the possibility of adapting this model in the outdoor thermal environment. Skin temperature from 17 local body segments along with thermal perception feelings from human subjects were used in this analysis. We tested the multi-nodal thermal regulation model developed by the UC Berkeley through comparing its predictions of human body skin temperature, thermal sensation vote (TSV), and thermal comfort vote (TCV) with our onsite human subject measurements and questionnaire survey, in order to identify the causes of the errors between the prediction and measurements. Corresponding to the thermal neutral status, the field-measured data recorded wider local skin temperature ranges than the simulated ones. We proposed using a "null zone” instead of “set-point” in the thermal comfort model to accommodate the possible adaptation of human subjects to the highly fluctuating wind environment in open spaces. The forehead was suggested to be counted as one of the dominant local body parts when defining the overall thermal sensation. The correlation coefficient $R^2$ between the prediction and the field measured TSV improved to 93.7% for the revised model from 76.2% of the original model.

## 5.2 General description of the microclimate conditions

Table. 5.1 The microclimate condition distribution of experiment

| Location | Hong Kong | | | | Sydney | | | |
|---|---|---|---|---|---|---|---|---|
| | Mean | Max | Min | Standard deviation | Mean | Max | Min | Standard deviation |
| Air temperature ($T_a$, ℃) | 26.7 | 33.2 | 16.8 | 2.9 | 18.7 | 21.9 | 15.5 | 1.9 |
| Mean radiant temperature ($T_{mrt}$, ℃) | 31.5 | 57.6 | 16.9 | 9.8 | 41.6 | 56.3 | 15.8 | 13.0 |
| Wind speed ($\nu$, m/s) | 1.0 | 4.6 | 0.1 | 0.8 | 1.1 | 2.2 | 0.4 | 0.4 |
| Relative humidity ($Rh$, %) | 63.9 | 78.4 | 31.9 | 8.4 | 36.7 | 69.7 | 20.8 | 14.4 |

All the microclimate conditions in the available dataset are shown in Table 5.1. For the winter experiment in Sydney, $T_a$ (air temperature) was in the range of 15.5 to 21.9 ℃ and $T_{mrt}$ (mean radiant temperature) was in the range of 15.8 to 56.3 ℃. The ν (wind speed) was in the range of 0.4 to 2.2 m/s. Wind blew from the central Australia makes the winter in Sydney very dry, and the *RH* (relative humidity) was between 20.8 to 69.7%.

We also had limited winter experiment samples from Hong Kong, which covered the $T_a$ range of 16.8 to 19.8 ℃. The dataset from transitional seasons and summer recorded the $T_a$ range of 23.6 to 33.2 ℃. The $T_{mrt}$ was from 16.9 to 57.6 ℃ while ν was from 0.1 to 4.6 m/s. The RH was from 31.9% to 78.4%. The distribution of $T_{mrt}$ was either very closed to $T_a$ (heavy cloudy) or at its extreme level (cloudless), which explains the high level of standard deviation. The partly sunny or partly cloudy conditions were limited in our dataset. The mean wind speed in the experiment of Hong Kong was recorded in a wider range than that in Sydney, with twice the standard deviation than Sydney. Still, above 90% of the observed cases in Hong Kong concentrated below 2.14 m/s.

### 5.3 Primary comparison of the field data and the simulated data

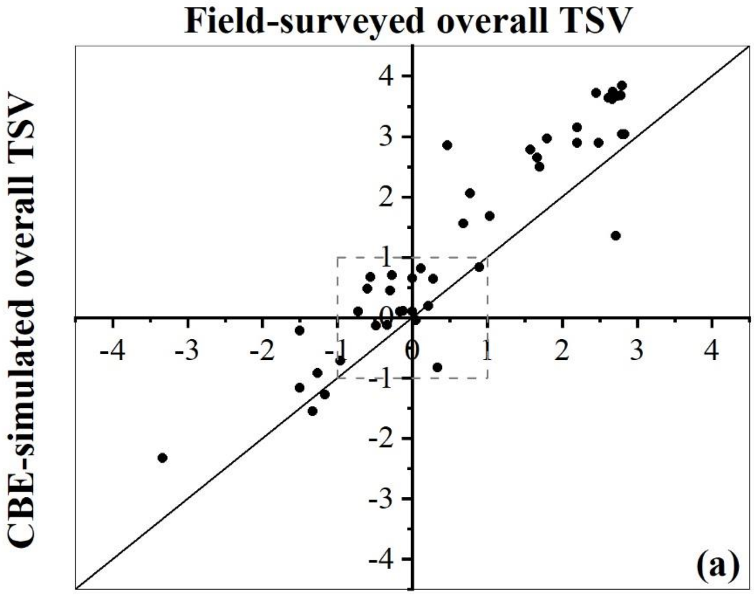


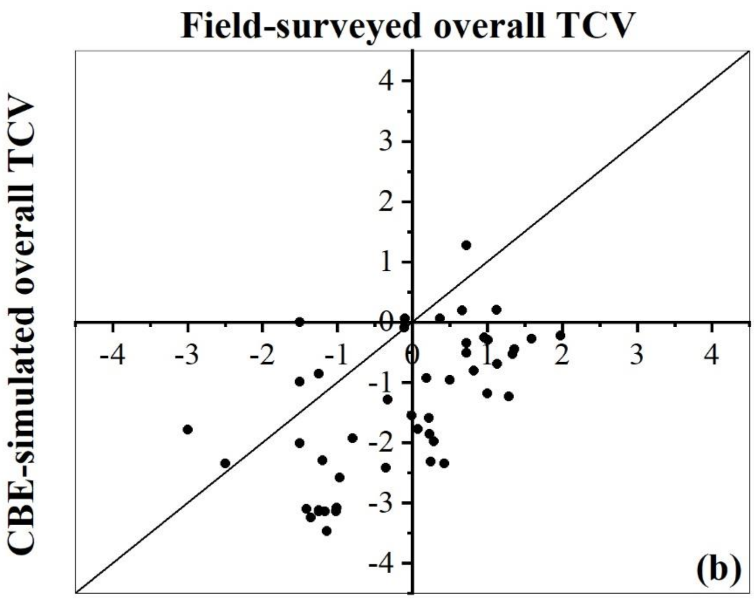


Figure 5.1 The relation between the field surveyed and simulated: (a) thermal

sensation vote (TSV); (b) thermal comfort votes (TCV). (*The simulated TSV and TCV data were obtained by using the measured environmental parameters, and the surveyed subject physiology data as inputs.)

The data comparison between the field-surveyed data, and the simulated data will be started with the primary comparison of the overall TSV (thermal sensation vote) and TCV (thermal comfort vote). The simulated results in were developed using the original CBE software and the meteorological parameters as input. Therefore, the simulated results in Fig. 5.1 are the comprehensive product of the 65-node thermoregulation model and the CBE comfort model. As an integrated environmental parameter, the operative temperature ( $T_{op}$ ) was chosen as the representative to make the primary comparison. Each point shown in Fig. 5.1 was the average result based on $T_{op}$. The $T_{op}$ coved the range of 15.7 to 45.7 ℃. The $T_{op}$ in both the winter of Sydney and Hong Kong were mild, the cases of below 20.0 ℃ were limited. Therefore, only minimal data points are located in the lower extreme level of field-surveyed thermal sensation. The following analysis will be focused on the dataset of transitional seasons and summer.

Our previous study has proved that thermal neutral status does not equivalent to "TSV = 0" through the independent t-test of comparing a field-surveyed dataset, which consists of more than one thousand samples and a randomly generated dataset.

The statistic results show that people make no distinction among the categories of "slightly cool", "neutral" and "slightly warm" (Yongxin Xie et al., 2019). In other words, people who stayed in the outdoor environment tended to vote from "slightly cool" to "slightly warm" in their thermal neutrality (Yongxin Xie et al., 2019). This finding provides us the evidence to define “TSV = -1” and “TSV = 1” also as thermal neutral status when an integer is used as the survey input. Though the CBE model generates continuous voting, this study used the same range in defining thermal neutrality to unify the criteria for comparison.

Fig. 5.1 shows the comparison results of the thermal sensation vote. The simulated data points locate almost above the 45-degree line, indicating that the simulated data are higher than the field-surveyed data covering the whole range. In the thermal neutral status, almost all the simulated data located in the TSV > 0 side when the field-surveyed data voted in the range of [-1,1]. Extreme simulated data points existed when the field-surveyed data was in the range of [0,1].

From the aspect of thermal comfort (Fig.5.1 (b)), the CBE-simulated TCV was calculated in the stable phase. The rule of calculating overall TCV in a transient environment (H. Zhang et al., 2010b) was not applied here. Because the transient thermal environment mentioned in most of the thermal comfort studies refers to the case of transient changing of temperature, which is not applicable to our case.

Regarding the wind environment, if wind speed keeps fluctuating in a limited range (no gust wind happens), such a case is referred to as enhanced convective heat transfer but not transient thermal environment. Furthermore, the existing studies are not able to describe the convective heat transfer effect of the outdoor wind environment due to limited experiment results in high turbulent intensity, needless to mention the transient effect by gust wind (R. J. de Dear et al., 1997). In the wind tunnel experiment from Yu et al. (Yu et al., 2019), they have confirmed that stronger heat transfer process existed under high turbulence intensity level. Therefore, we remained using the TCV results in a stable phase for comparison. The field survey results had more than half of the points located on the comfort side. Most of the surveyed responses located on the uncomfortable side were quite close to "TCV = -1", which corresponded to "slightly uncomfortable". More data points located on the comfortable side than in the thermal neutral zone, meaning people still feel thermally comfortable even when the thermal status is slightly away from the thermal neutrality in the outdoor environment. Compared with the field-surveyed results, most of the CBE-simulated results located on the uncomfortable side, and some were closed to the lower extremity.

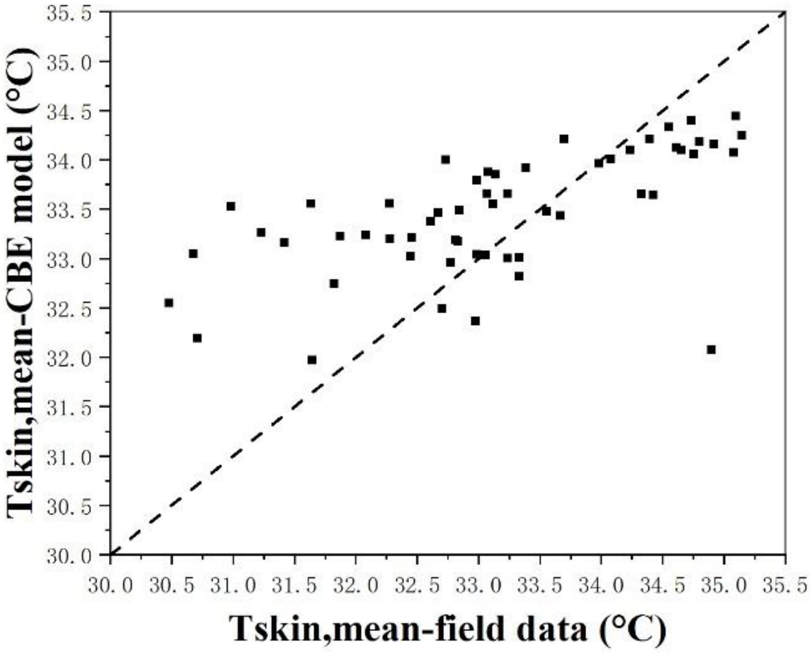


Figure 5.2 Comparison between the measured and simulated mean skin temperatures ($T_{skin,m}$)

The comparison results of field measured, and CBE-simulated $T_{skin,m}$ (mean skin temperature) are shown in Fig. 5.2. The CBE-simulated mean skin temperature was the simulation results of the multi-nodal thermal regulation model based on the meteorological parameters. The CBE dataset was well reported by other researchers of having higher predictive value than their datasets (Z. Wang et al., 2019; Zhou et al., 2014). However, from our comparison results, the measured and simulated $T_{skin,m}$ were similar in the range of 32.5 and 34.0 ℃. The measured $T_{skin,m}$ was much lower than the simulated data when lower than 32.5 ℃ and higher than the simulated data when higher than 34.0 ℃. The results here show that the prediction gap exists between the multi-nodal thermal regulation model and the field-measured data. And the main difference exists in the cold case. We compared our results with that from the mild cases conducted in the outdoor environment of Tianjin listed in the study of Lai et al. (Lai et al., 2017a), within which the mild cases refer to $T_a$ from 13.8 to 22.3 ℃ with the average solar radiation of 226.8 $W/m^2$. The meteorological conditions of the mild cases in Tianjin was similar to our experiment conditions in winter. The measured $T_{skin,m}$ from their study in the mild case was from 30.5 to 32.0 ℃ (Lai et al., 2017a), which was similar with our measurement results in the winter and supported the accuracy of our measurement results. We intended to use $T_{skin}$ as the bridge to link the meteorological parameters and the thermal sensation response. The measured skin temperature will be the input parameters in the CBE comfort model instead of the collected meteorological parameters to avoid the prediction difference generated by the multi-nodal thermal regulation model.

## 5.4 Comparison of the thermal sensation based on local and mean skin temperatures

This part will focus on the comparison of the field-measured, and the CBE-simulated thermal sensation votes, both the local and overall TSV will be discussed (shown in Fig. 5.3 (a-h)). The CBE-simulated TSV, including the local TSV and the overall TSV (Fig. 5.3 (a-h)), were generated using the measured skin temperature as input to the CBE comfort model. The CBE comfort model was reproduced using Matlab based on the original logic, set-points, and the listed coefficients from their previous publications (H. Zhang et al., 2010a, 2010b, 2010c; Zhao et al., 2014). The updates of the model detail were also addressed [34]. The reproduced CBE comfort model was validated using the simulated datasets from the original CBE comfort software. The relation between the overall TSV and $T_{skin,m}$ (mean skin temperature) will be discussed along with the local TSV of seven body parts used in the calculation of $T_{skin,m}$ (H. Zhang, 2003). The mean skin temperature was calculated using the 7-point method, the same as which used in the CBE model (H. Zhang, 2003). The seven local body parts used in the 7-point method, such as forehead, abdomen, left lower arm, left hand, left upper leg, left lower leg, and left foot were included in the analysis.

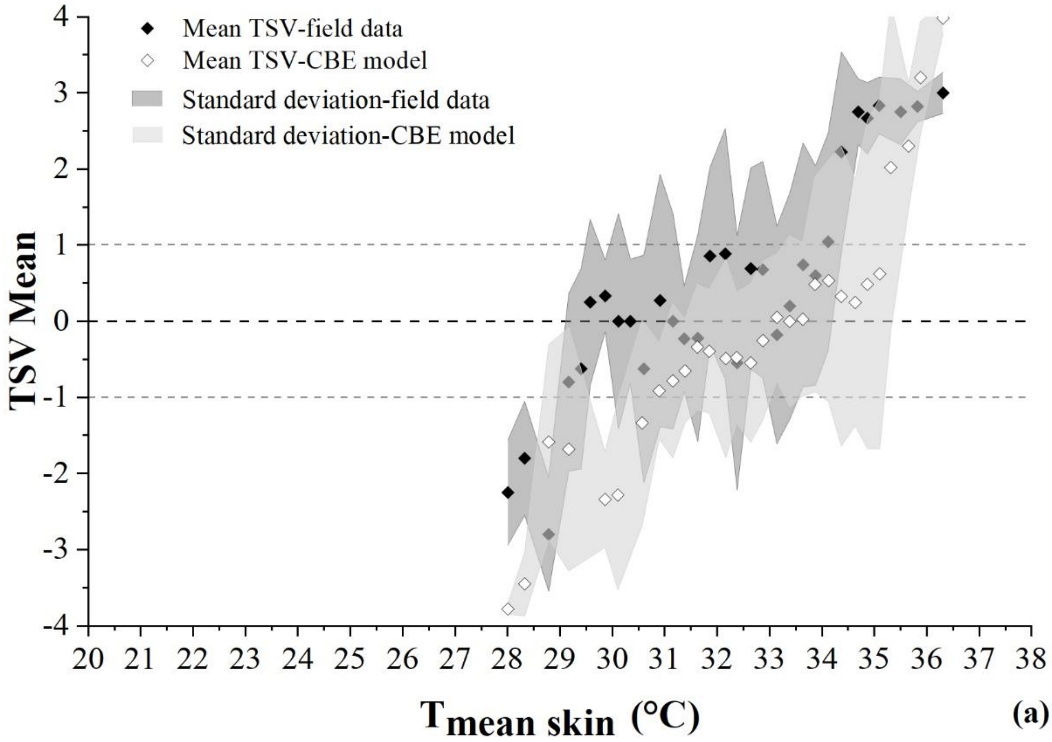
Mean TSV-field data
Mean TSV-CBE model
Standard deviation-field data
Standard deviation-CBE model
TSV Mean
Tmean skin (°C)
(a)

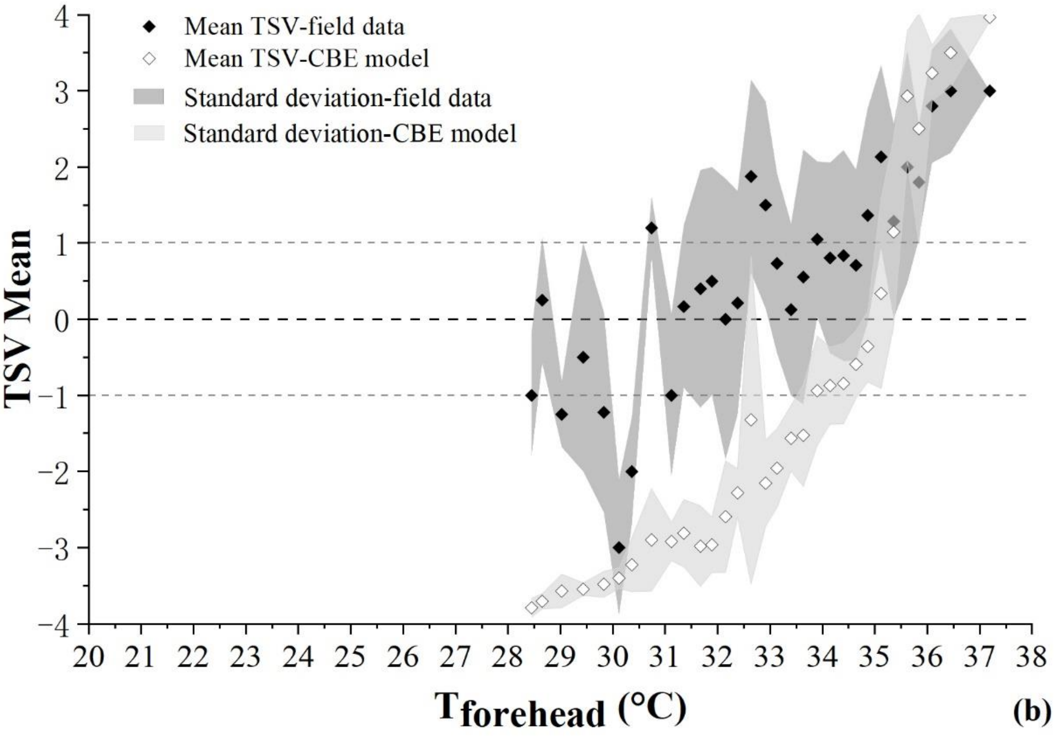
Mean TSV-field data
Mean TSV-CBE model
Standard deviation-field data
Standard deviation-CBE model
TSV Mean
Tforehead (°C)
(b)

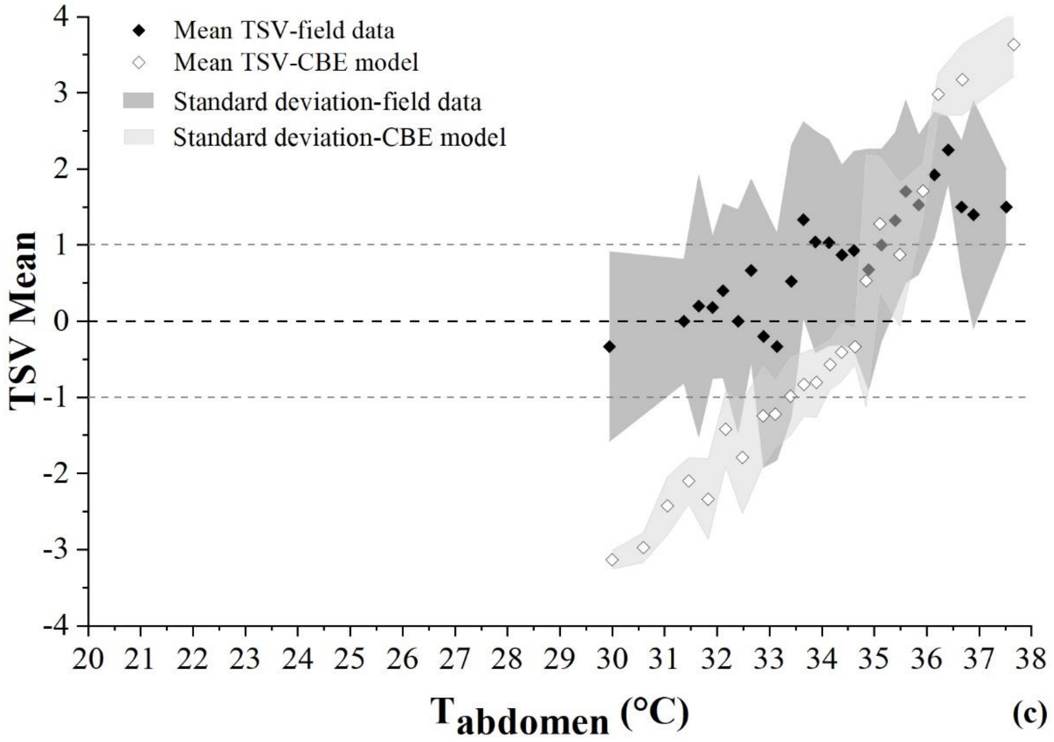
Mean TSV-field data
Mean TSV-CBE model
Standard deviation-field data
Standard deviation-CBE model
TSV Mean
4
3
2
1
0
-1
-2
-3
-4
20 21 22 23 24 25 26 27 28 29 30 31 32 33 34 35 36 37 38
T abdomen (°C)
(c)

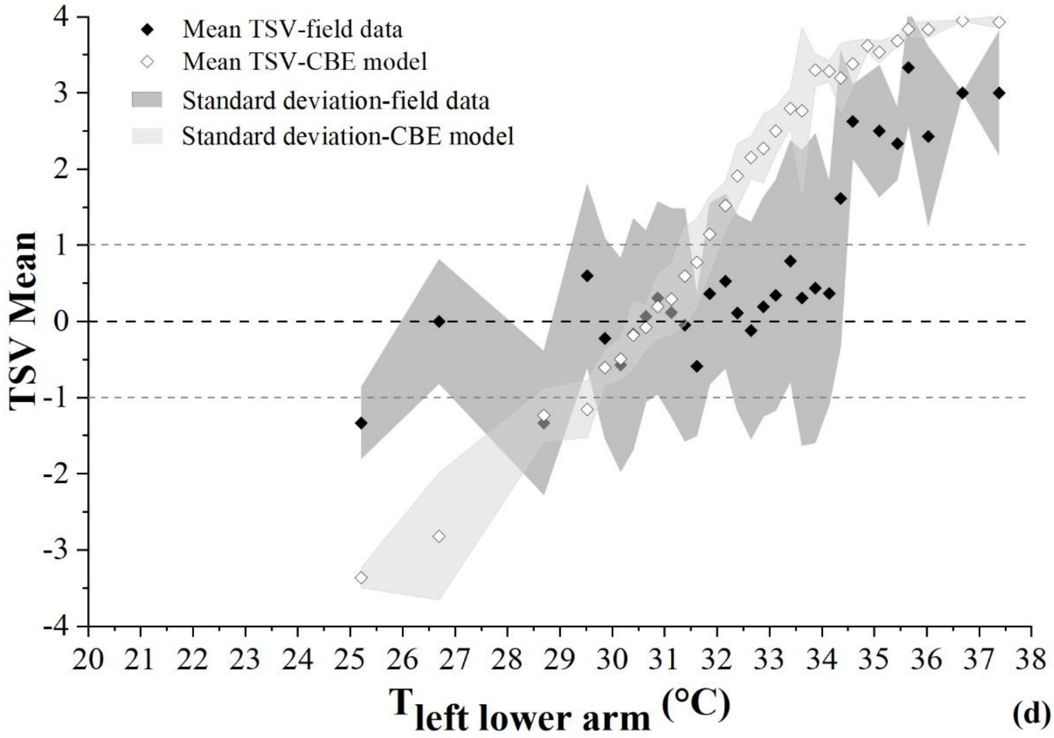
Mean TSV-field data
Mean TSV-CBE model
Standard deviation-field data
Standard deviation-CBE model
TSV Mean
4
3
2
1
0
-1
-2
-3
-4
20 21 22 23 24 25 26 27 28 29 30 31 32 33 34 35 36 37 38
T left lower arm (°C)
(d)

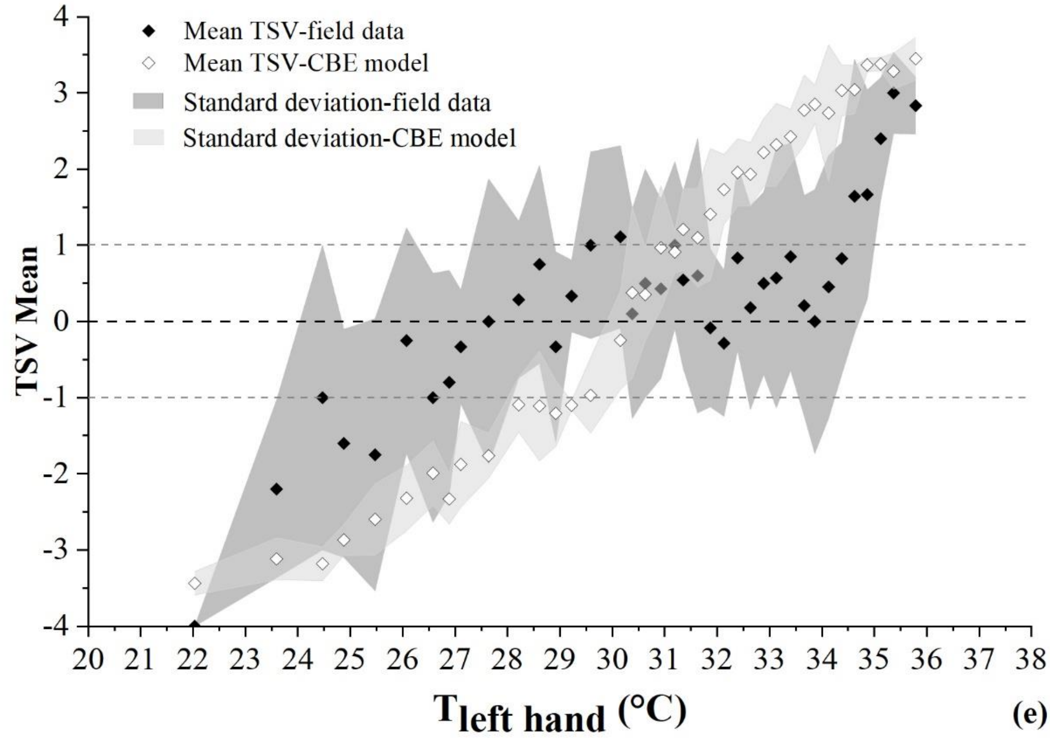
Mean TSV-field data
Mean TSV-CBE model
Standard deviation-field data
Standard deviation-CBE model
TSV Mean
$T_{left\ hand}$ (°C)
(e)

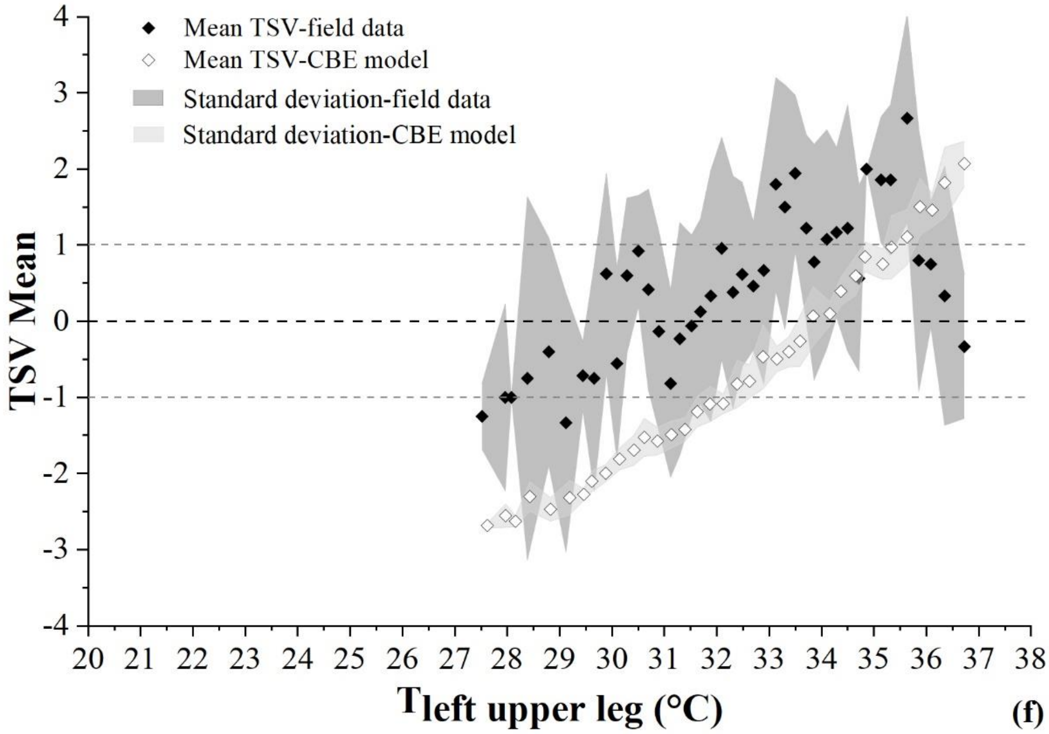
Mean TSV-field data
Mean TSV-CBE model
Standard deviation-field data
Standard deviation-CBE model
TSV Mean
$T_{left\ upper\ leg}$ (°C)
(f)

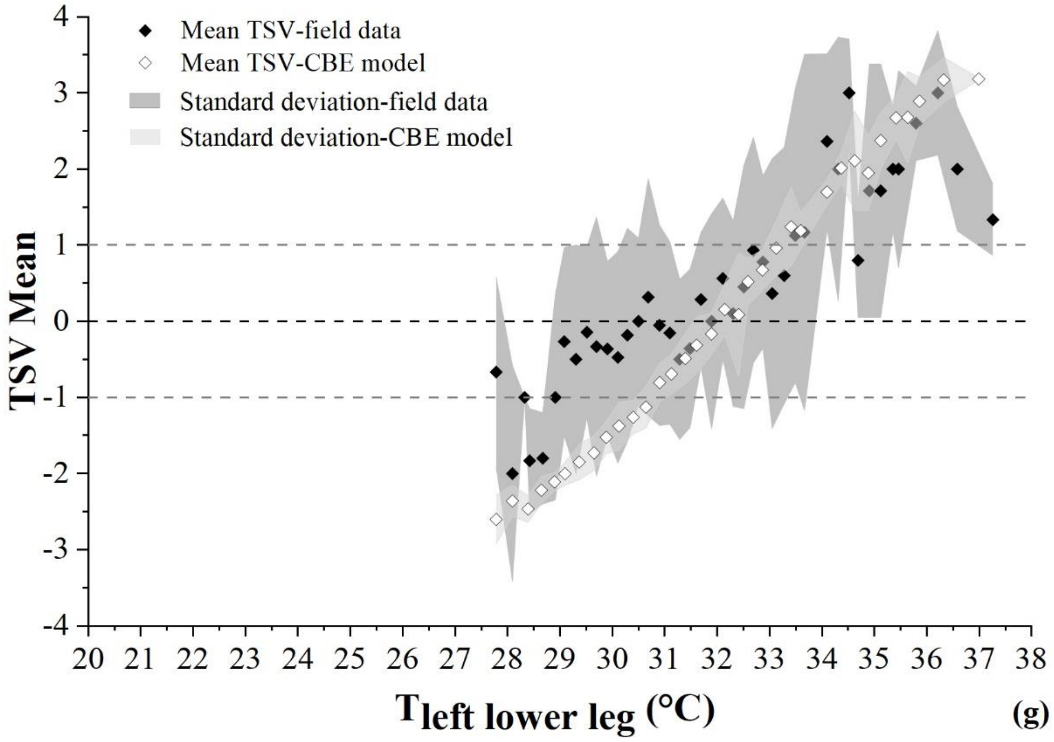


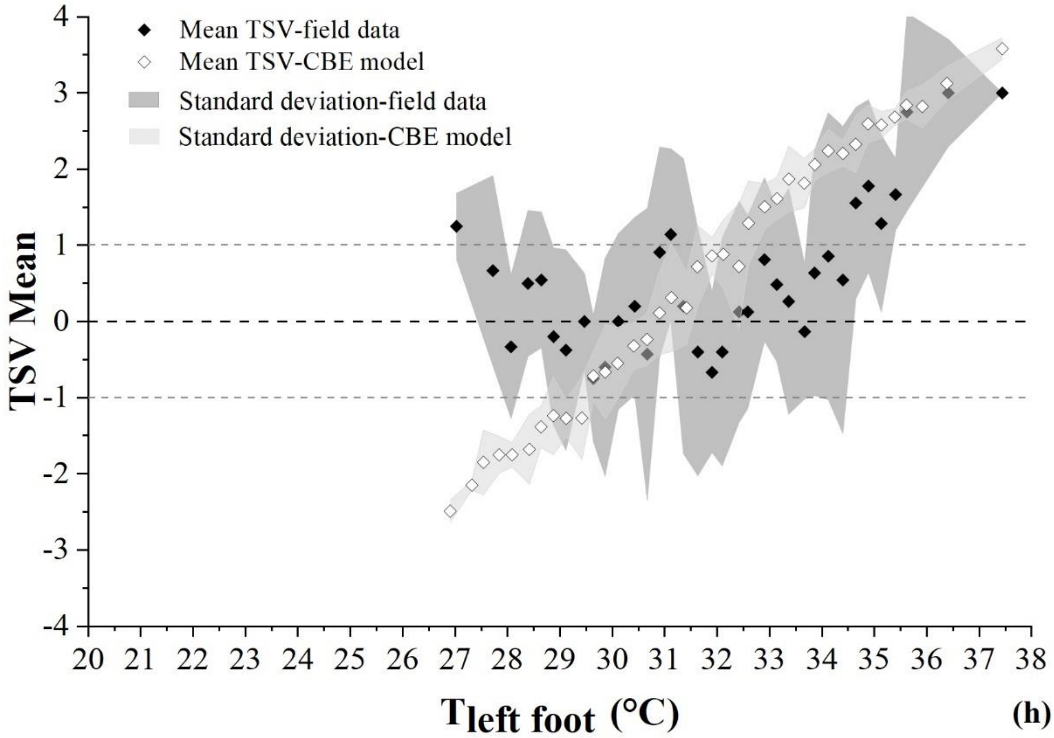


Figure 5.3 Correlation between thermal sensation vote (TSV) and skin temperature:

(a) between the overall TSV and mean skin temperature; and between the local TSVs and local skin temperatures: (b) Forehead; (c) Abdomen; (d) Left lower arm; (e) Left hand; (f) Left upper leg; (g) Left lower leg; (h) Left foot.

The measured $T_{skin,m}$ covered the range from 28.0 ℃ to 36.3 ℃. The corresponded $T_{skin,m}$ to the field-surveyed thermal neutral zone was from 29.1 to 34.2 ℃, while that corresponded to the simulated thermal neutral zone was from 30.9 to 35.1 ℃. The measured $T_{skin,m}$ corresponded to broader thermal neutral status in the surveyed results than the simulated results. If assuming “TSV = 0” as thermal neutral status, it is noticeable that the simulated data only had a limited range corresponded to “TSV = 0”, ranging from 33.1 to 33.6 ℃. However, the field-measured $T_{skin,m}$ was concentrated around “TSV = 0” from 30.9 to 33.4 ℃, which was similar to that corresponding to the extended thermal neutral range. Moreover, the surveyed data points were almost distributed around “TSV = 0” symmetrically in this range of $T_{skin,m}$. When the voted thermal sensation was larger than “TSV = +1”, the increasing trend of TSV with the increase of $T_{skin,m}$ was clearer.

The overall TSV is a comprehensive thermal feeling of different local body parts. Moreover, as $T_{skin,m}$ is the weighted average of seven local skin temperatures. It is needed to observe the relation between local skin temperature and local TSV individually. The temperature ranges of different local body parts vary from each other. In the coldest case of the experiment set, the lowest temperature of the abdomen was still close to 30.0 ℃, which was the highest local skin temperature in the coldest set. Being the closest local body part within all the seven mentioned body parts to the core and the body part easy to store fat, it is reasonable for the abdomen to have a limited range of temperature change. The forehead recorded the second-highest temperature (28.5 ℃) in the coldest experiment. The extremities, however, had a large temperature drop when the weather conditions were cold. The left lower arm had the lowest recorded temperature of 25.2 ℃, while the left hand had a much lower recording of 22.0 ℃. The closer to the end of the extremities, the lower the recorded local temperature it had. The lower body part had a similar pattern. The left foot had the lowest temperature of 27.0 ℃, followed by the left lower leg (27.8 ℃) and left upper leg (27.5 ℃). The reason for the left upper leg not having the recording higher than the left lower leg might due to a much thicker layer of fat surrounding the left upper leg than the left lower leg.

The relation between the local skin temperature and local thermal sensation varies in different local body parts. As for the abdomen, it was always covered with clothing which is suitable according to the weather conditions. Therefore, a wide range of abdomen temperatures were corresponded to the thermal neutral zone (from 29.9 to 35.1 ℃), and no extreme TSV was found. Much different than the surveyed dataset in the abdomen, the CBE-simulated TSV response of the abdomen was close to “cold” (TSV = -3.1) in the lowest measured abdomen temperature and close to “very hot” (TSV = 3.6) in the highest measured abdomen temperature. The surveyed thermal sensation in the forehead was more sensitive to low local skin temperature. However, when the temperature raised to above 31.0 ℃, the thermal sensation entered the thermal neutral zone and stayed there until 34.6 ℃. Compared with the field-measured data, the CBE-simulated TSV did not enter the thermal neutral zone until the forehead temperature raised to 33.9 ℃, and it left the thermal neutral zone at 35.1 ℃, making the thermal neutral range in forehead much narrower than the field-surveyed results. These two local body parts in the trunk area, which in total contributed 42% in the calculation of $T_{skin,m}$, all showed a wider local skin temperature range corresponded to the thermal neutral zone from the field measurement.

The extremities, compared with the trunk area, had a much more apparent retention phenomenon of staying in the thermal neutral zone or even staying around the point of “TSV = 0”. The left lower arm had limited points voted cooler than "slightly cool". The temperature range of staying in the thermal neutral zone was from 29.5 to 34.1 ℃. The left hand had a much wider range corresponded to the thermal neutral zone from 26.1 to 34.4 ℃. As for the lower body parts, the range in the thermal neutral zone for the left upper leg and left lower leg was 29.4 to 32.9 ℃ and 29.1 to 33.3 ℃ respectively. The left foot had the range from 27.7 to 34.4 ℃

corresponded to the thermal neutral zone, and it did not have the recording lower than "TSV = -1". Compared to the field-measured data, all the CBE-simulated TSV of the extremities crossed the thermal neutral zone in a straight line. The retention effect during thermal neutrality observed in the field measurement illustrates a need for replacing the set-point with a broader range of data.

### 5.5 The concept of "null zone" versus "set-point"

The microclimate in the urban environment is known as a highly unstable thermal environment. The relatively short exposure during each survey period enables limited changes in $T_{mrt}$ and $T_a$, yet the wind environment can change instantly. Unlike the experiment conducted in the controlled climate chamber, the field experiment in the outdoor environment could not control the microclimate variables. Therefore, the field measured skin temperature data in the outdoor environment can illustrate how it reacts and adapts to the continuous fluctuating thermal stimulus.

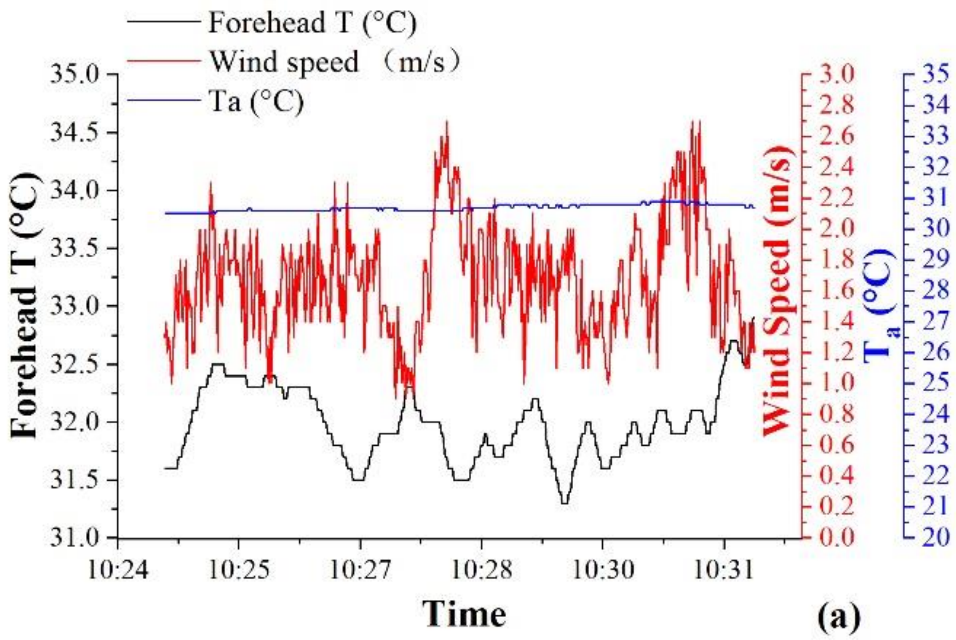


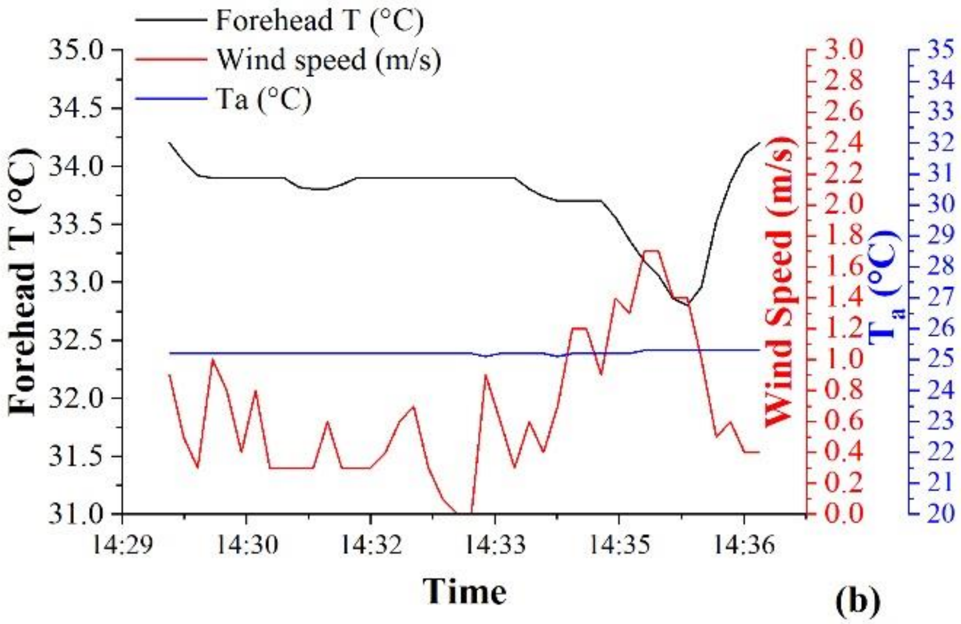


Figure 5.4 Forehead skin temperature change with the change of wind speed (a)

continuous sensible wind environment; (b) sudden strong wind environment

Fig. 5.4 shows the behaviour pattern of the forehead skin temperature with the change of wind speed. The forehead was chosen as an example because it was one of the unclothed body parts. Wind speed in the micro-urban climate has recorded severe fluctuations during the short-term experiment exposure. Two typical wind environment cases were chosen: a continuous sensible wind environment (Fig. 5.4 (a)) and a suddenly changed wind environment (Fig. 5.4 (b)). The recorded mean wind speed during the timeslot was about 1.7 m/s for the continuous sensible wind environment (Fig. 5.4 (a)), and about 0.7 m/s for the case with an immediate changing wind environment. The change of forehead temperature showed an apparent negative correlation with the change of wind speed. The forehead temperature almost raised immediately as the wind speed decreased and dropped while the wind speed increased from Fig. 5.4 (a). As the $T_a$ that day was relatively high at about 30.5 ℃, the range of change of the convective heat loss caused by the change of wind speed was small, and thus the changing range of the forehead temperature was narrow, from 31.3 to 32.9 ℃. For the case of sudden intense wind speed (Fig. 5.4 (b)), the forehead temperature did not variate much at the beginning as the wind speed kept fluctuating in the low range (under 1.0 m/s). However, when the wind speed suddenly increased from 1.1 m/s to 1.7 m/s, the forehead temperature almost decreased immediately from 33.7 to 32.8 ℃.

It is noticeable that the unclothed skin temperature can have a wide range of variation in the outdoors due to the fluctuating wind environment. The range of change of the local skin temperature depends on the temperature difference between the human body and the outside thermal environment and the strength of the wind speed. Fig. 5.4 (a) is the typical representative of the continuous changing thermal stimulus in the urban environment. The wind environment in the urban open space kept fluctuating at a certain level. The controlled wind speed of a particular point like the indoor environment is not realistic in the outdoors and thus leads to a doubt of whether the physiological dataset observed in the indoor chamber can represent the real outdoor conditions. Interestingly, corresponding to the continuous changing forehead temperature was the retention effect of the TSV in thermal neutrality, as shown in Fig. 6 (a). The retention effect of the TSV observed in the forehead area showed that human subjects adapt to the continuous disturbance created by the changing wind speed in the urban environment quite well.

In the control theory of thermoregulation, the peripheral thermoreceptors response to both the temperature and the change of temperature (Herbert Hensel, 1982). They follow the properties of differential control in dynamic phases (experiencing air temperature change in the climate chamber) while following the properties of proportional control during steady-state (Jürgen Werner, 2010), which is also applicable to the thermal comfort studies. According to Werner (Jürgen Werner, 2010), the property of differential control is impossible to be the exclusive control property in the peripheral area, because it only reacts to transient changes of disturbance, but does not counteract to a permanent disturbance. Therefore, proportional control takes the lead when a permanent disturbance happens. The question is whether transient changing wind environment in the outdoors should be treated as a permanent disturbance or transient disturbance.

The indoor environment has limited air movement and usually can be kept at an unnoticeable level. In that case, a slight increase in wind speed levels can create thermal sensation difference. Regarding the urban environment, fluctuating wind environment is unavoidable, if wind speed changes in a particular frequency and a certain amplitude, human seems able to adapt to it quickly. As the case in Fig. 5.4 (a), the wind speed kept changing frequently, but the variation range was kept between 0.9 to 2.7 m/s, no obvious sudden change was observed. Human subjects adapt to such kind of wind environment quite well; thus, we prefer to treat it as a permanent disturbance. However, when the given wind pattern was destroyed by changing the amplitude or frequency, further thermal sensation difference can be created. The case in Fig. 5.4 (b) could be an example, within which the wind speed fluctuated at low level (about 0.6 m/s) at the beginning of the experiment period and suddenly increased to a new level (about 1.7 m/s) in a very short period, we prefer to treat it as transient changes of disturbance. This discussion will not be expanded further in this study, but a proper mathematic description is needed to make a proper description of the disturbance created by different wind environments in the urban setting, and it will be discussed more in our future study. By analyzing the wind environment pattern here, the aim is to bring in the idea that the variability of local skin temperature should be allowed when the urban thermal environment is considered.

Moreover, it is widely accepted that the thermoeffector in thermoregulation reacts proportionally to body temperature. The proportional control works based on the "load error", which is the deviation of the regulated variable. That means the threshold of the regulated variable determines the output of the regulation and also thermal sensation as a side product. The misconception in thermal comfort research derives from defining the "load error" as the deviation of the body temperature and a fixed "set-point" (Parkinson, & De Dear, 2015). If a "set-point" used in the thermal regulation model is applied to the outdoors, it is almost impossible for a human body to remain its thermally stable state. However, the slight fluctuation of the unclothed local skin temperature with the change of wind speed and together with the retention effect shown in the thermal neutral status, indicates that human subjects feel thermally neutral in a certain range instead of a given value. It means either thermal balance could be remained in a range or the thermal sensation feelings be insensitive to a slight fluctuation of thermal imbalance. Therefore, applying set-point in the thermal sensation models cannot accommodate the fluctuation in thermal neutrality, and an inevitable variability should be allowed when the human body is experiencing an outdoor environment. Based on the listed reasons, we proposed using the concept of the "null zone" instead of "set-point” in the thermal regulation model.

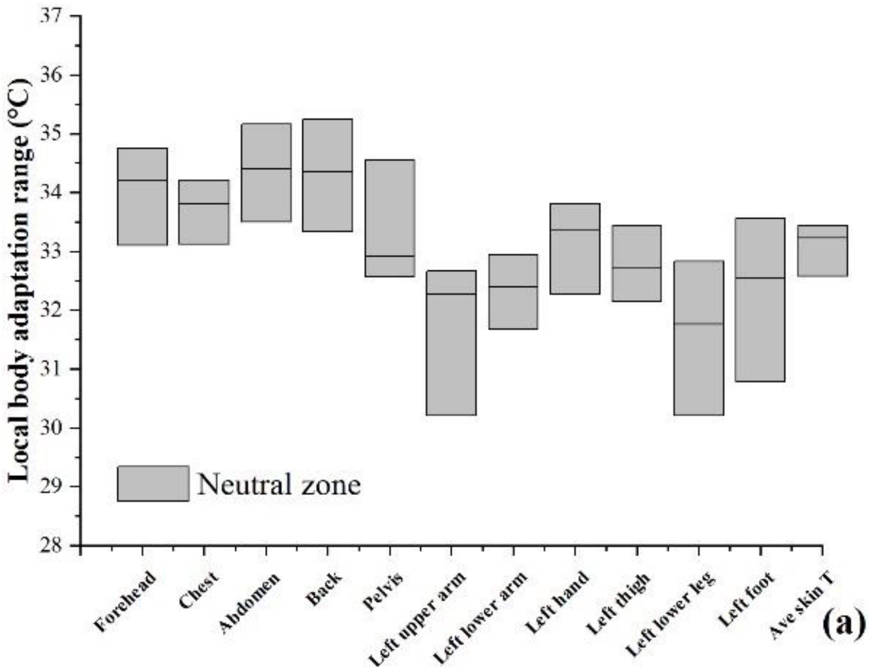

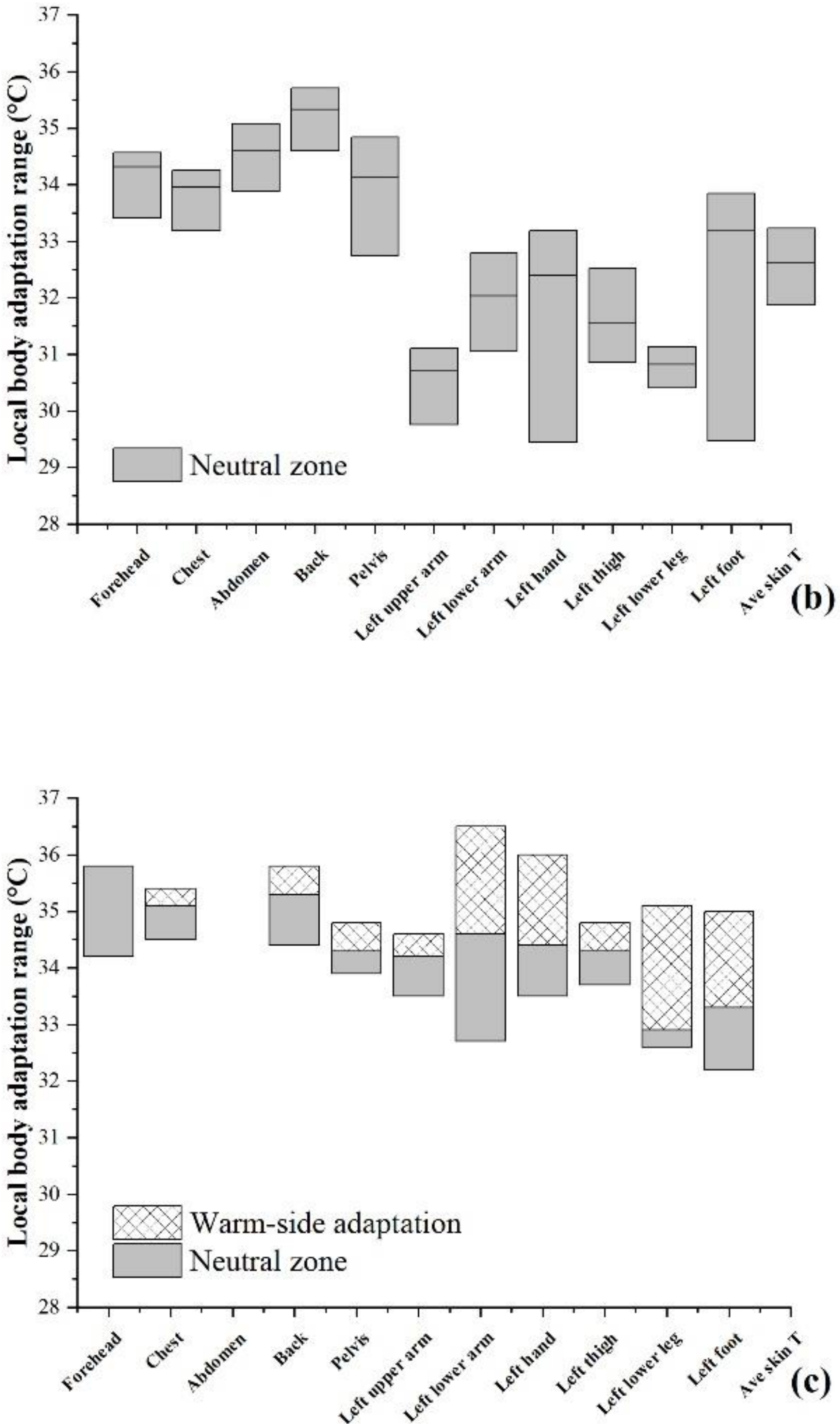


Figure 5.5 Local body temperature null zone in thermal neutral status (a) Male; (b)

Female (c) thermal adaptation range derived from Zhang's study (H. Zhang, 2003)

The concept of the "null zone" is first defined as a central temperature range associated with limited autonomic regulatory activity (Parkinson, & De Dear, 2015). It can also be referred to as "dead band" and "thermoneutral zone". Body temperature fluctuates within this threshold will not trigger further thermoregulation actions (Taylor et al., 2008). Therefore, the human body can minimize the need for regulatory remediation and thus conserve resources (Parkinson, & De Dear, 2015). The "load error" which drives further thermoregulation actions and stronger thermal sensation in this study are defined as the deviation from the thresholds of the null zone. This study will merely discuss the null zone range of local skin temperature; the null zone range of core temperature still needs more data support. The measured local skin temperature data within the null zone was selected by limiting the overall and every local thermal sensation between "-1 to 1", in order to search for the dataset that each local body part and overall thermal sensation feeling is thermal neutral. The filtrated dataset includes 31 human subjects in total, which includes 16 males and 15 females. The local skin temperature null zones are listed in Fig. 5.5, separating into male and female datasets. The lower and upper limits of the null zone are defined as the value located at the 25% and 75% of the filtrated data in an increasing trend. The medium measured skin temperature values for each local body parts are also shown in Fig. 5.5 (a, b). The thermal adaptation range in the neutral status and the warm-side adaptation of the CBE model are also reproduced for comparison (Fig. 5.5 (c)) (H. Zhang, 2003). The thermal adaptation range in neutral status was obtained from the limited indoor neutral conditions, while the warm-side adaptation range was retrieved from the regression results of the dataset in the extremely hot conditions (H. Zhang, 2003).

Almost all the local body parts for the thermal adaptation range in the CBE model were higher than the field measured null zone results. The reason for that might be due to the difference of dressing pattern: the human subjects joined the CBE experiment wore leotard which was able to tie up the temperature sensors on the skin, while the human subjects for our outdoor experiment wore their own regular clothing. The width of range in the field measured null zone results were much wider than the CBE adaptation range if only focus on its neutral zone; however, if counted in its warm-side adaptation, the width of the field measured and model ranges would be similar. Still, the field measured null zone for the extremities is noticeably lower than the CBE adaptation ranges. The distribution of body parts in the trunk area for male was quite uniform in the range of 33.1 to 35.3 ℃, except for the pelvis where was recorded lower null zone range from 32.6 to 34.6 ℃. The back was recorded as the highest null zone range for females, followed by the abdomen. Forehead and chest recorded similar null zone range. The null zone ranges for pelvis were similar for both males and females. Similar to the adaptation range in the CBE model, the extremities show a much broader null zone range than the trunk parts. The highest value of the extremities for males was recorded as 33.8 ℃ in the left hand while the lowest value was recorded as 30.2 ℃ in both left upper arm and left lower leg. Females had a wider null zone range for the end of the extremities, recorded from 29.4 to 33.2 ℃ for left hand and 29.5 to 33.8 ℃ for the left foot.

The null zone ranges were obtained by limiting the thermal sensation vote, while no limitation on clothing and environmental conditions, which ensures the dataset can apply directly to the real-life outdoor conditions. The thermal neutral range measured in our field study was a comprehensive result of physiological acclimation (adaptation to thermal stimulus), behavioural adjustment (comfortable dressing pattern for different climate conditions), and phycological expectation (willingness for staying in the outdoor environment) (Brager, & De Dear, 1998). This set of null zone data was used in the further development of the multi-nodal model to replace "set-point".

### 5.6 Further development of the multi-nodal model

$$\text{Local sensation}_{static} = 4\left(\frac{2}{1+e^{\left[-(C1+K1)\left(T_{skin,i}-T_{skin,i,null\ zone}\right)+K1\left(T_{skin,m}-T_{skin,m,null\ zone}\right)\right]}}-1\right) \quad \text{Equation (5.1)}$$

$$R^2 = 1-\frac{\sum(Y_{actual}-Y_{predict})^2}{\sum(Y_{actual}-Y_{mean})^2} \quad \text{Equation (5.2)}$$

The further development of the CBE comfort model mainly focused on two parts: local sensation prediction and the selection of dominant local body parts. Equation 5.1 illustrates the new equation for predicting the static part of a local sensation. The null zone results in part 5.4 were used in Equation 5.1. The coefficients and the logic of the local and overall thermal sensation prediction still follow the original model (shown in Fig. 2.3). According to the original model, only the chest, pelvis, abdomen, and back were chosen as the dominant body parts, and such body parts dominant the cool sensation. In the real-life outdoor conditions, such body parts are normally covered with clothing and thus hardly would approach the cold extreme unless local cooling is applied. Compared with the mentioned dominant local body parts, the forehead is normally the unclothed local body part, and it is closed to the body core. Moreover, it showed a strong positive correlation ($R^2 = 96.0\%$) with the overall thermal sensation (shown in Fig. 5.6). To further confirm our conjecture, the spearman correlation coefficient $r_s$ was used to measure the correlation strength between the selected local body temperatures and the overall thermal sensation. The absolute value of $r_s$ is between 0 and 1 (Dowdy et al., 2011). The higher the absolute $r_s$, the stronger the association it is. The $r_s$ results are shown in Table 5.2. Forehead showed the highest $r_s$ of 0.73 among the other dominant local body parts. This result indicates the importance of the forehead, and thus, it should also be listed as one of the dominant body parts.

Yet this revision focuses only on the relation between the skin temperature and thermal sensation, using skin temperature as the comprehensive parameters of the reflection for the outside thermal environment and personal clothing. The field-surveyed TSV was used to compare with the revised model. We did not separate the original dataset into the dataset for model development and the dataset for verification because the revised model was developed based on merely the measured skin temperature instead of the statistic regression using the subjective voting.

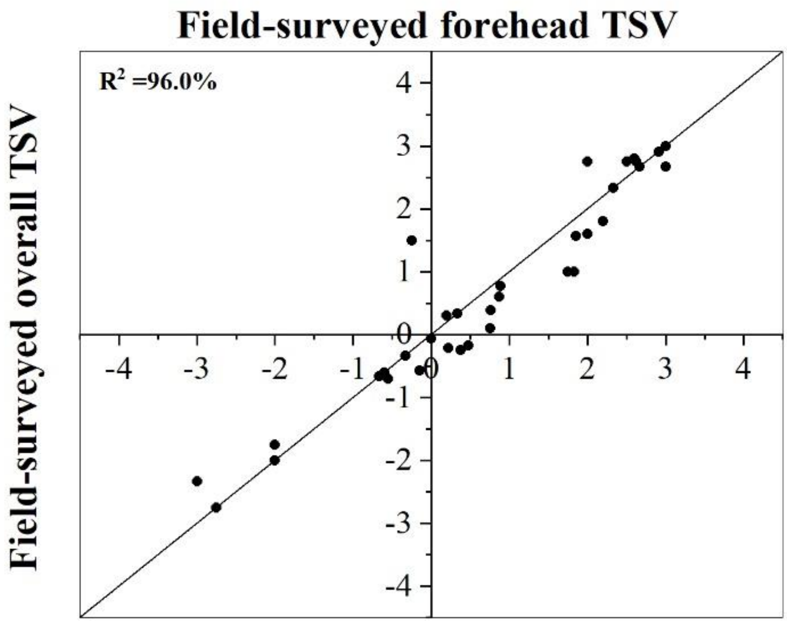


Figure 5.6 The relation between field-surveyed forehead TSV and overall TSV

Table 5.2. Spearman correlation coefficient ($r_s$) for the correlation between selected local body parts and the overall thermal sensation vote

| Local body parts | Forehead | Chest | Abdo | Back | Pelvis |
|---|---|---|---|---|---|
| $r_s$ | 0.73 | 0.30 | 0.66 | 0.32 | 0.43 |

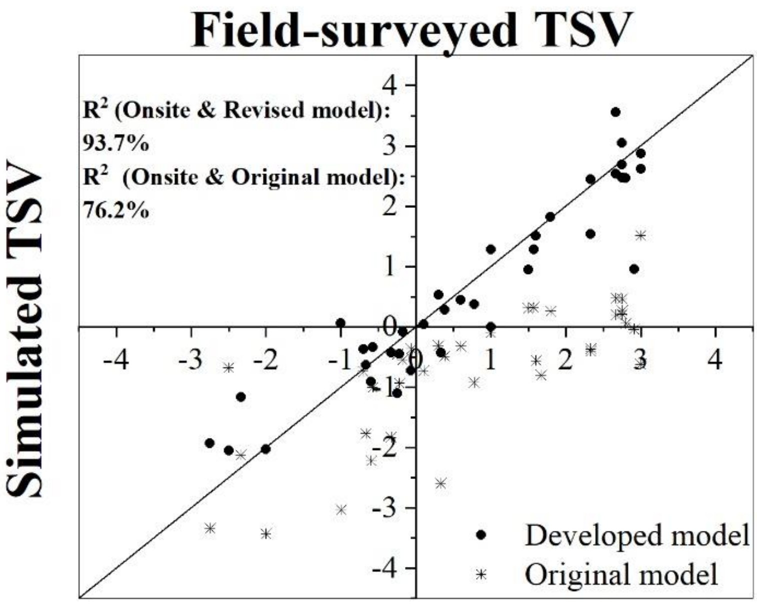


Figure 5.7 Prediction results compared with the field survey data (the revised model vs. the original model)

Fig. 5.7 shows the comparison results of the simulated data and the field-surveyed data. Two datasets are shown in Fig. 5.7: the dataset using the original model framework and the original CBE thresholds shown in Fig. 5.5 (c) and the dataset using the null zone data (shown in Fig. 5.5 (a, b)) and the developed logic structure for the calculation of overall thermal sensation. A 45-degree auxiliary line was added. The data points of the revised model were much closer to the 45-degree line than the prediction data of the original model. As the thresholds for local body parts in the original model were relatively high, the deviations of the measured local body temperature and the upper bound of the threshold were not large and thus very limited data points of the original model located in the extreme hot side. On the contrary, the cold extreme was easy to be approached in this case. $R^2$ was used to evaluate the performance of the revised model (Equation 5.2). $R^2$ of the revised model was 93.7%, while that of the original model was 76.2%. An improvement of 17.5% was realized through the revision.

# Chapter 6 Outdoor thermal sensation and logistic regression analysis of comfort range of meteorological parameters in Hong Kong

## 6.1 Introduction

Warm and hot days account for most of the time in Hong Kong. Outdoor thermal comfort studies in Hong Kong should give its first consideration to warm and hot days. This chapter presents investigations about thermal comfort through 1600 human subject responses from the onsite survey with concurrent meteorological parameter measurements. Probit analysis was used for searching the thermal neutral range of Hong Kong residents in a year span. Logistic regression was used for locating the meteorological parameter ranges for thermal neutral and comfort conditions. It is shown that people had difficulties defining their actual thermal feelings near the thermal neutral status when being asked to use the nine-point thermal sensation scale. Obvious thermal adaptation effect for thermal neutral conditions were observed among Hong Kong residents over the seasons in a year. The transitional seasons had wider thermal neutral range than that of winter and summer. Summer had the narrowest thermal neutral range. Wind and solar radiation had an interaction effect with air temperature in determining thermal sensation and thermal comfort. Wind can effectively offset the negative effect of solar radiation in summer when the air temperature was lower than 31 °C. The thermal comfort condition allowed a higher limit of solar radiation than the thermal neutral condition when the air temperature was lower than 31 °C. The investigations in this part provide some unique insights into the way to assess urban thermal comfort in the building design stage.

### 6.2 Hong Kong air temperature data analysis

The result and discussion part starts with the analysis of the air temperature collected in the King’s Park observation point by the Hong Kong Observatory. The King’s Park observation point is located in the Kowloon city of Hong Kong, where has a high density of high-rise buildings and living population. The data collected at this observation point is more appropriate in representing the air temperature within the city considered the heat island effect. Fig. 6.1 presents the monthly average air temperature throughout the past 10 years. It is noticeable that nearly half of the time of every year had a monthly recorded history higher than 26 °C, started from May and ended in October. The average air temperature within the city has been raising in the past 10 years. The most obvious increase occurs in summer, with an increase of 1.17 °C from the year of 2008 to 2017. Fig. 6.2 shows the number of extreme hot days in Hong Kong from the year of 2008 to 2017(daytime and nighttime records respectively). It is obvious that the number of daytime temperature over 33 °C kept increasing in the past ten years with slight fluctuation. The occurrence of such record has move forward from July to June. The number of nighttime temperature over 28 °C increased from 81 days in the year of 2008 to 118 days in the year of 2017. Among the past ten years, October recorded an ascending trend of extreme hot nights. All these evidences prove that Hong Kong is getting hotter. Hence, when considering the practical measures to improve outdoor thermal comfort, more efforts should be placed at targeting the intolerable hot conditions.

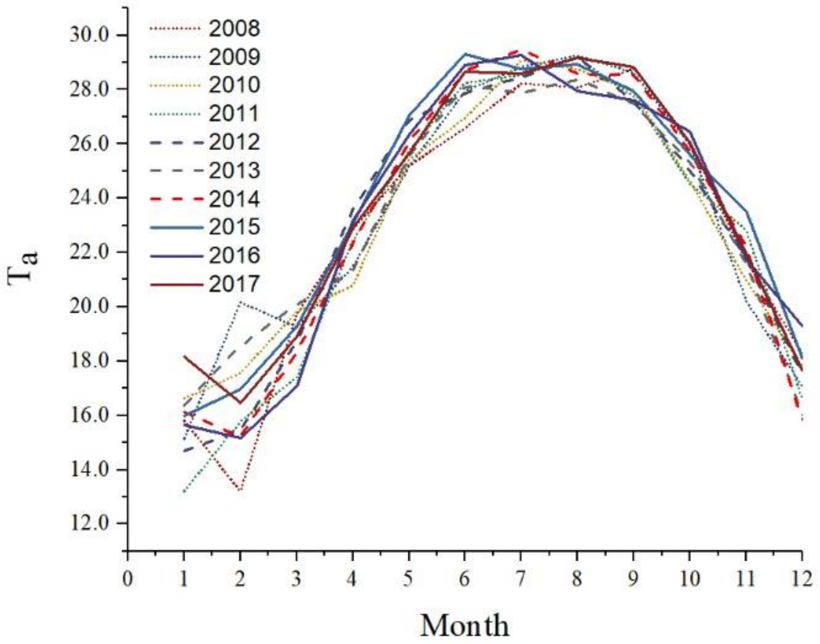


Figure 6.1 Monthly average air temperature for the past 10 years in King's Park Observation point

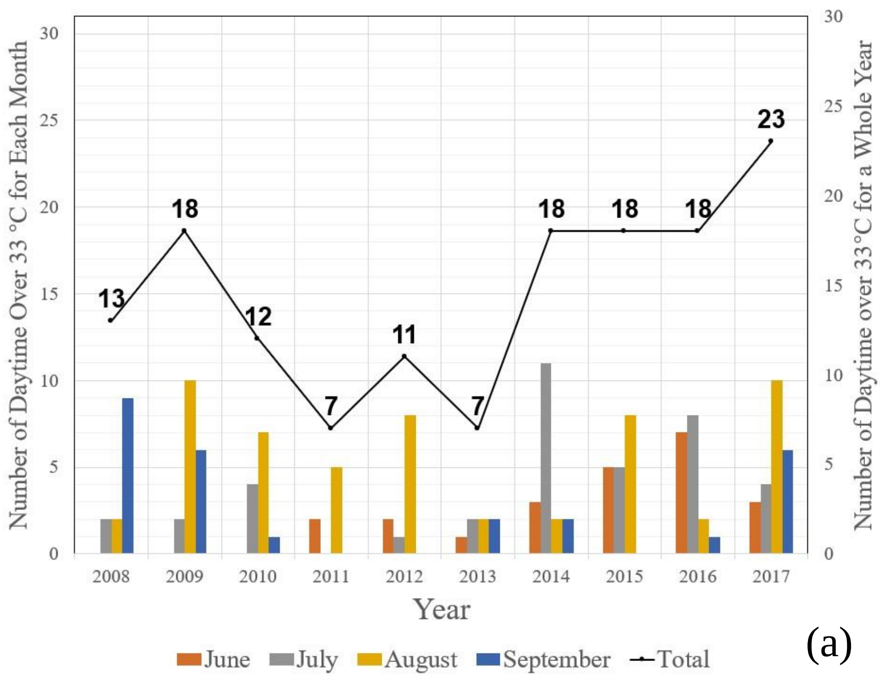


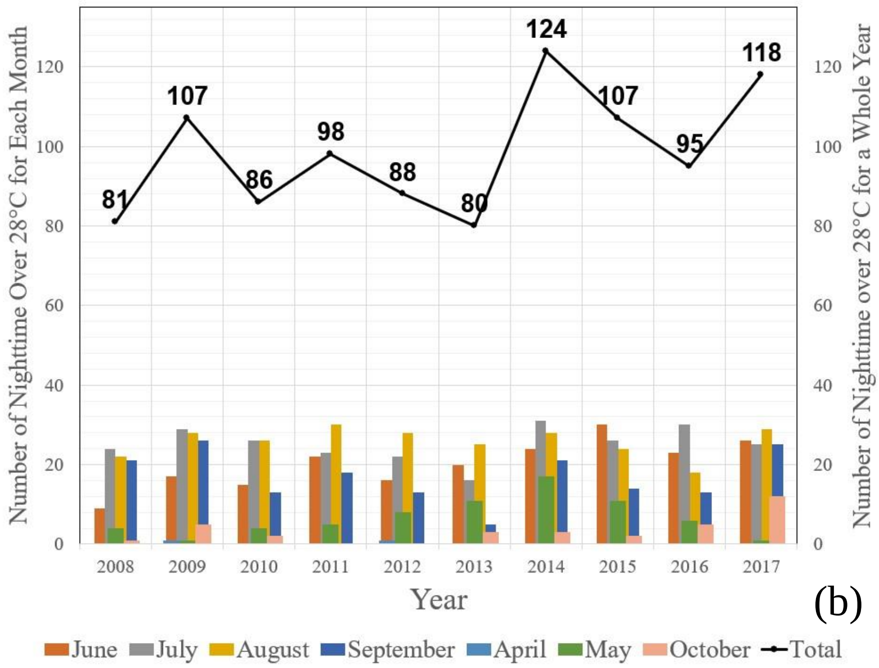


Figure 6.2 The record of extreme hot days in Hong Kong in the past 10 years (a) daytime record; (b) nighttime record

### 6.3 Data analysis related to the thermal neutral condition

### 6.3.1 Unclear voting around the thermal neutral range

To answer the question of whether TSV = 0 could represent “thermally neutral” or not, the original surveyed dataset was compared with the dataset including the generated random values. In the dataset with random values, the target values were replaced with the random integer generated by Matlab within a certain range. For example, the original voting ranging from “-2” to “0” were sorted out and replaced with a random integer ranging from “-2” to “0” to form a random dataset. In total, six new random datasets were built as shown in Table 6.1. These new datasets were compared with the original surveyed dataset by the independent t-test. The null hypothesis was that the two datasets were from the same population. If the null hypothesis was satisfied, the actual voting of the certain range had no difference with random voting. From the results shown in Table 6.1, it is noticeable that both replacing the actual voting “-1”, “0” and “0”, “1” with the random values in these two ranges created no differences when compared to the original voting group (p-value much higher than 0.05). But further replacing the range to “±2” or “±3” could create differences (p-value below 0.05). This comparison was able to illustrate a phenomenon that when people were in their thermal neutrality, they tended to vote from “slightly cool” to “slightly warm”. People had confusion on deciding the appropriate voting to describe their thermal status when they were around thermal neutrality. However, when the thermal condition tended to the warm or cool side, their voting started to reflect their actual thermal feelings. Thus, TSV from “slightly cool” to “slightly warm” was used when considering the concept of “thermal neutrality” in the further analysis of this study. This present finding only used the data obtained from the outdoor environment, the data of indoor thermal sensation was not included, which makes this finding only applicable to the outdoor thermal environment so far.

Table. 6.1 Significant level of comparison between original data and random data

| **Cool side** | ***p*-value** | **Warm side** | ***p*-value** |
|---|---|---|---|
| Random number [-1,0] | 0.956 | Random number [0,1] | 0.413 |
| Random number [-2,0] | 0.015* | Random number [0,2] | 0.023* |
| Random number [-3,0] | 0* | Random number [0,3] | 0* |

* p-value<0.05.

### 6.3.2 Defining outdoor thermal neutral range in Hong Kong

Fig. 6.3 and Fig. 6.4 show the P-P plot (probability–probability plot) and the residual plot of the surveying TSV. The data points basically followed the theoretical line of $y = x$ as shown in Fig. 6.3. Fig. 6.4 shows the distribution of the difference between the calculated cumulative normal distribution value and the observed cumulative value. The data points were distributed evenly around $y = 0$ with a slight fluctuation. As the absolute deviation was lower than 0.05, which was within the range of allowable distribution probability difference, the on-site survey TSV data was considered as following the normal distribution.

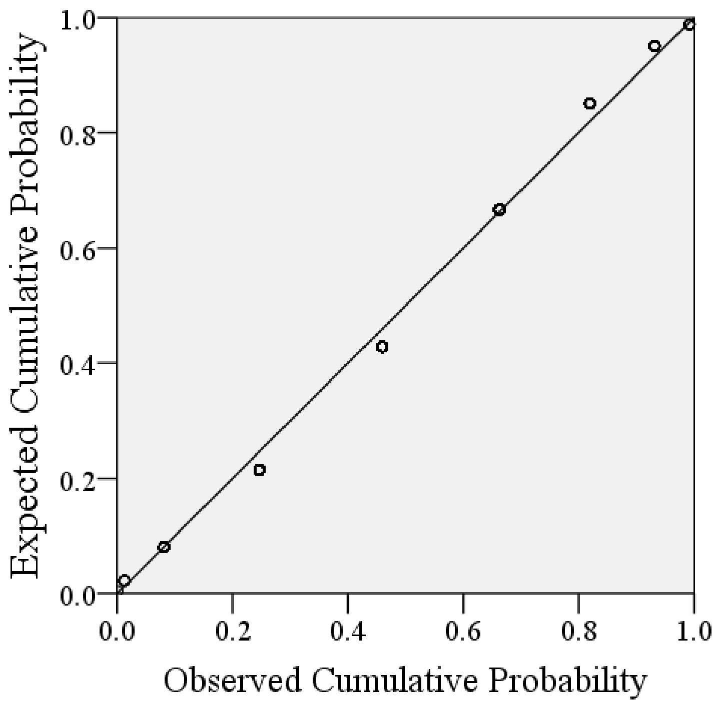


Figure 6.3 P-P plot of on-site survey thermal sensation vote data

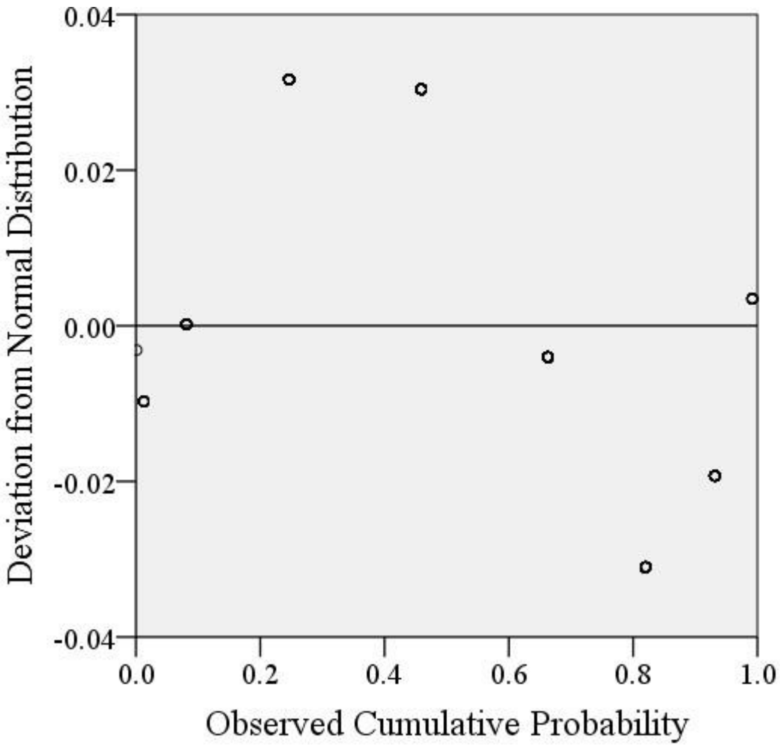


Figure 6.4 Normal distribution residual plot of on-site survey thermal sensation vote data

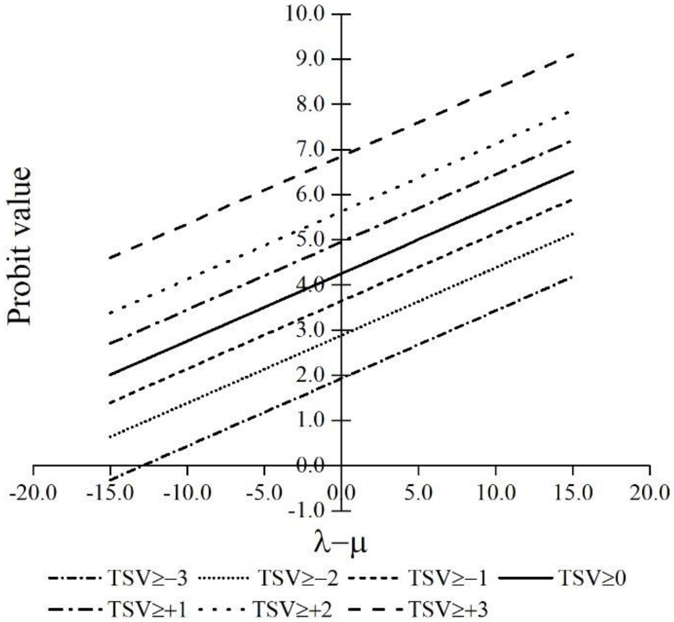


Figure 6.5 The seven probit regression lines

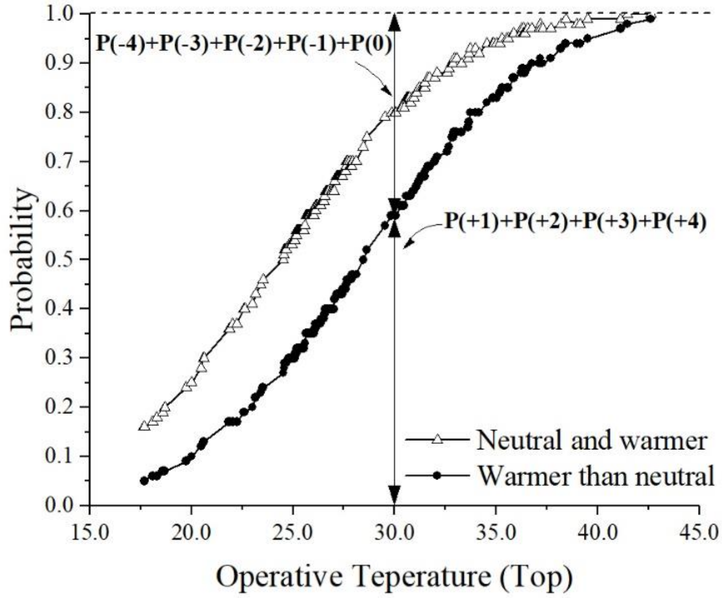


Figure 6.6 Sigmoid curves of the “neutral and warmer” and “warmer than neutral” groups

The whole set of original data was used in the probit analysis. Totally seven out of eight probit regression lines were generated as shown in Fig. 6.5, because the data "TSV = +4" was very limited in the experiment in Hong Kong. These regression lines followed the same slope of 0.15 but different intercepts. The probit regression lines were translated to the sigmoid curves by probit transmission. Fig. 6.6 shows two of the sigmoid curves. These were the cumulative distribution curves of the corresponding normal distributions. In the example of the "warmer than neutral" curve, $P$ here represents the probability of people voting for "TSV ≥ +1" at a certain $T_{op}$, *1-P* represents the probability of people voting for "TSV ≤ 0". Defined in the study of Nikolopoulou and Lykoudis (Nikolopoulou, & Lykoudis, 2006), the "neutral and warmer" curve was the transition curve describing the probability of someone changing the voting from the cool side to the neutral and warm side; and the "warmer than neutral" curve was the transition curve describing the probability of someone changing the voting from the cool and neutral side to the warm side (Nikolopoulou, & Lykoudis, 2006).

Along the two transition curves, the points where the probability equaled 50% were what needed to be concerned with. Because of the physical feature of the normal distribution curve, the derivation of the cumulative distribution curve was the rate of increase in the response for such groups against per unit increase in the operative temperature. Take the "neutral and warmer" curve as an example, the derivation of it namely described the percentage of people who would change their voting from “cooler than neutral” to “neutral and warmer” at a certain unit of operative temperature. Along the line of 50% in the $y$-axis shown in Fig. 6.7, when $T_{op}$ reached the threshold of stimulating 50% probability of the “neutral and warmer” transition curve, it was termed entering the neutrality zone; and when $T_{op}$ reached that of the “warmer than neutral” curve, leaving the neutrality zone. The definition of neutrality zone using probit analysis was first brought by Ballantyne et al. (Ballantyne et al., 1977), who also introduced the concept of defining the point of thermal neutral temperature as the midpoint of these two values (Ballantyne et al., 1977). However, it was hard to decide whether people just cannot tell the difference when the voting was around thermal neutral status, or this status might last for a certain range of thermal stimulus in the outdoor environment. The concept of the thermal neutral zone could be an alternative, which was also used in the present study.

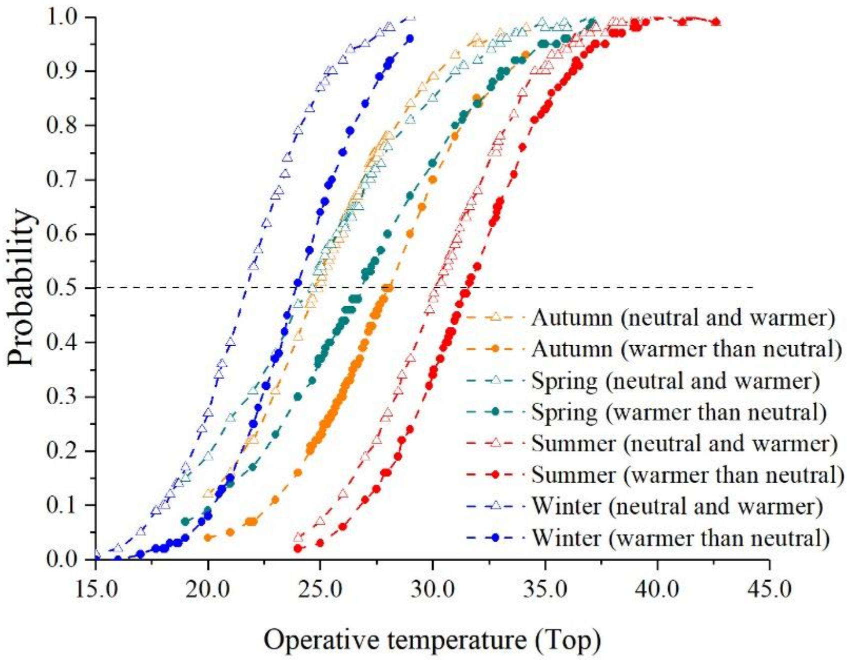


Figure 6.7 Transitional curves of thermal neutral for different seasons in Hong Kong

Fig. 6.7 shows four sets of transition curves for different seasons in Hong Kong. The thermal neutral zones for transitional seasons were much wider among four seasons. Thermal adaptation can be found when comparing the thermal neutral ranges of two transitional seasons. Almost similar $T_{op}$ (around 24.5 °C) started to stimulate thermal neutral feeling for spring and autumn, but the $T_{op}$ for leaving the thermal neutral zone (28.0 °C) in autumn was slightly higher than that of spring (26.8 °C). This phenomenon might be due to the recent thermal history of the previous season. The thermal sensation feeling in autumn was affected by the thermal history in summer, which made people more tolerable to high temperature.

However, the warm winter during our experiment in Hong Kong made it not able to provide a strong contrast for cold thermal sensation feeling, thus the starting point of $T_{op}$ to enter the thermal neutral zone in spring was very close to that in autumn.

It is noticeable that the thermal neutral zone increased from winter to summer. The thermal neutral zone for winter was the lowest, ranging from 21.5 to 23.7 °C; while for summer it was the highest, ranging from 30.1 to 31.6 °C. The similar increasing pattern was also found in the study of Nikolopoulou and Lykoudis (Nikolopoulou, & Lykoudis, 2006) which focused on thermal comfort for the open area of European countries. The thermal neutral zone for summer was within that of autumn from their observation, and the upper limit of the thermal neutral zone in summer was the same as in autumn (around 32.0 °C) (Nikolopoulou, & Lykoudis, 2006). However, the thermal neutral zone in summer was much higher than the other seasons for Hong Kong residents. Observed in Fig. 6.7, the $T_{op}$ for entering the neutrality zonein the Hong Kong summer was 30.01 °C while $T_{op}$ for leaving the neutrality zone for the other seasons was merely 28.0 °C.

Though winter and summer were both not as pleasant as the transitional seasons, the thermal neutral zone in summer was much narrower compared to winter. The temperature difference between two transition curves for winter was 2.2 °C while for summer it was merely 1.5 °C. This phenomenon illustrates that achieving thermal neutrality was the hardest in summer through the whole year in Hong Kong and that the thermal condition of the outdoor environment was the severest in summer. Therefore, when city planners try to make effort to improve the thermal conditions in the public open area, summer should be given the top priority. The upgrade projects targeted at the warm and hot conditions will be the optimized ones for the consideration of both resource utilization and solving the most serious problem.

## 6.4 Thermal neutral and comfort ranges of meteorological parameters in Hong Kong summer

Facing the fact that the air temperature in the outdoor environment was non-adjustable and that almost one-third of the whole year had air temperature over 30 °C in Hong Kong, improving the outdoor thermal environment should rely on improving the wind and solar radiation condition by the arrangement of buildings and the greenery. If the air temperature, wind, and solar radiation were treated as a whole system, achieving its best performance by driving each parameter to the best level might be inefficient and impracticable. The rational way is to find out the tolerable ranges that enable the target condition to be achieved. Therefore, this part will focus on searching for the suitable ranges of the meteorological parameters that can provide thermal neutrality or thermal comfort.

Logistic regression was used to predict the combination of wind and solar radiation conditions covering the whole air temperature range (from 25 to 35 °C) in summer. The maximum radiant temperature was up to 65 °C as observed in our on-site measurement; while that of the mean wind speed was up to 3 m/s. The positive response of thermal neutral condition was termed as "TSV = -1, 0 and +1" because of the proven wider range of thermal neutral in the previous part. The positive response of thermal comfort was defined as the TCV voting in the comfort side.

Our previous study has assessed the change of sensitivity of solar radiation and wind speed toward a one-unit change of TSV under different ranges of air temperature (Yongxin Xie et al., 2018). The effect of wind and solar radiation on outdoor thermal sensation has also been revealed a dependent relationship with air temperature in literature (Andrade et al., 2011; Eduardo L Krüger, & Rossi, 2011; Nikolopoulou, & Lykoudis, 2006). Namely, the conditional effect exists between the variables. The effect of wind on thermal sensation depends on the level of air temperature and so is the effect of solar radiation. As a kind of heat source that has a similar effect as air temperature to thermal sensation, it is reasonable to infer that wind and solar radiation also have an interaction effect on thermal sensation. Therefore, both the main effects and the interaction effects should be considered in the logistic regression model. Centered variables were used for the interaction terms and further in the regression to avoid the multicollinearity problem.

The prediction of response depended on the calculated probability of the logistic regression model. The default classification cutoff for a positive response was $P \geq 0.5$. It should be refined by the ROC curve to increase the true positive rate and reduce the false positive rate as well. The ROC curves are generated by the saturated logistic models and its results are shown in Fig. 6.8 (a-b). The area under the ROC curves of the thermal neutral and thermal comfort logistic regression results were 0.830 and 0.889, respectively. The higher area under the curve, the better the regression fitted with the original data. Fig. 6.8 (c-d) present the difference between the sensitivity and 1-specificity in the ROC curves. The largest difference meant the highest true positive rate and the lowest false positive rate, and the classification cutoff points corresponded to what was chosen in the further regression. The classification cutoffs for thermal neutral and thermal comfort logistic regression were 0.415 and 0.701, respectively.

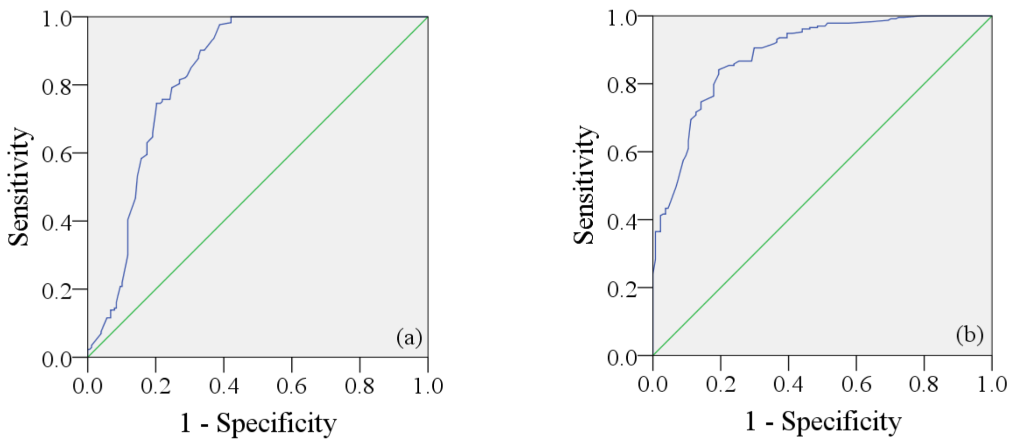

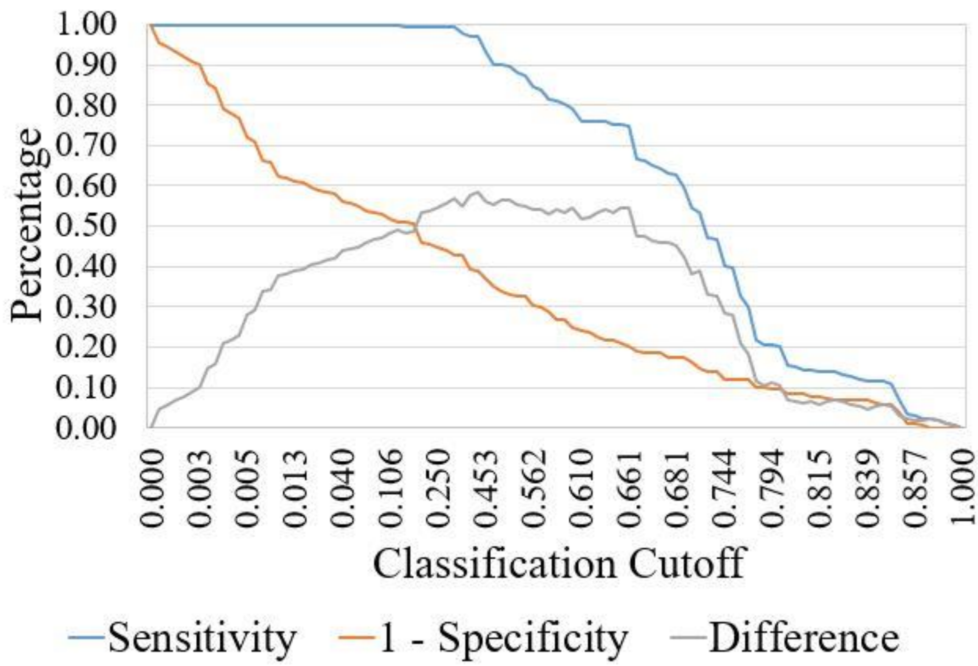


(c)

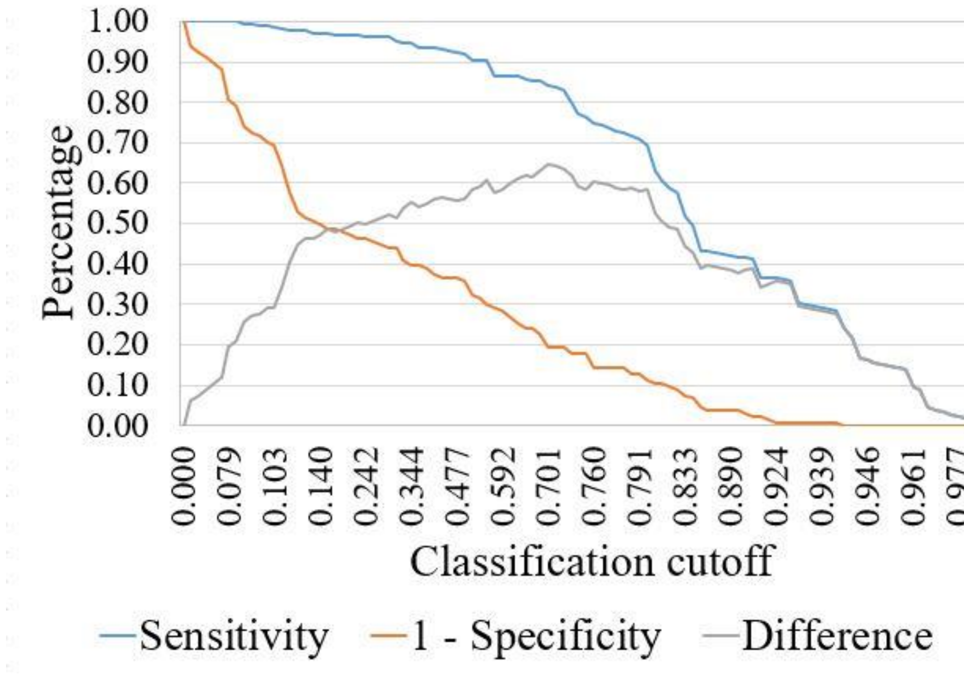


(d)

Figure 6.8 Determining the classification cutoff points (a) ROC curve of thermal neutral from the saturated logistic model; (b) ROC curve of thermal comfort from the saturated logistic model; (c) the difference between the sensitivity and 1-specificity in the ROC curve of thermal neutral logistic regression result; (d) the difference between the sensitivity and 1-specificity in the ROC curve of thermal comfort logistic regression result

Table. 6.2 Independent variables and the evaluation index in the logistics regression of thermal neutrality

| **Overall accuracy** | **Independent variables** | **-2 Log likelihood** | **Cox & Snell $R^2$** | **Nagelkerke $R^2$** |
|---|---|---|---|---|
| 49.3% | $v'^{**}$ | 486.497 | 0 | 0 |
| 66.1% | $T_a'$ | 429.858 | 0.149 | 0.199 |
| 78.1% | $[T_{mrt}-T_a]'$ | 334.464 | 0.352 | 0.469 |
| 76.4% | $[T_{mrt}-T_a]'$, $v'$ | 330.668 | 0.359 | 0.478 |
| 65.5% | $T_a'$, $v'$ | 426.216 | 0.158 | 0.210 |
| 76.9% | $T_a'$, $[T_{mrt}-T_a]'$ | 327.748 | 0.364 | 0.485 |
| 76.6% | $T_a'$, $[T_{mrt}-T_a]'$, $v'^{**}$ | 326.932 | 0.365 | 0.487 |
| 76.6% | $T_a'$, $[T_{mrt}-T_a]'$, $v'$, $T_a'\times v'$ | 315.321 | 0.386 | 0.515 |
| 78.9% | $T_a'^{**}$, $[T_{mrt}-T_a]'$, $v'^{**}$, $[T_{mrt}-T_a]'\times v'$ | 322.273 | 0.374 | 0.498 |
| 76.9% | $T_a'^{*}$, $[T_{mrt}-T_a]'$, $v'^{**}$, $T_a'\times[T_{mrt}-T_a]'^{**}$ | 326.422 | 0.366 | 0.488 |
| **78.1%** | $\boldsymbol{T_a'}$, $\boldsymbol{[T_{mrt}-T_a]'}$, $\boldsymbol{v'}$, $\boldsymbol{T_a'\times v'}$, $\boldsymbol{[T_{mrt}-T_a]'\times v'^{*}}$ | **313.139** | **0.390** | **0.520** |
| 78.1% | $T_a'$, $[T_{mrt}-T_a]'$, $v'$, $T_a'\times v'$, $T_a'\times[T_{mrt}-T_a]'^{**}$ | 315.183 | 0.386 | 0.515 |
| 78.9% | $T_a'^{**}$, $[T_{mrt}-T_a]'^{**}$, $v'^{**}$, $[T_{mrt}-T_a]'\times v'$, $T_a'\times[T_{mrt}-T_a]'^{**}$ | 322.040 | 0.374 | 0.499 |
| 78.1% | $T_a'^{**}$, $[T_{mrt}-T_a]'$, $v'$, $[T_{mrt}-T_a]'\times v'^{**}$, $T_a'\times v'$, $T_a'\times[T_{mrt}-T_a]'^{**}$ | 312.874 | 0.390 | 0.520 |
| 79.2 | $T_a'$, $[T_{mrt}-T_a]'$, $v'^{*}$, $T_a'\times[T_{mrt}-T_a]'\times v'$ | 316.358 | 0.384 | 0.512 |
| 78.1% | $T_a'$, $[T_{mrt}-T_a]'$, $v'$, $T_a'\times[T_{mrt}-T_a]'\times v'^{*}$, $T_a'\times v'^{*}$ | 312.602 | 0.391 | 0.521 |
| 79.2% | $T_a'$, $[T_{mrt}-T_a]'$, $v'^{*}$, $T_a'\times[T_{mrt}-T_a]'\times v'$, $[T_{mrt}-T_a]'\times v'$ | 312.147 | 0.392 | 0.522 |
| 79.2% | $T_a'$, $[T_{mrt}-T_a]'$, $v'$, $T_a'\times[T_{mrt}-T_a]'\times v'$, $T_a'\times[T_{mrt}-T_a]'$ | 316.326 | 0.384 | 0.512 |
| 78.1% | $T_a'$, $[T_{mrt}-T_a]'$, $v'^{**}$, $T_a'\times[T_{mrt}-T_a]'\times v'^{**}$, $T_a'\times v'^{**}$, $[T_{mrt}-T_a]'\times v'^{**}$ | 312.123 | 0.392 | 0.522 |
| 78.1% | $T_a'^{*}$, $[T_{mrt}-T_a]'$, $v'$, $T_a'\times[T_{mrt}-T_a]'\times v'$, $T_a'\times v'$, $T_a'\times[T_{mrt}-T_a]'$ | 312.310 | 0.391 | 0.522 |

| | | | | |
|---|---|---|---|---|
| 79.2% | $T_a'^{*}$, $[T_{mrt}-T_a]'$, $v'^{*}$, $T_a'\times[T_{mrt}-T_a]'\times v'$, $[T_{mrt}-T_a]'\times v'$, $T_a'\times[T_{mrt}-T_a]'^{*}$ | 311.865 | 0.392 | 0.523 |
| 79.2% (Saturated model) | $T_a'^{*}$, $[T_{mrt}-T_a]'$, $v'^{**}$, $T_a'\times[T_{mrt}-T_a]'\times v'^{**}$, $[T_{mrt}-T_a]'\times v'^{**}$, $T_a'\times v'^{**}$, $T_a'\times[T_{mrt}-T_a]'^{**}$ | 311.808 | 0.392 | 0.523 |
| Classification cutoff: $P$ = 0.415<br>$^{**}p > 0.1$; $^{*}0.1 > p > 0.05$ | | | | |

Table. 6.3 Independent variables and the evaluation index in the logistics regression of thermal comfort

| **Overall accuracy** | **Independent variables** | **-2 Log likelihood** | **Cox & Snell $R^2$** | **Nagelkerke $R^2$** |
|---|---|---|---|---|
| 41% | $v'^{*}$ | 461.829 | 0.007 | 0.010 |
| 67.8% | $T_a'$ | 351.770 | 0.272 | 0.373 |
| 85.9% | $[T_{mrt}-T_a]'$ | 262.759 | 0.434 | 0.594 |
| 85.6% | $[T_{mrt}-T_a]'$, $v'^{*}$ | 262.284 | 0.435 | 0.595 |
| 64.1% | $T_a'$, $v'$ | 340.956 | 0.294 | 0.403 |
| 83.3% | $T_a'$, $[T_{mrt}-T_a]'$ | 235.117 | 0.477 | 0.652 |
| 83.3% | $T_a'$, $[T_{mrt}-T_a]'$, $v'^{**}$ | 234.504 | 0.478 | 0.654 |
| 84.7% | $T_a'$, $[T_{mrt}-T_a]'$, $v'$, $T_a'\times v'$ | 223.135 | 0.494 | 0.676 |
| 83.3% | $T_a'$, $[T_{mrt}-T_a]'$, $v'^{*}$, $[T_{mrt}-T_a]'\times v'^{*}$ | 228.347 | 0.487 | 0.666 |
| 83.3% | $T_a'$, $[T_{mrt}-T_a]'$, $v'^{*}$, $T_a'\times[T_{mrt}-T_a]'^{**}$ | 234.229 | 0.478 | 0.654 |
| **84.7%** | $\boldsymbol{T_a'}$, $\boldsymbol{[T_{mrt}-T_a]'}$, $\boldsymbol{v'}$, $\boldsymbol{T_a'\times v'}$, $\boldsymbol{[T_{mrt}-T_a]'\times v'^{*}}$ | **220.606** | **0.498** | **0.681** |
| 85.9% | $T_a'$, $[T_{mrt}-T_a]'$, $v'$, $T_a'\times v'$, $T_a'\times[T_{mrt}-T_a]'$ | 222.043 | 0.496 | 0.678 |
| 83.3% | $T_a'$, $[T_{mrt}-T_a]'$, $v'^{*}$, $[T_{mrt}-T_a]'\times v'$, $T_a'\times[T_{mrt}-T_a]'^{**}$ | 227.757 | 0.487 | 0.667 |
| 85.0% | $T_a'$, $[T_{mrt}-T_a]'$, $v'$, $[T_{mrt}-T_a]'\times v'^{*}$, $T_a'\times v'$, $T_a'\times[T_{mrt}-T_a]'^{**}$ | 219.279 | 0.500 | 0.684 |
| 84.2% | $T_a'$, $[T_{mrt}-T_a]'$, $v'$, $T_a'\times[T_{mrt}-T_a]'\times v'$ | 225.816 | 0.490 | 0.671 |
| 85.3% | $T_a'$, $[T_{mrt}-T_a]'$, $v'$, $T_a'\times[T_{mrt}-T_a]'\times v'^{*}$, $T_a'\times v'$ | 220.105 | 0.498 | 0.682 |
| 84.7% | $T_a'$, $[T_{mrt}-T_a]'$, $v'$, $T_a'\times[T_{mrt}-T_a]'\times v'$, $[T_{mrt}-T_a]'\times v'$ | 221.681 | 0.496 | 0.679 |
| 84.2% | $T_a'$, $[T_{mrt}-T_a]'$, $v'$, $T_a'\times[T_{mrt}-T_a]'\times v'$, $T_a'\times[T_{mrt}-T_a]'^{*}$ | 225.357 | 0.491 | 0.672 |

| | | | | |
|---|---|---|---|---|
| 84.7% | $T_a'$, $[T_{mrt}-T_a]'$, $v'^{*}$, $T_a'\times[T_{mrt}-T_a]'\times v'^{**}$, $T_a'\times v'^{**}$, $[T_{mrt}-T_a]'\times v'^{**}$ | 219.630 | 0.499 | 0.682 |
| 84.7% | $T_a'$, $[T_{mrt}-T_a]'$, $v'$, $T_a'\times[T_{mrt}-T_a]'\times v'$, $T_a'\times v'$, $T_a'\times[T_{mrt}-T_a]'^{*}$ | 221.146 | 0.497 | 0.680 |
| 85.0% | $T_a'$, $[T_{mrt}-T_a]'$, $v'$, $T_a'\times[T_{mrt}-T_a]'\times v'^{*}$, $[T_{mrt}-T_a]'\times v'$, $T_a'\times[T_{mrt}-T_a]'^{**}$ | 218.826 | 0.500 | 0.685 |
| 85.0% (Saturated model) | $T_a'$, $[T_{mrt}-T_a]'$, $v'$, $T_a'\times[T_{mrt}-T_a]'\times v'^{**}$, $[T_{mrt}-T_a]'\times v'^{**}$, $T_a'\times v'^{*}$, $T_a'\times[T_{mrt}-T_a]'^{**}$ | 218.461 | 0.501 | 0.685 |
| Classification cutoff: $P$ = 0.701<br>$^{**}p > 0.1$; $^{*}0.1 > p > 0.05$ | | | | |

Table 6.2 and Table 6.3 list all the tested independent variables in the thermal neutral and thermal comfort logistic regression model and the index for regression evaluation as well. The overall accuracy shows how well is the regression model fit with the original data. The value of $-2\,ln\,L$ (-2 Log likelihood) was the deviance from the likelihood function of the logistic model and it was able to evaluate the prediction effect of the logistic model. The regression model gave better prediction when $-2\,ln\,L$ was lower compared to the others. Specifically, the saturated model had the lowest value of $-2\,ln\,L$. Cox & Snell $R^2$ and Nagelkerke $R^2$ (Allison, 2012) evaluated the ratio of the total variation of the dependent variable being described by the independent variables in the given model. The model was better in fitting with the original data when the Cox & Snell $R^2$ and Nagelkerke $R^2$ were higher (Allison, 2012). The saturated model had the highest value of Cox & Snell $R^2$ and Nagelkerke $R^2$ but introduced some redundant independent variables into the model. All the independent variables including the first-order variables ($T_a'$, $[T_{mrt}-T_a]'$, $v'$), the

second-order product terms ($[T_{mrt}-T_a]'\times v'$, $T_a{}'\times v'$, $T_a{}'\times[T_{mrt}-T_a]'$) and the third-order product term ($T_a{}'\times[T_{mrt}-T_a]'\times v'$) were tested in the logistic regression model. In the model of thermal neutral prediction, $[T_{mrt}-T_a]'$had the highest fitting accuracy of 78.1% and the lowest value of $-2\,ln\,L$ value of 334.464 among all the first-order independent variables. However, decreasing two degrees of freedom by accounting for $T_a'$ and $v'$ into the model could further reduce the value of $-2\,ln\,L$ to 326.932. A difference of 7.532 in $-2\,ln\,L$ was significant at the level of $\alpha$ = 0.025 (>$x^2{}_{(df\,=\,2,\alpha\,=\,0.025)}$), which means the model including independent variables of $[T_{mrt}-T_a]'$, $T_a{}'$ and $v'$ could predict better than the model contains only $[T_{mrt}-T_a]'$. Considering the interaction terms, decreasing one degree of freedom by accounting for $T_a{}'\times v'$ or $[T_{mrt}-T_a]'\times v'$ could decrease the value of $-2\,ln\,L$ to a further level of 315.321 (>$x^2{}_{(df\,=\,1,\alpha\,=\,0.005)}$) and 322.273 ((>$x^2{}_{(df\,=\,1,\alpha\,=\,0.05)}$), respectively. Though the first-order variable $v'$ itself showed no statistical significance at the level of $\alpha$ = 0.05, its interaction terms $T_a'\times v'$ and $[T_{mrt}-T_a]'\times v'$ were non-negligible in the regression. Thus, the first-order variable $v'$ itself should also be included in the regression (Aiken et al., 1991; Cleary, & Kessler, 1982; Yu Xie, 2013). The interaction term $T_a'\times[T_{mrt}-T_a]'$did not make a statistical difference when it was compared with the first-order variable model ($T_a'$, $[T_{mrt}-T_a]', v'$). The second-order interaction terms $T_a'\times v'$ and $[T_{mrt}-T_a]'\times v'$ with its first-order parameters together had the closest $-2\,ln\,L$ value (313.139) to the saturated model

(311.808) while the least independent variables were needed. Further decreasing the degree of freedoms could not make any statistical difference at the level of $\alpha$ = 0.05. Therefore, the model containing independent variables of $T_a'$, $[T_{mrt} - T_a]'$, $v'$, $T_a' \times v'$ and $[T_{mrt} - T_a]' \times v'$ was used in the thermal neutral prediction of different combinations of meteorological parameters (shown as bold in Table 6.2).

The similar analytical method was used in filtering the independent variables for the thermal comfort logistic regression model. The model containing independent variables of $T_a'$, $[T_{mrt} - T_a]'$, $v'$, $T_a' \times v'$ and $[T_{mrt} - T_a]' \times v'$ was selected in the thermal comfort prediction as well (shown as bold in Table 6.3). In general, the logistic regression model for thermal comfort prediction had higher accuracy than that for thermal neutrality with lower $-2\,ln\,L$ value (220.606) and higher pseudo $R^2$ (0.498 and 0.681). Equation (6.1) and (6.2) describe the logistic regression equations for thermal neutrality and thermal comfort prediction, respectively.

$$\mathrm{P}_{thermal\ neutral} = \frac{\exp\,(0.662 - 0.240T_a' - 0.293[T_{mrt} - T_a]' + 1.686v' - 0.309(T_a' \times v') + 0.078([T_{mrt} - T_a]' \times v')}{1 + \exp\,(0.662 - 0.240T_a' - 0.293[T_{mrt} - T_a]' + 1.686v' - 0.309(T_a' \times v') + 0.078([T_{mrt} - T_a]' \times v')}$$

Equation (6.1)

$$\mathrm{P}_{thermal\ comfort} = \frac{\exp\,(3.714 - 0.632T_a' - 0.254[T_{mrt} - T_a]' + 2.825v' - 0.487(T_a' \times v') + 0.054([T_{mrt} - T_a]' \times v')}{1 + \exp\,(3.714 - 0.632T_a' - 0.254[T_{mrt} - T_a]' + 2.825v' - 0.487(T_a' \times v') + 0.054([T_{mrt} - T_a]' \times v')}$$

Equation (6.2)

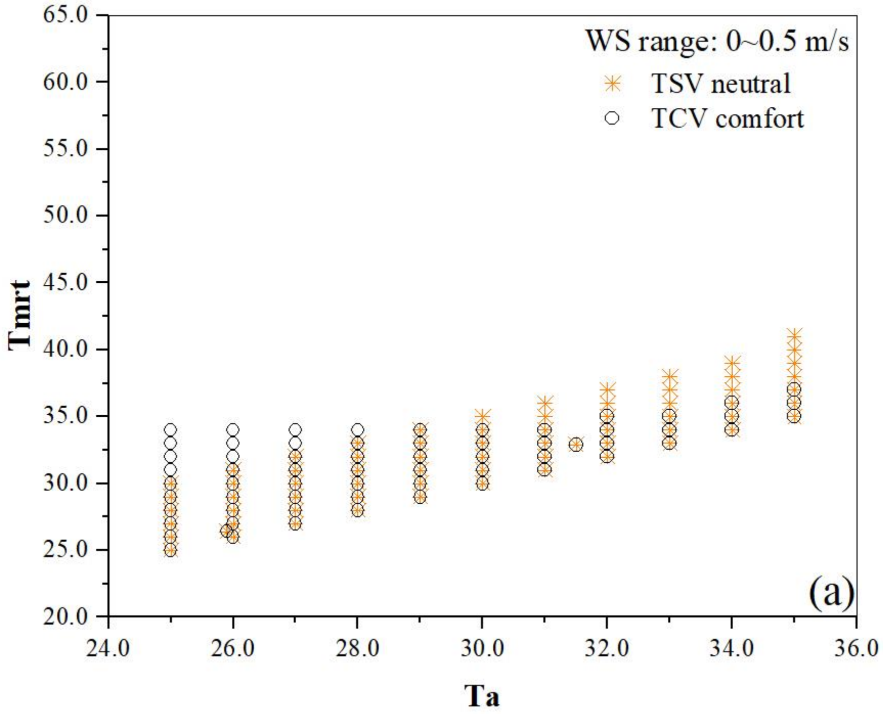
WS range: 0~0.5 m/s
TSV neutral
TCV comfort
Tmrt
Ta
(a)

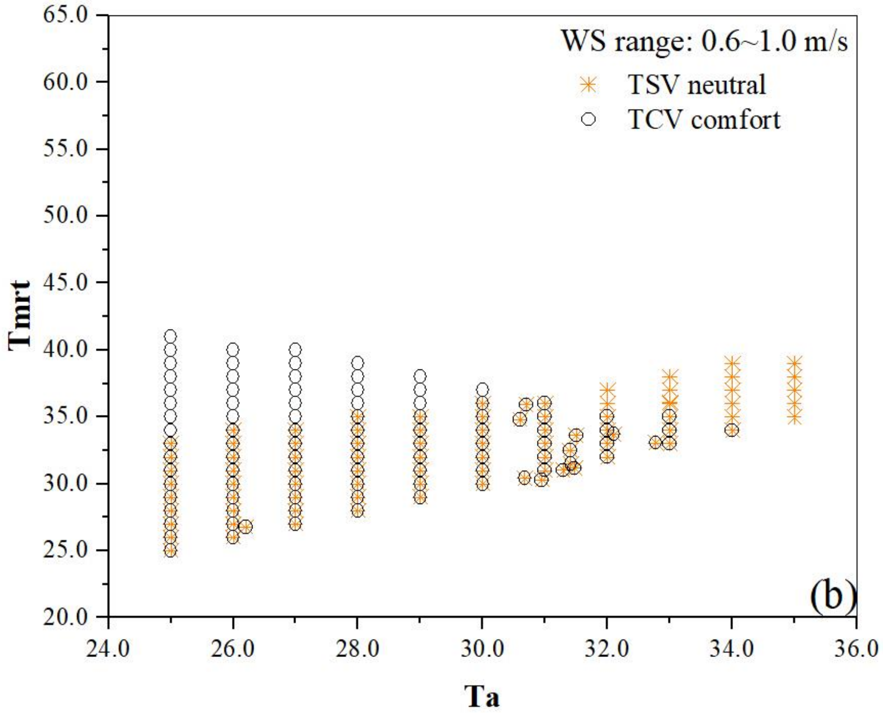
WS range: 0.6~1.0 m/s
TSV neutral
TCV comfort
Tmrt
Ta
(b)

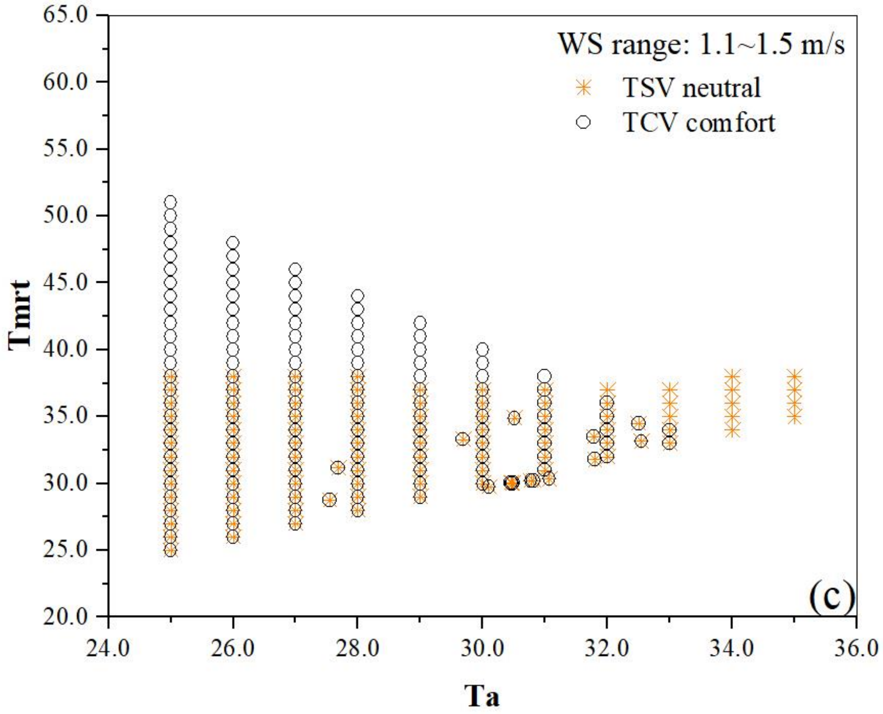
WS range: 1.1~1.5 m/s
TSV neutral
TCV comfort
Tmrt
Ta
(c)

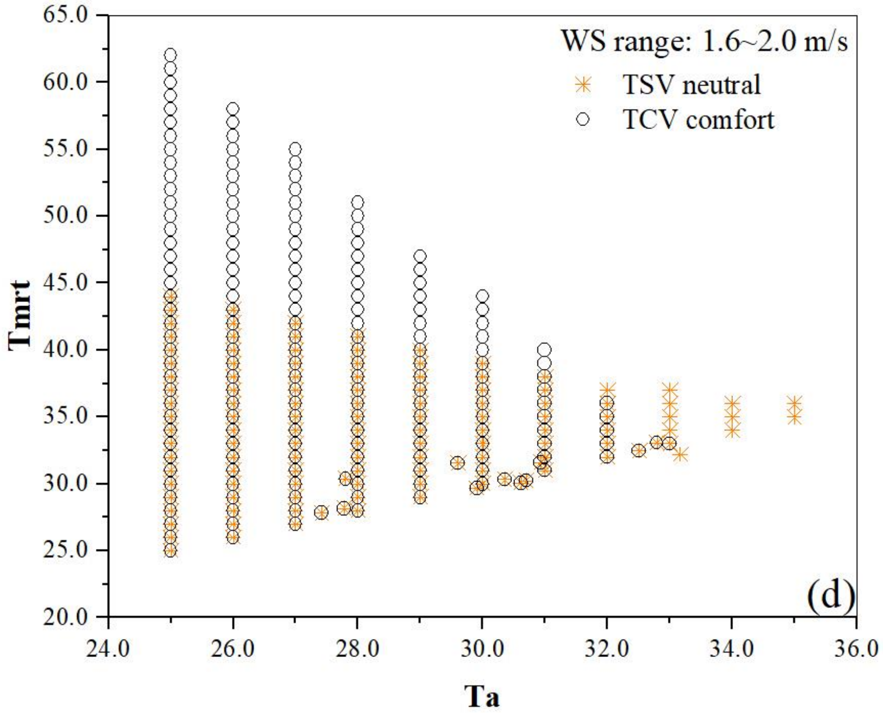
WS range: 1.6~2.0 m/s
TSV neutral
TCV comfort
Tmrt
Ta
(d)

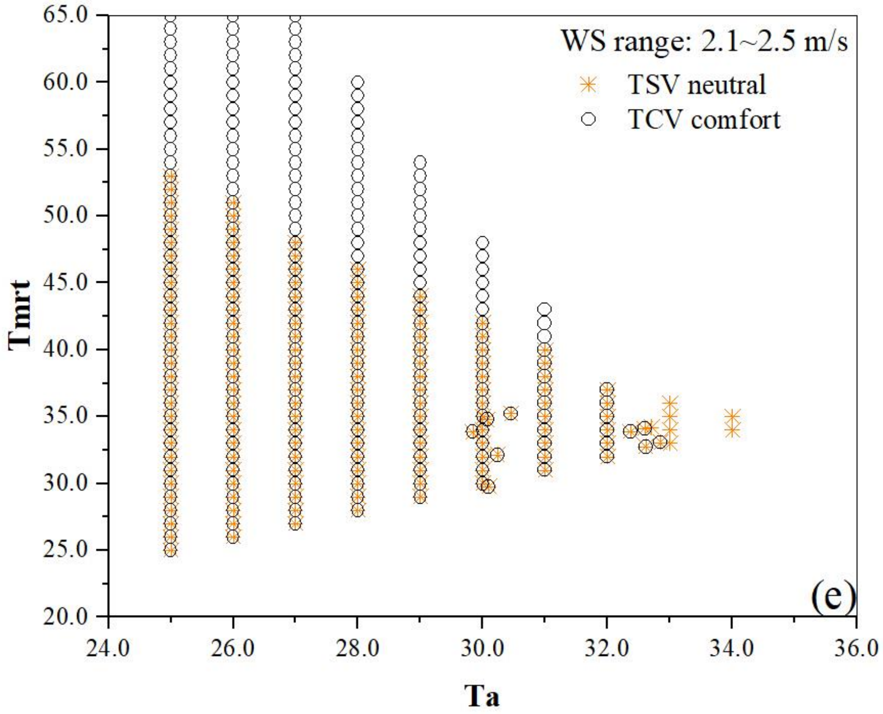
WS range: 2.1~2.5 m/s
TSV neutral
TCV comfort
Tmrt
Ta
(e)

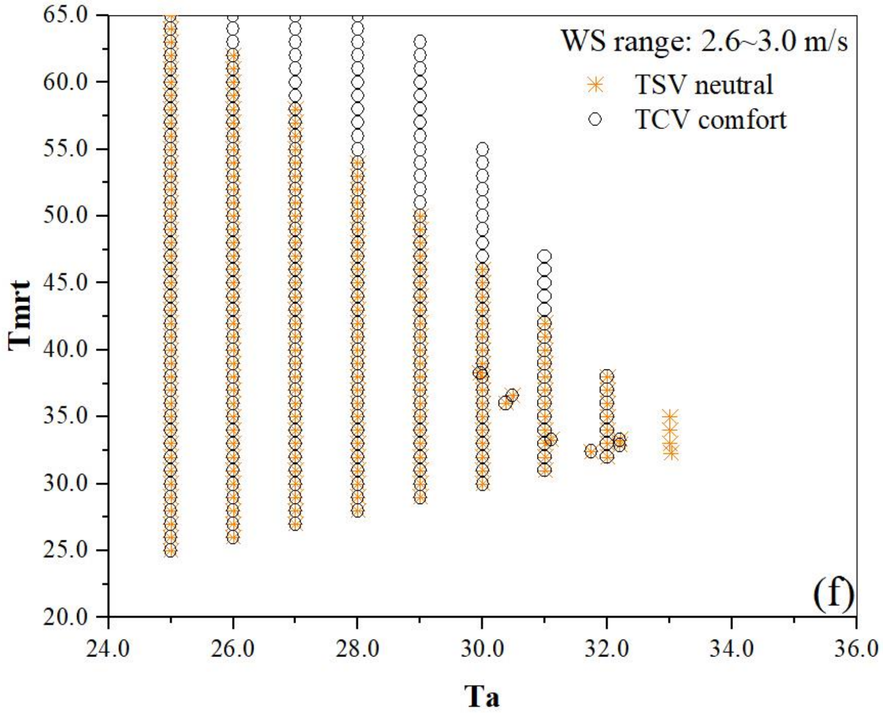
WS range: 2.6~3.0 m/s
TSV neutral
TCV comfort
Tmrt
Ta
(f)

Fig.6.9 The meteorological parameters combinations for thermal neutrality and thermal comfort in the Hong Kong summer (a) Wind speed range: 0~0.5 m/s; (b) Wind speed range: 0.6~1.0 m/s; (c) Wind speed range: 1.1~1.5 m/s; (d) Wind speed range: 1.6~2.0 m/s; (e) Wind speed range: 2.1~2.5 m/s; (f) Wind speed range: 2.5~3.0 m/s.

The prediction result of thermal neutrality and thermal comfort cases is shown in Fig. 6.9. The result covers the $T_a$ from 25 to 35 °C. An increase level of 0.5 m/s of wind speed was used as a partition zone. Increasing wind speed could counterbalance the effect of $T_{mrt}$ have on bringing the thermal sensation feelings to the hotter level when $T_a$ < 32 °C. In low wind speed zone (0 to 0.5 m/s), the allowable $T_{mrt}$ for thermal neutrality was only 5 °C higher than $T_a$ and was free of influence from the increase of $T_a$ level. However, when wind speed was as high as the range of 2.6 to 3.0 m/s, the feeling of thermal neutrality could be achieved in the condition of $T_{mrt}$ up to 65 °C provided that $T_a$ was 25 °C. But when $T_a$ was 30 °C, the upper limit of $T_{mrt}$ for thermal neutrality was only limited to around 46 °C. The rate of decrease in the allowable upper limit of $T_{mrt}$ for thermal neutrality in per unit increase of $T_a$ became larger with the increase of wind speed zone. This phenomenon indicates that providing thermal neutrality under direct solar radiation condition by the means of increasing wind speed was more promising when $T_a$ was in a pleasant range than that in a severe hot range. In the severe hot conditions, increasing wind speed might bring negative effect when achieving thermal neutrality was considered. Increasing wind speed was almost useless on offsetting the hot feelings resulted from $T_{mrt}$ when $T_a$ = 32 °C. The upper limit for thermal neutrality of $T_{mrt}$ remained unchanged at around 37 °C when $T_a$ = 32 °C regardless of the increase of wind speed. When $T_a$ was above 32 °C, thermal neutral feeling became less or even disappeared although wind speed was increased. This is possible if the surrounded $T_a$ was almost similar to the skin temperature, less cooling effect would be provided by only increasing wind speed on enhancing convective heat transfer in this case. The wind would be felt as hot wave in this case.

The influence of increasing wind speed in achieving thermal comfort was more obvious than achieving thermal neutrality. When $T_a$ = 25 °C, every 0.5 m/s raise of wind speed could offset the discomfort feeling by at least 10 °C raise of $T_{mrt}$ (Fig. 6.9 (a)). The strongest observed solar radiation level ($T_{mrt}$ close or equal to 65 °C), which was the condition of direct solar radiation from a clear sky in the midday of Hong Kong summer, was also able to provide the thermal comfort feeling in the condition of $v \geq 2.1$ m/s and $T_a \leq 27$ °C or of $v \geq 2.6$ m/s and $T_a \leq 28$ °C. Increasing wind speed could still enable extra solar radiation acceptance when $T_a \geq 30$ °C, but its influence was less than that of the cases of $T_a < 30$ °C. The highest allowable $T_{mrt}$ condition for thermal comfort limited to only 5 °C higher than $T_a$ when $T_a$ = 32 °C, which was a typical cloudy day in Hong Kong summer.

The conditions which were able to provide thermal comfort did not necessarily coincide with those able to provide thermal neutrality. It has been suggested in indoor environment (R. J. De Dear, & Brager, 2002; Nicol, & Humphreys, 2010) and recently indicated in an outdoor study that people felt thermally comfortable in slightly warm status in the cold season and slightly cool status in the hot season (D. Lai, D. Guo, et al., 2014). From the result of the present study, the thermal comfort condition covered much wider combination of meteorological parameters, which indicates that the requirement to achieve thermal comfort was not as strict as achieving thermal neutrality. It can be discovered from both the coefficient of wind speed in the Equation (3.2) and the rate of change of the upper limit of $T_{mrt}$ with the increase of wind speed level. In the cases of $T_a \leq 31$ °C, the conditions for achieving thermal comfort was less strict than that for thermal neutrality. Wind speed amplification could improve the range of thermal comfort but not thermal neutrality in the cases with higher solar radiation. Meanwhile, thermal comfort was harder to be achieved than thermal neutrality when $T_a \geq 32$ °C. It is not easy to achieve thermal comfort in the windy environment when $T_a > 32$ °C. With such high air temperature and high humidity in Hong Kong summer, the wind is felt hot and sticky and hence uncomfortable when $T_a > 32$ °C. Notably, this aforementioned analysis is not able to conclude which kind of thermal sensation feeling it is in the cases of achieving thermal comfort but not thermal neutrality due to the limitation of the category. Last but not least, as relative humidity was not included as one of the independent variables in the logstic regression, the above results and discussions are only applicable to the citis located in the subtropical area with high relative humidity level in summer.

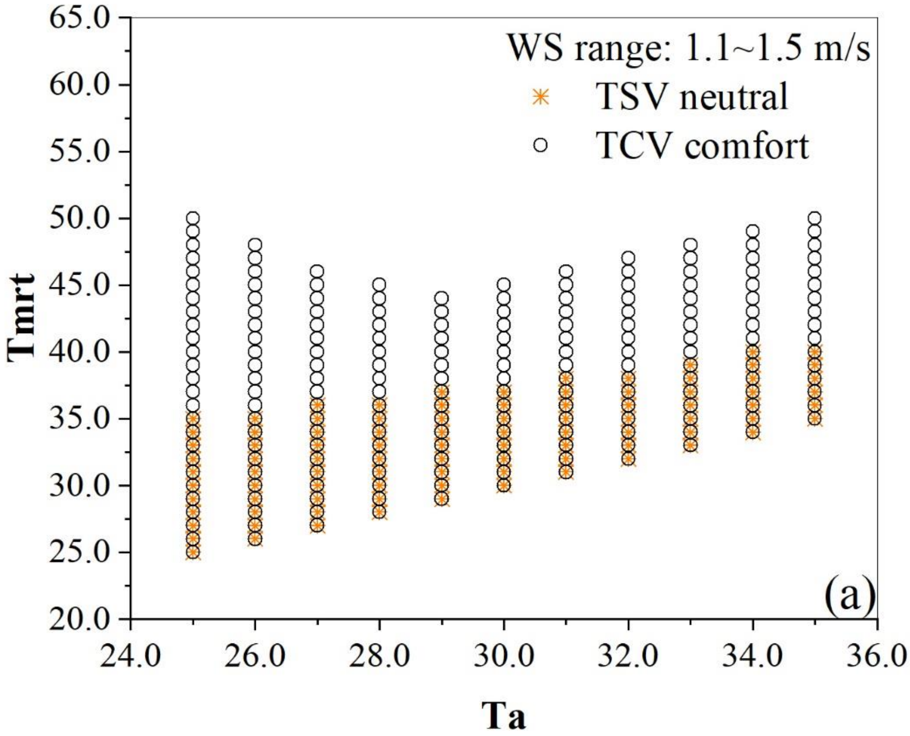

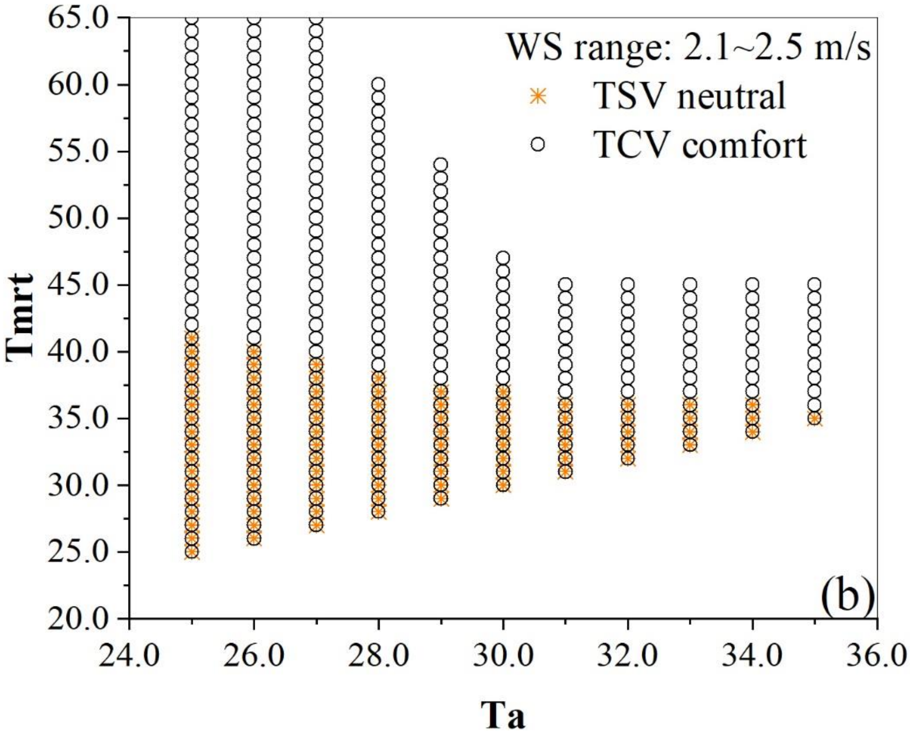


Fig.6.10 The meteorological parameters combinations for thermal neutrality and thermal comfort in the September of Hong Kong (a) Wind speed range: 1.1~1.5 m/s; (b) Wind speed range: 2.1~2.5 m/s.

Fig.6.10 shows the meteorological paprameter combinations for thermal neutrality and thermal comfort in the September of Hong Kong. The prediction data for September still use the same mathmatic structure and the independent variables described in the previous part, but feed in merely the data collected in September. Two prediciton datasets, wind speed in the range of 1.1 to 1.5 m/s and 2.1 to 2.5 m/s are presented here as examples. By comparing the prediction results based on the dataset of whole summer and that of September, we are able to figure out the difference of thermal neutrality and comfort ranges of the meteorological parameter combinations between monthly and seasonal calculation. September is choosen because it represent the end of summer month. The thermal feelings in this month can be the reflection of thermal adaptation after a whole season.

When thermal neutral is under discussion, it is noticable that the thermal neutral conditions in September in the wind speed range of 1.1 to 1.5 m/s is similar to that in the whole summer. However, for the wind speed range of 2.1 to 2.5 m/s, the thermal neutral conditions in September corresponding to the air temperature between 25 and 32 °C is less than that in the whole summer, especially when the air temperature is lower than 30 °C. In other words, when the wind condition increase to 2.1 to 2.5 m/s, less high radiation cases in the September dataset locate in thermal neutral condition than that in whole summer. As the prediction results cannot distinguish whether the points that not locating in thermal neutrality correspond to the cool side or warm side. We make an inference by combining with the thermal comfort prediciton results in September that the those cases might locate in the cool side for the reason because the comfort cases were similar to the whole summer prediciton shown in Fig. 6.9. This might be the result of thermal adaptation after a long summer. People are more sensitive to cool conditions in late summer than early summer.

Another interesting finding from Fig. 6.10 is that more allowable high radiation cases in high air temperature range ($T_a > 30$ °C) for thermal comfort in September than that in the whole summer. This is also the thermal adaptation result of a long summer: people are more tolerable to high radiation conditions than early summer.

By the comparison analysis between prediciton results from September and the whole summer, we notice that the effect of thermal adaptation is very obvious after a season and cannot be ignored in the outdoor thermal comfort studies.

## 6.5 Design recommendations for outdoor thermal comfort improvement

The target of outdoor thermal environment design is to provide as more comfortable condition as possible. Designs which focus on alleviating the hot feelings from hot days will aggravate the cool feelings in cold days. The special condition for Hong Kong is that summer-time accounts for one third of the time in a year and the winter-time is short and the uncomfortable level is mild. Therefore, the design recommendations for improving outdoor thermal comfort conditions should focus on hot days.

From the previous analysis, solar radiation is the main factor which contributes to the uncomfortable hot feeling. And it is obvious that improving wind speed can effectively offset the uncomfortable feelings caused by increased solar radiation level when the air temperature is no higher than 32 °C. Therefore, the main recommendations for better outdoor thermal environment focus on providing more shading and improving wind environment. Some of the recommendations for upgrading outdoor thermal conditions are listed as below with actual cases.

### 6.5.1 Improving pedestrian wind environment

The following strategies are recommended for improving pedestrian wind environment.

**Elevated buildings**: The design of elevated buildings refer to the buildings with an elevated floor from the ground lifted using columns, shear walls, central core or a combination of them (X. Zhang et al., 2018a) (shown in Fig. 6.11). Such kind of buildings can provide space underneath the elevated floor for wind to circulate through and is advantageous to improve the urban wind environment. Xia et al. (2017) demonstrated significant decrease of the areas with low wind speeds underneath the elevated buildings by transforming the ordinary buildings into buildings with elevated structure through CFD and wind tunnel test. This kind of structure should be recommended in the cities with weak wind environment.


Fig. 6.11 Example of the area under the elevated building

**Reduction of building ground coverage**: It can be achieved by the step-down podium design and the separations between buildings as shown in Fig. 6.12. It helps to improve urban ventilation in pedestrian level. Yuan and Ng (2012) did a parametric analysis of different types of building structure and confirmed that step-down design can lead air flow to the pedestrian level and the separations between buildings significantly accelerate turbulent level in the podium level.

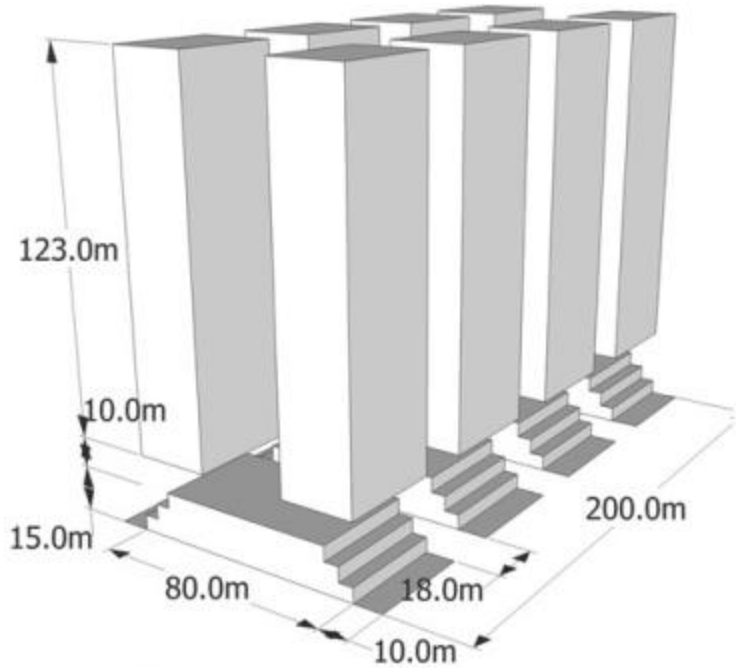


Fig. 6.12 Example of stepped podium design with building separations and tall towers (derived from Yuan and Eg (2012))

**Porous buildings**: The concept of porous building is similar to the previous two recommendations. Hong Kong government has issued a sustainable building design guidelines (HKBD (Hong Kong Buildings Department), 2016), which requires up to one third of the vertically projected façade area to be permeable. As a result of that, we can notice that the newly-built landmarks in Hong Kong can be categorized as porous buildings, such as the Hong Kong government building (shown in Fig. 6.13).

Fig. 6.13 Hong Kong government building

**Breezeway and air path**: The general idea for high-dense city is that the better air ventilation in the city, the better it will be for the dense urban areas (Ng, 2006). This is more important for the major roads which are along the direction of prevailing wind direction. Widening the major road or creating proper open plazas along the prevailing wind direction can ensure the prevailing wind penetrate deep in the densely urban area (Ng, 2006) and thus improving the pedestrian-level wind environment in the high-dense urban area. However, this rule is not applicable to all the roads, especially for those small roads which are not along the prevailing wind direction. To achieve thermal comfort, the width of the road should be considered along with its orientation and the buildings along the road. Designs with wider street does allow higher air ventilation rate, but at the same time such design cannot create much shading and thus allow more solar access. In the case of high-density city located in the sub-tropical area, whether the benefit of improving wind environment by widen street could overcome the negative effect from less shading in hot summer condition should be further discussed. The quantitative analysis between these two factors from this part could provide some insights.

### 6.5.2 Providing shading

**Urban greening:** The concept of "urban greening" has been proposed to alleviate urban heat island effect. Urban greening includes tree planting, urban parks and green roofs etc. An early review by Bowler et al. (2010) pointed out the evidence of lower air temperature within a park recorded of 0.94 °C cooler than other urban areas. Lin et al. (2010) found SVF (sky view factor) significantly influence outdoor thermal comfort condition in Taiwan where has hot summer and mild winter. They built the relation between SVF (sky view factor) and the percentage of thermal comfort period over a year and found low SVF (highly shaded) corresponded to longer thermal comfort period (T.-P. Lin et al., 2010). On the evidence of the above research, it is proved that shading can effectively improve thermal comfort condition for the subtropical area. But designers have to concern about choosing tree types and the arrangement of trees, because planting trees can also effectively reduce wind speed in pedestrian level.

**Shading device**: Providing shading using shading devices such as sunshade umbrella and overhang balcony are useful to overcome heat stress in sub-tropical area. Lau et al. (2019) conducted experiment in the urban area of Hong Kong in summer to study the dynamic thermal response of pedestrian under outdoor walking routes: one group was exposed to continuous solar radiation, the other group was with discrete shading provided by trees or overhang balcony. They found the group went through discrete shading expressed more satisfied thermal feeling and they attribute this observation to “thermal alliestheisia” (Lau et al., 2019; Parkinson, & De Dear, 2015). The immediate thermal pleasant thermal history under shading has influence on the thermal perception under direct solar radiation. This study shows the importance of providing shading by changing the urban geometry design for creating better pedestrian environment in high-density cities.

# Chapter 7 Conclusions and recommendations for future study

## 7.1 Summary of main works

This thesis has investigated the issues related to outdoor thermal comfort in the city on the scale of the neighborhood using the method of onsite monitoring and surveys. This study aims at quantifying the thermal effect of the outdoor environment on human body. The main contributions are summarized below.

(1) A microclimate station was used to monitor the meteorological parameters in three different kinds of outdoor thermal conditions: the semi-outdoor environment with less wind, the open environment where received direct solar radiation, and the semi-outdoor environment with strong wind. At the meantime, human subjects were invited to experience the actual outdoor environments and express their thermal perceptions. The survey results show that the outdoor thermal environment varies a lot with different design of building structures and the placement of buildings. The actual users were sensitive to the fluctuating wind environment, especially when the operative temperature was below 34°C. Increasing wind speed from breeze to mild wind could create a cooling effect. The users could tolerate high air temperature well as long as the solar radiation was low.

(2) Appling the CBE model directly to the outdoor environment leads to

prediction errors. The comparison results of the CBE model and the field survey results show that the CBE model over predicted the thermal sensation in hot conditions, especially when the solar radiation level was low. The model was not sensitive to the change of the wind environment.

(3) The skin temperature of 17 local body parts were measured for the human subjects who joined the outdoor experiment. The measurement results show a wide range of local skin temperatures corresponded to the thermal neutral status, and it was termed as “null-zone”. The actual users in the outdoor environment could adapt to the fluctuating wind environment quite well.

(4) Some revisions were done in the CBE model, to further develop the CBE model for the better evaluation of the outdoor thermal environment. The field measured “null-zone” of different body parts were included in the CBE model. The forehead was also included as one of the dominant local body parts. The model accuracy was improved to 93.7% after the revision.

(5) An independent t-test was presented to identify whether the residents could tell the difference near thermal neutrality. The probit analysis was utilized to figure the thermal neutral zone in different seasons. Summer had the narrowest thermal neutral range of merely 1.51 °C in operative temperature, making summer the severest season for Hong Kong.

(6) A logistic model was developed to predict the thermal neutral and thermal comfort ranges. Thermal comfort was easier to be achieved than thermal neutrality when the air temperature was no higher than 31 °C. When the air temperature was higher than 32 °C, it was hard to achieve either thermal neutrality or thermal comfort by increased wind speed.

### 7.2 Evaluation of a multi-nodal thermal regulation model for assessment of outdoor thermal comfort- Sensitivity to wind speed and solar radiation

This section compared the surveyed thermal sensation data and the simulated data using the CBE model and verified its usage in outdoor environments from a sensitivity point of view. Two fast-changing meteorological parameters – wind speed and solar radiation – were discussed in this study.

The CBE model did not respond well to the changes in wind speed. The on-site data show that increasing wind speed from breeze group to mild wind group could create a considerable cooling effect when the operative temperature was lower than 34° C. However, the CBE-simulated results showed no thermal sensation difference between two wind speed groups. Subjects' thermal sensation in an actual outdoor environment was more sensitive to wind environment than predicted in the model.

Subjects better tolerated high air temperatures outdoors when the solar radiation was low. They preferred low radiation and disliked medium or high radiation. The mid and high radiation groups made a leap in TSV compared with the low radiation group in the on-site data, but this was not observed in the CBE-simulated data. The CBE model may over-predicted the TSV of the low radiation group. The sensitivity of these two parameters was examined under different operative temperature ranges. Subjects' sensitivity to wind speed and solar radiation did not remain the same at all operative temperature ranges. They were more sensitive to changes in wind speed when the environment got hotter.

Their sensitivity to mean radiant temperature remained more or less the same, except for the condition that subjects stayed in neutral thermal status. The CBE-simulated data showed a similar pattern. However, for a one-degree change in TSV, the CBE data allowed less change in wind speed and solar radiation than the on-site data, which implies that the CBE model was less sensitive to these two parameters than the actual outdoor survey results showed.

We have to state the limitation of this comparison due to the reason of thermal adaptation. The dataset covered about three fourths of whole-year length. Seasonal thermal adaptation might be one of the important factors influencing the thermal response in the field survey results. Thermal adaptation is complex because it involves physiological, psychological and behavioral factors. However, the CBE model is a pure physiological model which does not take into account of the psychological and behavioral factors. Therefore, the influence of thermal adaptation on thermal responses could not be covered in this model.

To better reveal the relation between outdoor transient and asymmetric thermal environment and thermal sensation feelings and for the purpose of better application of the multi-nodal thermal regulation model in the outdoors, additional direct measurement of subject physiological parameters such as core and skin temperatures in outdoor environments may be helpful.

## 7.3 Development of a multi-nodal thermal regulation and comfort model for the outdoor environment

This section focuses on the application of the CBE model in the outdoor environment. A primary comparison of the overall TSV and TCV from the field-collected and the CBE-simulated datasets organized using $T_{op}$ started the discussion. The CBE-simulated TSV was higher than the field-surveyed TSV. The CBE-simulated TCV was mainly located in the uncomfortable side, while above half of the surveyed TCV was located in the comfortable side. To further locate the problem causing the difference in TSV prediction. A comparison between the field measured, and CBE-simulated mean skin temperature was conducted. A difference exists between the measured and simulated mean skin temperature. Therefore, the measured skin temperature was used as the input in the original CBE comfort model in further analysis to avoid the prediction difference generated by the multi-nodal thermal regulation model. Noticeable retention effect exists in the thermal neutral status of the local body parts when showing the relation between the local and mean body temperature and field-surveyed TSV. This phenomenon differs a lot from the CBE-simulated local and overall TSV datasets where “set-point” was applied in the simulation.

A discussion about the "null zone" and "set-point” was brought forward from two aspects: the adaptation to persistent thermal stimulus and the mechanism of the control theory for temperature regulation. Considered the fluctuating characteristics of the wind environment in the outdoors, it is proposed using the "null zone" instead of "set-point" in the calculation of "load error". A revised definition of “load error” used in thermal comfort studies was proposed as the deviation between the regulated variable and its threshold of null zone. The null zone range of skin temperature for different local body parts was defined for the first time in the real-life outdoor environment.

Finally, the CBE comfort model was further developed to fit in outdoor settings. The revision mainly focused on two aspects: applying the measured null zone range in the calculation of local thermal sensation, adding the forehead as one of the dominant body parts when determining overall thermal sensation. About 93.7% of the variation in the field-surveyed overall TSV was addressed by the revised CBE comfort model.

This section focuses on improving the prediction accuracy of thermal sensation when applying the CBE comfort model in the outdoor conditions where no noticeable temperature change of air temperature and solar radiation. The improvement of the thermal comfort prediction is not the main issue under discussion, and we will address the thermal comfort issue in future studies. The dataset includes the winter experiment conducted in Sydney, during which visiting scholars from multiple climate zones of China were invited to the experiment. It is needed to point out that thermal adaptation for the participants who originate from different parts of China might lead to the different thermal perception to similar thermal stimulation.

## 7.4 Outdoor thermal sensation and logistic regression analysis of comfort range of meteorological parameters in Hong Kong

This section discussed the outdoor thermal comfort issues in Hong Kong. The changes of air temperature in Hong Kong from the past 10 years were presented along with the number of days over 30 °C based on the statistics from the Hong Kong Observatory. The confusion of defining thermal sensation feeling around thermal neutral status was studied using the independent t-test. Hong Kong residents could not tell the difference from "slightly cool" to "slightly warm" when they were around thermal neutrality but could have explicit thermal sensation voting when the thermal condition was away from thermal neutrality. The probit analysis was utilized to figure out the thermal neutral zone in four seasons in Hong Kong. Obvious thermal adaptation effect was found in Hong Kong residents from the phenomenon that autumn had higher thermal neutral range than spring. Summer had the narrowest thermal neutral range of merely 1.51 °C in operative temperature, making the thermal comfort problem the severest in this season for Hong Kong. Therefore, logistic regression was used to search for the meteorological parameter combination to achieve thermal comfort and thermal neutrality focusing on the warm and hot conditions in Hong Kong. The model contains independent variables of $\mathrm{Ta}'$, $[\mathrm{Tmrt}-\mathrm{Ta}]'$, $v'$, $\mathrm{Ta}'\times v'$ and $[\mathrm{Tmrt}-\mathrm{Ta}]'\times v'$ had the best prediction effect in both thermal neutrality and thermal comfort. Wind could offset the negative effect of solar radiation on both thermal neutrality and thermal comfort, but its effect decreased with the increase of air temperature. Thermal comfort was easier to be achieved than thermal neutrality when the air temperature was no higher than 31 °C, with higher upper limit solar radiation acceptable. When the air temperature was higher than 32 °C, it was hard to achieve either thermal neutrality or thermal comfort by increased wind speed. The combination of meteorological parameters suitable for achieving thermal neutrality or thermal comfort is only applicable to the subtropical area with high relative humidity.

### 7.5 Recommendations for the future study

Despite the findings obtained from this thesis, this thesis still exhibits a few limitations, which are recommended to be done in future studies.

(1) This thesis presents merely the local skin temperature and its relationship with the CBE model. The whole modification was based merely on the local skin temperature. However, other physiological parameters are also closely related to thermal perceptions, such as core temperature, sweating rate, and metabolic rate. It is recommended that future studies should focus on the listed physiological parameters and investigate its influence on outdoor thermal perceptions. The revisions of CBE model for the outdoor environment focus on its logic structure, the coefficients of local thermal sensation, comfort, and overall sensation, comfort were not modified due to limit data support. Therefore, there is still lots of work to do for the modification of the CBE model.

(2) Though the existing models are confirmed not suitable for applying directly to the outdoor environment. The models target at higher turbulence intensity level, and fluctuating wind environment was not developed yet. Future research should focus more on the thermal comfort model targeted at a high turbulence level.

(3) Most of the human subjects for this study are students and young colleges. The middle-aged and elderly were not the main participants. It is suggested that the survey range should be extended to all ages, to investigate the application range to the revised CBE model and the thermal neutrality and thermal comfort ranges for Hong Kong.

(4) The onsite survey for the investigation of transient wind characteristics was 5 minutes one set. It aimed to catch the transient thermal effect of the fluctuating wind environment, but the fixed time constant for distributing the survey was not the most efficient way for catching the transient thermal characteristics of gust wind. Therefore, it is suggested that in the future study.

# Reference


Ahmed, K. S. (2003). Comfort in urban spaces: defining the boundaries of outdoor thermal comfort for the tropical urban environments. *Energy and Buildings, 35*(1), 103-110.

Aiken, L. S., West, S. G., & Reno, R. R. (1991). *Multiple regression: Testing and interpreting interactions*: Sage.

Ali-Toudert, F., & Mayer, H. (2006). Numerical study on the effects of aspect ratio and orientation of an urban street canyon on outdoor thermal comfort in hot and dry climate. *Building and Environment, 41*(2), 94-108. doi:10.1016/j.buildenv.2005.01.013

Ali-Toudert, F., & Mayer, H. (2007). Effects of asymmetry, galleries, overhanging facades and vegetation on thermal comfort in urban street canyons. *Solar Energy, 81*(6), 742-754.

Allison, P. D. (2012). *Logistic regression using SAS: Theory and application*: SAS Institute.

Andrade, H., Alcoforado, M. J., & Oliveira, S. (2011). Perception of temperature and wind by users of public outdoor spaces: relationships with weather parameters and personal characteristics. *International journal of Biometeorology, 55*(5), 665-680.

Antoniou, N., Montazeri, H., Neophytou, M., & Blocken, B. (2019). CFD simulation of urban microclimate: Validation using high-resolution field measurements. *Science of the total environment, 695*, 133743.

Arens, E., & Bosselmann, P. (1989). Wind, sun and temperature—Predicting the thermal comforf of people in outdoor spaces. *Building and Environment, 24*(4), 315-320.

Arens, E. A., & Zhang, H. (2006). The skin's role in human thermoregulation and comfort. In *Thermal and Moisture Transport in Fibrous Materials* (pp. 560-602): Woodhead Publishing Ltd.

ASHRAE Standard Committee. (2010). Standard 55-2010:“Thermal Environmental Conditions for Human Occupancy”; ASHRAE. *Atlanta USA*.

ASHRAE Standard Committee. (2013). *ASHRAE handbook: fundamentals 2013*:

Ashrae.

ASHRAE Standard Committee. (2017a). *ASHRAE handbook: fundamentals 2017*: American Society of Heating, Refrigerating and Air-Conditioning Engine.

ASHRAE Standard Committee. (2017b). Standard 55-2017:“Thermal Environmental Conditions for Human Occupancy”; ASHRAE. *Atlanta USA*.

Ballantyne, E., Hill, R., & Spencer, J. (1977). Probit analysis of thermal sensation assessments. *International journal of Biometeorology, 21*(1), 29-43.

Belding, H., & Hatch, T. (1955). Index for evaluating heat stress in terms of resulting physiological strains. *Heating, piping and air conditioning, 27*(8), 129-136.

Bittel, J. (1987). Heat debt as an index for cold adaptation in men. *Journal of applied physiology, 62*(4), 1627-1634.

Blazejczyk, K., Epstein, Y., Jendritzky, G., Staiger, H., & Tinz, B. (2012). Comparison of UTCI to selected thermal indices. *International journal of Biometeorology, 56*(3), 515-535.

Bligh, J. (2006). A theoretical consideration of the means whereby the mammalian core temperature is defended at a null zone. *Journal of applied physiology, 100*(4), 1332-1337.

Blocken, B., & Carmeliet, J. (2004). Pedestrian wind environment around buildings: Literature review and practical examples. *Journal of Thermal Envelope and Building Science, 28*(2), 107-159.

Blocken, B., & Carmeliet, J. (2004). Pedestrian Wind Environment around Buildings: Literature Review and Practical Examples. *Journal of Building Physics, 28*(2), 107-159. doi:10.1177/1097196304044396

Blocken, B., & Carmeliet, J. (2007). Validation of CFD simulations of wind-driven rain on a low-rise building facade. *Building and Environment, 42*(7), 2530-2548. doi:10.1016/j.buildenv.2006.07.032

Blocken, B., & Persoon, J. (2009). Pedestrian wind comfort around a large football stadium in an urban environment: CFD simulation, validation and application of the new Dutch wind nuisance standard. *Journal of Wind Engineering and Industrial Aerodynamics, 97*(5-6), 255-270.

Blocken, B., Stathopoulos, T., Carmeliet, J., & Hensen, J. L. (2011). Application of computational fluid dynamics in building performance simulation for the outdoor environment: an overview. *Journal of Building Performance Simulation, 4*(2), 157-184.

Bottema, M. (2000). A method for optimisation of wind discomfort criteria. *Building and Environment, 35*(1), 1-18.

Bowler, D. E., Buyung-Ali, L., Knight, T. M., & Pullin, A. S. (2010). Urban greening to cool towns and cities: A systematic review of the empirical evidence. *Landscape and Urban Planning, 97*(3), 147-155.

Bradley, A. V., Thornes, J. E., Chapman, L., Unwin, D., & Roy, M. (2002). Modelling spatial and temporal road thermal climatology in rural and urban areas using a GIS. *Climate Research, 22*(1), 41-55.

Brager, G. S., & De Dear, R. J. (1998). Thermal adaptation in the built environment: a literature review. *Energy and Buildings, 27*(1), 83-96.

Bröde, P., Fiala, D., Błażejczyk, K., Holmér, I., Jendritzky, G., Kampmann, B., . . . Havenith, G. (2012). Deriving the operational procedure for the Universal Thermal Climate Index (UTCI). *International journal of Biometeorology, 56*(3), 481-494.

Brode, P., Kruger, E. L., Rossi, F. A., & Fiala, D. (2012). Predicting urban outdoor thermal comfort by the Universal Thermal Climate Index UTCI--a case study in Southern Brazil. *Int J Biometeorol, 56*(3), 471-480. doi:10.1007/s00484-011-0452-3

Brück, K., Baum, E., & Schwennicke, H. P. (1976). Cold-adaptive modifications in man induced by repeated short-term cold-exposures and during a 10-day and-night cold-exposure. *Pflügers Archiv, 363*(2), 125-133.

Buildings Department. (2014). *Design and Construction Requirements for Energy Efficiency of Residential Buildings Hong Kong Retrieved fromhttp*. Retrieved from

Chan, S. Y., Chau, C. K., & Leung, T. M. (2017). On the study of thermal comfort and perceptions of environmental features in urban parks: A structural equation modeling approach. *Building and Environment, 122*, 171-183. doi:10.1016/j.buildenv.2017.06.014

Chen, L., & Ng, E. (2012). Outdoor thermal comfort and outdoor activities: A review of research in the past decade. *Cities, 29*(2), 118-125. doi:10.1016/j.cities.2011.08.006

Chen, L., & Ng, E. (2013). Simulation of the effect of downtown greenery on thermal comfort in subtropical climate using PET index: a case study in Hong Kong. *Architectural Science Review, 56*(4), 297-305.

Cheng, C., Matsukawa, T., Sessler, D. I., Makoto, O., Kurz, A., Merrifield, B., . . . Olofsson, P. (1995). Increasing mean skin temperature linearly reduces the core-temperature thresholds for vasoconstriction and shivering in humans. *The Journal of the American Society of Anesthesiologists, 82*(5), 1160-1168.

Cheng, V., & Ng, E. (2006). Thermal comfort in urban open spaces for Hong Kong. *Architectural Science Review, 49*(3), 236-242.

Cheng, V., Ng, E., Chan, C., & Givoni, B. (2009). *An experiment of urban human thermal comfort in hot and humid sub-tropical city of Hong Kong under high density urban morphological conditions, Hong Kong.* Paper presented at the JAPANESE-GERMAN MEETING ON URBAN CLIMATOLOGY.

Cheng, V., Ng, E., Chan, C., & Givoni, B. (2012). Outdoor thermal comfort study in a sub-tropical climate: a longitudinal study based in Hong Kong. *International journal of Biometeorology, 56*(1), 43-56.

Cheung, C. S., & Hart, M. A. (2014). Climate change and thermal comfort in Hong Kong. *Int J Biometeorol, 58*(2), 137-148. doi:10.1007/s00484-012-0608-9

Cheung, C. S. C., & Hart, M. A. (2014). Climate change and thermal comfort in Hong Kong. *International journal of Biometeorology, 58*(2), 137-148.

Cheung, P. K., & Jim, C. (2018). Subjective outdoor thermal comfort and urban green space usage in humid-subtropical Hong Kong. *Energy and Buildings*.

Cheung, P. K., & Jim, C. Y. (2018). Subjective outdoor thermal comfort and urban green space usage in humid-subtropical Hong Kong. *Energy and Buildings, 173*, 150-162.

Cleary, P. D., & Kessler, R. C. (1982). The estimation and interpretation of modifier effects. *Journal of Health and Social Behavior*, 159-169.

Cotter, J. D., & Taylor, N. A. (2005). The distribution of cutaneous sudomotor and alliesthesial thermosensitivity in mildly heat‐stressed humans: an open‐loop approach. *The Journal of physiology, 565*(1), 335-345.

Cox, D. R. (2018). *Analysis of binary data* (2nd Edition ed.): Routledge, New York.

Craig, A. (2003). Pain mechanisms: labeled lines versus convergence in central processing. *Annual review of neuroscience, 26*(1), 1-30.

De Dear, R. (2011). Revisiting an old hypothesis of human thermal perception: alliesthesia. *Building Research & Information, 39*(2), 108-117.

de Dear, R. J., Arens, E., Hui, Z., & Oguro, M. (1997). Convective and radiative heat transfer coefficients for individual human body segments. *International journal of Biometeorology, 40*(3), 141-156.

De Dear, R. J., & Brager, G. S. (2002). Thermal comfort in naturally ventilated buildings: revisions to ASHRAE Standard 55. *Energy and Buildings, 34*(6), 549-561.

DeGroot, D. W., & Kenney, W. L. (2007). Impaired defense of core temperature in aged humans during mild cold stress. *American journal of Physiology-Regulatory, integrative and comparative Physiology, 292*(1), R103-R108.

Dimoudi, A., Kantzioura, A., Zoras, S., Pallas, C., & Kosmopoulos, P. (2013). Investigation of urban microclimate parameters in an urban center. *Energy and Buildings, 64*, 1-9.

Dowdy, S., Wearden, S., & Chilko, D. (2011). *Statistics for research* (Vol. 512): John Wiley & Sons.

Du, Y., Mak, C. M., Huang, T., & Niu, J. (2017). Towards an integrated method to assess effects of lift-up design on outdoor thermal comfort in Hong Kong. *Building and Environment, 125*, 261-272. doi:10.1016/j.buildenv.2017.09.001

Du, Y., Mak, C. M., & Li, Y. (2018). Application of a multi-variable optimization method to determine lift-up design for optimum wind comfort. *Building and Environment, 131*, 242-254.

Du, Y., Mak, C. M., Liu, J., Xia, Q., Niu, J., & Kwok, K. C. (2017). Effects of lift-up design on pedestrian level wind comfort in different building configurations under three wind directions. *Building and Environment, 117*, 84-99.

Engineers, A. S. o. C. (2003). *Outdoor Human Comfort and Its Assessment: State of the Art*.

Fang, Z., Feng, X., & Lin, Z. (2017). Investigation of PMV Model for Evaluation of the Outdoor Thermal Comfort. *Procedia Engineering, 205*, 2457-2462.

Fang, Z., Feng, X., Liu, J., Lin, Z., Mak, C. M., Niu, J., . . . Xu, X. (2019). Investigation into the differences among several outdoor thermal comfort indices against field survey in subtropics. *Sustainable Cities and Society, 44*, 676-690.

Fang, Z., Lin, Z., Mak, C. M., Niu, J., & Tse, K.-T. (2018). Investigation into sensitivities of factors in outdoor thermal comfort indices. *Building and Environment, 128*, 129-142. doi:10.1016/j.buildenv.2017.11.028

Fiala, D. (1998). *Dynamic simulation of human heat transfer and thermal comfort.* De Montfort University Leicester, UK,

Fiala, D., Havenith, G., Bröde, P., Kampmann, B., & Jendritzky, G. (2012). UTCI-Fiala multi-node model of human heat transfer and temperature regulation. *International journal of Biometeorology, 56*(3), 429-441.

Fiala, D., Lomas, K. J., & Stohrer, M. (2001). Computer prediction of human thermoregulatory and temperature responses to a wide range of environmental conditions. *International journal of Biometeorology, 45*(3), 143-159.

Fiala, D., Psikuta, A., Jendritzky, G., Paulke, S., Nelson, D. A., van Marken Lichtenbelt, W. D., & Frijns, A. J. (2010). Physiological modeling for technical, clinical and research applications. *Front Biosci S, 2*, 939-968.

Finney, D. J., & Tattersfield, F. (1952). *Probit analysis*: Cambridge University Press, Cambridge.

Foda, E., & Sirén, K. (2011). A new approach using the Pierce two-node model for different body parts. *International journal of Biometeorology, 55*(4), 519-532.

Frank, S. M., Raja, S. N., Bulcao, C. F., & Goldstein, D. S. (1999). Relative contribution of core and cutaneous temperatures to thermal comfort and autonomic responses in humans. *Journal of applied physiology, 86*(5), 1588-1593.

Franke, J. (2005). *Numerical simulation of the flow across an asymmetric street intersection.* Paper presented at the Proc. 4^< th> European & African Conference on Wind Engineering, Prague, 2005.

Gagge, A. (1973). *Standard effective temperature-A single temperature index of temperature sensation an thermal discomfort.* Paper presented at the Proc. of the CIB Commission W45 (Human Requirements), Symposium, Thermal Comfort and Moderate Heat Stress, 1973.

Gagge, A. P. (1971). An effective temperature scale based on a simple model of human physiological regulatory response. *Ashrae Trans., 77*, 247-262.

Gagge, A. P., Burton, A. C., & Bazett, H. C. (1941). A practical system of units for the description of the heat exchange of man with his environment. *science, 94*(2445), 428-430.

Givoni, B., Noguchi, M., Saaroni, H., Pochter, O., Yaacov, Y., Feller, N., & Becker, S. (2003). Outdoor comfort research issues. *Energy and Buildings, 35*(1), 77-86.

Golasi, I., Salata, F., de Lieto Vollaro, E., & Coppi, M. (2018). Complying with the demand of standardization in outdoor thermal comfort: A first approach to the Global Outdoor Comfort Index (GOCI). *Building and Environment, 130*, 104-119.

Gulyás, Á., Unger, J., & Matzarakis, A. (2006). Assessment of the microclimatic and human comfort conditions in a complex urban environment: modelling and measurements. *Building and Environment, 41*(12), 1713-1722.

Hadianpour, M., Mahdavinejad, M., Bemanian, M., Haghshenas, M., & Kordjamshidi, M. (2019). Effects of windward and leeward wind directions on outdoor thermal and wind sensation in Tehran. *Building and Environment, 150*, 164-180.

Hadianpour, M., Mahdavinejad, M., Bemanian, M., & Nasrollahi, F. (2018). Seasonal differences of subjective thermal sensation and neutral temperature in an outdoor shaded space in Tehran, Iran. *Sustainable Cities and Society, 39*, 751-764. doi:https://doi.org/10.1016/j.scs.2018.03.003

Hall, J. E. (2011). Guyton and Hall textbook of medical physiology. *Philadelphia: Saunders Elisever*.

Harlan, S. L., Brazel, A. J., Prashad, L., Stefanov, W. L., & Larsen, L. (2006). Neighborhood microclimates and vulnerability to heat stress. *Soc Sci Med, 63*(11), 2847-2863. doi:10.1016/j.socscimed.2006.07.030

Hensel, H. (1982). *Thermal sensations and thermoreceptors in man*: Charles C. Thomas.

Hensel, H., & Schafer, K. (1984). Thermoreception and temperature regulation in man. In *Recent advances in medical thermology* (pp. 51-64): Springer.

HKBD (Hong Kong Buildings Department). (2016). APP-152: Sustainable Building

Design Guidelines.

Hong, B., & Lin, B. (2015). Numerical studies of the outdoor wind environment and thermal comfort at pedestrian level in housing blocks with different building layout patterns and trees arrangement. *Renewable Energy, 73*, 18-27. doi:10.1016/j.renene.2014.05.060

Höppe, P. (1999). The physiological equivalent temperature–a universal index for the biometeorological assessment of the thermal environment. *International journal of Biometeorology, 43*(2), 71-75.

Höppe, P. (2002). Different aspects of assessing indoor and outdoor thermal comfort. *Energy and Buildings, 34*(6), 661-665.

Hosker, R. (1984). Flow and diffusion near obstacles. *Atmospheric science and power production*.

Howell, J. R., Menguc, M. P., & Siegel, R. (2010). *Thermal radiation heat transfer*: CRC press.

HQInc. (2019). CorTemp Sensor. Retrieved from https://hqinc.net/home/cortemp/cortemp-products/cortemp-sensor/

Huang, T., Li, J., Xie, Y., Niu, J., & Mak, C. M. (2017). Simultaneous environmental parameter monitoring and human subject survey regarding outdoor thermal comfort and its modelling. *Building and Environment, 125*, 502-514.

Huizenga, C., Hui, Z., & Arens, E. (2001). A model of human physiology and comfort for assessing complex thermal environments. *Building and Environment, 36*(6), 691-699.

Hunt, J., Poulton, E., & Mumford, J. (1976a). The effects of wind on people; new criteria based on wind tunnel experiments. *Building and Environment*

*11*(1), 15-28.

Hunt, J., Poulton, E., & Mumford, J. (1976b). The effects of wind on people; new criteria based on wind tunnel experiments. *Building and Environment, 11*(1), 15-28.

Hwang, R.-L., & Lin, T.-P. (2007). Thermal Comfort Requirements for Occupants of Semi-Outdoor and Outdoor Environments in Hot-Humid Regions. *Architectural Science Review, 50*(4), 357-364. doi:10.3763/asre.2007.5043

Jendritzky, G., de Dear, R., & Havenith, G. (2012). UTCI—why another thermal index? *International journal of Biometeorology, 56*(3), 421-428.

Jessen, C. (1981). Independent clamps of peripheral and central temperatures and their effects on heat production in the goat. *The Journal of physiology, 311*(1), 11-22.

Johansson, E. (2006). Influence of urban geometry on outdoor thermal comfort in a hot dry climate: A study in Fez, Morocco. *Building and Environment, 41*(10), 1326-1338.

Klemm, W., Heusinkveld, B. G., Lenzholzer, S., & van Hove, B. (2015). Street greenery and its physical and psychological impact on thermal comfort. *Landscape and Urban Planning, 138*, 87-98. doi:10.1016/j.landurbplan.2015.02.009

Kong, L., Lau, K. K.-L., Yuan, C., Chen, Y., Xu, Y., Ren, C., & Ng, E. (2017a). Regulation of outdoor thermal comfort by trees in Hong Kong. *Sustainable Cities and Society, 31*, 12-25. doi:10.1016/j.scs.2017.01.018

Kong, L., Lau, K. K. L., Yuan, C., Chen, Y., Xu, Y., Ren, C., & Ng, E. (2017b). Regulation of outdoor thermal comfort by trees in Hong Kong. *Sustainable Cities and Society, 31*, 12-25.

Krüger, E. L., Minella, F. O., & Rasia, F. (2011). Impact of urban geometry on outdoor thermal comfort and air quality from field measurements in Curitiba, Brazil. *Building and Environment*, *46*(3), 621-634. doi:10.1016/j.buildenv.2010.09.006

Krüger, E. L., & Rossi, F. A. (2011). Effect of personal and microclimatic variables on observed thermal sensation from a field study in southern Brazil. *Building and Environment*, *46*(3), 690-697.

Krüger, E. L., Tamura, C. A., Bröde, P., Schweiker, M., & Wagner, A. (2017). Short- and long-term acclimatization in outdoor spaces: Exposure time, seasonal and heatwave adaptation effects. *Building and Environment*, *116*, 17-29.

Lai, D., Guo, D., Hou, Y., Lin, C., & Chen, Q. (2014). Studies of outdoor thermal comfort in northern China. *Building and Environment, 77*, 110-118. doi:10.1016/j.buildenv.2014.03.026

Lai, D., Zhou, C., Huang, J., Jiang, Y., Long, Z., & Chen, Q. (2014). Outdoor space quality: A field study in an urban residential community in central China.

*Energy and Buildings, 68*, 713-720.

Lai, D., Zhou, X., & Chen, Q. (2017a). Measurements and predictions of the skin temperature of human subjects on outdoor environment. *Energy and Buildings, 151*, 476-486. doi:10.1016/j.enbuild.2017.07.009

Lai, D., Zhou, X., & Chen, Q. (2017b). Modelling dynamic thermal sensation of human subjects in outdoor environments. *Energy and Buildings, 149*, 16-25.

Lai, D. Y., Guo, D. H., Hou, Y. F., Lin, C. Y., & Chen, Q. Y. (2014). Studies of outdoor thermal comfort in northern China. *Building and Environment, 77,* 110-118. doi:10.1016/j.buildenv.2014.03.026

Lam, C. K. C., & Lau, K. K. L. (2018). Effect of long-term acclimatization on summer thermal comfort in outdoor spaces: a comparative study between Melbourne and Hong Kong. *International journal of Biometeorology, 62*(7), 1311–1324.

Lau, K. K., Shi, Y., & Ng, E. Y. (2019). Dynamic response of pedestrian thermal comfort under outdoor transient conditions. *Int J Biometeorol, 63*(7), 979-989. doi:10.1007/s00484-019-01712-2

Lawson, T. (1975). *The effect of wind on people in the vicinity of buildings.* Paper presented at the 4th Int. Conf. on Wind Effects on Buildings and Structures, London, 1975.

Lee, H., Mayer, H., & Chen, L. (2016). Contribution of trees and grasslands to the mitigation of human heat stress in a residential district of Freiburg, Southwest Germany. *Landscape and Urban Planning, 148,* 37-50. doi:10.1016/j.landurbplan.2015.12.004

Li, J., Niu, J., Mak, C. M., Huang, T., & Xie, Y. (2018). Assessment of outdoor thermal comfort in Hong Kong based on the individual desirability and acceptability of sun and wind conditions. *Building and Environment, 145*, 50-61. doi:10.1016/j.buildenv.2018.08.059

Lin, B., Li, X., Zhu, Y., & Qin, Y. (2008). Numerical simulation studies of the different vegetation patterns' effects on outdoor pedestrian thermal comfort. *Journal of Wind Engineering and Industrial Aerodynamics, 96*(10-11), 1707-1718. doi:10.1016/j.jweia.2008.02.006

Lin, T.-P. (2009). Thermal perception, adaptation and attendance in a public square in hot and humid regions. *Building and Environment, 44*(10), 2017-2026.

doi:10.1016/j.buildenv.2009.02.004

Lin, T.-P., de Dear, R., & Hwang, R.-L. (2011). Effect of thermal adaptation on seasonal outdoor thermal comfort. *International Journal of Climatology, 31*(2), 302-312. doi:10.1002/joc.2120

Lin, T.-P., Matzarakis, A., & Hwang, R.-L. (2010). Shading effect on long-term outdoor thermal comfort. *Building and Environment*, *45*(1), 213-221. doi:10.1016/j.buildenv.2009.06.002

Lin, T. P., & Matzarakis, A. (2008). Tourism climate and thermal comfort in Sun Moon Lake, Taiwan. *International journal of Biometeorology, 52*(4), 281-290.

Lin, T. P., Tsai, K. T., Hwang, R. L., & Matzarakis, A. (2012). Quantification of the effect of thermal indices and sky view factor on park attendance. *Landscape and Urban Planning*, *107*(2), 137-146.

Liu, J., & Niu, J. (2016). CFD simulation of the wind environment around an isolated high-rise building: An evaluation of SRANS, LES and DES models. *Building and Environment*, *96*, 91-106.

Liu, J., & Niu, J. (2019). Delayed detached eddy simulation of pedestrian-level wind around a building array–The potential to save computing resources. *Building and Environment*, *152*, 28-38.

Liu, J., Niu, J., Du, Y., Mak, C. M., & Zhang, Y. (2019). LES for pedestrian level wind around an idealized building array—Assessment of sensitivity to influencing parameters. *Sustainable Cities and Society*

*44*, 406-415.

Liu, J., Niu, J., Mak, C. M., & Xia, Q. (2017). Detached eddy simulation of pedestrian-level wind and gust around an elevated building. *Building and Environment*, *125*, 168-179.

Liu, J., Niu, J., & Xia, Q. (2016). Combining measured thermal parameters and simulated wind velocity to predict outdoor thermal comfort. *Building and Environment*, *105*, 185-197. doi:10.1016/j.buildenv.2016.05.038

Liu, J., Zhang, X., Niu, J., & Tse, K. T. (2019). Pedestrian-level wind and gust around buildings with a 'lift-up' design: Assessment of influence from surrounding buildings by adopting LES. *Building Simulation, 12*(6), 1107-1118. doi:10.1007/s12273-019-0541-5

Makhoul, A., Ghali, K., & Ghaddar, N. (2013). Desk fans for the control of the convection flow around occupants using ceiling mounted personalized ventilation. *Building and Environment, 59*, 336-348.

Maruani, T., & Amit-Cohen, I. (2007). Open space planning models: A review of approaches and methods. *Landscape and Urban Planning, 81*(1-2), 1-13. doi:10.1016/j.landurbplan.2007.01.003

Matzarakis, A., Mayer, H., & Iziomon, M. G. (1999). Applications of a universal thermal index: physiological equivalent temperature. *International journal of Biometeorology, 43*(2), 76-84.

Mayer, H., & Hoppe, P. (1987). Thermal comfort of man in different urban environments. *Theoretical and Applied Climatology, 38*(1), 43-49. doi:10.1007/bf00866252

Mekjavic, I. B., Sundberg, C. J., & Linnarsson, D. (1991). Core temperature" null zone". *Journal of applied physiology, 71*(4), 1289-1295.

Melikov, A. K., Popiolek, Z., Silva, M., Care, I., & Sefker, T. (2007). Accuracy limitations for low-velocity measurements and draft assessment in rooms. *HVAC&R Research, 13*(6), 971-986.

Middel, A., Lukasczyk, J., & Maciejewski, R. (2017). Sky View Factors from Synthetic Fisheye Photos for Thermal Comfort Routing—A Case Study in Phoenix, Arizona. *Urban Planning, 2*(1), 19-30.

Mochida, A., & Lun, I. Y. F. (2008). Prediction of wind environment and thermal comfort at pedestrian level in urban area. *Journal of Wind Engineering and Industrial Aerodynamics, 96*(10-11), 1498-1527. doi:10.1016/j.jweia.2008.02.033

Morakinyo, T. E., Kong, L., Lau, K. K.-L., Yuan, C., & Ng, E. (2017). A study on the impact of shadow-cast and tree species on in-canyon and neighborhood's thermal comfort. *Building and Environment, 115*, 1-17. doi:10.1016/j.buildenv.2017.01.005

Murakami, S., Iwasa, Y., & Morikawa, Y. (1986). Study on acceptable criteria for assessing wind environment at ground level based on residents' diaries. *Journal of Wind Engineering and Industrial Aerodynamics, 24*(1), 1-18.

Murakami, S., Ooka, R., Mochida, A., Yoshida, S., & Kim, S. (1999). CFD analysis of wind climate from human scale to urban scale. *Journal of Wind*

*Engineering and Industrial Aerodynamics, 81*(1), 57-81.

Murakami, S., Uehara, K., & Deguchi, K. (1980). Wind effects on pedestrians: New criteria based on outdoor observation of over 2000 persons. In *Wind Engineering* (pp. 277-288): Elsevier.

Ndetto, E. L., & Matzarakis, A. (2013). Effects of urban configuration on human thermal conditions in a typical tropical African coastal city. *Advances in Meteorology, 2013*.

Ng, E. (2006). *Air ventilation assessment system for high density planning and design.* Paper presented at the Proceedings of PLEA International Conference.

Ng, E. (2009). Policies and technical guidelines for urban planning of high-density cities–air ventilation assessment (AVA) of Hong Kong. *Building and Environment, 44*(7), 1478-1488.

Ng, E., Chen, L., Wang, Y., & Yuan, C. (2012). A study on the cooling effects of greening in a high-density city: An experience from Hong Kong. *Building and Environment, 47*, 256-271. doi:10.1016/j.buildenv.2011.07.014

Ng, E., & Cheng, V. (2012). Urban human thermal comfort in hot and humid Hong Kong. *Energy and Buildings, 55*, 51-65.

Ng, E., & Ren, C. (2015). *The urban climatic map: A methodology for sustainable urban planning*: Routledge.

Nicol, F., & Humphreys, M. (2010). Derivation of the adaptive equations for thermal comfort in free-running buildings in European standard EN15251. *Building and Environment, 45*(1), 11-17.

Nicol, F., Humphreys, M., & Roaf, S. (2012). *Adaptive thermal comfort: principles and practice*: Routledge, London.

Nikolopoulou, M., Baker, N., & Steemers, K. (2001). Thermal comfort in outdoor urban spaces: understanding the human parameter. *Solar Energy, 70*(3), 227-235.

Nikolopoulou, M., & Lykoudis, S. (2006). Thermal comfort in outdoor urban spaces: analysis across different European countries. *Building and Environment, 41*(11), 1455-1470.

Niu, J., Liu, J., Lee, T.-C., Lin, Z., Mak, C. M., Tse, K.-T., . . . Kwok, K. C. S. (2015). A new method to assess spatial variations of outdoor thermal comfort: Onsite monitoring results and implications for precinct planning. *Building and Environment, 91*, 263-270. doi:10.1016/j.buildenv.2015.02.017

Norton, B. A., Coutts, A. M., Livesley, S. J., Harris, R. J., Hunter, A. M., & Williams, N. S. G. (2015). Planning for cooler cities: A framework to prioritise green infrastructure to mitigate high temperatures in urban landscapes. *Landscape and Urban Planning, 134*, 127-138. doi:10.1016/j.landurbplan.2014.10.018

Oke, T. R., Mills, G., Christen, A., & Voogt, J. A. (2017). *Urban climates*: Cambridge University Press.

Osmond, P., & Sharifi, E. (2017). Guide to urban cooling strategies. *Low Carbon Living CRC*.

Pantavou, K., Lykoudis, S., Nikolopoulou, M., & Tsiros, I. X. (2018). Thermal sensation and climate: a comparison of UTCI and PET thresholds in different climates. *International journal of Biometeorology, 62*(9), 1695-1708.

Pantavou, K., Theoharatos, G., Santamouris, M., & Asimakopoulos, D. (2013). Outdoor thermal sensation of pedestrians in a Mediterranean climate and a comparison with UTCI. *Building and Environment, 66*, 82-95. doi:10.1016/j.buildenv.2013.02.014

Parkinson, T., & De Dear, R. (2015). Thermal pleasure in built environments: physiology of alliesthesia. *Building Research and Information, 43*(3), 288-301.

Pearlmutter, D., Berliner, P., & Shaviv, E. (2006). Physical modeling of pedestrian energy exchange within the urban canopy. *Building and Environment, 41*(6), 783-795. doi:10.1016/j.buildenv.2005.03.017

Pickup, J., & de Dear, R. (2000). *An outdoor thermal comfort index (OUT_SET*)-part I-the model and its assumptions.* Paper presented at the Biometeorology and urban climatology at the turn of the millenium. Selected papers from the Conference ICB-ICUC.

Ramponi, R., & Blocken, B. (2012). CFD simulation of cross-ventilation for a generic isolated building: Impact of computational parameters. *Building and Environment, 53*, 34-48. doi:10.1016/j.buildenv.2012.01.004

Richards, P., Mallinson, G., McMillan, D., & Li, Y. (2002). Pedestrian level wind speeds in downtown Auckland. *Wind and Structures, 5*(2_3_4), 151-164.

Rodríguez-Algeciras, J., Tablada, A., & Matzarakis, A. (2018). Effect of asymmetrical street canyons on pedestrian thermal comfort in warm-humid climate of Cuba. *Theoretical and Applied Climatology, 133*(3-4), 663-679.

Romanovsky, A. A. (2007). Thermoregulation: some concepts have changed. Functional architecture of the thermoregulatory system. *American journal of Physiology-Regulatory, integrative and comparative Physiology, 292*(1), R37-R46.

Saaroni, H., & Ziv, B. (2003). The impact of a small lake on heat stress in a Mediterranean urban park: the case of Tel Aviv, Israel. *International journal of Biometeorology, 47*(3), 156-165.

Sakurada, S., Shido, O., Fujikake, K., & Nagasaka, T. (1993). Relationship between body core and peripheral temperatures at the onset of thermoregulatory responses in rats. *The Japanese journal of physiology, 43*(5), 659-667.

Salata, F., Golasi, I., de Lieto Vollaro, R., & de Lieto Vollaro, A. (2016). Outdoor thermal comfort in the Mediterranean area. A transversal study in Rome, Italy. *Building and Environment, 96*, 46-61. doi:10.1016/j.buildenv.2015.11.023

Schellen, L., Loomans, M., Kingma, B., De Wit, M., Frijns, A., & van Marken Lichtenbelt, W. (2013). The use of a thermophysiological model in the built environment to predict thermal sensation: coupling with the indoor environment and thermal sensation. *Building and Environment, 59*, 10-22.

Skelhorn, C., Lindley, S., & Levermore, G. (2014). The impact of vegetation types on air and surface temperatures in a temperate city: A fine scale assessment in Manchester, UK. *Landscape and Urban Planning, 121*, 129-140. doi:10.1016/j.landurbplan.2013.09.012

Soligo, M. J., Irwin, P. A., Williams, C. J., & Schuyler, G. D. (1998). A comprehensive assessment of pedestrian comfort including thermal effects. *Journal of Wind Engineering and Industrial Aerodynamics, 77*, 753-766.

Spagnolo, J., & de Dear, R. (2003). A field study of thermal comfort in outdoor and semi-outdoor environments in subtropical Sydney Australia. *Building and Environment, 38*(5), 721-738. doi:10.1016/s0360-1323(02)00209-3

Stolwijk, J., Nadel, E., Mitchell, J., & Saltin, B. (1971). Modification of central sweating drive at the periphery. *International journal of Biometeorology, 15*(2), 268-272.

Stolwijk, J. A. (1971). A mathematical model of physiological temperature regulation in man.

Sun, R., Chen, A., Chen, L., & Lü, Y. (2012). Cooling effects of wetlands in an urban region: the case of Beijing. *Ecological Indicators, 20*, 57-64.

Sun, S., Xu, X., Lao, Z., Liu, W., Li, Z., García, E. H., . . . Zhu, J. (2017). Evaluating the impact of urban green space and landscape design parameters on thermal comfort in hot summer by numerical simulation. *Building and Environment, 123*, 277-288.

Sund‐Levander, M., Forsberg, C., & Wahren, L. K. (2002). Normal oral, rectal, tympanic and axillary body temperature in adult men and women: a systematic literature review. *Scandinavian journal of caring sciences, 16*(2), 122-128.

Syafii, N. I., Ichinose, M., Wong, N. H., Kumakura, E., Jusuf, S. K., & Chigusa, K. (2016). Experimental Study on the Influence of Urban Water Body on Thermal Environment at Outdoor Scale Model. *Procedia Engineering, 169*, 191-198. doi:10.1016/j.proeng.2016.10.023

Taleghani, M., Kleerekoper, L., Tenpierik, M., & van den Dobbelsteen, A. (2015). Outdoor thermal comfort within five different urban forms in the Netherlands. *Building and Environment, 83*, 65-78. doi:10.1016/j.buildenv.2014.03.014

Tanabe, S.-i., Kobayashi, K., Nakano, J., Ozeki, Y., & Konishi, M. (2002). Evaluation of thermal comfort using combined multi-node thermoregulation (65MN) and radiation models and computational fluid dynamics (CFD). *Energy and Buildings, 34*(6), 637-646.

Tansey, E. A., & Johnson, C. D. (2015). Recent advances in thermoregulation. *Advances in physiology education, 39*(3), 139-148.

Taylor, N., Werner, J., & Mekjavic, I. B. (2008). Concepts in physiological regulation: a thermoregulatory perspective.

Thorsson, S., Honjo, T., Lindberg, F., Eliasson, I., & Lim, E.-M. (2007). Thermal comfort and outdoor activity in Japanese urban public places. *Environment and Behavior, 39*(5), 660-684.

Thorsson, S., Lindberg, F., Björklund, J., Holmer, B., & Rayner, D. (2011). Potential changes in outdoor thermal comfort conditions in Gothenburg, Sweden due to climate change: the influence of urban geometry. *International Journal of*

*Climatology, 31*(2), 324-335.

Tikuisis, P., & Giesbrecht, G. G. (1999). Prediction of shivering heat production from core and mean skin temperatures. *European journal of applied physiology and occupational physiology, 79*(3), 221-229.

Toparlar, Y., Blocken, B., Maiheu, B., & van Heijst, G. J. F. (2017). A review on the CFD analysis of urban microclimate. *Renewable and Sustainable Energy Reviews, 80*, 1613-1640. doi:10.1016/j.rser.2017.05.248

Toparlar, Y., Blocken, B., Vos, P., van Heijst, G. J. F., Janssen, W. D., van Hooff, T., . . . Timmermans, H. J. P. (2015). CFD simulation and validation of urban microclimate: A case study for Bergpolder Zuid, Rotterdam. *Building and Environment, 83*, 79-90. doi:10.1016/j.buildenv.2014.08.004

Tseliou, A., Tsiros, I. X., Lykoudis, S., & Nikolopoulou, M. (2010). An evaluation of three biometeorological indices for human thermal comfort in urban outdoor areas under real climatic conditions. *Building and Environment, 45*(5), 1346-1352.

van Druenen, T., van Hooff, T., Montazeri, H., & Blocken, B. (2019). CFD evaluation of building geometry modifications to reduce pedestrian-level wind speed. *Building and Environment, 163*. doi:10.1016/j.buildenv.2019.106293

Van Hoof, J. (2008). Forty years of Fanger's model of thermal comfort: comfort for all? *Indoor Air, 18*(3), 182-201.

Vignola, F., Michalsky, J., & Stoffel, T. (2016). *Solar and infrared radiation measurements*: CRC press.

Wang, Y., Berardi, U., & Akbari, H. (2016). Comparing the effects of urban heat island mitigation strategies for Toronto, Canada. *Energy and Buildings, 114*, 2-19. doi:10.1016/j.enbuild.2015.06.046

Wang, Z., Yu, H., Luo, M., Wang, Z., Zhang, H., & Jiao, Y. (2019). Predicting older people's thermal sensation in building environment through a machine learning approach: Modelling, interpretation, and application. *Building and Environment*, 106231.

Webb, C. (1959). An analysis of some observations of thermal comfort in an equatorial climate. *Occupational and Environmental Medicine, 16*(4), 297-310.

Wei, R., Song, D., Wong, N. H., & Martin, M. (2016). Impact of Urban Morphology Parameters on Microclimate. *Procedia Engineering, 169*, 142-149. doi:10.1016/j.proeng.2016.10.017

Weihs, P., Staiger, H., Tinz, B., Batchvarova, E., Rieder, H., Vuilleumier, L., . . . Jendritzky, G. (2012). The uncertainty of UTCI due to uncertainties in the determination of radiation fluxes derived from measured and observed meteorological data. *Int J Biometeorol, 56*(3), 537-555. doi:10.1007/s00484-011-0416-7

Weinbaum, S., Jiji, L., & Lemons, D. (1984). Theory and experiment for the effect of vascular microstructure on surface tissue heat transfer—Part I: Anatomical foundation and model conceptualization.

Werner, J. (1980). The concept of regulation for human body temperature. *Journal of Thermal Biology, 5*(2), 75-82.

Werner, J. (1988). Functional mechanisms of temperature regulation, adaptation and fever: complementary system theoretical and experimental evidence. *Pharmacology and therapeutics, 37*(1), 1-23.

Werner, J. (2010). System properties, feedback control and effector coordination of human temperature regulation. *European journal of applied physiology, 109*(1), 13-25.

Wing-lui, G., Tsz-cheung, L., & Kin-yu, C. (2010). Past and future changes in the climate of Hong Kong. *Journal of Meteorological Research, 24*(2), 163-175.

Wissler, E. (1985). Mathematical simulation of human thermal behavior using whole body models. *Heat transfer in medicine and biology, 1*(13), 325-373.

Wu, L.-J., Sweet, T.-B., & Clapham, D. E. (2010). International Union of Basic and Clinical Pharmacology. LXXVI. Current progress in the mammalian TRP ion channel family. *Pharmacological reviews, 62*(3), 381-404.

Xi, T., Li, Q., Mochida, A., & Meng, Q. (2012). Study on the outdoor thermal environment and thermal comfort around campus clusters in subtropical urban areas. *Building and Environment, 52*, 162-170. doi:10.1016/j.buildenv.2011.11.006

Xia, Q., Liu, X., Niu, J., & Kwok, K. C. (2017). Effects of building lift-up design on the wind environment for pedestrians. *Indoor and Built Environment, 26*(9), 1214-1231.

Xie, Y. (2013). *Regression Analysis*. BeiJing: Social Sciences Academic Press (China).

Xie, Y., Huang, T., Li, J., Liu, J., Niu, J., Mak, C. M., & Lin, Z. (2018). Evaluation of a multi-nodal thermal regulation model for assessment of outdoor thermal comfort: Sensitivity to wind speed and solar radiation. *Building and Environment*, *132*, 45-56.

Xie, Y., Liu, J., Huang, T., Li, J., Niu, J., Mak, C. M., & Lee, T.-c. (2019). Outdoor thermal sensation and logistic regression analysis of comfort range of meteorological parameters in Hong Kong. *Building and Environment*.

Xu, M., Hong, B., Mi, J., & Yan, S. (2018). Outdoor thermal comfort in an urban park during winter in cold regions of China. *Sustainable Cities and Society, 43*, 208-220. doi:https://doi.org/10.1016/j.scs.2018.08.034

Yang, W., Wong, N. H., & Zhang, G. (2013). A comparative analysis of human thermal conditions in outdoor urban spaces in the summer season in Singapore and Changsha, China. *Int J Biometeorol*, *57*(6), 895-907. doi:10.1007/s00484-012-0616-9

Yau, R., Au, B., Leung, D., Fort-Brescia, B., & Dutton, H. (2017). *Bringing Sustainable Neighborhood Design into Reality – Case Sharing by Brickell City Centre, Miami* Paper presented at the World Sustainable Built Environment Conference 2017 Hong Kong, Hong Kong.

Yoshida, A., Hisabayashi, T., Kashihara, K., Kinoshita, S., & Hashida, S. (2015). Evaluation of effect of tree canopy on thermal environment, thermal sensation, and mental state. *Urban Climate, 14*, 240-250. doi:10.1016/j.uclim.2015.09.004

Yoshie, R., Mochida, A., Tominaga, Y., Kataoka, H., Harimoto, K., Nozu, T., & Shirasawa, T. (2007). Cooperative project for CFD prediction of pedestrian wind environment in the Architectural Institute of Japan. *Journal of Wind Engineering and Industrial Aerodynamics, 95*(9-11), 1551-1578. doi:10.1016/j.jweia.2007.02.023

Yu, Y., Liu, J., Chauhan, K., de Dear, R., & Niu, J. (2019). Experimental study on convective heat transfer coefficients for the human body exposed to turbulent wind conditions. *Building and Environment*, 106533.

Yuan, C., & Ng, E. (2012). Building porosity for better urban ventilation in high-density cities–A computational parametric study. *Building and Environment*, *50*, 176-189.

Zhang, H. (2003). Human thermal sensation and comfort in transient and non-uniform thermal environments. *Center for the Built Environment*.

Zhang, H., Arens, E., Huizenga, C., & Han, T. (2010a). Thermal sensation and comfort models for non-uniform and transient environments, part II: Local comfort of individual body parts. *Building and Environment, 45*(2), 389-398.

Zhang, H., Arens, E., Huizenga, C., & Han, T. (2010b). Thermal sensation and comfort models for non-uniform and transient environments, part III: Whole-body sensation and comfort. *Building and Environment, 45*(2), 399-410.

Zhang, H., Arens, E., Huizenga, C., & Han, T. (2010c). Thermal sensation and comfort models for non-uniform and transient environments: Part I: Local sensation of individual body parts. *Building and Environment, 45*(2), 380-388.

Zhang, X., Tse, K.-T., Weerasuriya, A. U., Li, S., Kwok, K. C., Mak, C. M., . . . Lin, Z. (2017). Evaluation of pedestrian wind comfort near 'lift-up'buildings with different aspect ratios and central core modifications. *Building and Environment*

*124*, 245-257.

Zhang, X., Tse, K., Weerasuriya, A., Kwok, K., Niu, J., Lin, Z., & Mak, C. M. (2018a). Pedestrian-level wind conditions in the space underneath lift-up buildings. *Journal of Wind Engineering and Industrial Aerodynamics, 179*, 58-69.

Zhang, X., Tse, K., Weerasuriya, A., Kwok, K., Niu, J., Lin, Z., & Mak, C. M. (2018b). Pedestrian-level wind conditions in the space underneath lift-up buildings. *Journal of Wind Engineering and Industrial Aerodynamics*

*179*, 58-69.

Zhang, X., Tse, K. T., Weerasuriya, A. U., Li, S. W., Kwok, K. C. S., Mak, C. M., . . . Lin, Z. (2017). Evaluation of pedestrian wind comfort near 'lift-up' buildings with different aspect ratios and central core modifications. *Building and Environment, 124*, 245-257. doi:10.1016/j.buildenv.2017.08.012

Zhang, Y., Du, X., & Shi, Y. (2017). Effects of street canyon design on pedestrian thermal comfort in the hot-humid area of China. *International journal of Biometeorology, 61*(8), 1421-1432.

Zhao, Y., Zhang, H., Arens, E. A., & Zhao, Q. (2014). Thermal sensation and comfort models for non-uniform and transient environments, part IV: Adaptive neutral setpoints and smoothed whole-body sensation model. *Building and Environment, 72,* 300-308.

Zhou, X., Zhang, H., Lian, Z., & Zhang, Y. (2014). A model for predicting thermal sensation of Chinese people. *Building and Environment, 82,* 237-246.

Zolfaghari, A., & Maerefat, M. (2010). A new simplified thermoregulatory bioheat model for evaluating thermal response of the human body to transient environments. *Building and Environment, 45*(10), 2068-2076.